Density Model for Minke Whale (*Balaenoptera acutorostrata*) for the U.S. East Coast: Supplementary Report

Duke University Marine Geospatial Ecology Lab*

Model Version 8.4 - 2016-04-21

Citation

When referencing our methodology or results generally, please cite our open-access article:

Roberts JJ, Best BD, Mannocci L, Fujioka E, Halpin PN, Palka DL, Garrison LP, Mullin KD, Cole TVN, Khan CB, McLellan WM, Pabst DA, Lockhart GG (2016) Habitat-based cetacean density models for the U.S. Atlantic and Gulf of Mexico. Scientific Reports 6: 22615. doi: 10.1038/srep22615

To reference this specific model or Supplementary Report, please cite:

Roberts JJ, Best BD, Mannocci L, Fujioka E, Halpin PN, Palka DL, Garrison LP, Mullin KD, Cole TVN, Khan CB, McLellan WM, Pabst DA, Lockhart GG (2016) Density Model for Minke Whale (*Balaenoptera acutorostrata*) for the U.S. East Coast Version 8.4, 2016-04-21, and Supplementary Report. Marine Geospatial Ecology Lab, Duke University, Durham, North Carolina.

Copyright and License

Revision History

Version	Date	Description of changes
1	2013-05-07	Initial version.
2	2013-05-08	Text edited to correct minor errors.
3	2014-03-01	Switched from four seasonal models to two. Reformulated density model using a Horvitz-Thompson estimator. Eliminated GAM for group size (consequence of above). Added group size as a candidate covariate in detection functions (benefit of above). Added survey ID as a candidate covariate in NOAA NARWSS detection functions. Took more care in selecting right-truncation distances. Fitted models with contemporaneous predictors, for comparison to climatological. Switched SST and SST fronts predictors from NOAA Pathfinder to GHRSST CMC0.2deg L4. Changed SST fronts algorithm to use Canny operator instead of Cayula-Cornillon. Switched winds predictors from SCOW to CCMP (SCOW only gives climatol. estimates.) Added DistToEddy predictors, based on Chelton et al. (2011) eddy database. Added cumulative VGPM predictors, summing productivity for 45, 90, and 180 days. Added North Atlantic Oscillation (NAO) predictor; included 3 and 6 month lags. Transformed predictors more carefully, to better minimize leverage of outliers. Implemented hybrid hierarchical-forward / exhaustive model selection procedure. Model selection procedure better avoids concurvity between predictors. Allowed GAMs to select between multiple formulations of dynamic predictors. Adjusted land mask to eliminate additional estuaries and hard-to-predict cells.

*For questions, or to offer feedback about this model or report, please contact Jason Roberts (jason.roberts@duke.edu)

4	2014-05-14	Added discussion of acoustic monitoring studies to text. Density models unchanged.
5	2014-05-20	Fixed bug in temporal variability plots. Density models unchanged.
6	2014-10-18	Added surveys: NJ-DEP, Virginia Aquarium, NARWSS 2013, UNCW 2013. Extended study area up Scotian Shelf. Added SEAPODYM predictors. Switched to mgcv estimation of Tweedie p parameter (family=tw()). Added Palka (2006) survey-specific g(0) estimates. Removed distance to eddy predictors and wind speed predictor from all models; they were not ecologically justified. Fixed missing pixels in several climatological predictors, which led to not all segments being utilized. Adjusted subregion extents. Eliminated Cape Cod Bay subregion.
7	2014-11-13	Reconfigured detection hierarchy and adjusted NARWSS detection functions based on additional information from Tim Cole. Switched to uniform distribution of density for southeast slope and abyss in winter. Removed CumVGPM180 predictor. Updated documentation.
8	2014-12-03	Fixed bug that applied the wrong detection function to segments NE_narwss_1999_widgeon_hapo dataset. Refitted model. Updated documentation.
8.1	2015-02-02	Updated the documentation. No changes to the model.
8.2	2015-05-14	Updated calculation of CVs. Switched density rasters to logarithmic breaks. No changes to the model.
8.3	2015-09-26	Updated the documentation. No changes to the model.
8.4	2016-04-21	Switched calculation of monthly 5% and 95% confidence interval rasters to the method used to produce the year-round rasters. (We intended this to happen in version 8.2 but I did not implement it properly.) Updated the monthly CV rasters to have value 0 where we assumed the species was absent, consistent with the year-round CV raster. No changes to the other (non-zero) CV values, the mean abundance rasters, or the model itself.

Survey Data

Survey	Period	Length (1000 km)	Hours	Sightings
NEFSC Aerial Surveys	1995-2008	70	412	86
NEFSC NARWSS Harbor Porpoise Survey	1999-1999	6	36	6
NEFSC North Atlantic Right Whale Sighting Survey	1999-2013	432	2330	819
NEFSC Shipboard Surveys	1995-2004	16	1143	101
NJDEP Aerial Surveys	2008-2009	11	60	0
NJDEP Shipboard Surveys	2008-2009	14	836	2
SEFSC Atlantic Shipboard Surveys	1992-2005	28	1731	1
SEFSC Mid Atlantic Tursiops Aerial Surveys	1995-2005	35	196	0
SEFSC Southeast Cetacean Aerial Surveys	1992-1995	8	42	0
UNCW Cape Hatteras Navy Surveys	2011-2013	19	125	4
UNCW Early Marine Mammal Surveys	2002-2002	18	98	0
UNCW Jacksonville Navy Surveys	2009-2013	66	402	9
UNCW Onslow Navy Surveys	2007-2011	49	282	2
UNCW Right Whale Surveys	2005-2008	114	586	0
Virginia Aquarium Aerial Surveys	2012-2014	9	53	1
Total		895	8332	1031

Table 2: Survey effort and sightings used in this model. Effort is tallied as the cumulative length of on-effort transects and hours the survey team was on effort. Sightings are the number of on-effort encounters of the modeled species for which a perpendicular sighting distance (PSD) was available. Off effort sightings and those without PSDs were omitted from the analysis.

Season	Months	Length (1000 km)	Hours	Sightings
Winter	Nov Dec Jan Feb Mar	326	2436	71
Summer	Apr May Jun Jul Aug Sep Oct	571	5896	960

Table 3: Survey effort and on-effort sightings having perpendicular sighting distances, summarized by season.

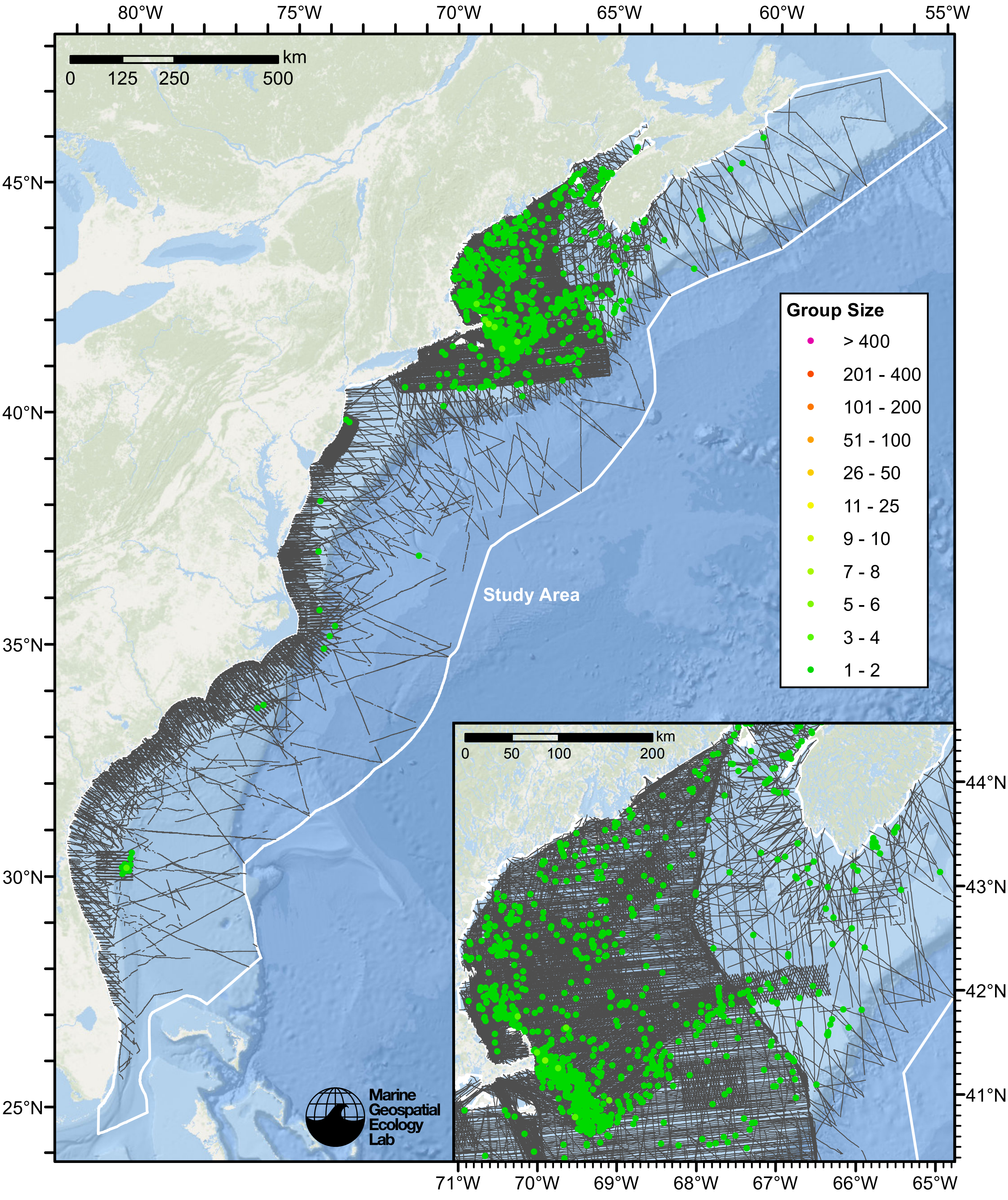

Figure 1: Minke whale sightings and survey tracklines.

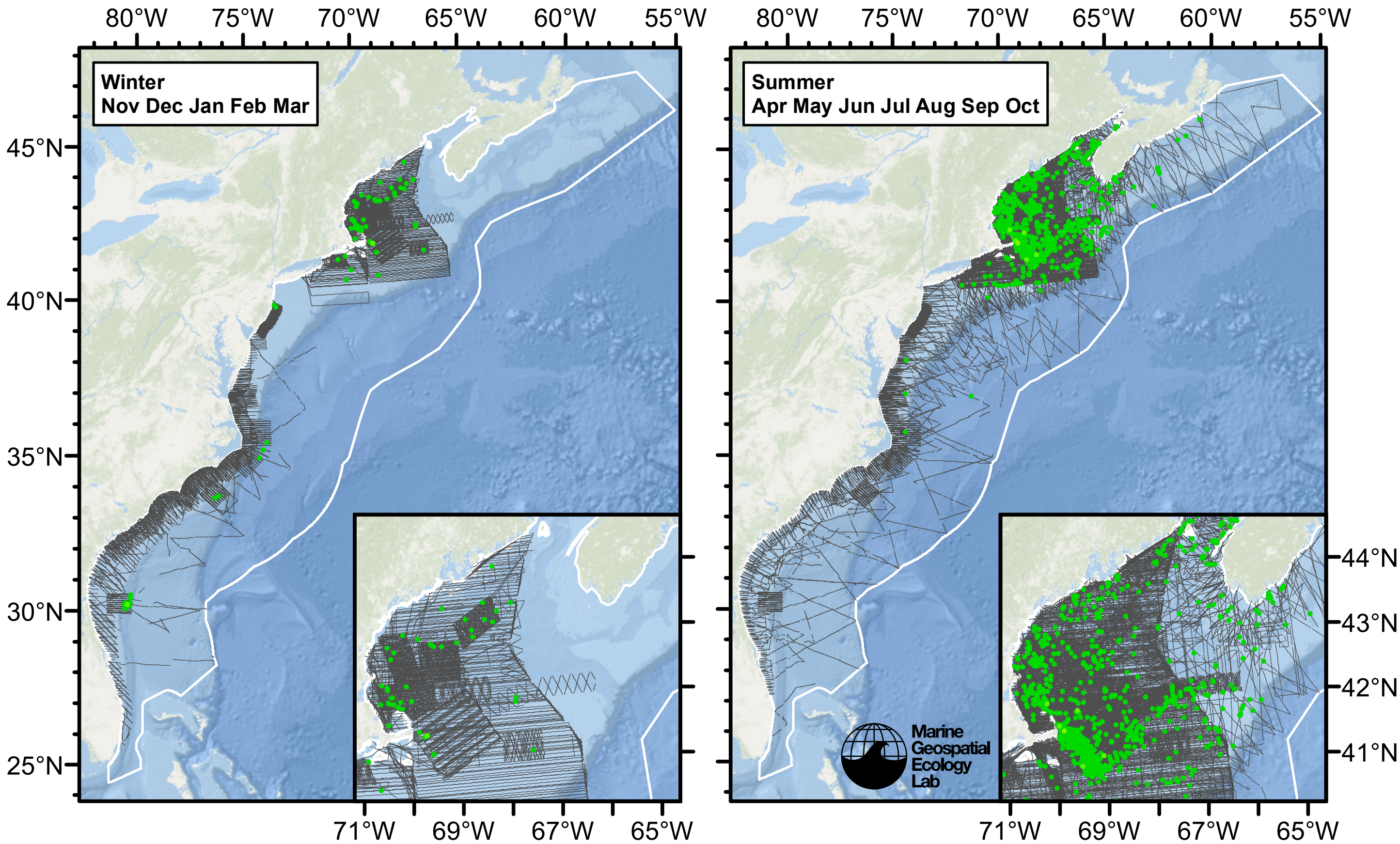

Figure 2: Minke whale sightings and survey tracklines, by season. Sighting colors are the same as the previous figure.

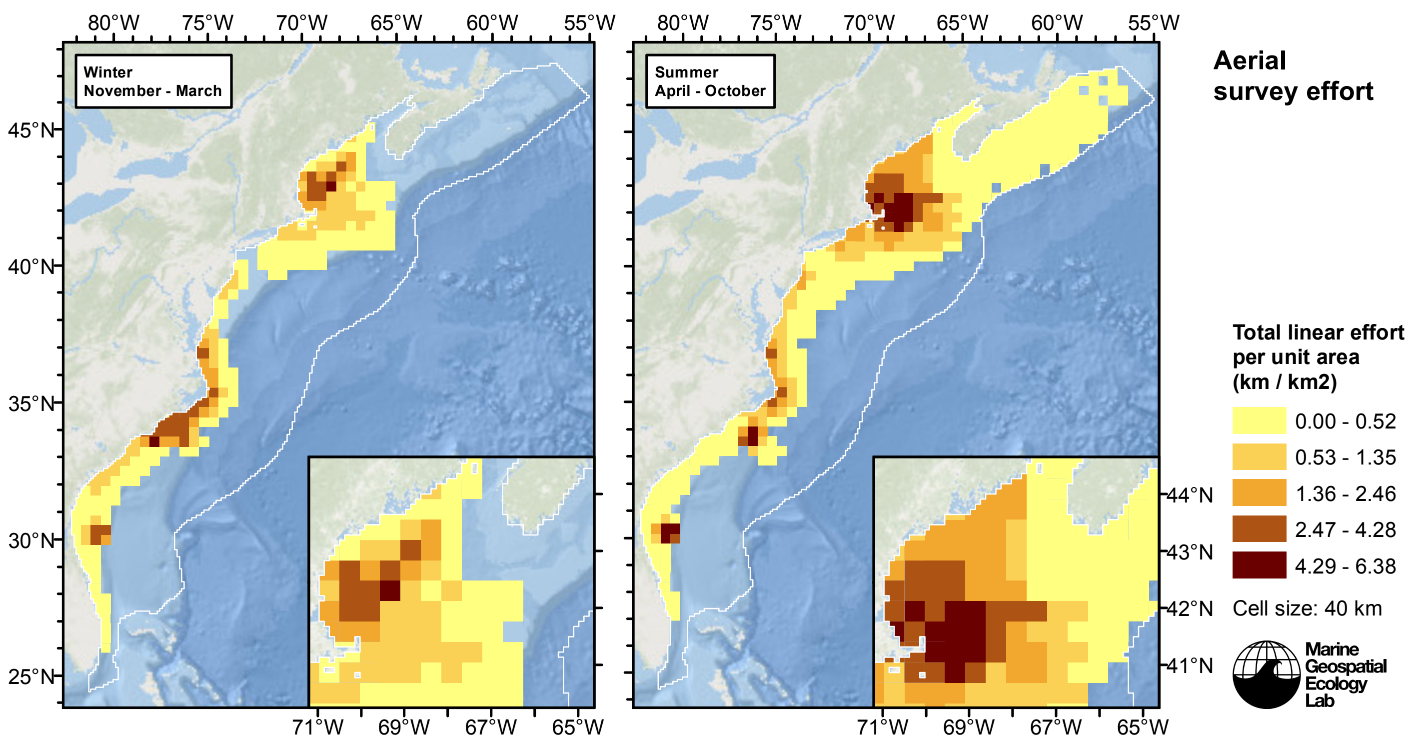

Figure 3: Aerial linear survey effort per unit area.

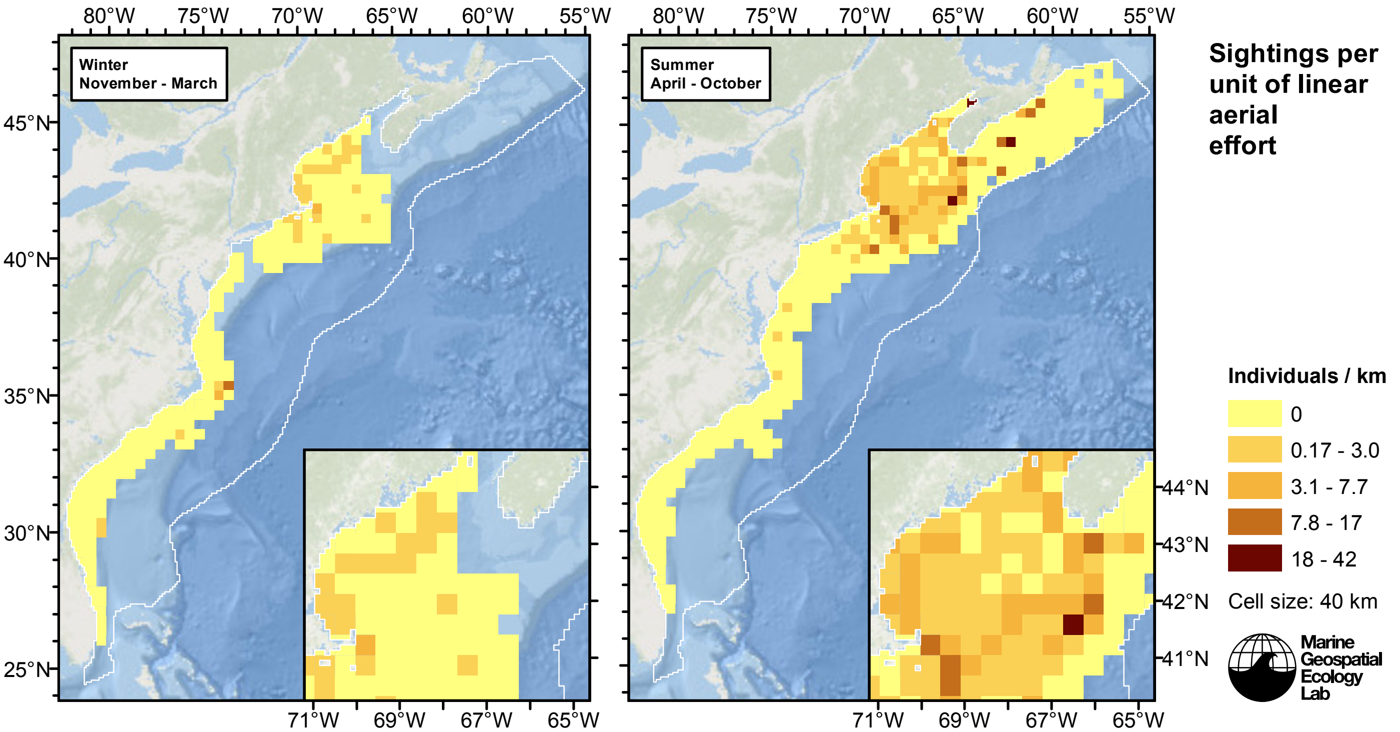

Figure 4: Minke whale sightings per unit aerial linear survey effort.

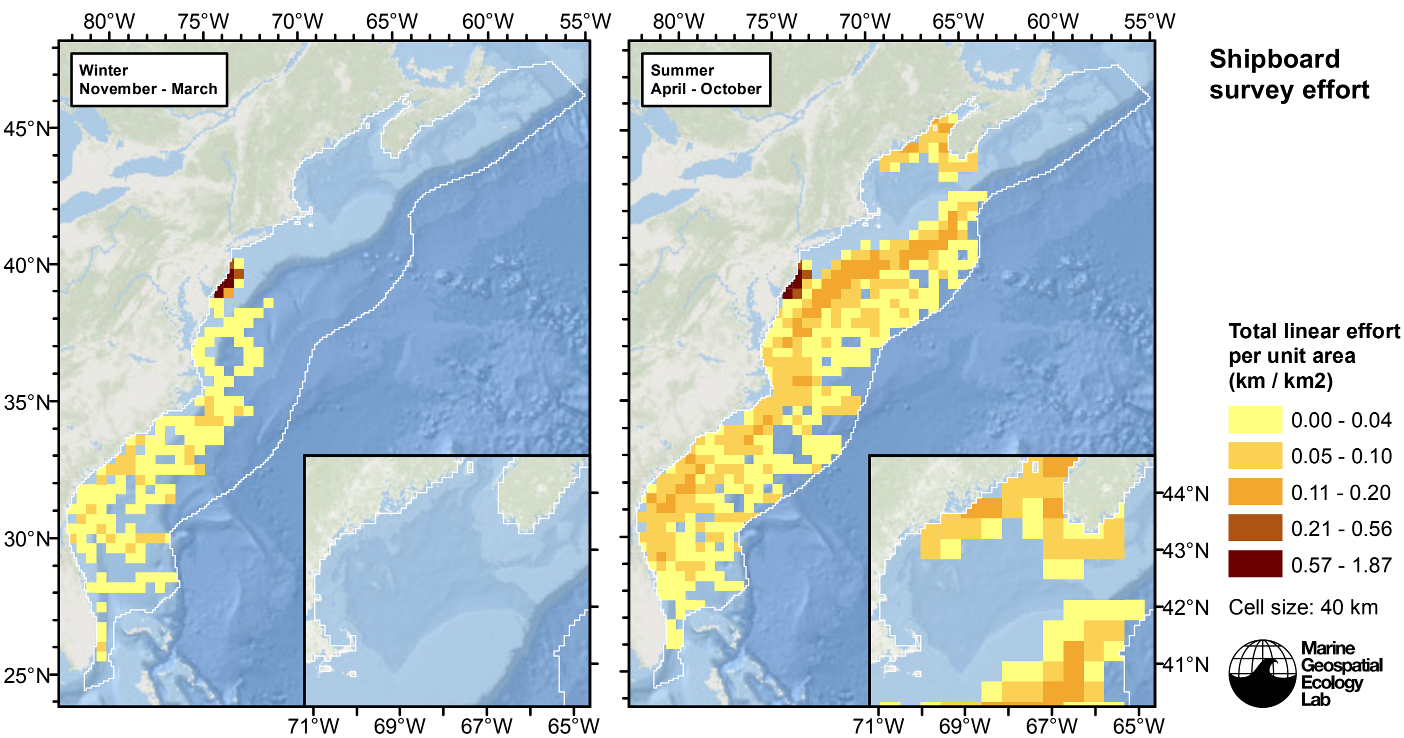

Figure 5: Shipboard linear survey effort per unit area.

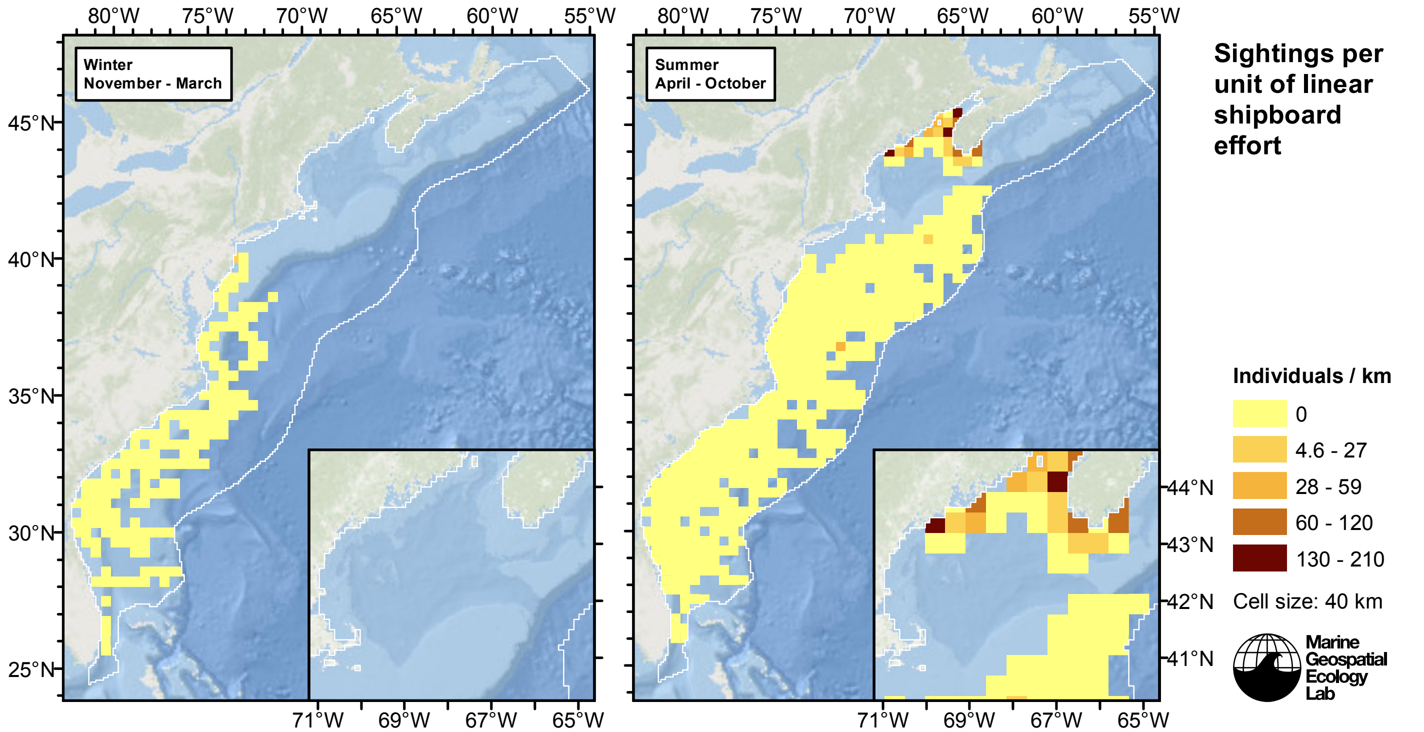

Figure 6: Minke whale sightings per unit shipboard linear survey effort.

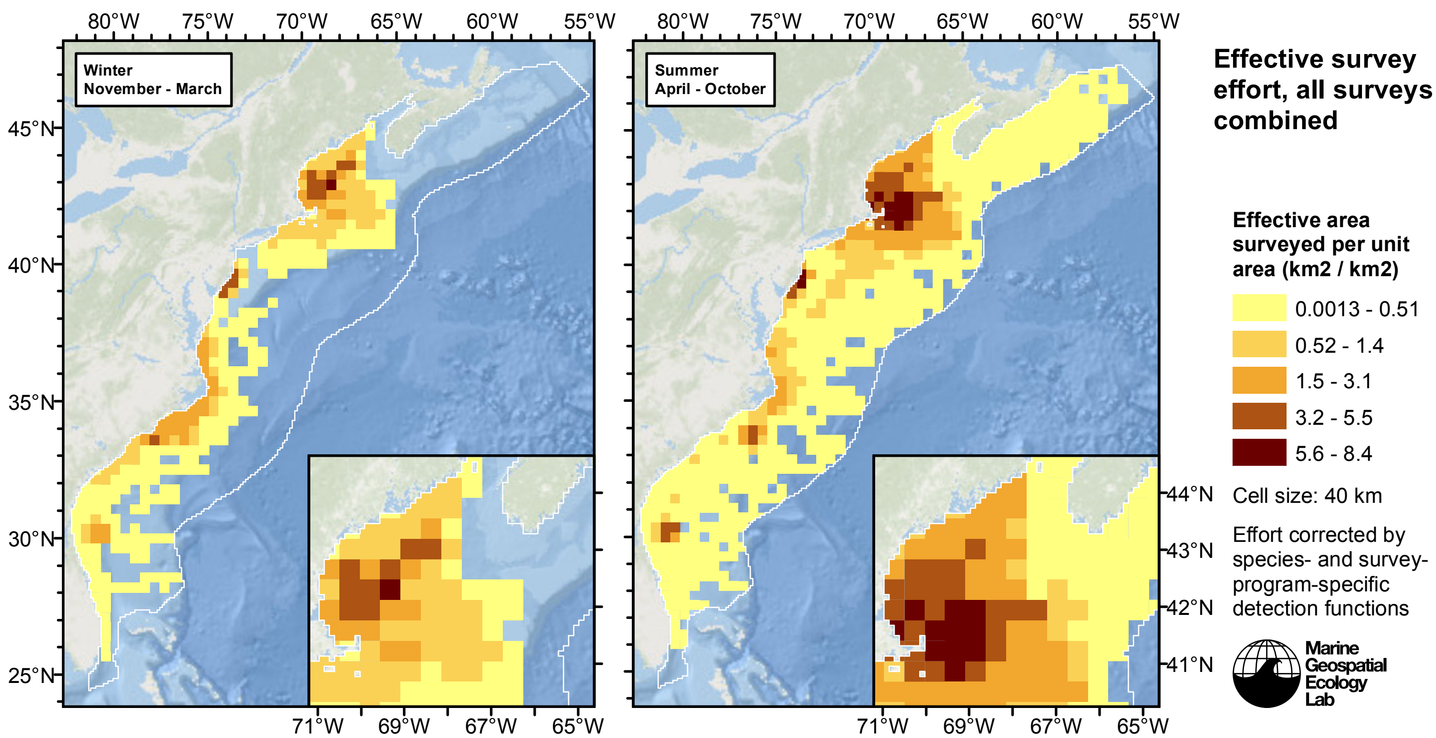

Figure 7: Effective survey effort per unit area, for all surveys combined. Here, effort is corrected by the species- and survey-program-specific detection functions used in fitting the density models.

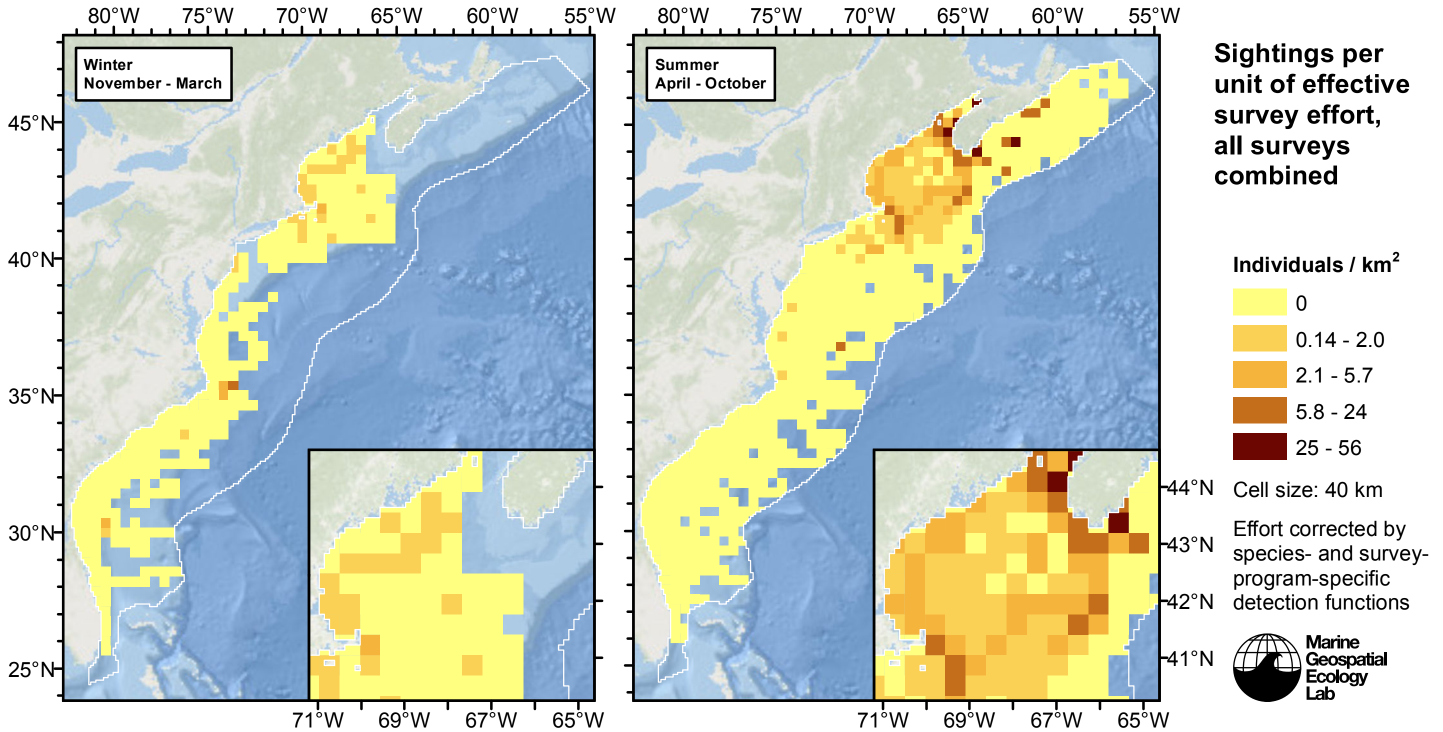

Figure 8: Minke whale sightings per unit of effective survey effort, for all surveys combined. Here, effort is corrected by the species- and survey-program-specific detection functions used in fitting the density models.

Detection Functions

The detection hierarchy figures below show how sightings from multiple surveys were pooled to try to achieve Buckland et. al's (2001) recommendation that at least 60-80 sightings be used to fit a detection function. Leaf nodes, on the right, usually represent individual surveys, while the hierarchy to the left shows how they have been grouped according to how similar we believed the surveys were to each other in their detection performance.

At each node, the red or green number indicates the total number of sightings below that node in the hierarchy, and is colored green if 70 or more sightings were available, and red otherwise. If a grouping node has zero sightings–i.e. all of the surveys within it had zero sightings–it may be collapsed and shown as a leaf to save space.

Each histogram in the figure indicates a node where a detection function was fitted. The actual detection functions do not appear in this figure; they are presented in subsequent sections. The histogram shows the frequency of sightings by perpendicular sighting distance for all surveys contained by that node. Each survey (leaf node) recieves the detection function that is closest to it up the hierarchy. Thus, for common species, sufficient sightings may be available to fit detection functions deep in the hierarchy, with each function applying to only a few surveys, thereby allowing variability in detection performance between surveys to be addressed relatively finely. For rare species, so few sightings may be available that we have to pool many surveys together to try to meet Buckland's recommendation, and fit only a few coarse detection functions high in the hierarchy.

A blue Proxy Species tag indicates that so few sightings were available that, rather than ascend higher in the hierarchy to a point that we would pool grossly-incompatible surveys together, (e.g. shipboard surveys that used big-eye binoculars with those that used only naked eyes) we pooled sightings of similar species together instead. The list of species pooled is given in following sections.

Shipboard Surveys

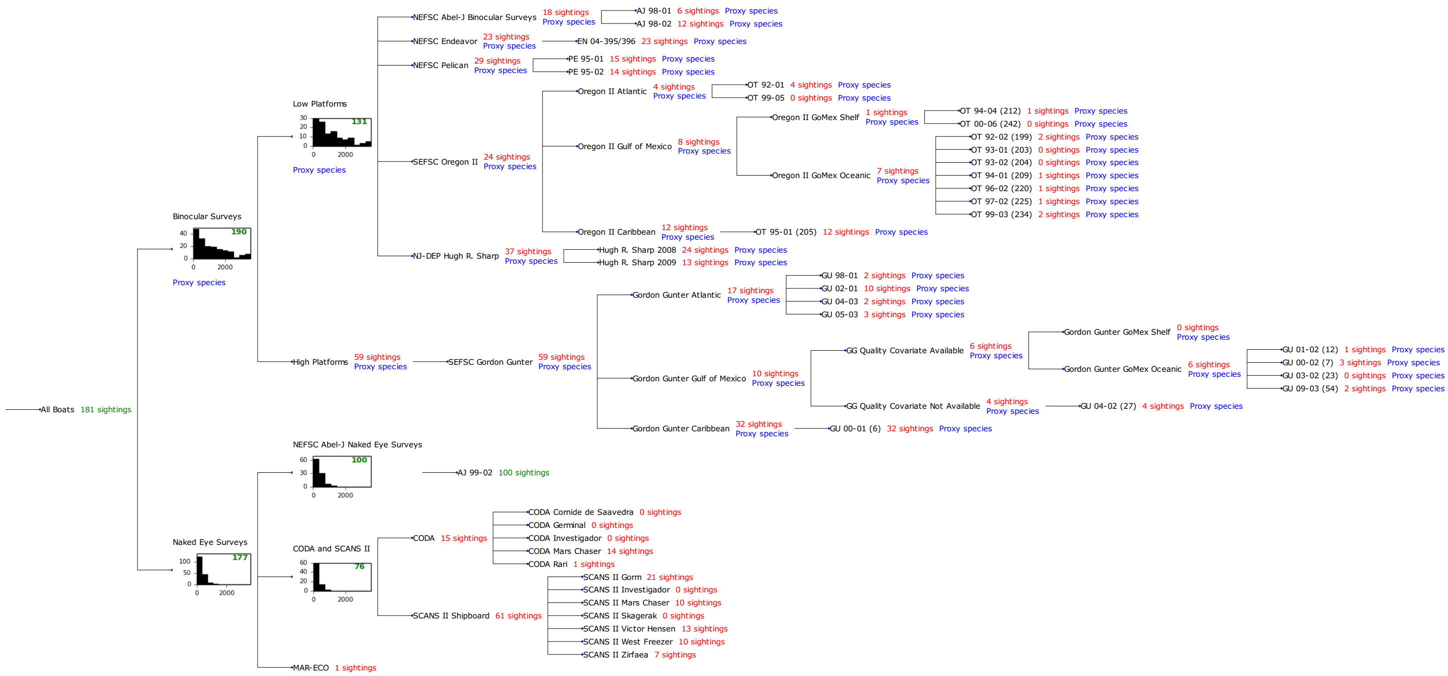

Figure 9: Detection hierarchy for shipboard surveys

Binocular Surveys

Because this taxon was sighted too infrequently to fit a detection function to its sightings alone, we fit a detection function to the pooled sightings of several other species that we believed would exhibit similar detectability. These "proxy species" are listed below.

Reported By Observer	Common Name	n
Balaenoptera	Balaenopterid sp.	8
Balaenoptera acutorostrata	Minke whale	4
Balaenoptera borealis	Sei whale	4
Balaenoptera borealis/edeni	Sei or Bryde's whale	6
Balaenoptera borealis/physalus	Fin or Sei whale	0
Balaenoptera edeni	Bryde's whale	21
Balaenoptera musculus	Blue whale	0
Balaenoptera physalus	Fin whale	98
Eubalaena glacialis	North Atlantic right whale	4
Eubalaena glacialis/Megaptera novaeangliae	Right or humpback whale	0
Megaptera novaeangliae	Humpback whale	46
Total		191

Table 4: Proxy species used to fit detection functions for Binocular Surveys. The number of sightings, n, is before truncation.

The sightings were right truncated at 5500m.

Covariate	Description
beaufort	Beaufort sea state.
size	Estimated size (number of individuals) of the sighted group.
vessel	Vessel from which the observation was made. This covariate allows the detection function to account for vessel-specific biases, such as the height of the survey platform.

Table 5: Covariates tested in candidate “multi-covariate distance sampling” (MCDS) detection functions.

Key	Adjustment	Order	Covariates	Succeeded	Δ AIC	Mean ESHW (m)
hr	poly	4		Yes	0.00	1354
hr			size	Yes	0.31	1757
hr				Yes	0.33	1542
hn	cos	2		Yes	1.52	1802
hr			beaufort, size	Yes	2.17	1780
hr			beaufort	Yes	2.24	1553
hr	poly	2		Yes	2.33	1542
hr			vessel, size	Yes	5.84	1920
hr			vessel	Yes	6.42	1605
hr			beaufort, vessel, size	Yes	7.56	1952
hr			beaufort, vessel	Yes	8.03	1675
hn	cos	3		Yes	9.44	1787
hn			size	Yes	11.39	2317
hn			beaufort, size	Yes	13.21	2319
hn			vessel, size	Yes	14.82	2298
hn			vessel	Yes	17.10	2301
hn				Yes	17.13	2311
hn			beaufort	Yes	18.72	2311
hn	herm	4		Yes	18.78	2306
hn			beaufort, vessel	No		
hn			beaufort, vessel, size	No		

Table 6: Candidate detection functions for Binocular Surveys. The first one listed was selected for the density model.

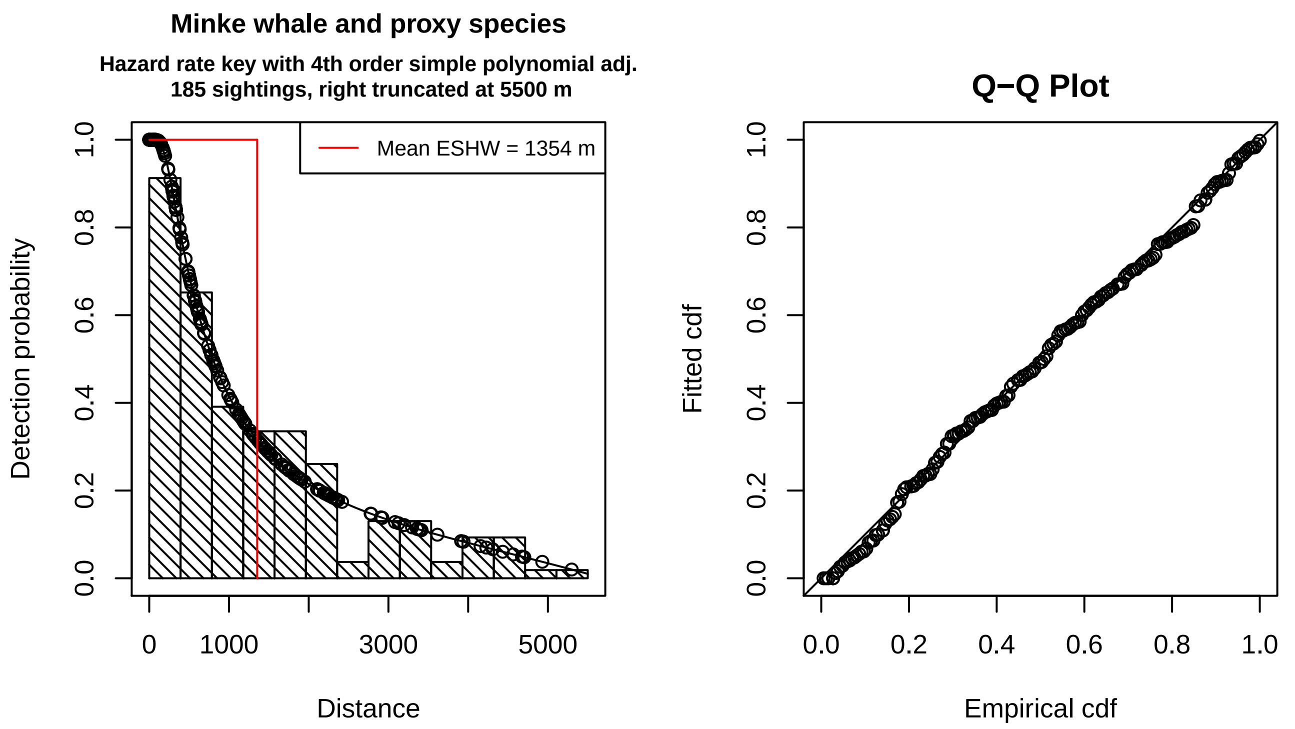

Figure 10: Detection function for Binocular Surveys that was selected for the density model

Statistical output for this detection function:

```
Summary for ds object
Number of observations :  185
Distance range         :  0  -  5500
AIC                    :  3030.414

Detection function:
 Hazard-rate key function with simple polynomial adjustment term of order 4

Detection function parameters
Scale Coefficients:
            estimate        se
(Intercept) 6.355815 0.3367864

Shape parameters:
             estimate        se
(Intercept) 0.1193933 0.1815256

Adjustment term parameter(s):
                estimate        se
poly, order 4 -0.8663169 0.2837938


Monotonicity constraints were enforced.
                       Estimate           SE         CV
Average p             0.2460911   0.03962055 0.1609995
N in covered region 751.7541457 130.19901860 0.1731936

Monotonicity constraints were enforced.
```

Additional diagnostic plots:

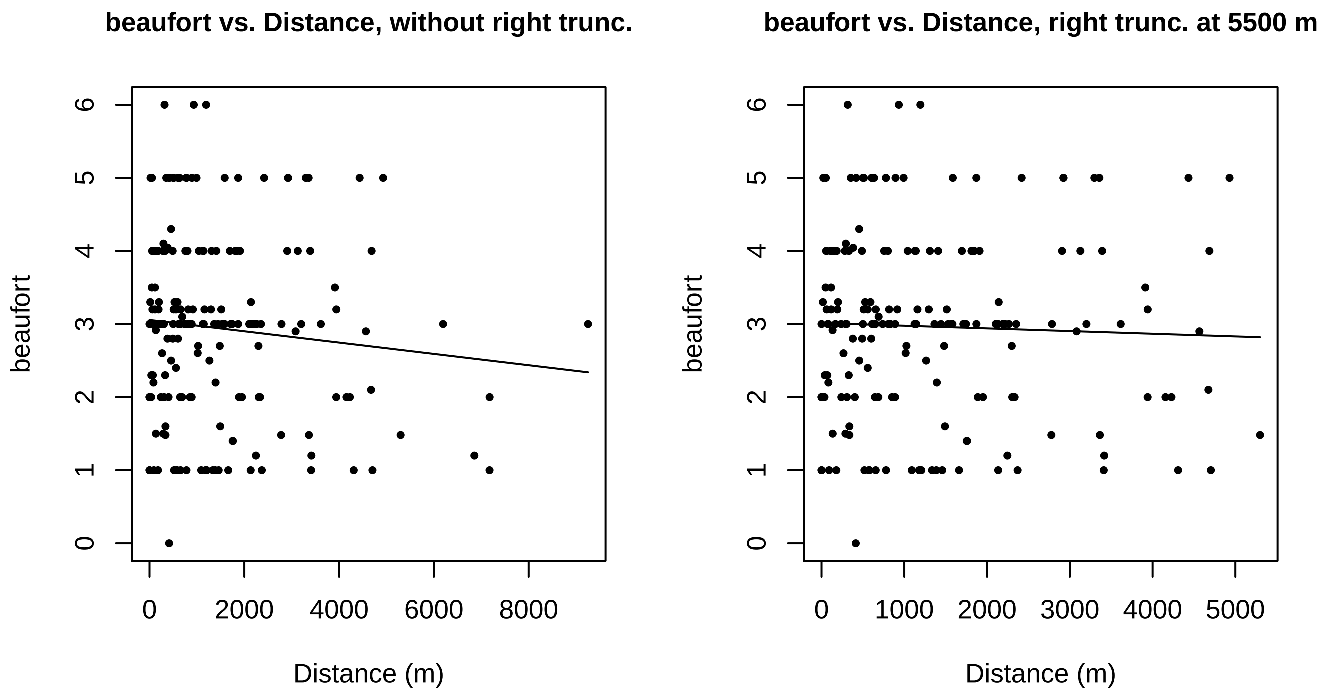

Figure 11: Scatterplots showing the relationship between Beaufort sea state and perpendicular sighting distance, for all sightings (left) and only those not right truncated (right). The line is a simple linear regression.

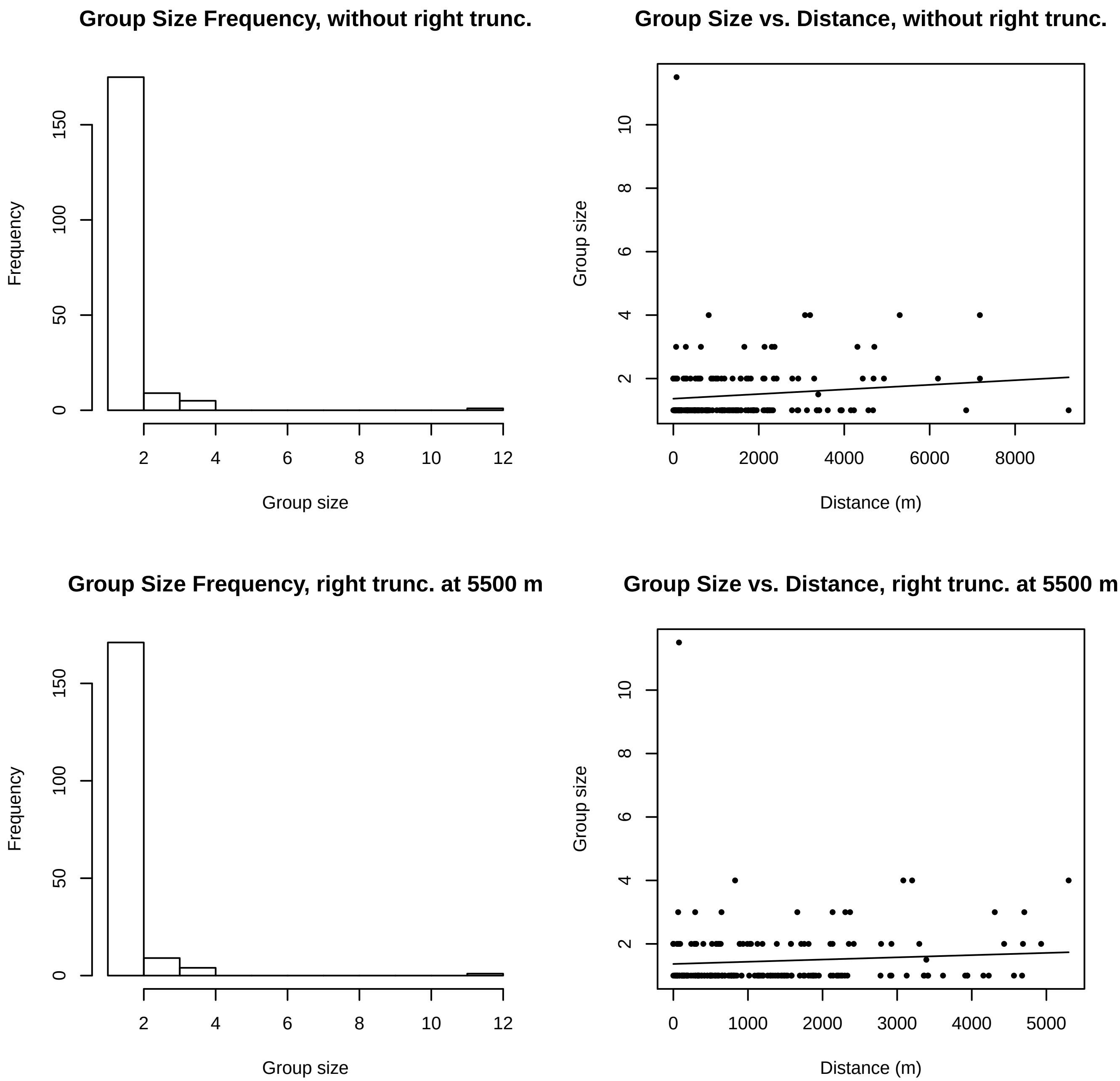

Figure 12: Histograms showing group size frequency and scatterplots showing the relationship between group size and perpendicular sighting distance, for all sightings (top row) and only those not right truncated (bottom row). In the scatterplot, the line is a simple linear regression.

Low Platforms

Because this taxon was sighted too infrequently to fit a detection function to its sightings alone, we fit a detection function to the pooled sightings of several other species that we believed would exhibit similar detectability. These "proxy species" are listed below.

Reported By Observer	Common Name	n
Balaenoptera	Balaenopterid sp.	1
Balaenoptera acutorostrata	Minke whale	3

Balaenoptera borealis	Sei whale	4
Balaenoptera borealis/edeni	Sei or Bryde's whale	5
Balaenoptera borealis/physalus	Fin or Sei whale	0
Balaenoptera edeni	Bryde's whale	7
Balaenoptera musculus	Blue whale	0
Balaenoptera physalus	Fin whale	86
Eubalaena glacialis	North Atlantic right whale	3
Eubalaena glacialis/Megaptera novaeangliae	Right or humpback whale	0
Megaptera novaeangliae	Humpback whale	23
Total		132

Table 7: Proxy species used to fit detection functions for Low Platforms. The number of sightings, n, is before truncation.

The sightings were right truncated at 5500m.

Covariate	Description
beaufort	Beaufort sea state.
size	Estimated size (number of individuals) of the sighted group.
vessel	Vessel from which the observation was made. This covariate allows the detection function to account for vessel-specific biases, such as the height of the survey platform.

Table 8: Covariates tested in candidate “multi-covariate distance sampling” (MCDS) detection functions.

Key	Adjustment	Order	Covariates	Succeeded	Δ AIC	Mean ESHW (m)
hr			size	Yes	0.00	1851
hn	cos	2		Yes	1.87	1764
hr				Yes	1.95	1652
hr			beaufort, size	Yes	1.99	1858
hr			vessel, size	Yes	2.55	2107
hr	poly	4		Yes	3.84	1634
hr	poly	2		Yes	3.89	1634
hr			beaufort, vessel, size	Yes	4.48	2116
hr			vessel	Yes	5.62	1830
hn			size	Yes	6.78	2311
hr			beaufort, vessel	Yes	7.51	1860
hn			vessel, size	Yes	8.30	2288
hn			beaufort, size	Yes	8.64	2312
hn	cos	3		Yes	11.49	1819

hn			vessel	Yes	13.80	2330
hn				Yes	15.66	2345
hn			beaufort	Yes	17.02	2343
hn	herm	4		Yes	17.38	2339
hr			beaufort	No		
hn			beaufort, vessel	No		
hn			beaufort, vessel, size	No		

Table 9: Candidate detection functions for Low Platforms. The first one listed was selected for the density model.

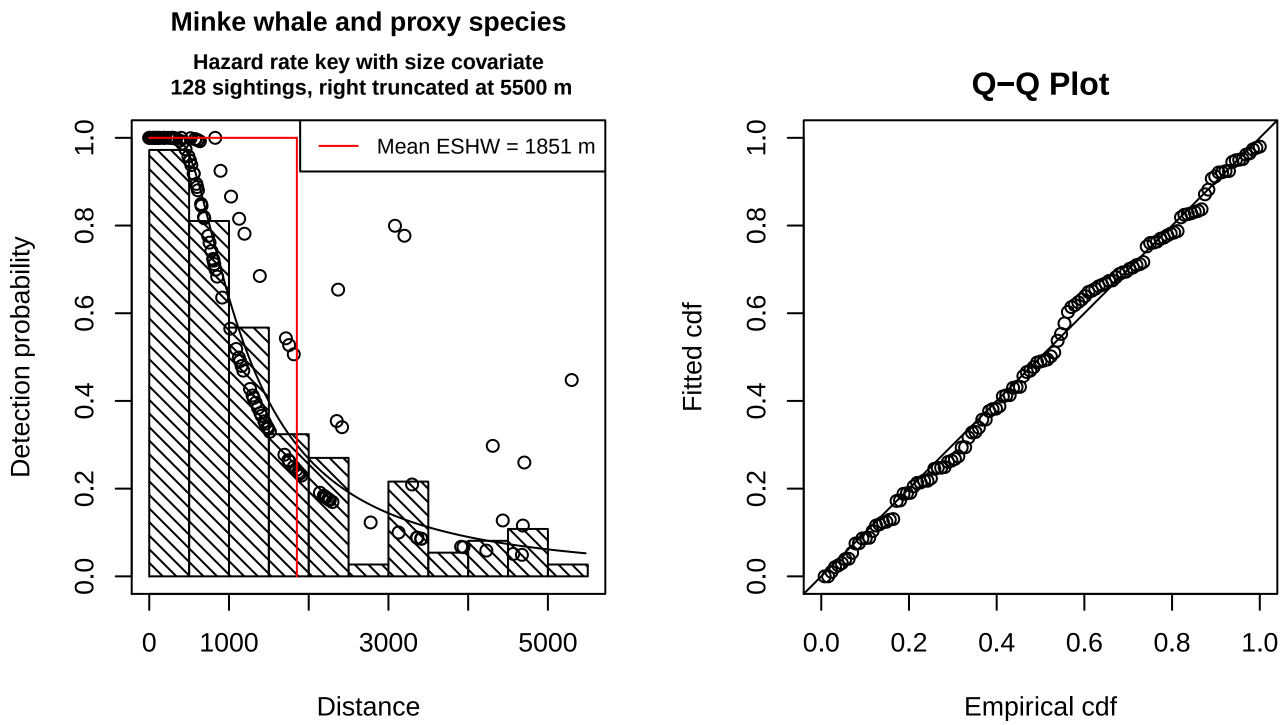

Figure 13: Detection function for Low Platforms that was selected for the density model

Statistical output for this detection function:

```
Summary for ds object
Number of observations :  128
Distance range         :  0  -  5500
AIC                    :  2096.769

Detection function:
 Hazard-rate key function

Detection function parameters
Scale Coefficients:
             estimate       se
(Intercept) 6.3349147 0.371540
size        0.4891423 0.206231
```

```
Shape parameters:
             estimate        se
(Intercept) 0.6088181 0.1772601

                        Estimate          SE        CV
Average p              0.3143138  0.03980726 0.1266481
N in covered region 407.2363117 59.81062771 0.1468696
```

Additional diagnostic plots:

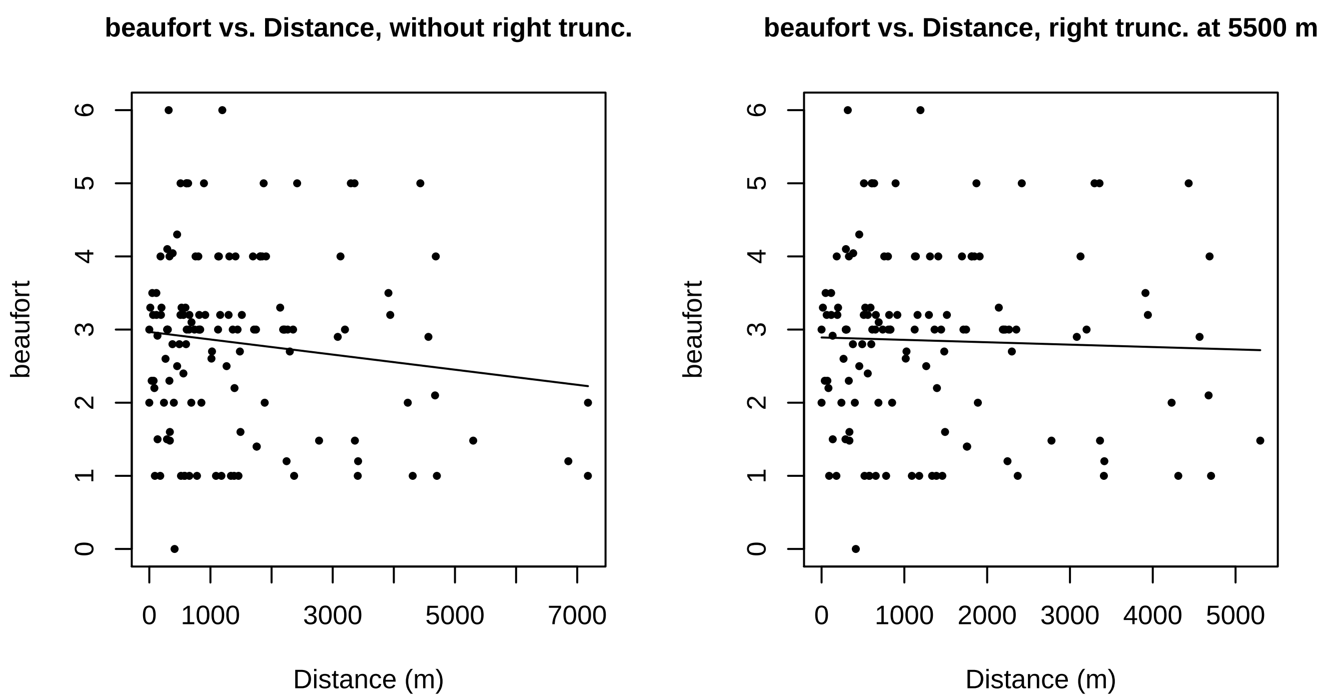

Figure 14: Scatterplots showing the relationship between Beaufort sea state and perpendicular sighting distance, for all sightings (left) and only those not right truncated (right). The line is a simple linear regression.

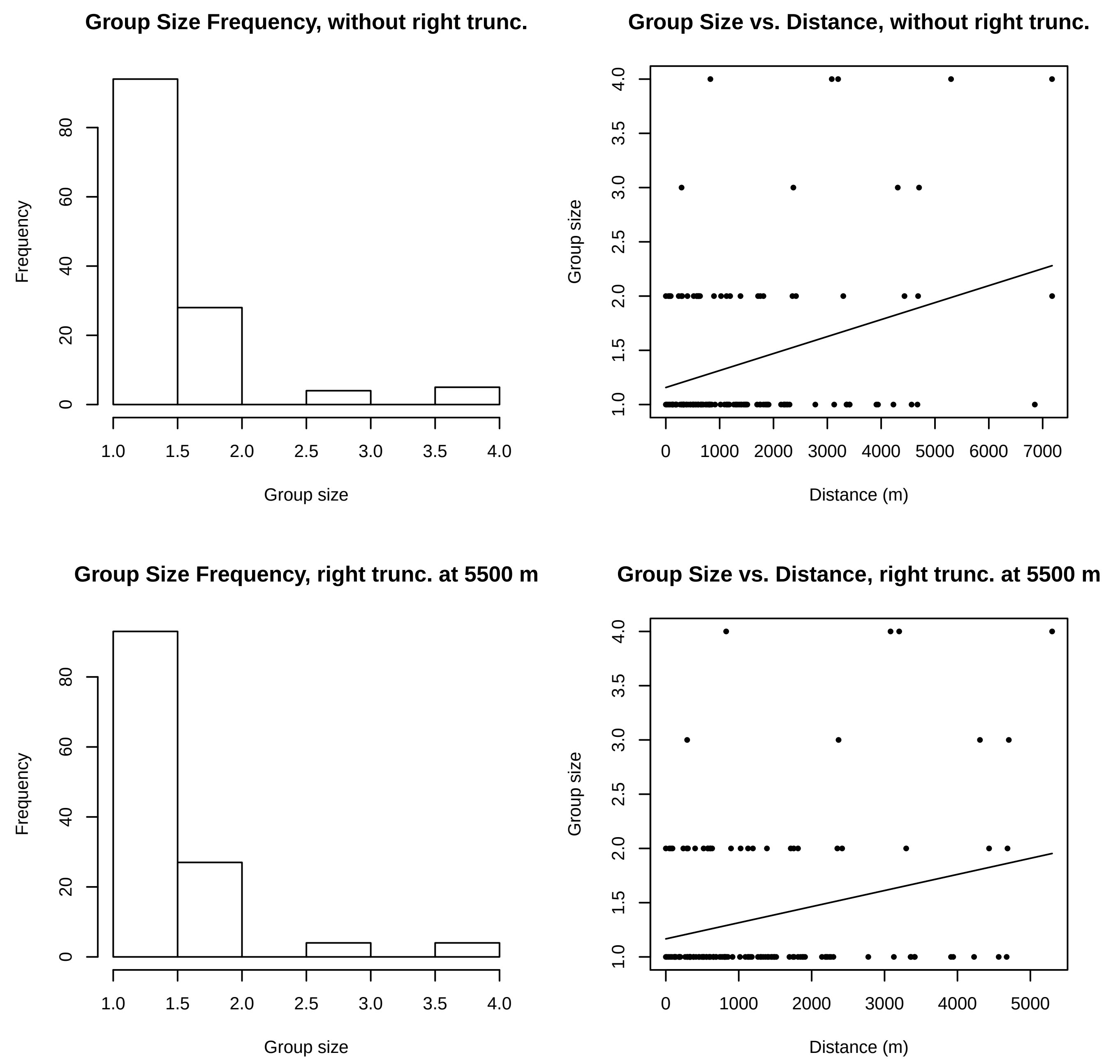

Figure 15: Histograms showing group size frequency and scatterplots showing the relationship between group size and perpendicular sighting distance, for all sightings (top row) and only those not right truncated (bottom row). In the scatterplot, the line is a simple linear regression.

Naked Eye Surveys

The sightings were right truncated at 1000m.

Covariate	Description
beaufort	Beaufort sea state.
size	Estimated size (number of individuals) of the sighted group.

Table 10: Covariates tested in candidate "multi-covariate distance sampling" (MCDS) detection functions.

Key	Adjustment	Order	Covariates	Succeeded	Δ AIC	Mean ESHW (m)
hn	cos	3		Yes	0.00	356
hn	cos	2		Yes	0.04	377
hr			beaufort	Yes	0.23	395
hr	poly	4		Yes	0.24	376
hr	poly	2		Yes	0.93	372
hr				Yes	1.13	386
hr			beaufort, size	Yes	2.22	395
hr			size	Yes	2.94	385
hn				Yes	2.97	441
hn			beaufort	Yes	3.59	442
hn	herm	4		Yes	4.83	439
hn			size	No		
hn			beaufort, size	No		

Table 11: Candidate detection functions for Naked Eye Surveys. The first one listed was selected for the density model.

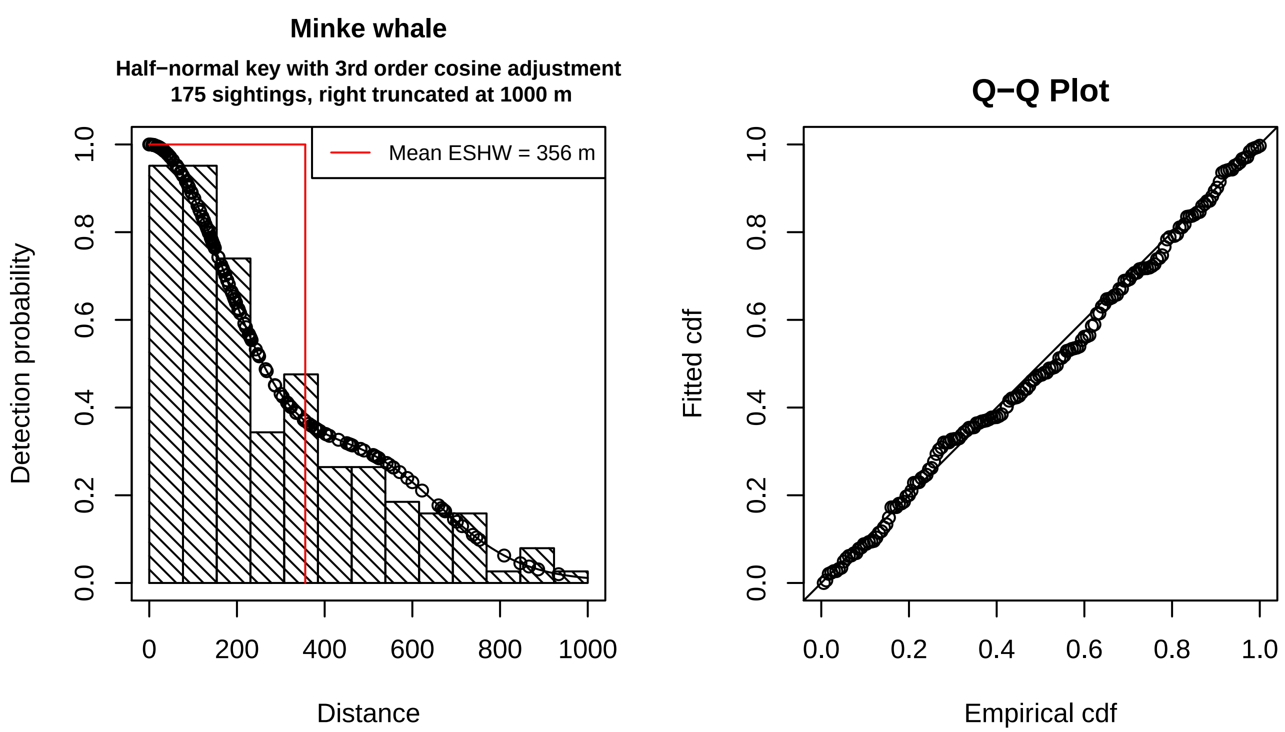

Figure 16: Detection function for Naked Eye Surveys that was selected for the density model

Statistical output for this detection function:

```
Summary for ds object
```

```
Number of observations :  175
Distance range         :  0  -  1000
AIC                    :  2297.655

Detection function:
 Half-normal key function with cosine adjustment term of order 3

Detection function parameters
Scale Coefficients:
            estimate         se
(Intercept) 5.870882 0.05476318

Adjustment term parameter(s):
              estimate        se
cos, order 3 0.2448755 0.1079304


Monotonicity constraints were enforced.
                       Estimate          SE         CV
Average p             0.3557862  0.03483433 0.09790805
N in covered region 491.8684419 56.65506177 0.11518336

Monotonicity constraints were enforced.
```

Additional diagnostic plots:

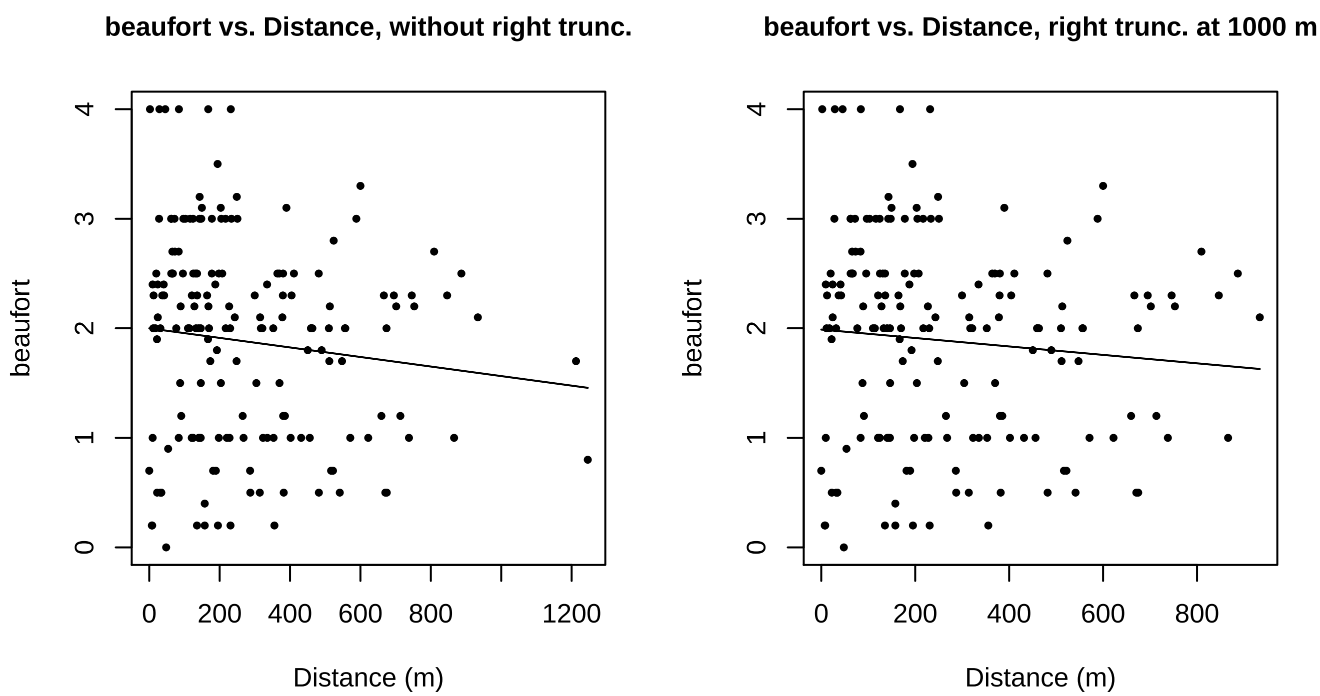

Figure 17: Scatterplots showing the relationship between Beaufort sea state and perpendicular sighting distance, for all sightings (left) and only those not right truncated (right). The line is a simple linear regression.

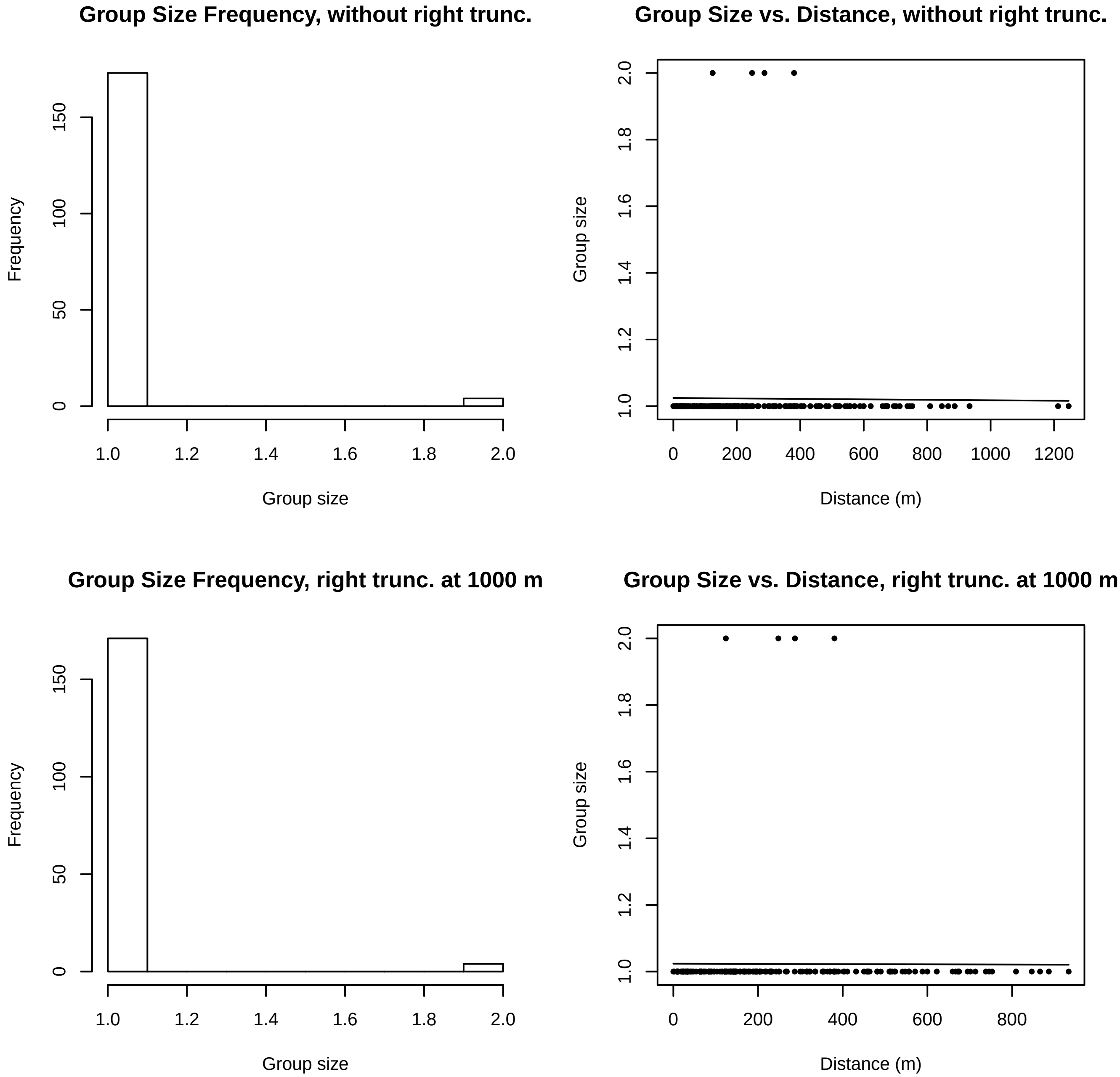

Figure 18: Histograms showing group size frequency and scatterplots showing the relationship between group size and perpendicular sighting distance, for all sightings (top row) and only those not right truncated (bottom row). In the scatterplot, the line is a simple linear regression.

NEFSC Abel-J Naked Eye Surveys

The sightings were right truncated at 1000m.

Covariate	Description
beaufort	Beaufort sea state.
quality	Survey-specific index of the quality of observation conditions, utilizing relevant factors other than Beaufort sea state (see methods).
size	Estimated size (number of individuals) of the sighted group.

Table 12: Covariates tested in candidate "multi-covariate distance sampling" (MCDS) detection functions.

Key	Adjustment	Order	Covariates	Succeeded	Δ AIC	Mean ESHW (m)
hn				Yes	0.00	500
hn	cos	3		Yes	1.29	445
hn	cos	2		Yes	1.48	462
hn	herm	4		Yes	1.98	499
hr				Yes	2.63	482
hr	poly	4		Yes	2.70	473
hr	poly	2		Yes	3.00	468
hr			size	Yes	4.52	478
hr			beaufort	No		
hn			beaufort	No		
hr			quality	No		
hn			quality	No		
hn			size	No		
hr			beaufort, quality	No		
hn			beaufort, quality	No		
hr			beaufort, size	No		
hn			beaufort, size	No		
hr			quality, size	No		
hn			quality, size	No		
hr			beaufort, quality, size	No		
hn			beaufort, quality, size	No		

Table 13: Candidate detection functions for NEFSC Abel-J Naked Eye Surveys. The first one listed was selected for the density model.

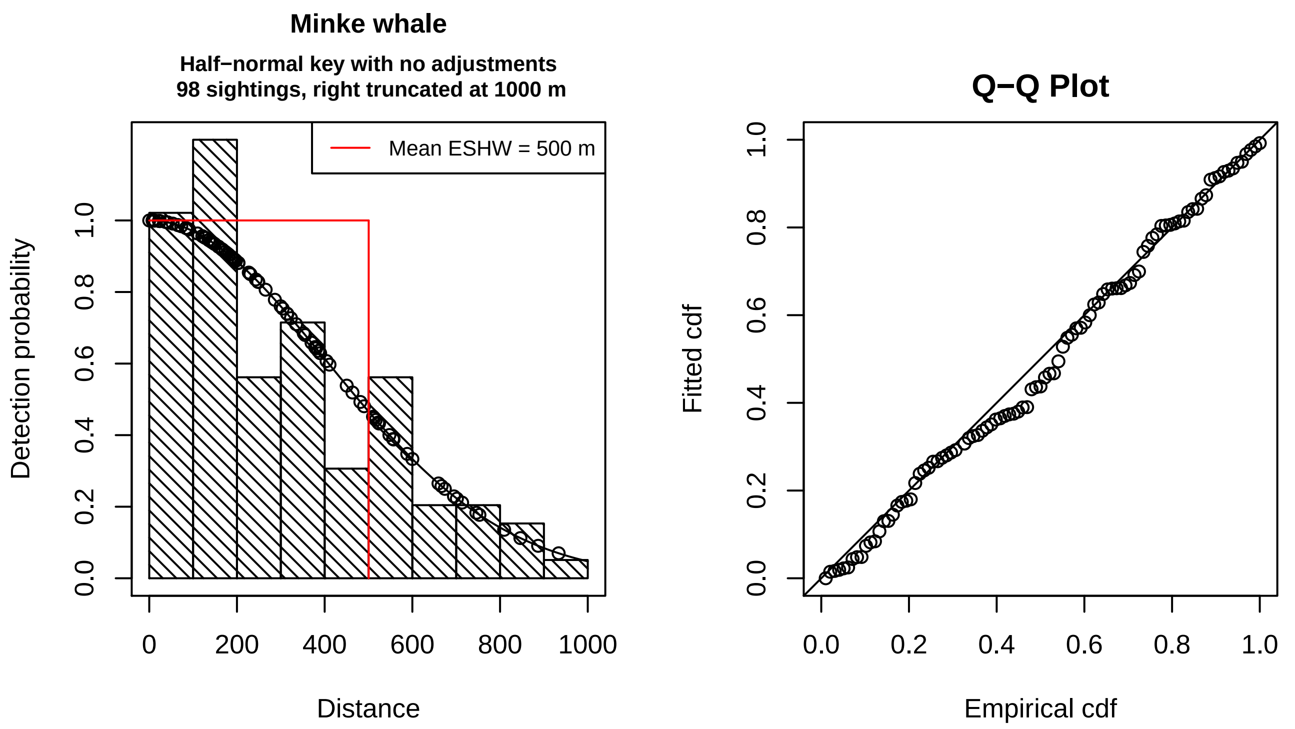

Figure 19: Detection function for NEFSC Abel-J Naked Eye Surveys that was selected for the density model

Statistical output for this detection function:

```
Summary for ds object
Number of observations :  98
Distance range         :  0  -  1000
AIC                    :  1308.981

Detection function:
 Half-normal key function

Detection function parameters
Scale Coefficients:
            estimate         se
(Intercept) 6.003282 0.08605204

                      Estimate          SE         CV
Average p             0.500439  0.03899114 0.07791387
N in covered region 195.828050 20.69498703 0.10567938
```

Additional diagnostic plots:

Figure 20: Scatterplots showing the relationship between Beaufort sea state and perpendicular sighting distance, for all sightings (left) and only those not right truncated (right). The line is a simple linear regression.

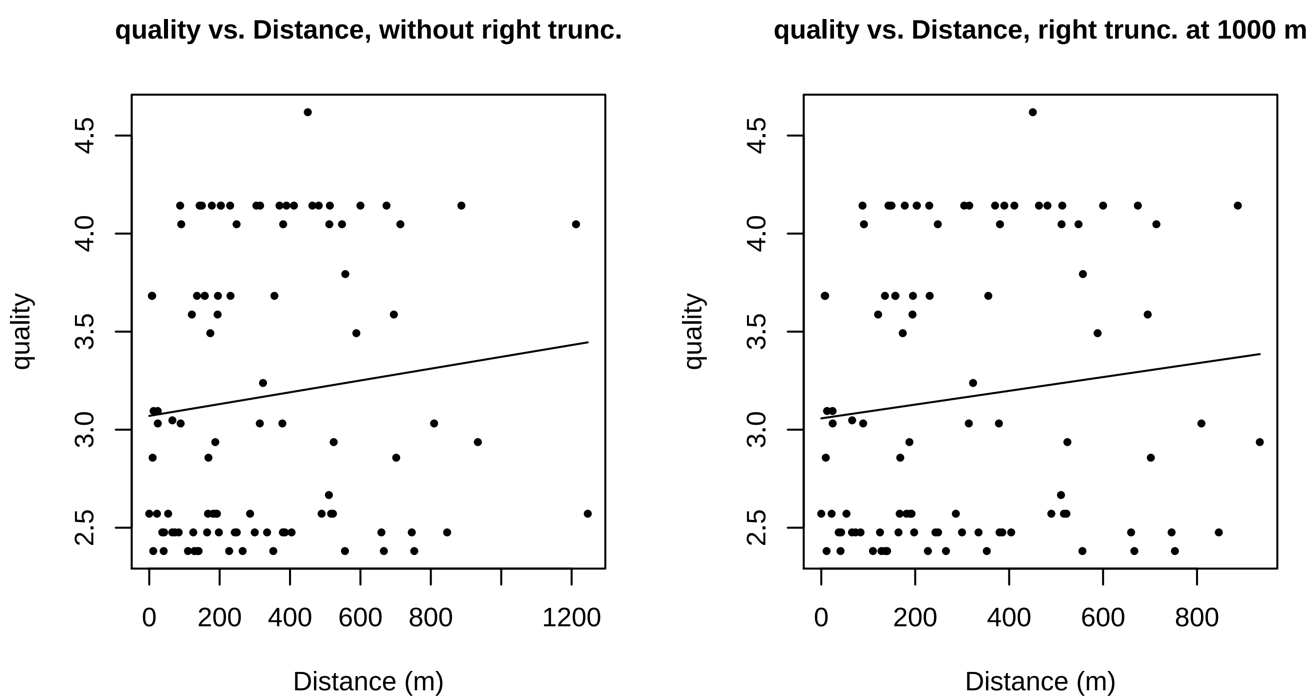

Figure 21: Scatterplots showing the relationship between the survey-specific index of the quality of observation conditions and perpendicular sighting distance, for all sightings (left) and only those not right truncated (right). Low values of the quality index correspond to better observation conditions. The line is a simple linear regression.

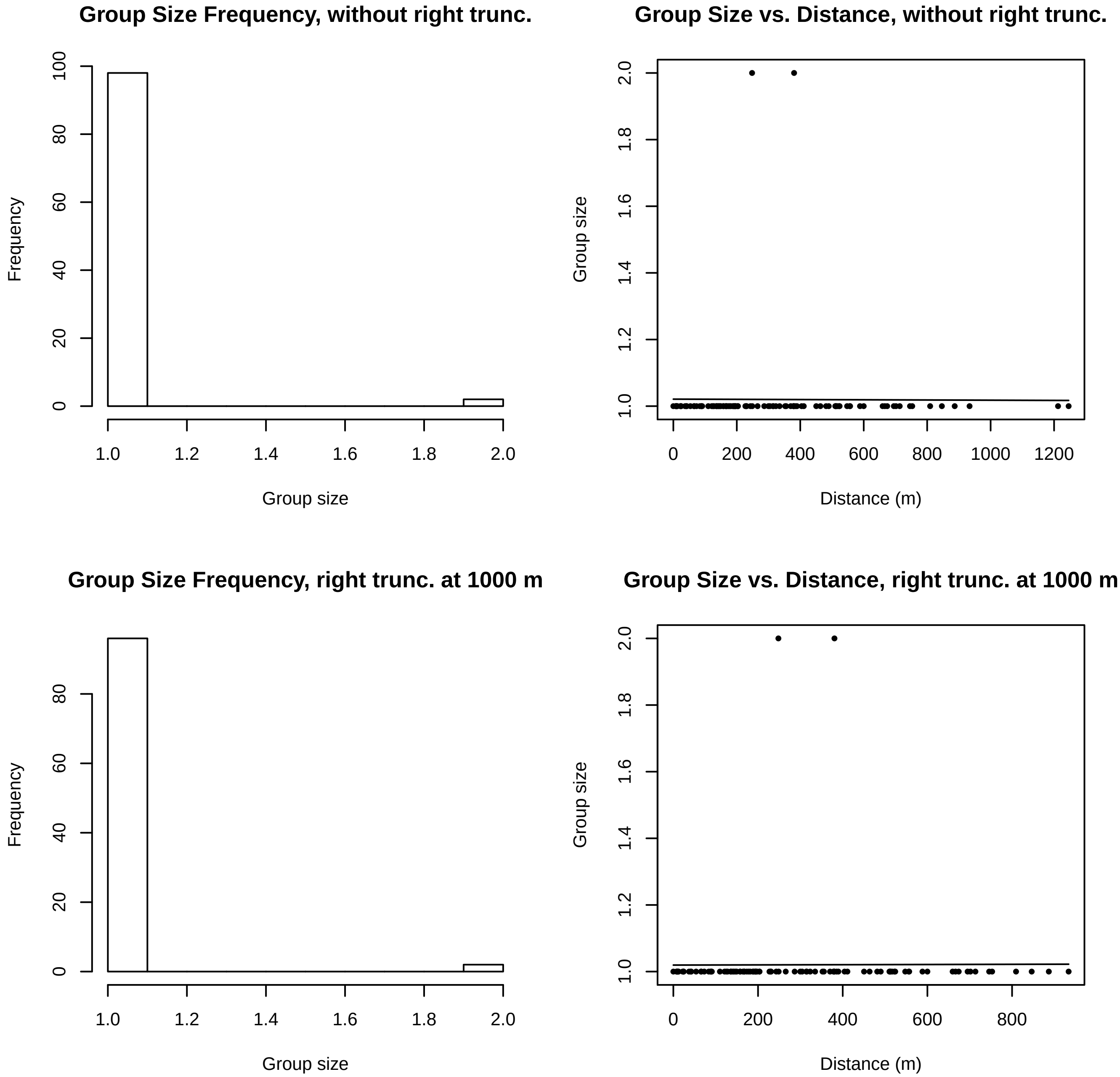

Figure 22: Histograms showing group size frequency and scatterplots showing the relationship between group size and perpendicular sighting distance, for all sightings (top row) and only those not right truncated (bottom row). In the scatterplot, the line is a simple linear regression.

CODA and SCANS II

The sightings were right truncated at 1000m.

Covariate	Description
beaufort	Beaufort sea state.
quality	Survey-specific index of the quality of observation conditions, utilizing relevant factors other than Beaufort sea state (see methods).
size	Estimated size (number of individuals) of the sighted group.

Table 14: Covariates tested in candidate “multi-covariate distance sampling” (MCDS) detection functions.

Key	Adjustment	Order	Covariates	Succeeded	Δ AIC	Mean ESHW (m)
hn			quality	Yes	0.00	341
hn			beaufort, quality	Yes	2.00	341
hn			beaufort	Yes	3.99	347
hr			quality	Yes	4.97	499
hr			beaufort	Yes	11.21	403
hr				Yes	18.69	297
hn	cos	3		Yes	18.79	266
hn	cos	2		Yes	19.59	301
hr	poly	4		Yes	19.76	293
hr	poly	2		Yes	20.16	290
hr			size	Yes	20.64	296
hn				Yes	22.73	361
hn	herm	4		Yes	24.65	361
hn			size	No		
hr			beaufort, quality	No		
hr			beaufort, size	No		
hn			beaufort, size	No		
hr			quality, size	No		
hn			quality, size	No		
hr			beaufort, quality, size	No		
hn			beaufort, quality, size	No		

Table 15: Candidate detection functions for CODA and SCANS II. The first one listed was selected for the density model.

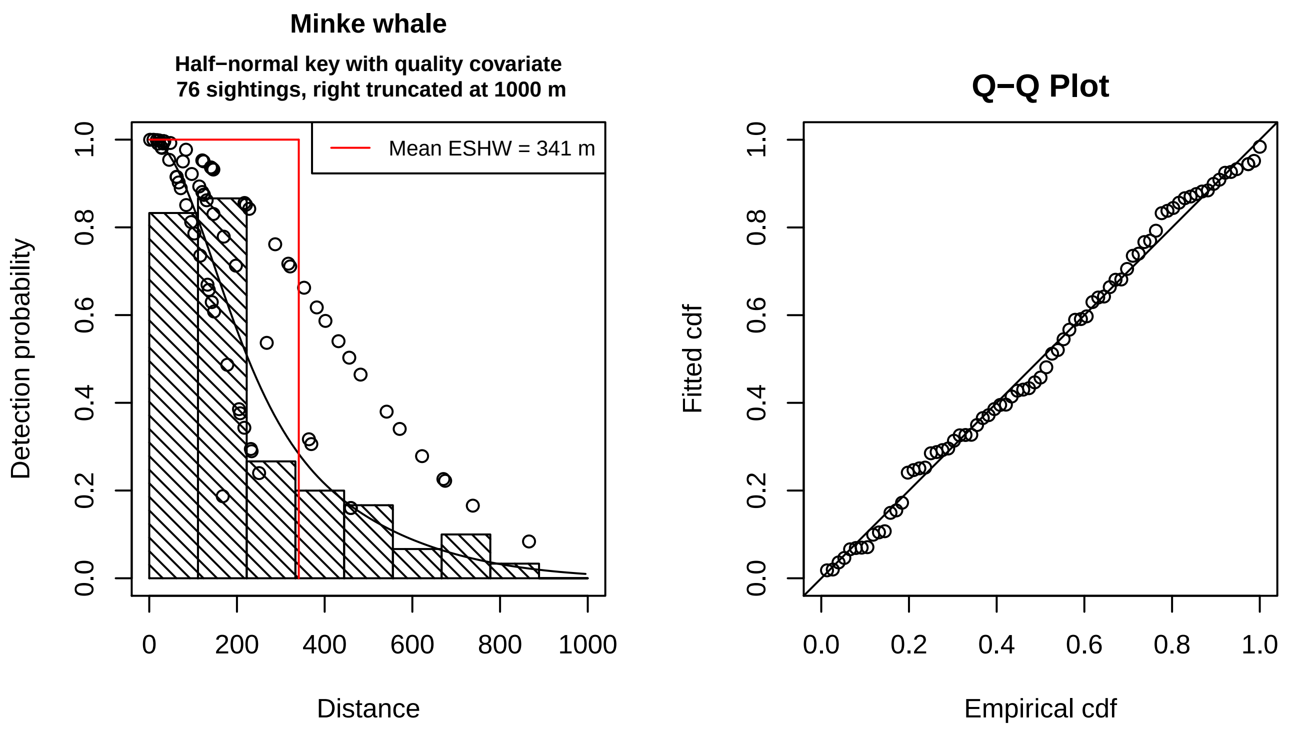

Figure 23: Detection function for CODA and SCANS II that was selected for the density model

Statistical output for this detection function:

```
Summary for ds object
Number of observations :  76
Distance range         :  0  -  1000
AIC                    :  949.968

Detection function:
 Half-normal key function

Detection function parameters
Scale Coefficients:
              estimate         se
(Intercept)  5.9637668 0.13121730
quality     -0.2894483 0.06248953

                        Estimate          SE        CV
Average p              0.2812759  0.03437786 0.1222212
N in covered region 270.1973721 42.87609404 0.1586843
```

Additional diagnostic plots:

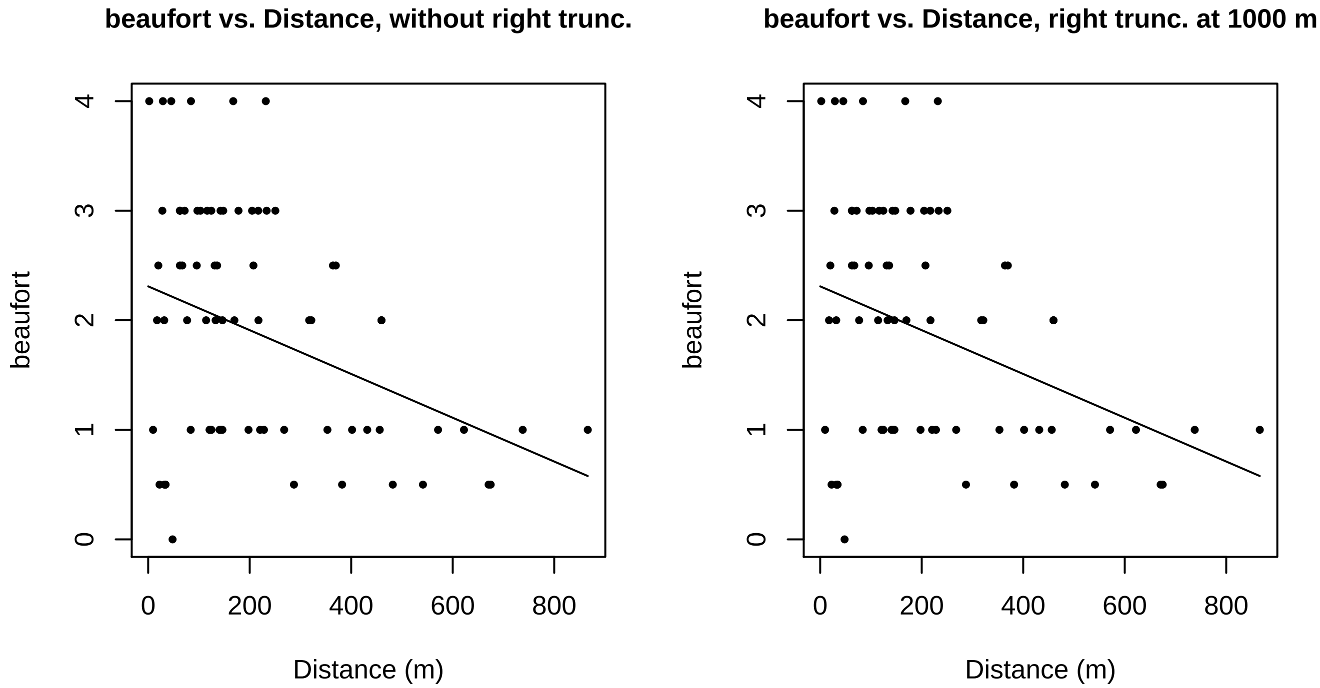

Figure 24: Scatterplots showing the relationship between Beaufort sea state and perpendicular sighting distance, for all sightings (left) and only those not right truncated (right). The line is a simple linear regression.

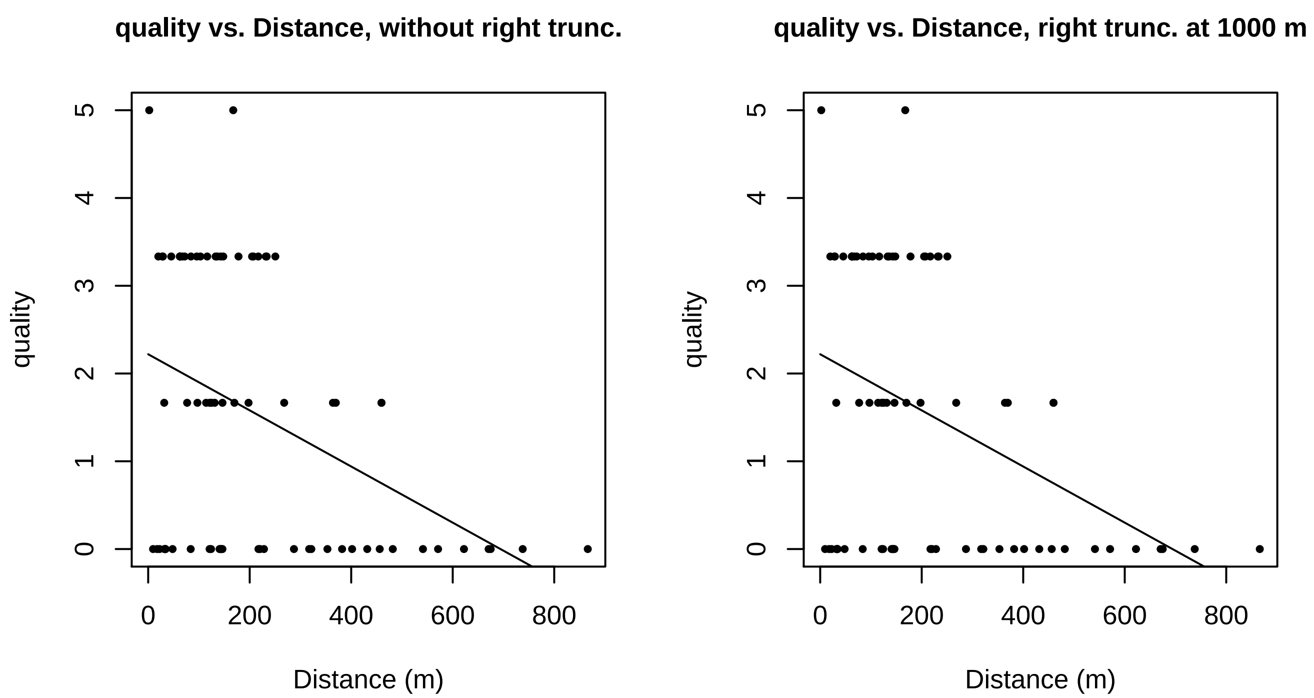

Figure 25: Scatterplots showing the relationship between the survey-specific index of the quality of observation conditions and perpendicular sighting distance, for all sightings (left) and only those not right truncated (right). Low values of the quality index correspond to better observation conditions. The line is a simple linear regression.

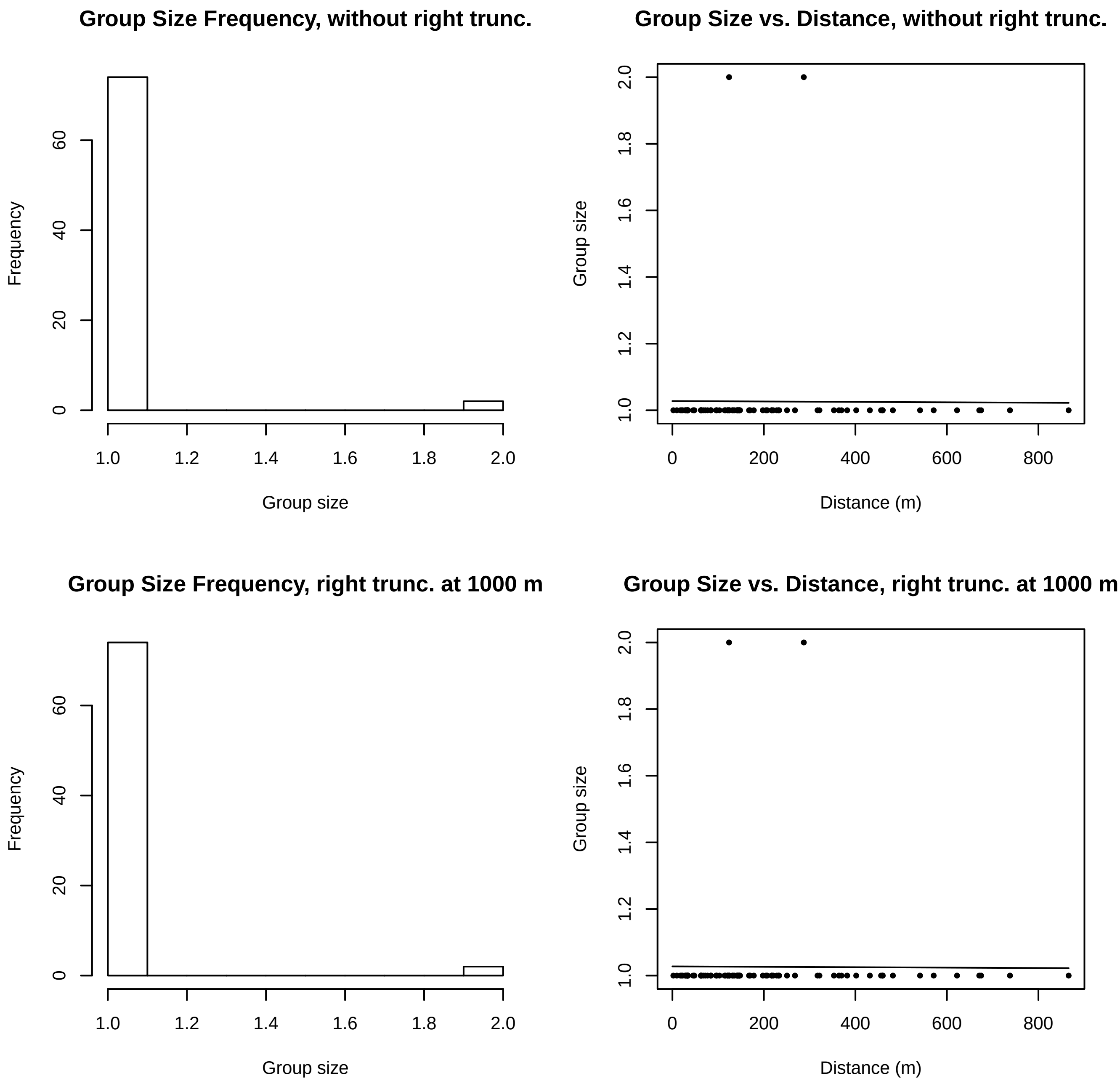

Figure 26: Histograms showing group size frequency and scatterplots showing the relationship between group size and perpendicular sighting distance, for all sightings (top row) and only those not right truncated (bottom row). In the scatterplot, the line is a simple linear regression.

Aerial Surveys

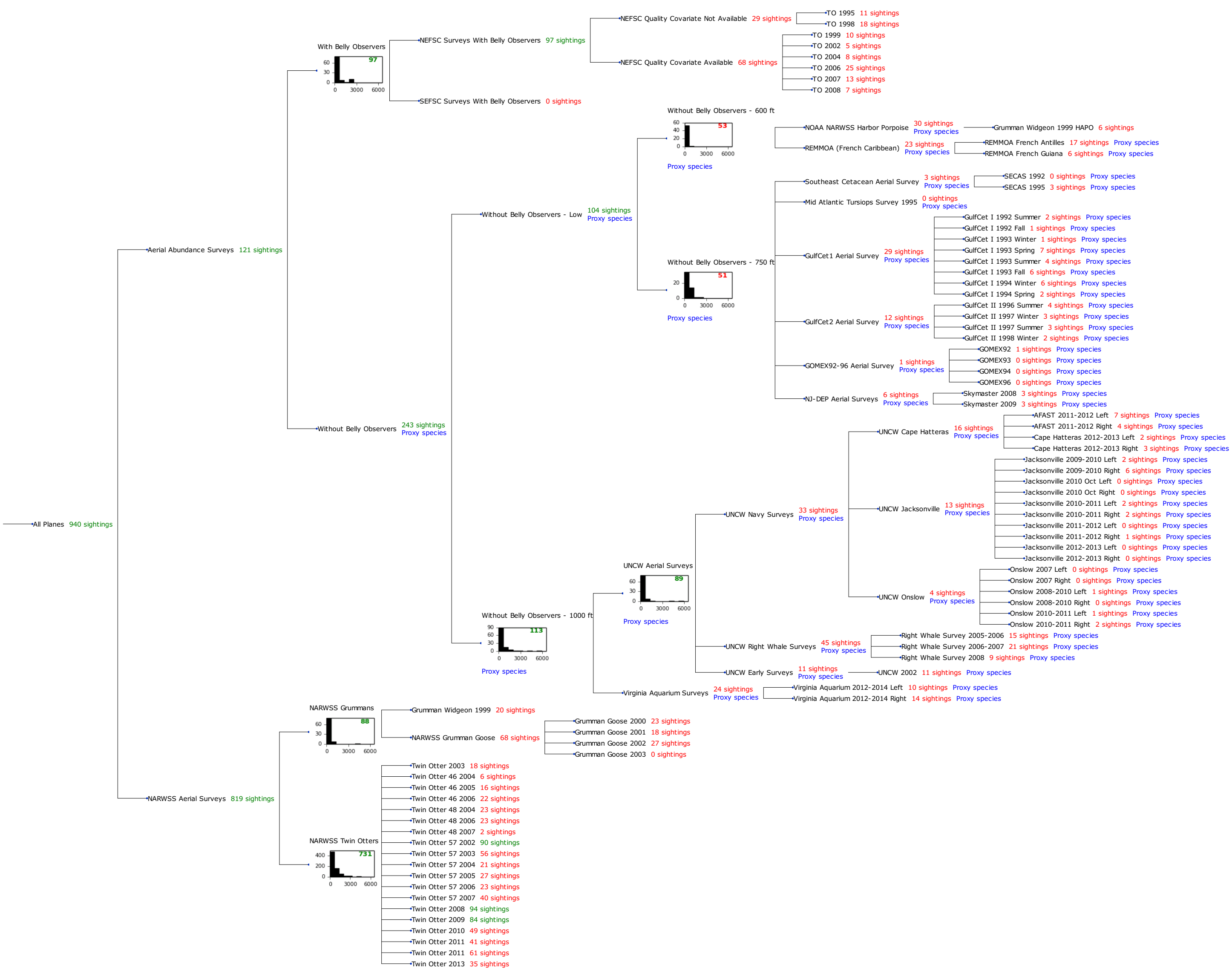

Figure 27: Detection hierarchy for aerial surveys

With Belly Observers

The sightings were right truncated at 1500m.

Covariate	Description
beaufort	Beaufort sea state.
size	Estimated size (number of individuals) of the sighted group.

Table 16: Covariates tested in candidate "multi-covariate distance sampling" (MCDS) detection functions.

Key	Adjustment	Order	Covariates	Succeeded	Δ AIC	Mean ESHW (m)
hr				Yes	0.00	386

hr			size	Yes	1.73	383
hn	cos	2		Yes	1.81	401
hr	poly	2		Yes	1.94	381
hr	poly	4		Yes	2.00	386
hn	cos	3		Yes	5.64	370
hn			beaufort	Yes	9.51	485
hn				Yes	10.11	489
hn			beaufort, size	Yes	11.43	485
hn			size	Yes	11.76	489
hn	herm	4		No		
hr			beaufort	No		
hr			beaufort, size	No		

Table 17: Candidate detection functions for With Belly Observers. The first one listed was selected for the density model.

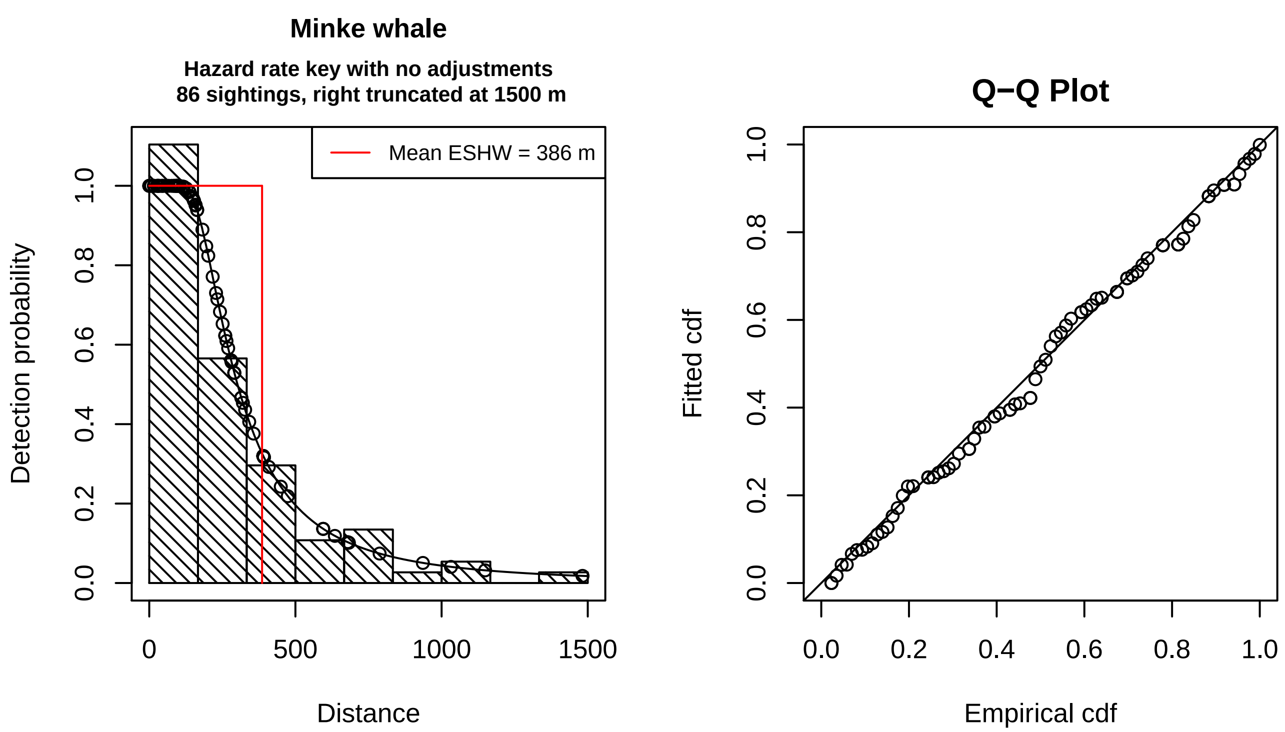

Figure 28: Detection function for With Belly Observers that was selected for the density model

Statistical output for this detection function:

```
Summary for ds object
Number of observations :  86
Distance range         :  0  -  1500
AIC                    :  1142.786
```

```
Detection function:
 Hazard-rate key function

Detection function parameters
Scale Coefficients:
            estimate        se
(Intercept) 5.549614 0.1842558

Shape parameters:
             estimate        se
(Intercept) 0.8277391 0.1754307

                        Estimate          SE        CV
Average p              0.2572932  0.03182451 0.1236897
N in covered region 334.2489812 51.71174183 0.1547102
```

Additional diagnostic plots:

Figure 29: Scatterplots showing the relationship between Beaufort sea state and perpendicular sighting distance, for all sightings (left) and only those not right truncated (right). The line is a simple linear regression.

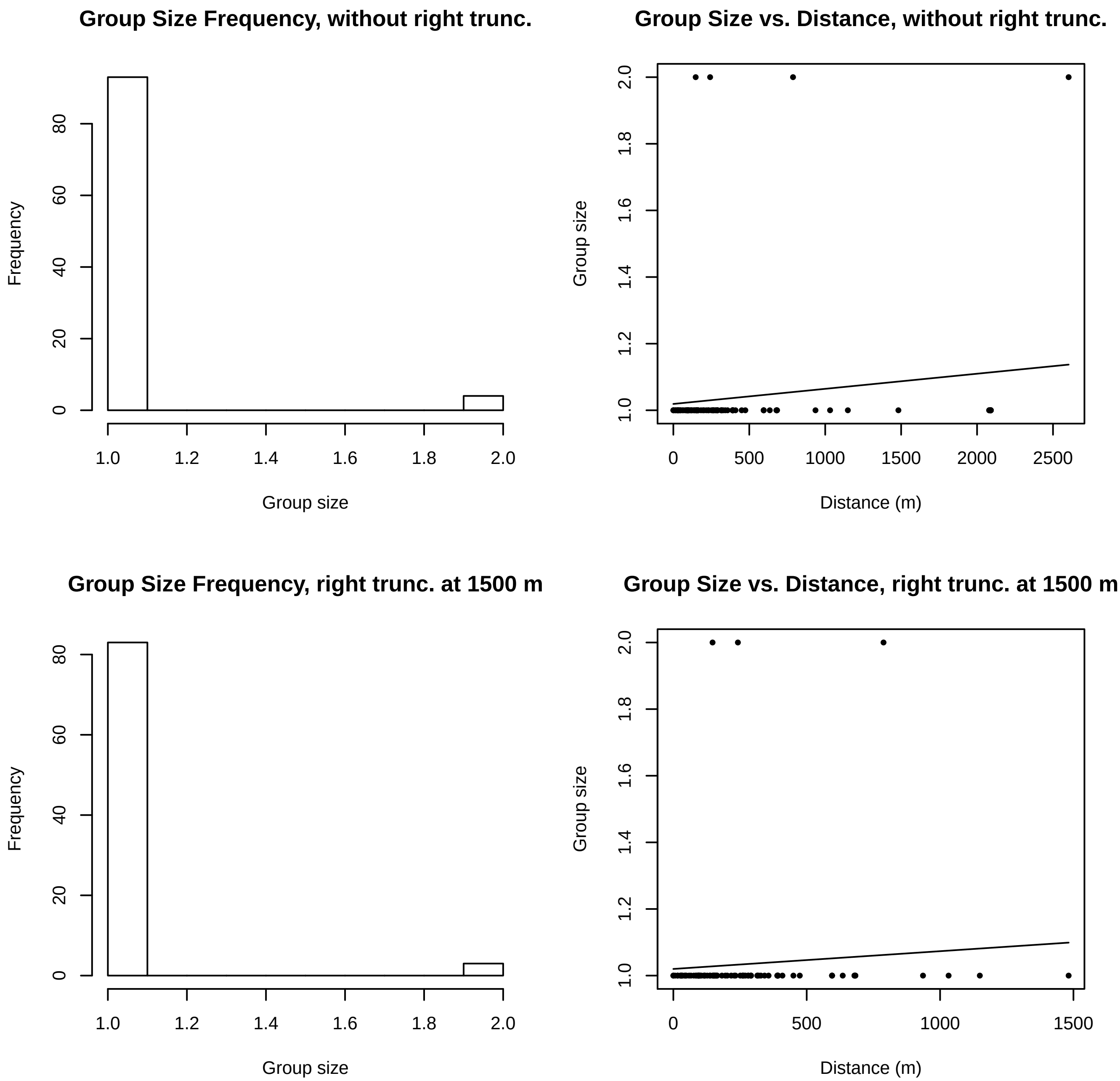

Figure 30: Histograms showing group size frequency and scatterplots showing the relationship between group size and perpendicular sighting distance, for all sightings (top row) and only those not right truncated (bottom row). In the scatterplot, the line is a simple linear regression.

Without Belly Observers - 600 ft

Because this taxon was sighted too infrequently to fit a detection function to its sightings alone, we fit a detection function to the pooled sightings of several other species that we believed would exhibit similar detectability. These "proxy species" are listed below.

Reported By Observer	Common Name	n
Balaenoptera	Balaenopterid sp.	2
Balaenoptera acutorostrata	Minke whale	8

Balaenoptera borealis	Sei whale	0
Balaenoptera borealis/edeni	Sei or Bryde's whale	0
Balaenoptera borealis/physalus	Fin or Sei whale	0
Balaenoptera edeni	Bryde's whale	0
Balaenoptera musculus	Blue whale	0
Balaenoptera physalus	Fin whale	15
Eubalaena glacialis	North Atlantic right whale	2
Eubalaena glacialis/Megaptera novaeangliae	Right or humpback whale	0
Megaptera novaeangliae	Humpback whale	16
Physeter macrocephalus	Sperm whale	10
Total		53

Table 18: Proxy species used to fit detection functions for Without Belly Observers - 600 ft. The number of sightings, n, is before truncation.

The sightings were right truncated at 600m. Due to a reduced frequency of sightings close to the trackline that plausibly resulted from the behavior of the observers and/or the configuration of the survey platform, the sightings were left truncted as well. Sightings closer than 32 m to the trackline were omitted from the analysis, and it was assumed that the the area closer to the trackline than this was not surveyed. This distance was estimated by inspecting histograms of perpendicular sighting distances.

Covariate	Description
beaufort	Beaufort sea state.
size	Estimated size (number of individuals) of the sighted group.

Table 19: Covariates tested in candidate "multi-covariate distance sampling" (MCDS) detection functions.

Key	Adjustment	Order	Covariates	Succeeded	Δ AIC	Mean ESHW (m)
hn				Yes	0.00	293
hr				Yes	1.14	318
hn			beaufort	Yes	1.57	293
hn	cos	3		Yes	1.65	311
hn	herm	4		Yes	1.93	291
hr			beaufort	Yes	1.97	326
hn	cos	2		Yes	1.97	283
hr	poly	2		Yes	3.14	318
hr	poly	4		Yes	3.14	318
hn			size	No		
hr			size	No		
hn			beaufort, size	No		
hr			beaufort, size	No		

Table 20: Candidate detection functions for Without Belly Observers - 600 ft. The first one listed was selected for the density model.

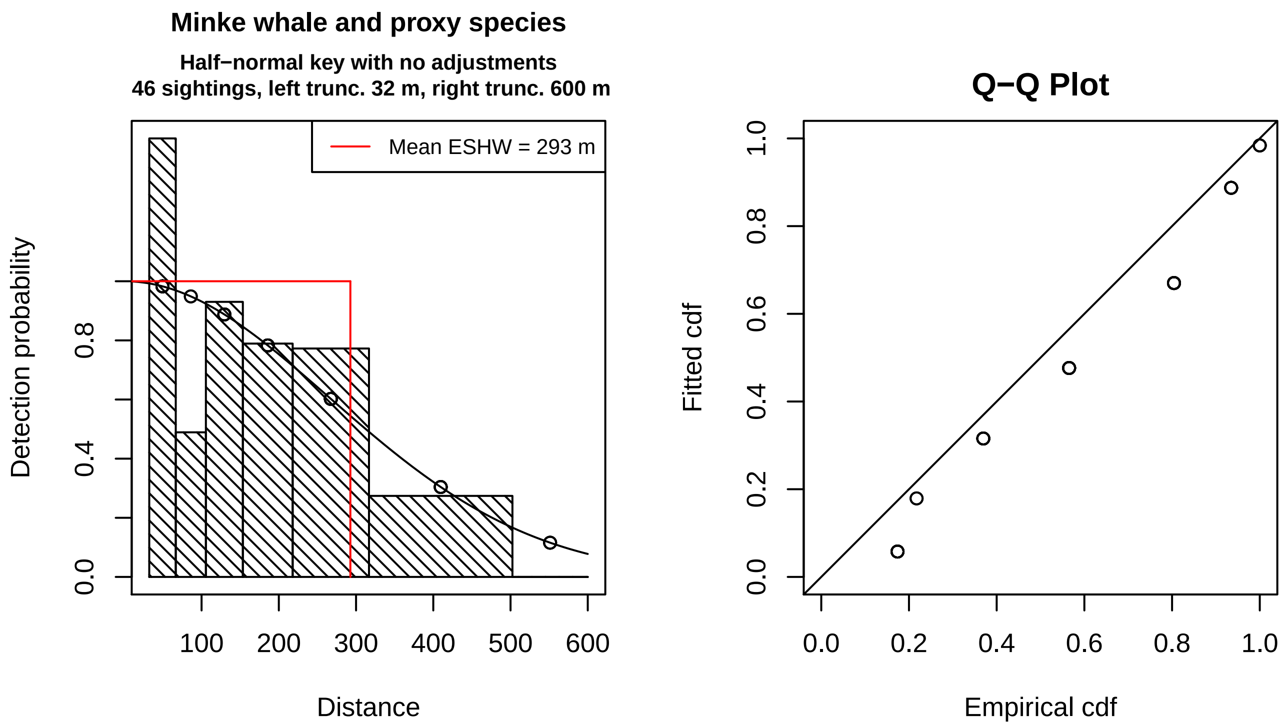

Figure 31: Detection function for Without Belly Observers - 600 ft that was selected for the density model

Statistical output for this detection function:

```
Summary for ds object
Number of observations :  46
Distance range         :  32.24668  -  600
AIC                    :  177.4011

Detection function:
 Half-normal key function

Detection function parameters
Scale Coefficients:
            estimate        se
(Intercept) 5.581559 0.1339955

                      Estimate          SE        CV
Average p             0.487738  0.06208134 0.1272842
N in covered region 94.312922 15.59372100 0.1653402
```

Additional diagnostic plots:

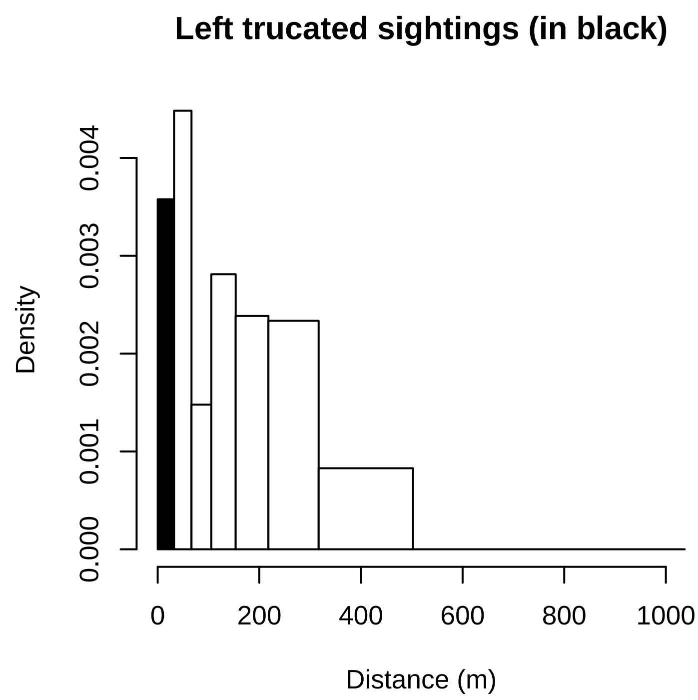

Figure 32: Density of sightings by perpendicular distance for Without Belly Observers - 600 ft. Black bars on the left show sightings that were left truncated.

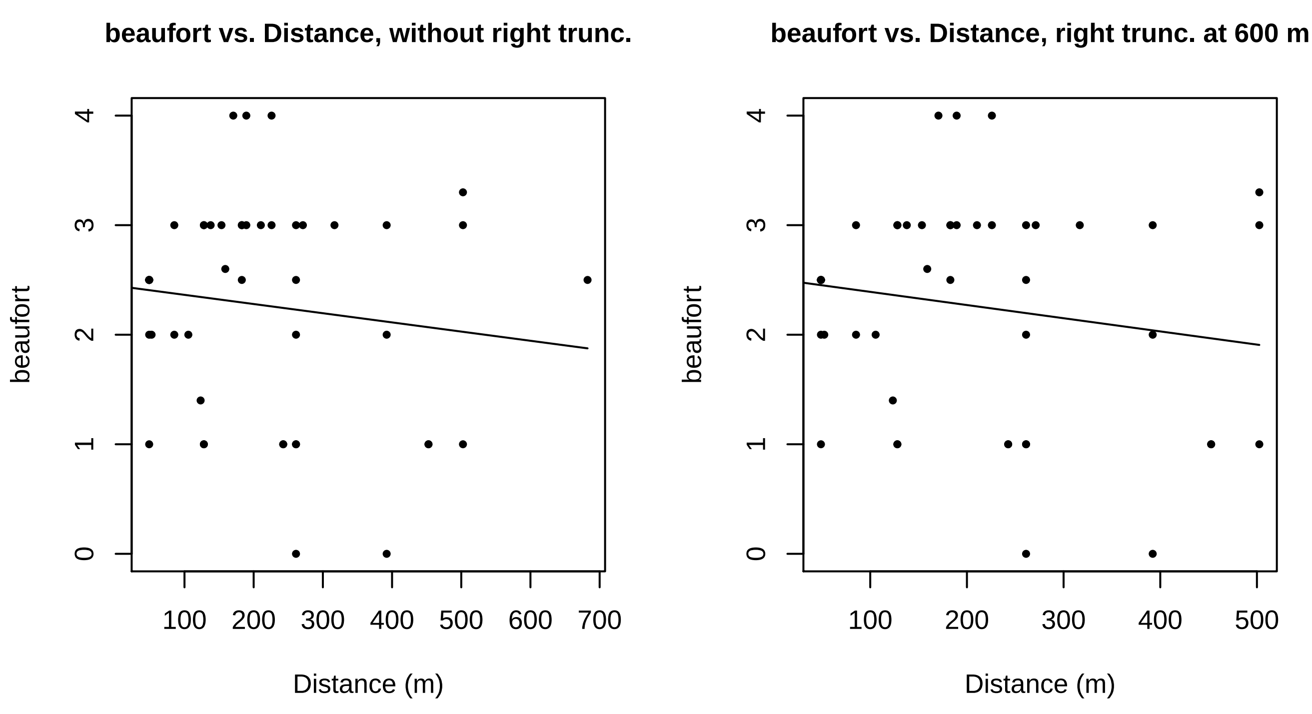

Figure 33: Scatterplots showing the relationship between Beaufort sea state and perpendicular sighting distance, for all sightings (left) and only those not right truncated (right). The line is a simple linear regression.

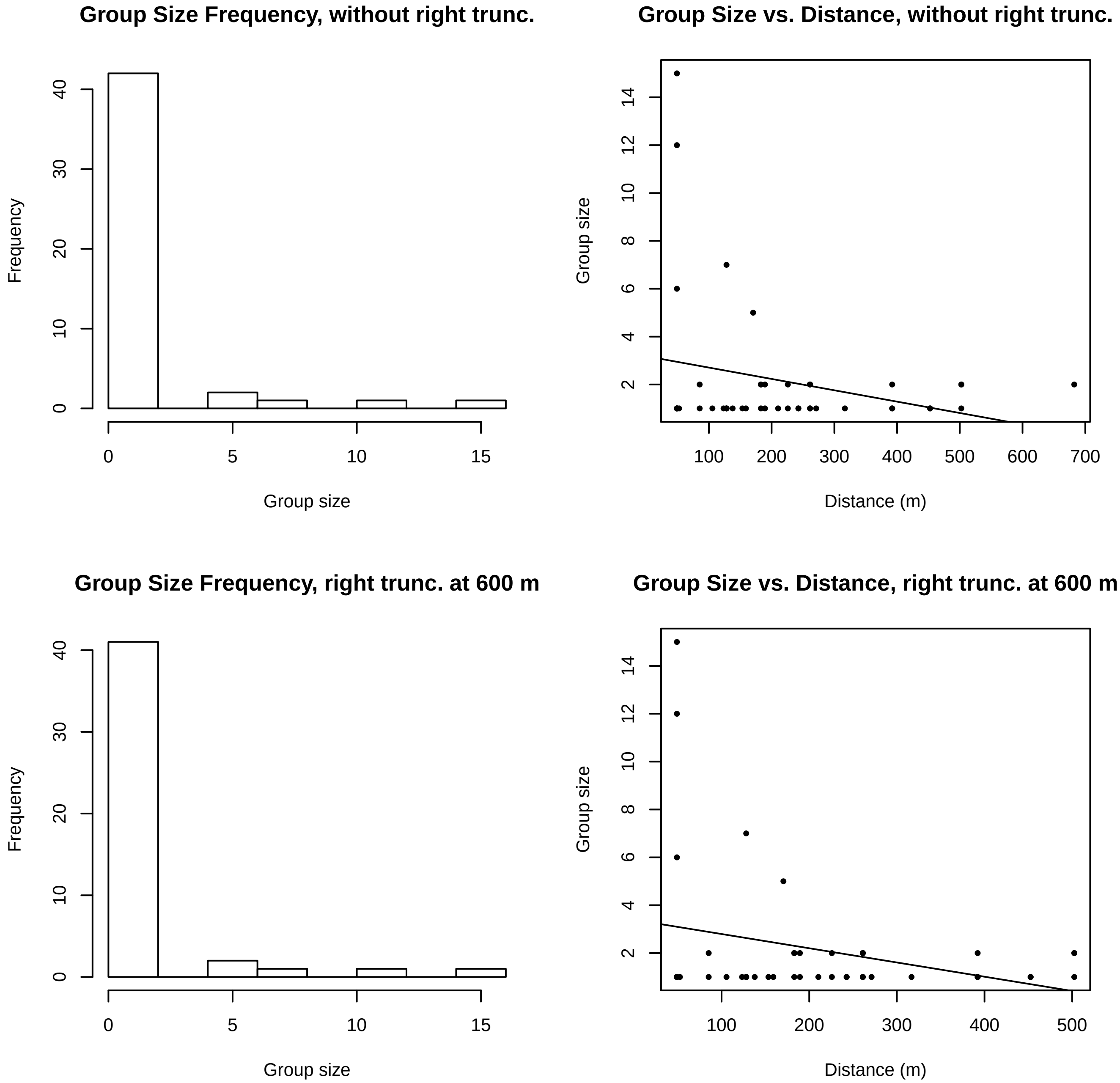

Figure 34: Histograms showing group size frequency and scatterplots showing the relationship between group size and perpendicular sighting distance, for all sightings (top row) and only those not right truncated (bottom row). In the scatterplot, the line is a simple linear regression.

Without Belly Observers - 750 ft

Because this taxon was sighted too infrequently to fit a detection function to its sightings alone, we fit a detection function to the pooled sightings of several other species that we believed would exhibit similar detectability. These "proxy species" are listed below.

Reported By Observer	Common Name	n
Balaenoptera	Balaenopterid sp.	1
Balaenoptera acutorostrata	Minke whale	0

Balaenoptera borealis	Sei whale	0
Balaenoptera borealis/edeni	Sei or Bryde's whale	2
Balaenoptera borealis/physalus	Fin or Sei whale	0
Balaenoptera edeni	Bryde's whale	3
Balaenoptera musculus	Blue whale	0
Balaenoptera physalus	Fin whale	2
Eubalaena glacialis	North Atlantic right whale	0
Eubalaena glacialis/Megaptera novaeangliae	Right or humpback whale	0
Megaptera novaeangliae	Humpback whale	6
Physeter macrocephalus	Sperm whale	37
Total		51

Table 21: Proxy species used to fit detection functions for Without Belly Observers - 750 ft. The number of sightings, n, is before truncation.

The sightings were right truncated at 600m. Due to a reduced frequency of sightings close to the trackline that plausibly resulted from the behavior of the observers and/or the configuration of the survey platform, the sightings were left truncted as well. Sightings closer than 40 m to the trackline were omitted from the analysis, and it was assumed that the the area closer to the trackline than this was not surveyed. This distance was estimated by inspecting histograms of perpendicular sighting distances. The vertical sighting angles were heaped at 10 degree increments, so the candidate detection functions were fitted using linear bins scaled accordingly.

Key	Adjustment	Order	Covariates	Succeeded	Δ AIC	Mean ESHW (m)
hn	cos	2		Yes	0.00	216
hr				Yes	0.59	251
hn	cos	3		Yes	2.31	255
hn	herm	4		Yes	2.46	316
hr	poly	2		Yes	2.59	251
hr	poly	4		Yes	2.71	220
hn				No		

Table 22: Candidate detection functions for Without Belly Observers - 750 ft. The first one listed was selected for the density model.

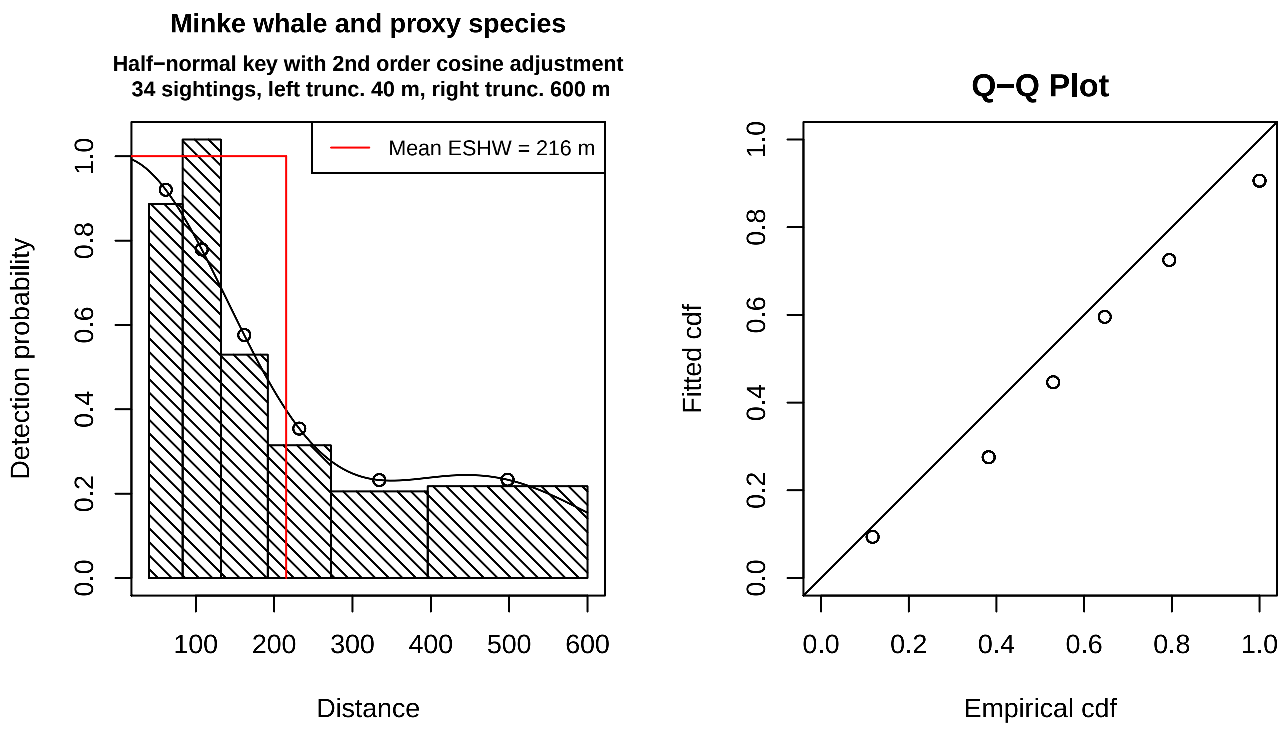

Figure 35: Detection function for Without Belly Observers - 750 ft that was selected for the density model

Statistical output for this detection function:

```
Summary for ds object
Number of observations :  34
Distance range         :  40.30835  -  600
AIC                    :  124.984

Detection function:
 Half-normal key function with cosine adjustment term of order 2

Detection function parameters
Scale Coefficients:
            estimate        se
(Intercept) 5.738324 0.1838281

Adjustment term parameter(s):
              estimate       se
cos, order 2 0.4333817 0.242253


Monotonicity constraints were enforced.
                      Estimate         SE        CV
Average p            0.3592782  0.0870934 0.2424122
N in covered region 94.6341980 26.3634680 0.2785829

Monotonicity constraints were enforced.
```

Additional diagnostic plots:

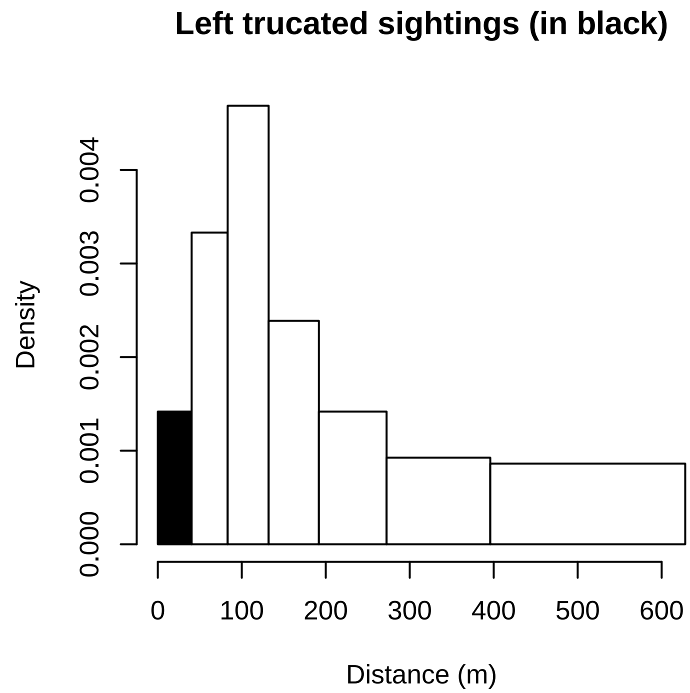

Figure 36: Density of sightings by perpendicular distance for Without Belly Observers - 750 ft. Black bars on the left show sightings that were left truncated.

Without Belly Observers - 1000 ft

Because this taxon was sighted too infrequently to fit a detection function to its sightings alone, we fit a detection function to the pooled sightings of several other species that we believed would exhibit similar detectability. These "proxy species" are listed below.

Reported By Observer	Common Name	n
Balaenoptera	Balaenopterid sp.	1
Balaenoptera acutorostrata	Minke whale	16
Balaenoptera borealis	Sei whale	0
Balaenoptera borealis/edeni	Sei or Bryde's whale	0
Balaenoptera borealis/physalus	Fin or Sei whale	0
Balaenoptera edeni	Bryde's whale	0
Balaenoptera musculus	Blue whale	0
Balaenoptera physalus	Fin whale	32
Eubalaena glacialis	North Atlantic right whale	34
Eubalaena glacialis/Megaptera novaeangliae	Right or humpback whale	0
Megaptera novaeangliae	Humpback whale	30
Total		113

Table 23: Proxy species used to fit detection functions for Without Belly Observers - 1000 ft. The number of sightings, n, is before truncation.

The sightings were right truncated at 1500m.

Covariate	Description
beaufort	Beaufort sea state.
quality	Survey-specific index of the quality of observation conditions, utilizing relevant factors other than Beaufort sea state (see methods).
size	Estimated size (number of individuals) of the sighted group.

Table 24: Covariates tested in candidate "multi-covariate distance sampling" (MCDS) detection functions.

Key	Adjustment	Order	Covariates	Succeeded	Δ AIC	Mean ESHW (m)
hr				Yes	0.00	434
hr	poly	4		Yes	1.58	424
hn	cos	2		Yes	1.71	462
hr	poly	2		Yes	1.92	427
hr			quality	Yes	1.96	433
hn	cos	3		Yes	3.64	418
hn				Yes	11.03	585
hn	herm	4		No		
hn			beaufort	No		
hr			beaufort	No		
hn			quality	No		
hn			size	No		
hr			size	No		
hn			beaufort, quality	No		
hr			beaufort, quality	No		
hn			beaufort, size	No		
hr			beaufort, size	No		
hn			quality, size	No		
hr			quality, size	No		
hn			beaufort, quality, size	No		
hr			beaufort, quality, size	No		

Table 25: Candidate detection functions for Without Belly Observers - 1000 ft. The first one listed was selected for the density model.

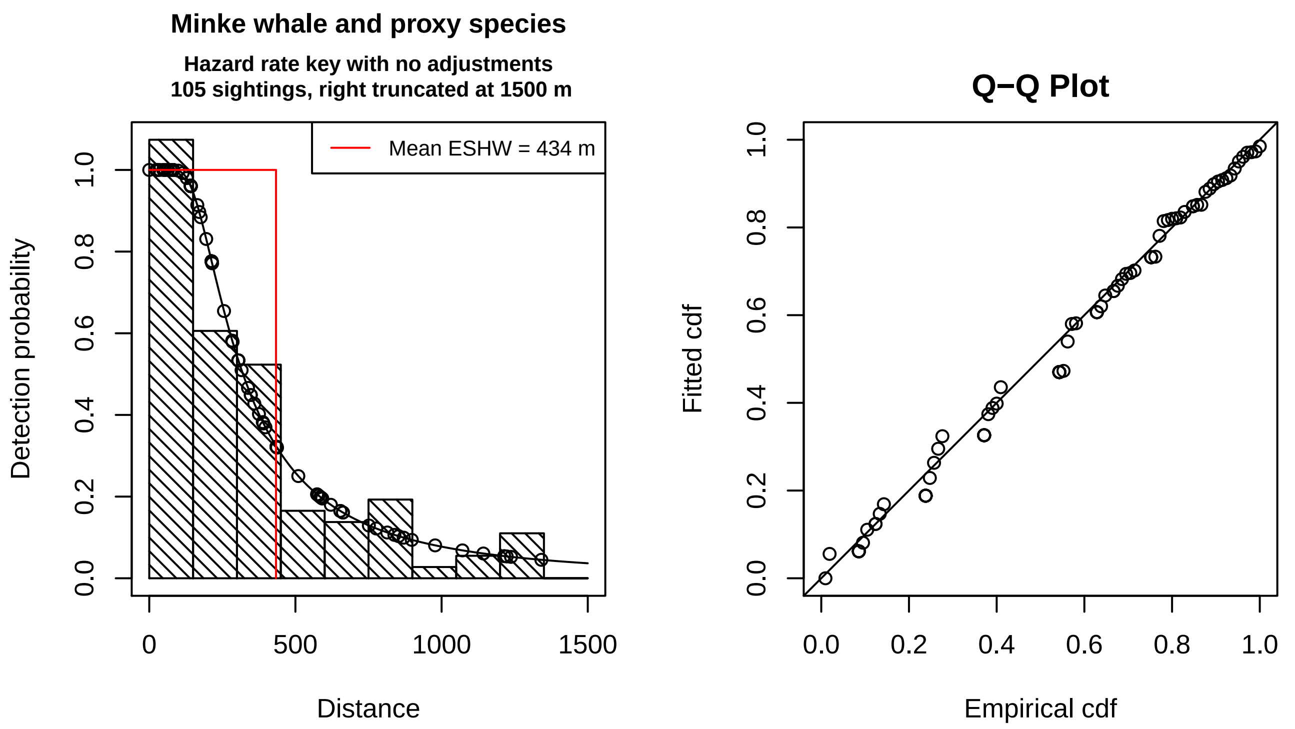

Figure 37: Detection function for Without Belly Observers - 1000 ft that was selected for the density model

Statistical output for this detection function:

```
Summary for ds object
Number of observations :  105
Distance range         :  0  -  1500
AIC                    :  1432.491

Detection function:
 Hazard-rate key function

Detection function parameters
Scale Coefficients:
            estimate        se
(Intercept) 5.576432 0.2232183

Shape parameters:
             estimate        se
(Intercept) 0.6374087 0.1752092

                        Estimate          SE        CV
Average p              0.2891295  0.03984493 0.1378100
N in covered region 363.1591175 58.28878285 0.1605048
```

Additional diagnostic plots:

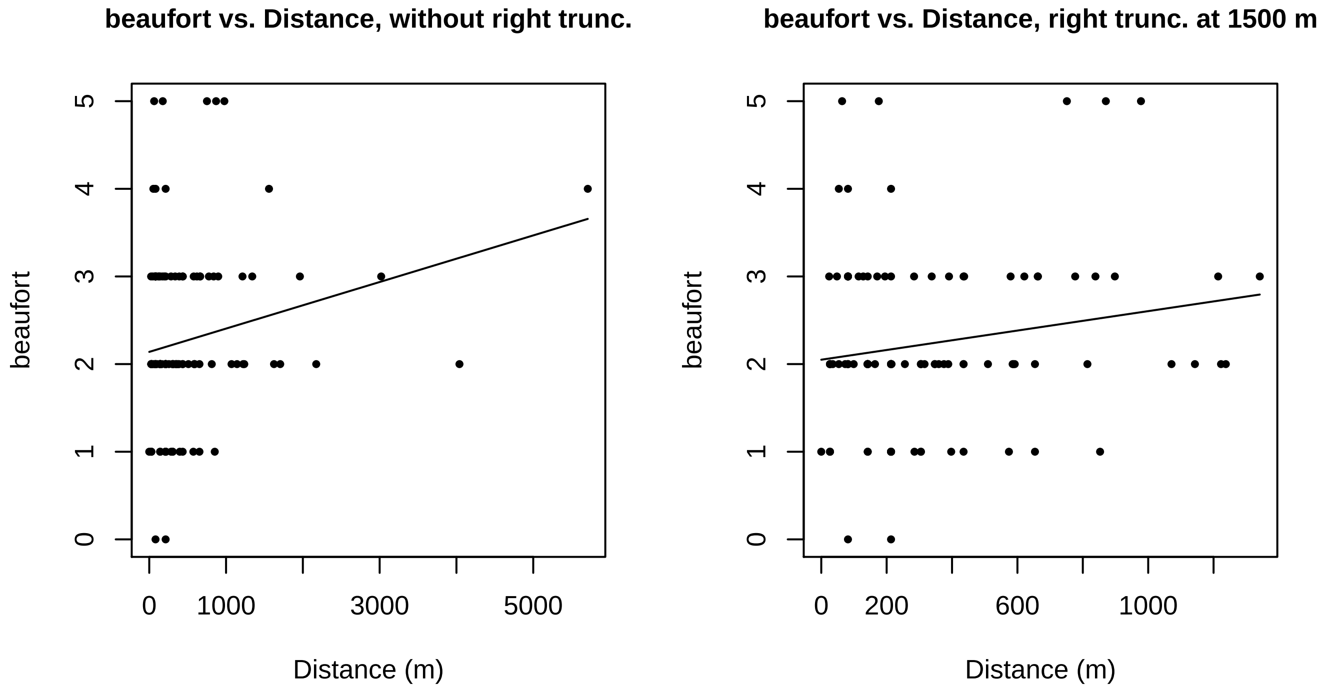

Figure 38: Scatterplots showing the relationship between Beaufort sea state and perpendicular sighting distance, for all sightings (left) and only those not right truncated (right). The line is a simple linear regression.

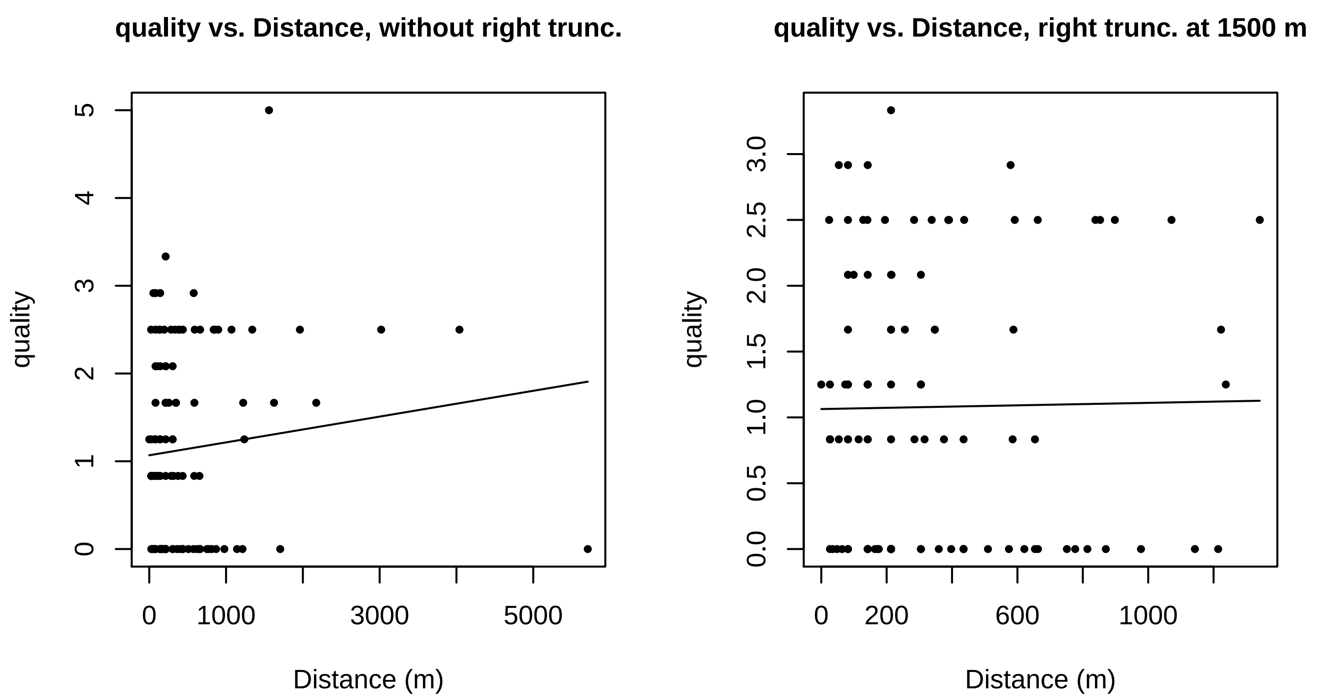

Figure 39: Scatterplots showing the relationship between the survey-specific index of the quality of observation conditions and perpendicular sighting distance, for all sightings (left) and only those not right truncated (right). Low values of the quality index correspond to better observation conditions. The line is a simple linear regression.

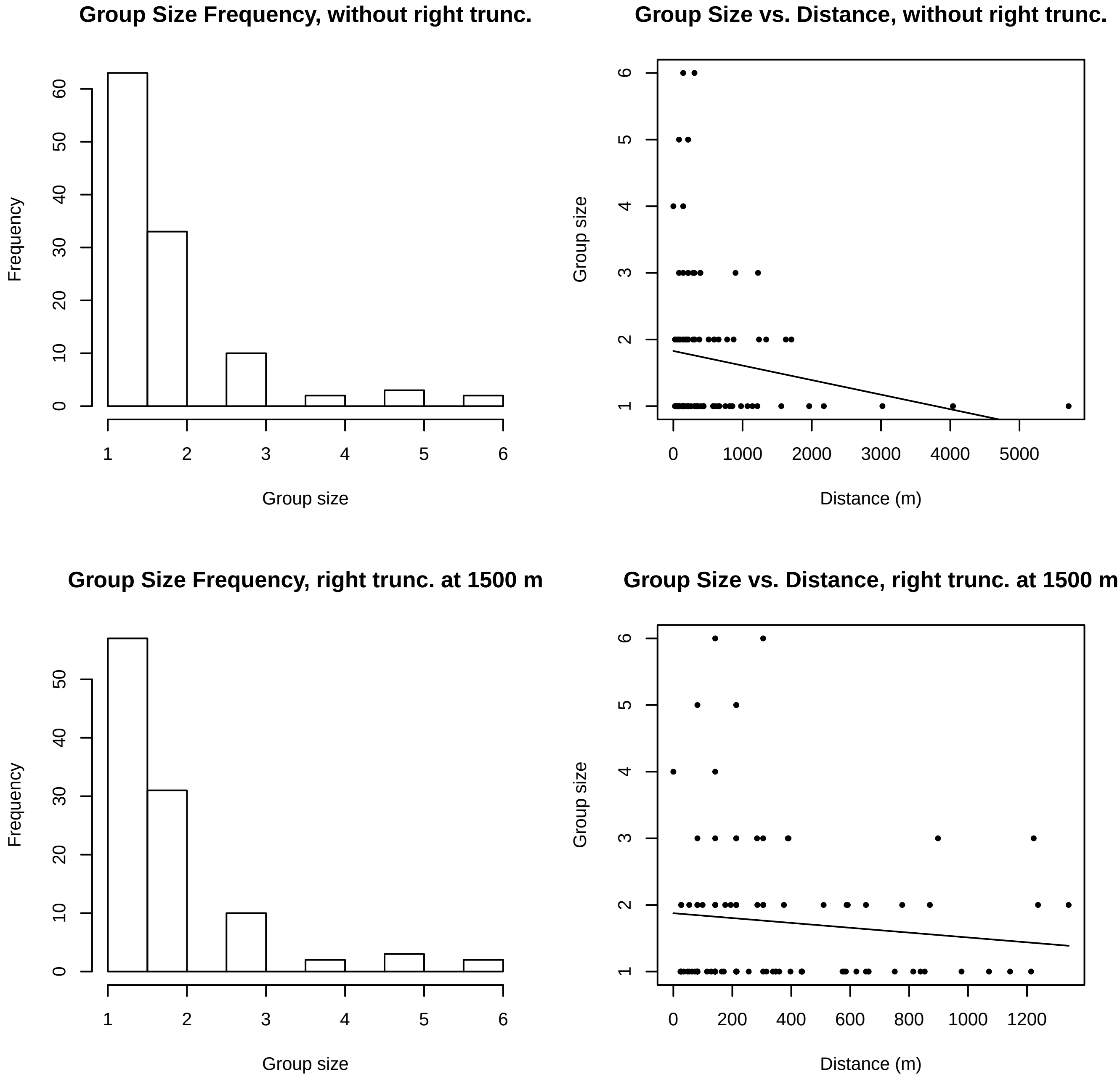

Figure 40: Histograms showing group size frequency and scatterplots showing the relationship between group size and perpendicular sighting distance, for all sightings (top row) and only those not right truncated (bottom row). In the scatterplot, the line is a simple linear regression.

UNCW Aerial Surveys

Because this taxon was sighted too infrequently to fit a detection function to its sightings alone, we fit a detection function to the pooled sightings of several other species that we believed would exhibit similar detectability. These “proxy species” are listed below.

Reported By Observer	Common Name	n
Balaenoptera	Balaenopterid sp.	1
Balaenoptera acutorostrata	Minke whale	15

Balaenoptera borealis	Sei whale	0
Balaenoptera borealis/edeni	Sei or Bryde's whale	0
Balaenoptera borealis/physalus	Fin or Sei whale	0
Balaenoptera edeni	Bryde's whale	0
Balaenoptera musculus	Blue whale	0
Balaenoptera physalus	Fin whale	19
Eubalaena glacialis	North Atlantic right whale	31
Eubalaena glacialis/Megaptera novaeangliae	Right or humpback whale	0
Megaptera novaeangliae	Humpback whale	23
Total		89

Table 26: Proxy species used to fit detection functions for UNCW Aerial Surveys. The number of sightings, n, is before truncation.

The sightings were right truncated at 1500m.

Covariate	Description
beaufort	Beaufort sea state.
quality	Survey-specific index of the quality of observation conditions, utilizing relevant factors other than Beaufort sea state (see methods).
size	Estimated size (number of individuals) of the sighted group.

Table 27: Covariates tested in candidate "multi-covariate distance sampling" (MCDS) detection functions.

Key	Adjustment	Order	Covariates	Succeeded	Δ AIC	Mean ESHW (m)
hn	cos	3		Yes	0.00	358
hr				Yes	0.01	397
hr	poly	4		Yes	0.85	391
hr	poly	2		Yes	1.03	386
hn	cos	2		Yes	1.24	409
hr			quality	Yes	1.55	396
hn				Yes	5.53	480
hn			quality	Yes	7.53	480
hn	herm	4		No		
hn			beaufort	No		
hr			beaufort	No		
hn			size	No		
hr			size	No		
hn			beaufort, quality	No		
hr			beaufort, quality	No		

hn	beaufort, size	No
hr	beaufort, size	No
hn	quality, size	No
hr	quality, size	No
hn	beaufort, quality, size	No
hr	beaufort, quality, size	No

Table 28: Candidate detection functions for UNCW Aerial Surveys. The first one listed was selected for the density model.

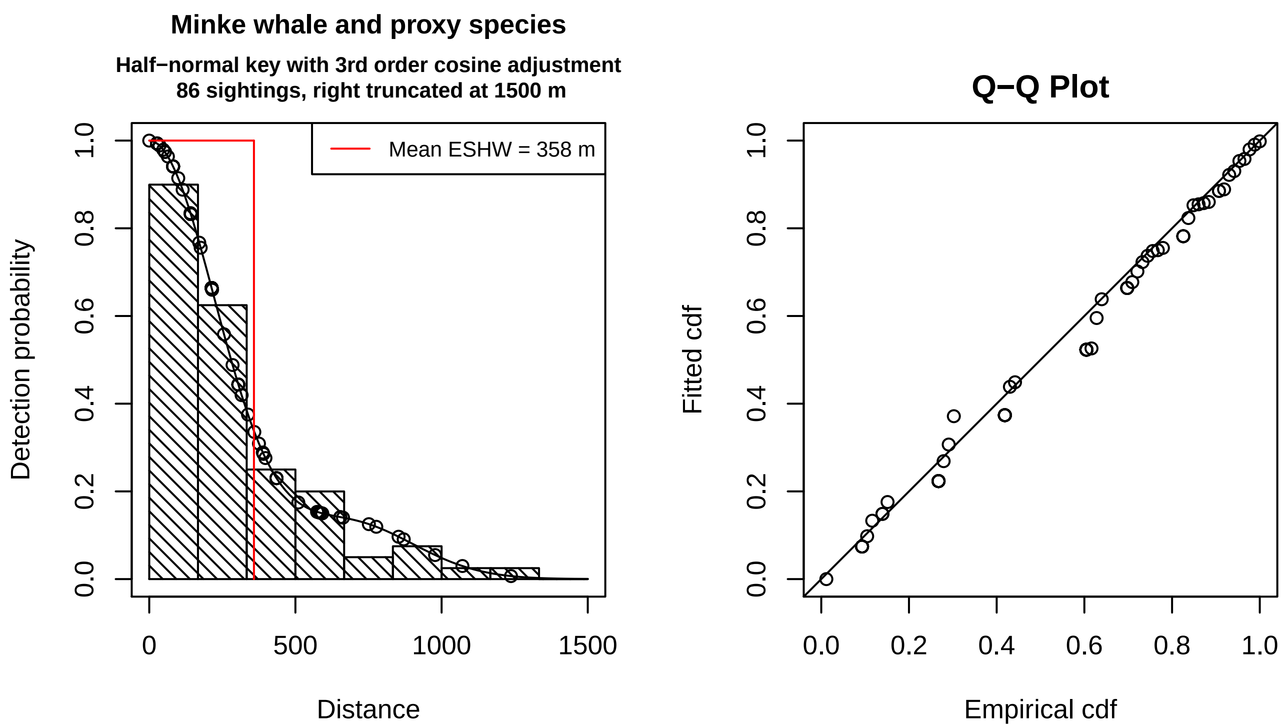

Figure 41: Detection function for UNCW Aerial Surveys that was selected for the density model

Statistical output for this detection function:

```
Summary for ds object
Number of observations :  86
Distance range         :  0  -  1500
AIC                    :  1144.166

Detection function:
 Half-normal key function with cosine adjustment term of order 3

Detection function parameters
Scale Coefficients:
            estimate         se
(Intercept) 6.006457 0.06897785

Adjustment term parameter(s):
```

```
              estimate        se
cos, order 3 0.4451316 0.1512901


Monotonicity constraints were enforced.
                       Estimate          SE        CV
Average p             0.2387636  0.02505434 0.1049337
N in covered region 360.1889061 50.76321099 0.1409350

Monotonicity constraints were enforced.
```

Additional diagnostic plots:

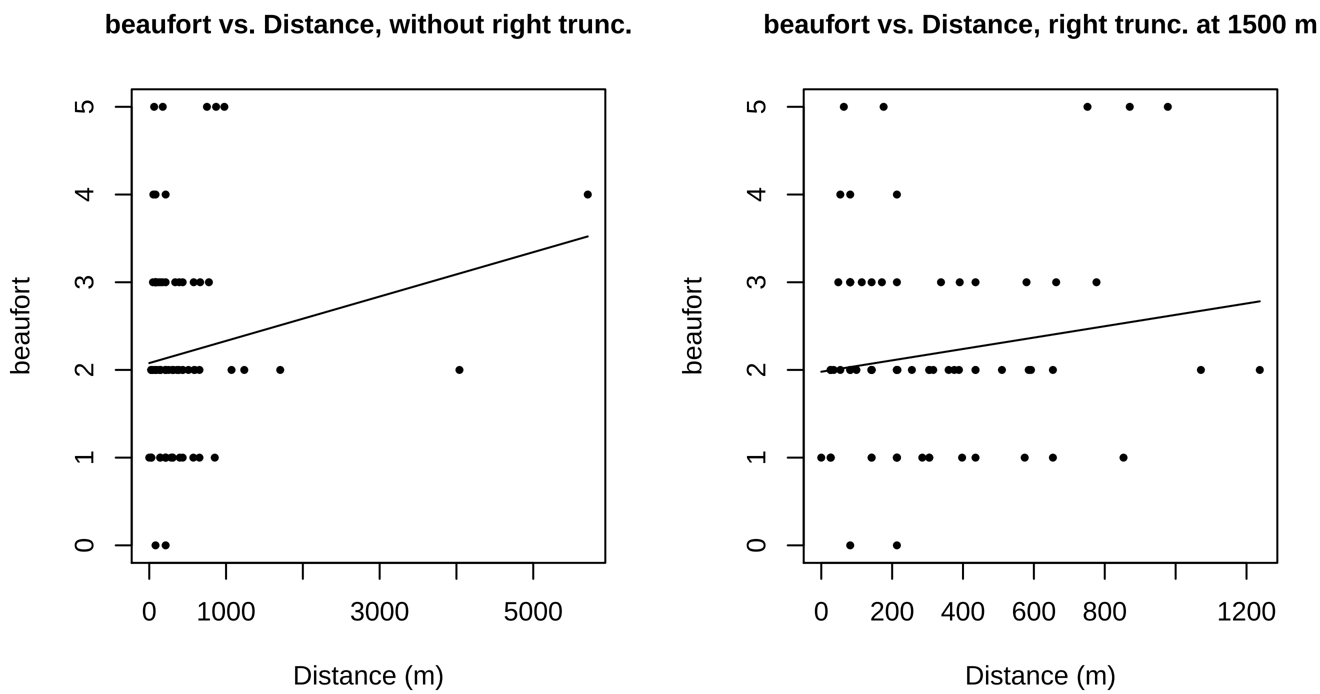

Figure 42: Scatterplots showing the relationship between Beaufort sea state and perpendicular sighting distance, for all sightings (left) and only those not right truncated (right). The line is a simple linear regression.

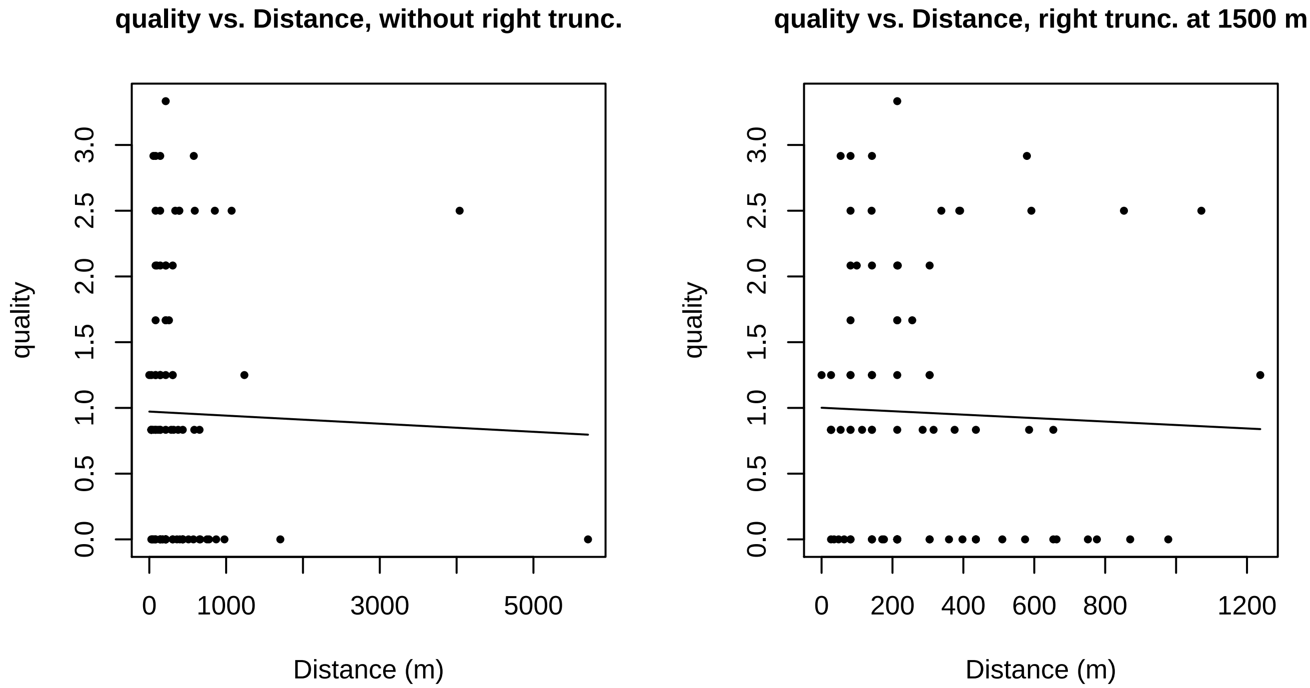

Figure 43: Scatterplots showing the relationship between the survey-specific index of the quality of observation conditions and perpendicular sighting distance, for all sightings (left) and only those not right truncated (right). Low values of the quality index correspond to better observation conditions. The line is a simple linear regression.

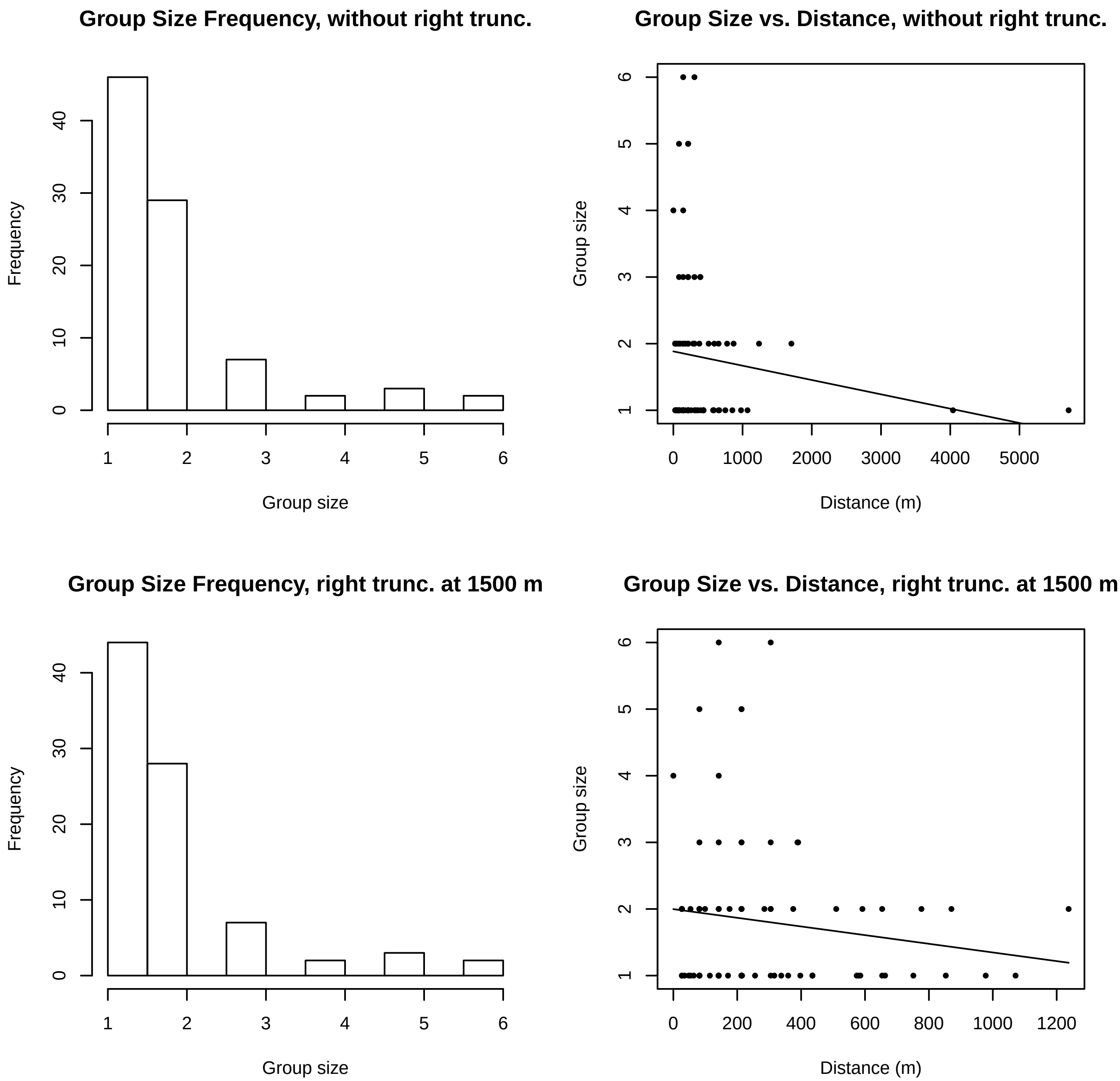

Figure 44: Histograms showing group size frequency and scatterplots showing the relationship between group size and perpendicular sighting distance, for all sightings (top row) and only those not right truncated (bottom row). In the scatterplot, the line is a simple linear regression.

NARWSS Grummans

The sightings were right truncated at 1500m. Due to a reduced frequency of sightings close to the trackline that plausibly resulted from the behavior of the observers and/or the configuration of the survey platform, the sightings were left truncted as well. Sightings closer than 107 m to the trackline were omitted from the analysis, and it was assumed that the the area closer to the trackline than this was not surveyed. This distance was estimated by inspecting histograms of perpendicular sighting distances.

Covariate	Description

beaufort	Beaufort sea state.
quality	Survey-specific index of the quality of observation conditions, utilizing relevant factors other than Beaufort sea state (see methods).
size	Estimated size (number of individuals) of the sighted group.

Table 29: Covariates tested in candidate “multi-covariate distance sampling” (MCDS) detection functions.

Key	Adjustment	Order	Covariates	Succeeded	Δ AIC	Mean ESHW (m)
hr			beaufort, quality	Yes	0.00	302
hr			quality	Yes	0.71	296
hr	poly	2		Yes	1.96	34
hr				Yes	1.97	145
hr	poly	4		Yes	2.31	92
hr			beaufort	Yes	2.55	195
hn	cos	2		Yes	5.67	259
hn	cos	3		Yes	6.79	209
hn			quality	Yes	12.34	323
hn				Yes	14.22	330
hn	herm	4		No		
hn			beaufort	No		
hn			size	No		
hr			size	No		
hn			beaufort, quality	No		
hn			beaufort, size	No		
hr			beaufort, size	No		
hn			quality, size	No		
hr			quality, size	No		
hn			beaufort, quality, size	No		
hr			beaufort, quality, size	No		

Table 30: Candidate detection functions for NARWSS Grummans. The first one listed was selected for the density model.

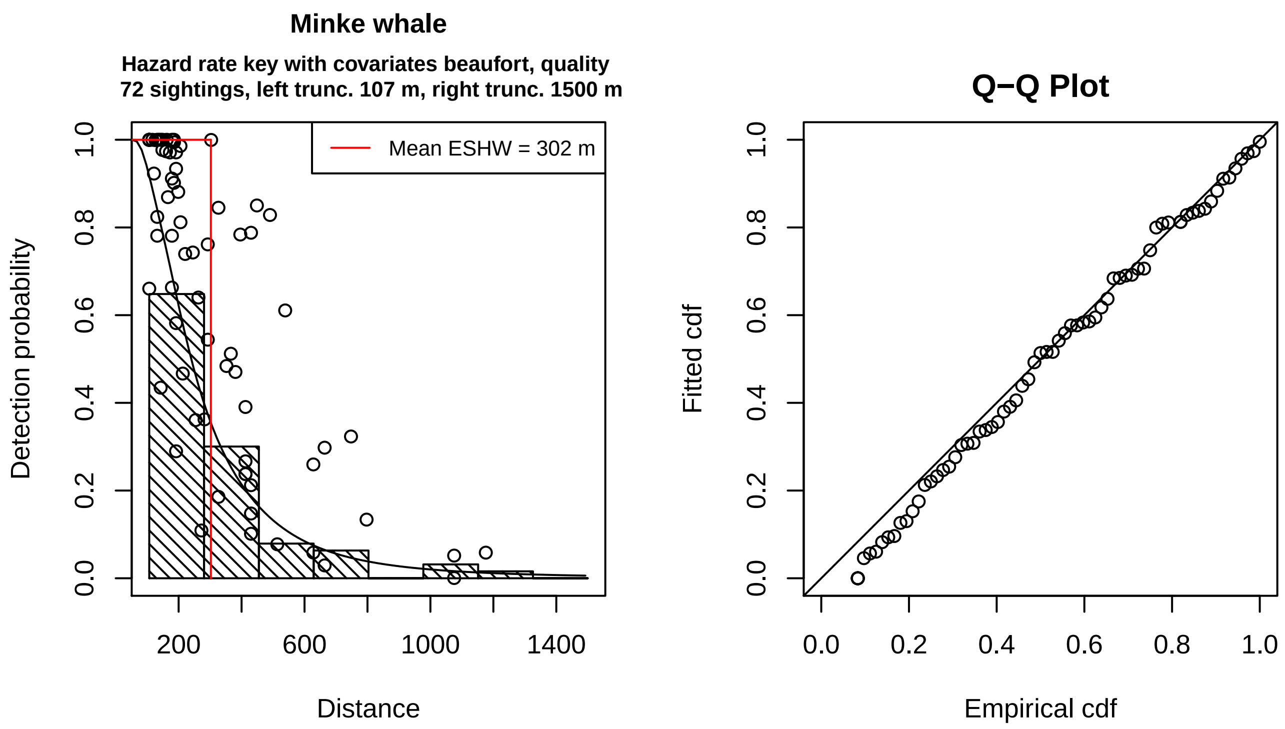

Figure 45: Detection function for NARWSS Grummans that was selected for the density model

Statistical output for this detection function:

```
Summary for ds object
Number of observations :  72
Distance range         :  106.5979  -  1500
AIC                    :  916.9474

Detection function:
 Hazard-rate key function

Detection function parameters
Scale Coefficients:
              estimate        se
(Intercept)  6.5939090 0.3651588
beaufort    -0.2158345 0.1636608
quality     -0.5009568 0.1736876

Shape parameters:
            estimate        se
(Intercept) 1.129938 0.1447496

                       Estimate          SE        CV
Average p             0.1321684   0.05084224 0.3846778
N in covered region 544.7596910 218.58027034 0.4012416
```

Additional diagnostic plots:

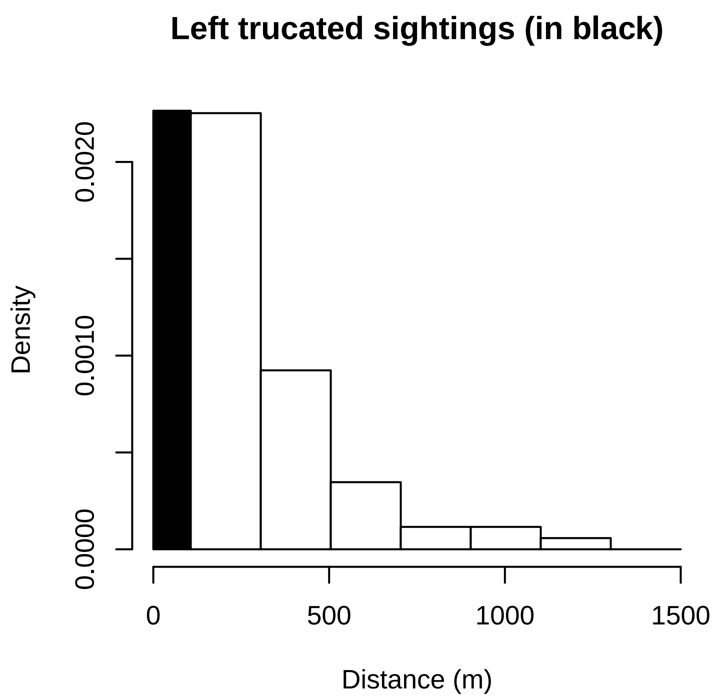

Figure 46: Density of sightings by perpendicular distance for NARWSS Grummans. Black bars on the left show sightings that were left truncated.

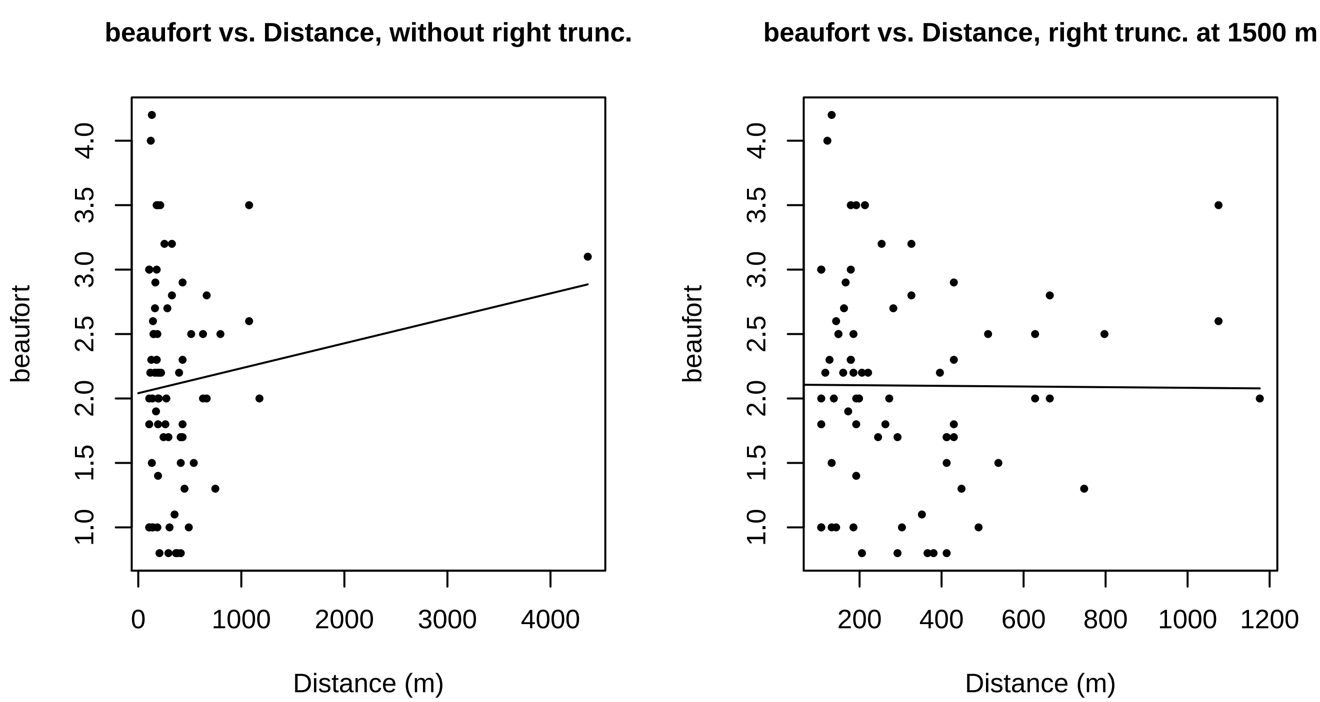

Figure 47: Scatterplots showing the relationship between Beaufort sea state and perpendicular sighting distance, for all sightings (left) and only those not right truncated (right). The line is a simple linear regression.

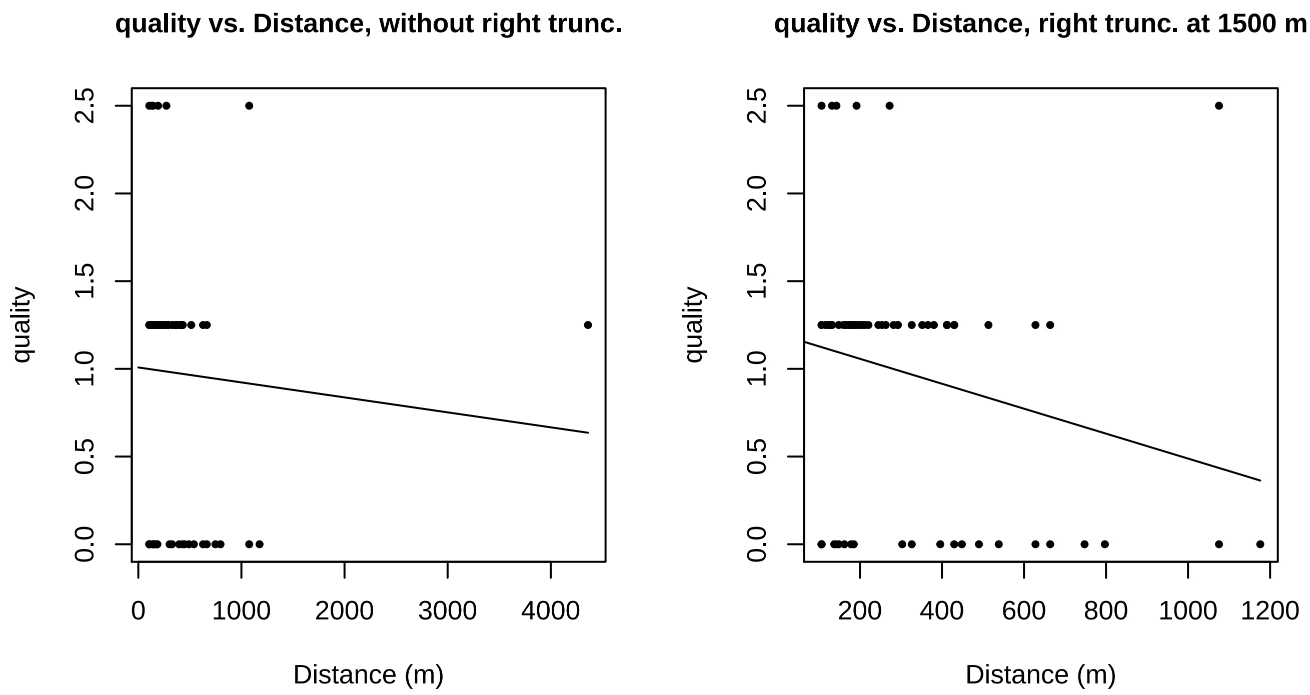

Figure 48: Scatterplots showing the relationship between the survey-specific index of the quality of observation conditions and perpendicular sighting distance, for all sightings (left) and only those not right truncated (right). Low values of the quality index correspond to better observation conditions. The line is a simple linear regression.

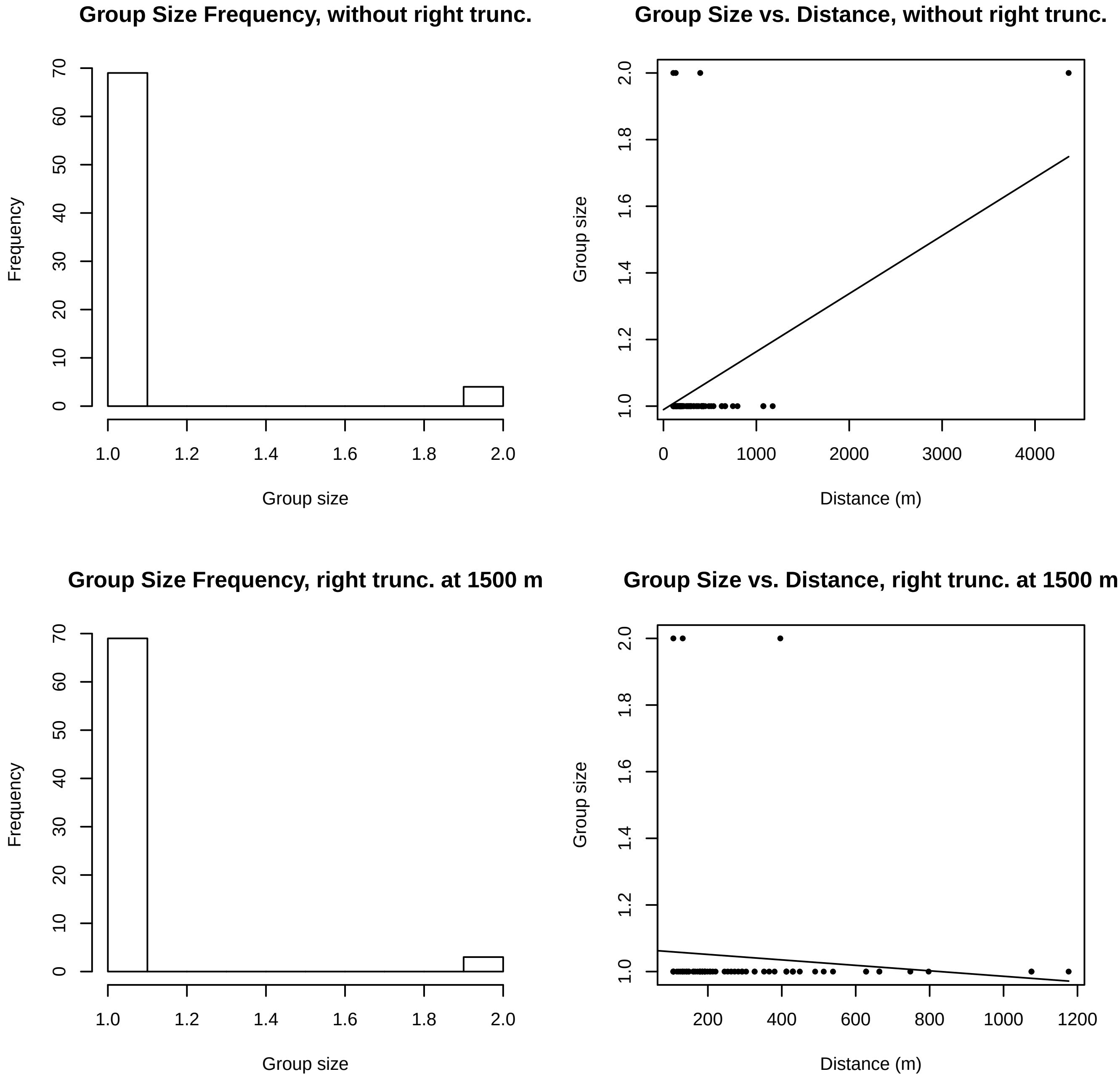

Figure 49: Histograms showing group size frequency and scatterplots showing the relationship between group size and perpendicular sighting distance, for all sightings (top row) and only those not right truncated (bottom row). In the scatterplot, the line is a simple linear regression.

NARWSS Twin Otters

The sightings were right truncated at 3000m. Due to a reduced frequency of sightings close to the trackline that plausibly resulted from the behavior of the observers and/or the configuration of the survey platform, the sightings were left truncted as well. Sightings closer than 107 m to the trackline were omitted from the analysis, and it was assumed that the the area closer to the trackline than this was not surveyed. This distance was estimated by inspecting histograms of perpendicular sighting distances. The vertical sighting angles were heaped at 10 degree increments up to 80 degrees and 1 degree increments thereafter, so the candidate detection functions were fitted using linear bins scaled accordingly.

Covariate	Description

beaufort	Beaufort sea state.
quality	Survey-specific index of the quality of observation conditions, utilizing relevant factors other than Beaufort sea state (see methods).
size	Estimated size (number of individuals) of the sighted group.

Table 31: Covariates tested in candidate “multi-covariate distance sampling” (MCDS) detection functions.

Key	Adjustment	Order	Covariates	Succeeded	Δ AIC	Mean ESHW (m)
hr				Yes	0.00	730
hr			size	Yes	1.21	732
hr			quality	Yes	1.45	725
hr			beaufort	Yes	1.73	732
hr	poly	2		Yes	1.88	722
hr	poly	4		Yes	1.95	726
hr			quality, size	Yes	2.70	727
hr			beaufort, size	Yes	2.93	734
hr			beaufort, quality	Yes	3.23	727
hr			beaufort, quality, size	Yes	4.47	729
hn	cos	2		Yes	6.21	729
hn	cos	3		Yes	41.04	670
hn				Yes	83.89	948
hn			quality	Yes	84.26	947
hn	herm	4		Yes	84.70	946
hn			size	Yes	85.12	948
hn			quality, size	Yes	85.51	947
hn			beaufort	Yes	85.72	948
hn			beaufort, quality	Yes	86.23	947
hn			beaufort, size	Yes	86.88	948
hn			beaufort, quality, size	Yes	87.44	947

Table 32: Candidate detection functions for NARWSS Twin Otters. The first one listed was selected for the density model.

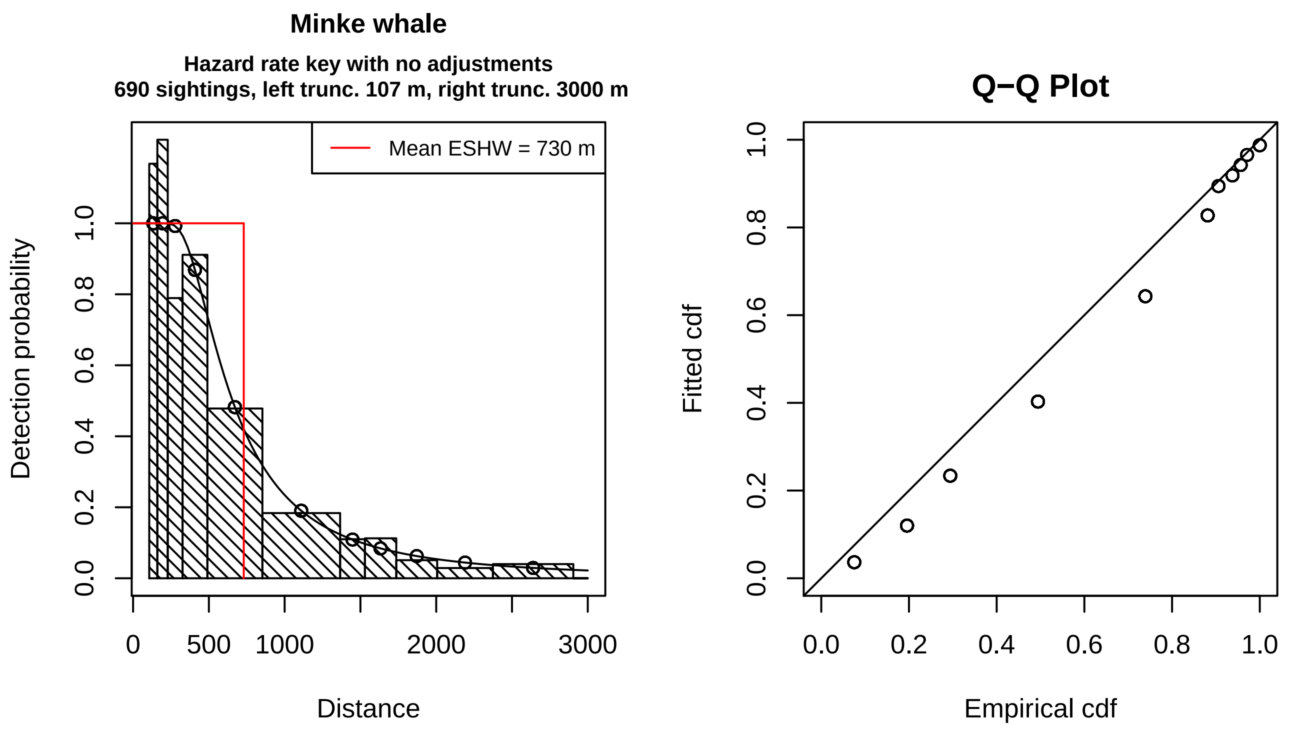

Figure 50: Detection function for NARWSS Twin Otters that was selected for the density model

Statistical output for this detection function:

```
Summary for ds object
Number of observations :  690
Distance range         :  106.5979  -  3000
AIC                    :  2870.708

Detection function:
 Hazard-rate key function

Detection function parameters
Scale Coefficients:
            estimate         se
(Intercept)  6.32497 0.07208426

Shape parameters:
             estimate         se
(Intercept) 0.8177279 0.06285359

                        Estimate           SE         CV
Average p              0.2434029   0.01353473 0.05560628
N in covered region 2834.8054751 183.46635588 0.06471920
```

Additional diagnostic plots:

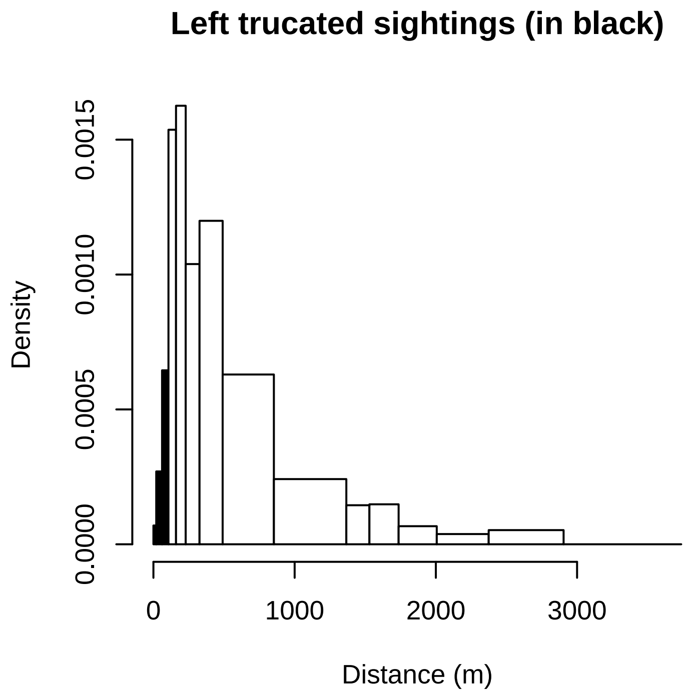

Figure 51: Density of sightings by perpendicular distance for NARWSS Twin Otters. Black bars on the left show sightings that were left truncated.

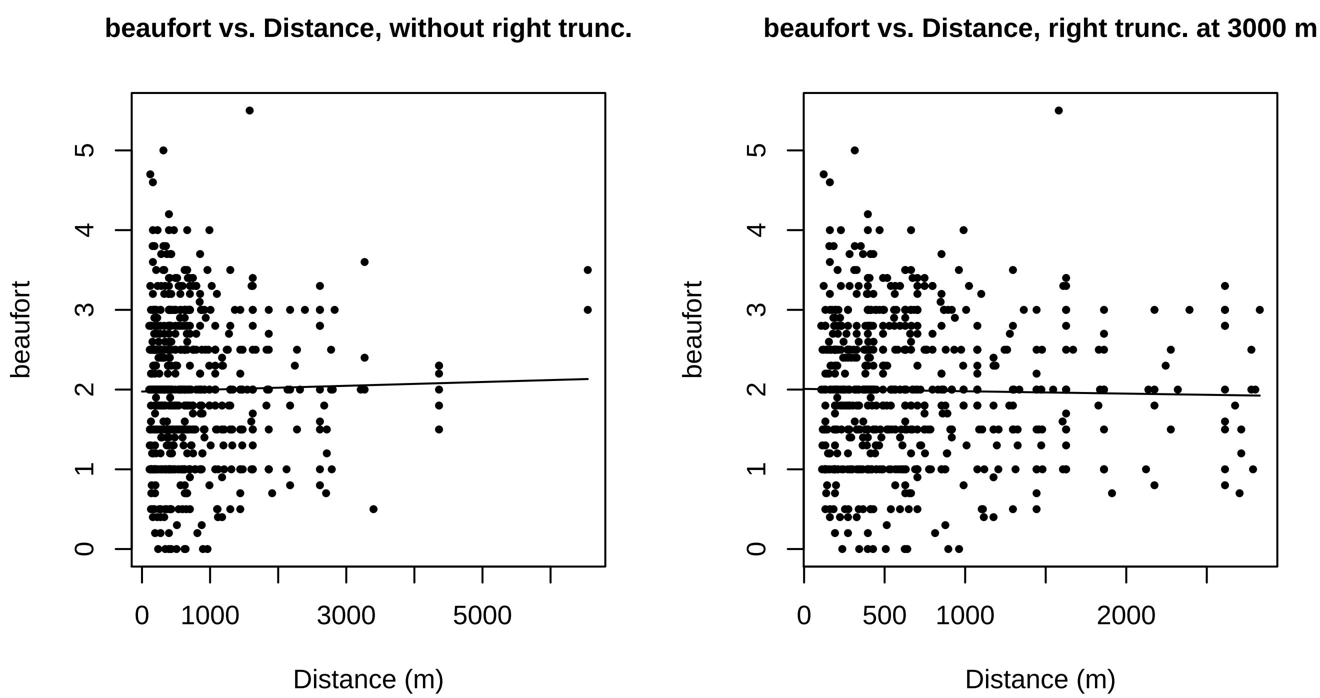

Figure 52: Scatterplots showing the relationship between Beaufort sea state and perpendicular sighting distance, for all sightings (left) and only those not right truncated (right). The line is a simple linear regression.

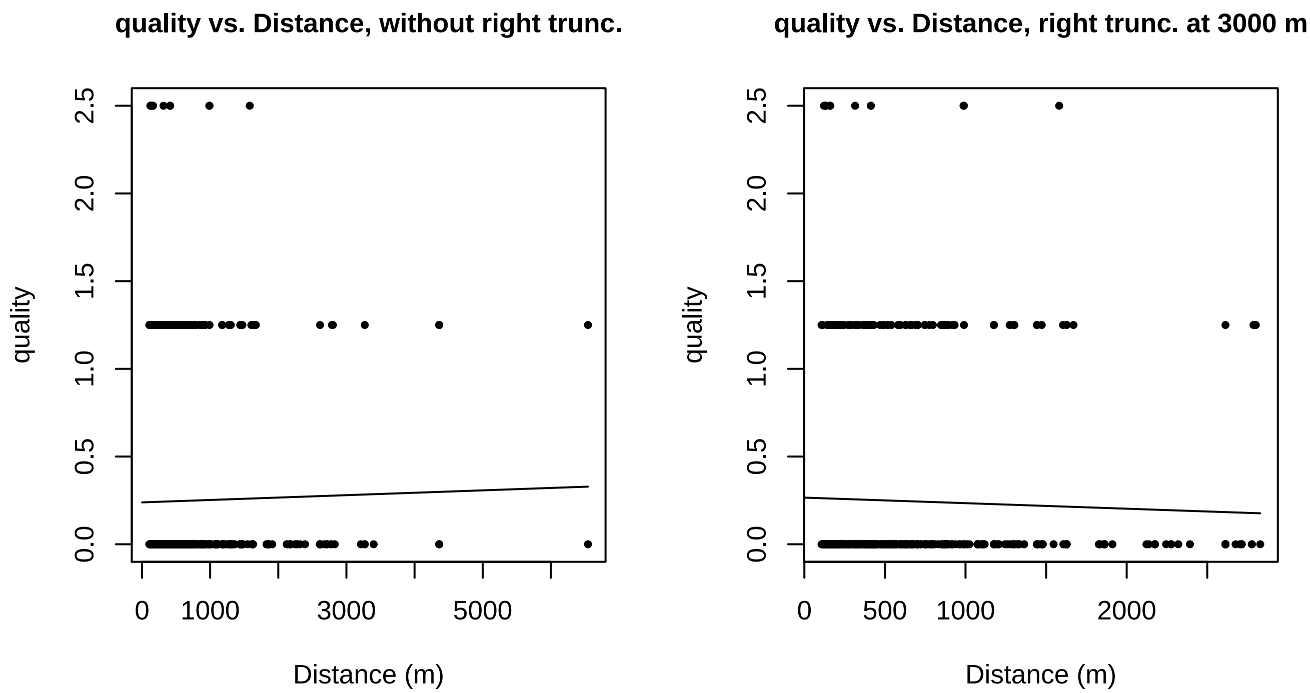

Figure 53: Scatterplots showing the relationship between the survey-specific index of the quality of observation conditions and perpendicular sighting distance, for all sightings (left) and only those not right truncated (right). Low values of the quality index correspond to better observation conditions. The line is a simple linear regression.

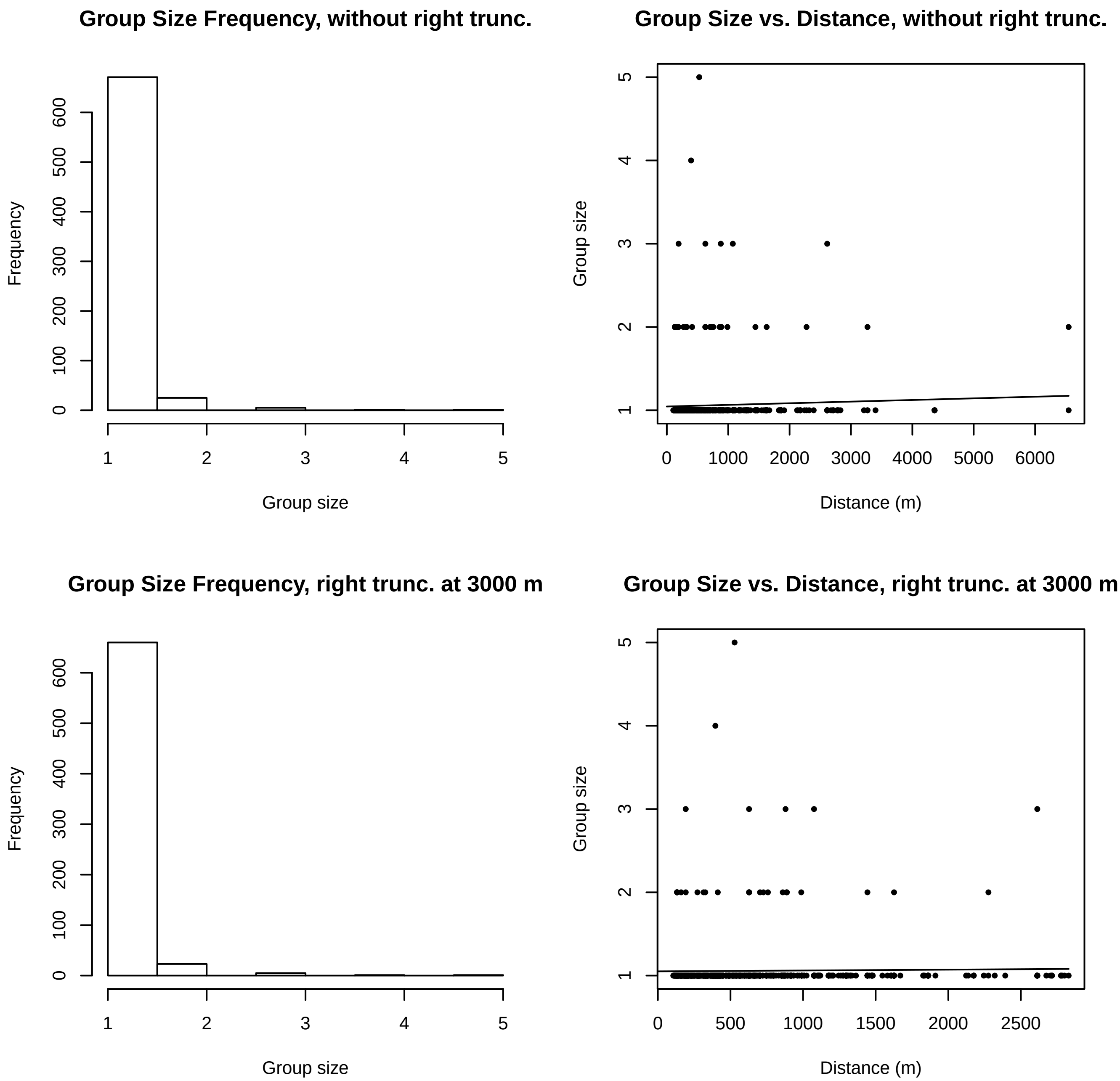

Figure 54: Histograms showing group size frequency and scatterplots showing the relationship between group size and perpendicular sighting distance, for all sightings (top row) and only those not right truncated (bottom row). In the scatterplot, the line is a simple linear regression.

g(0) Estimates

Platform	Surveys	Group Size	*g(0)*	Biases Addressed	Source
Shipboard	All	Any	0.69	Both	Palka (2006)
Aerial	All	Any	0.386	Availability	Carretta et al. (2000)

Table 33: Estimates of *g(0)* used in this density model.

According to Barlow and Forney (2007), as of 2007, there were no published estimates of g(0) for minke whales based on shipboard observers searching with 25x binoculars. Barlow and Forney based their g(0) estimate (0.846) on that for small groups of delphinids but acknowledged that minke whales are very difficult to detect. Bearing that in mind, we based our estimate on Palka's (2006) g(0) estimate (0.69) for minke whales observed by naked eye in the Gulf of Maine. We believed this would serve as a better proxy, as it was obtained only from minke whales, even if it was from a naked eye survey. In any case, the final abundance estimate is not sensitive to this choice, as very few minke whales were sighted from shipboard cruises that used binoculars.

For aerial surveys, we used Carretta et al.'s (2000) estimate of the availability bias component of g(0) for minke whales, estimated from dive data (Stern 1992) for aerial surveys conducted with two observers with bubble windows at an altitude of 213 m (700 ft) and an airspeed of 185 km/hr (100 kts). Carretta et al. did not estimate the perception bias component of g(0), asserting that perception bias for whales is expected to be negligible since they are rarely missed on the trackline.

Density Models

Less has been published about the spatiotemporal distribution of mike whales in U.S. Atlantic waters than about other balaenopterids. Waring et al. (2014) summarize minkes' spatiotemporal distribution:

> The minke whale is common and widely distributed within the U.S. Atlantic Exclusive Economic Zone (EEZ) (CETAP 1982). There appears to be a strong seasonal component to minke whale distribution. Spring and summer are times of relatively widespread and common occurrence, and when the whales are most abundant in New England waters. In New England waters during fall there are fewer minke whales, while during winter the species appears to be largely absent. Like most other baleen whales, minke whales generally occupy the continental shelf proper (< 100 m deep), rather than the continental shelf-edge region. Records summarized by Mitchell (1991) hint at a possible winter distribution in the West Indies, and in the mid-ocean south and east of Bermuda. As with several other cetacean species, the possibility of a deep-ocean component to the distribution of minke whales exists but remains unconfirmed.

Minke whales have been observed feeding in the Gulf of Maine from March-September (CETAP 1982). Similar to other balaenopterids, minke whales are believed to follow an annual migration pattern of moving to high latitudes in summer to feed and returning to low latitudes to breed.

We modeled minke whales using a two-season model. We fixed the summer/winter and winter/summer transitions at October/November and March/April based on the reduced presence of minkes in the Gulf of Maine in November-March, and the sighting of minkes in each month of December-March between Cape Hatteras and Florida.

Acoustic monitoring detected minkes close to the deep side of the continental shelf break in Jacksonville, Florida in December-March (Debich et al. 2013; Norris et al. 2014) with a single pulse train detected in June. A similar study detected minkes close to the deep side of the shelf break near Onslow Bay, North Carolina in November-April (Hodge and Read 2014) and at a more distant site September-November, with substantially more detections in November, and no monitoring performed in December-June (Debich et al. 2014). Finally, a similar study detected minkes close to the deep side of the shelf break near Cape Hatteras in March and April, the only months that were monitored (Stanistreet et al. 2013). Risch et al. (2014) synthesized these acoustic monitoring results into a summary view of the temporal dynamics of minke whale migrations in the region. Together, these results generally support our seasonal divisions.

Winter

In this season, the available survey effort was restricted to two areas: a northeast region comprised of the Gulf of Maine, southern New England, and part of Georges Bank, and a southeast region, mainly along the shelf, between New Jersey and Miami. Little effort was conducted off the shelf in either area.

In the northern part of the study area, all of the sightings were on the shelf, while in the southern part, all were off the shelf. Acoustic results confirm the presence of minkes off the shelf in the south, and aerial sightings of mother-calf pairs between North Carolina and Florida, as well as stranding records of calves, suggest the off-shelf southeast region may be a breeding and calving area for minke whales (Risch et al. 2014).

Proceeding from this hypothesis, we split the study area at Cape Hatteras, where the Gulf Stream leaves the continental shelf. South of this area, waters are warm and presumably more likely to be calving habitat. North of it, winter waters are cold, and we presume minke whales here are overwintering rather than breeding.

In the south, we split the study area again at the shelf break (we used the 125 m isobath). No sightings were reported on the shelf over many years of surveying. Risch et al. (2014) reported that acoustic instruments deployed near Jacksonville, Florida both on and off the shelf only detected minke whales off the shelf. This is consistent with the aerial surveys conducted in the same region conducted by University of Carolina at Wilmington (see Figure 55, dense tracklines at 30 N). In the southern on-shelf region, we assumed that minkes were absent.

In the off-shelf region, we estimated mean density across the area that was surveyed, clipping our model tightly to the survey tracklines to reflect our uncertainty about the area. We also investigated the possibility of fitting a model with one predictor, but this model selected distance to 125 m isobath as the best predictor, reflecting the close proximity of all of the sightings to the shelf break. This model predicted a very patchy distribution, with nearly all of the abundance concentrated at the shelf break. The Gulf Stream also follows the shelf break through this area; when we eliminated all static predictors from our experimental model, it selected total kinetic energy instead, concentrating minke abundance in the Gulf Stream.

Risch et al. (2014) speculated that minkes could be following the Gulf Stream during their northward spring migration. Some of the sightings in our database reported by surveys off North Carolina were in February and March; these could be consistent with Risch et al.'s hypothesis. But given the low, patchy survey effort in the area, we were reluctant to adopt a model that concentrated abundance so strongly in the Gulf Stream, particularly because acoustic results have also detected minkes far from it, including at the mid-Atlantic ridge (Risch et al. 2014). We reviewed our decision to not attempt a habitat-based model for the southern region with D. Risch in January 2015; she concurred with our decision.

In the north, there were sufficient sightings to fit a habitat-based model from environmental predictors. We did not split the study area at the shelf break, but again clipped the model tightly to the survey tracklines to reflect uncertainty.

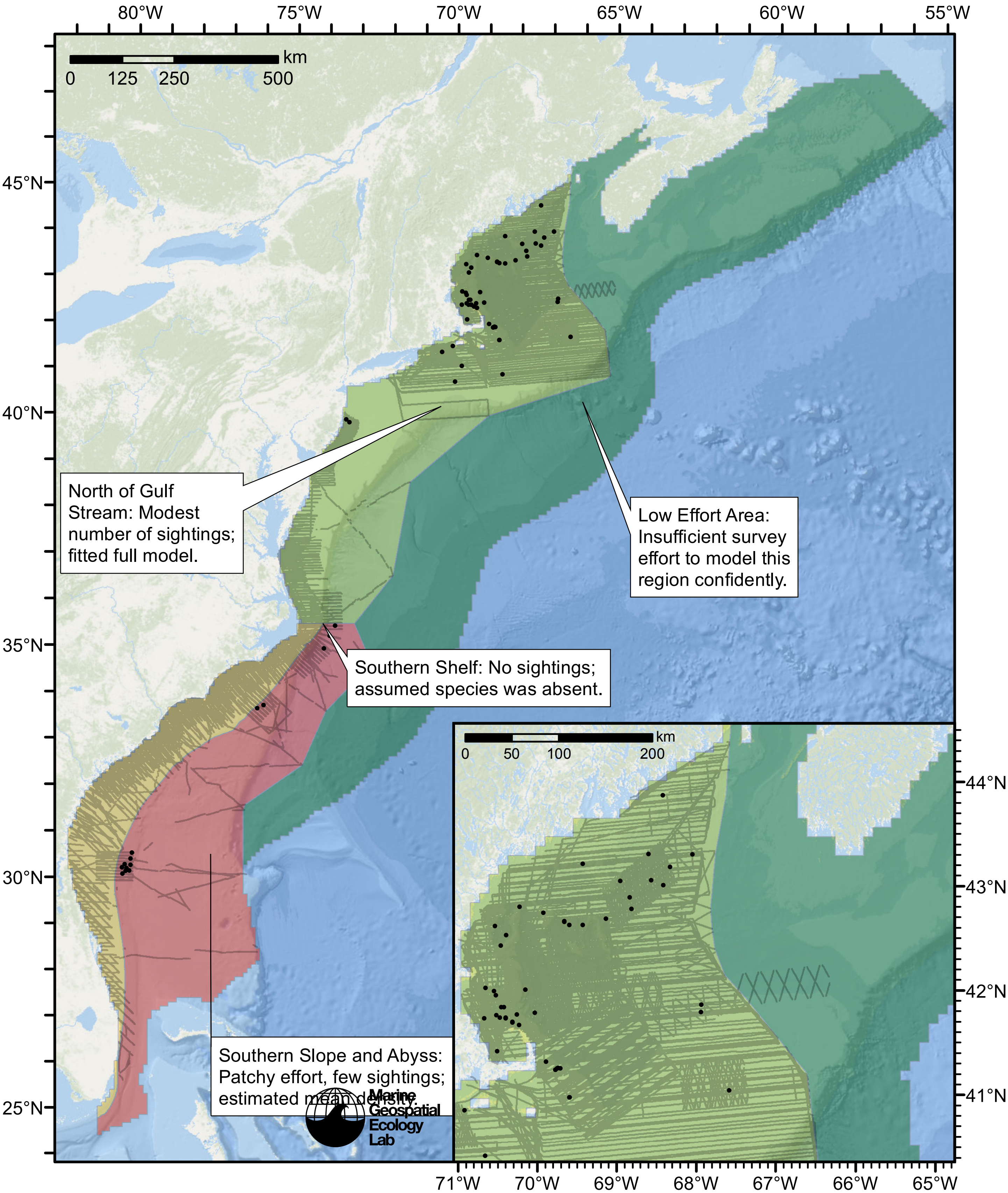

Figure 55: Minke whale density model schematic for Winter season. All on-effort sightings are shown, including those that were truncated when detection functions were fitted.

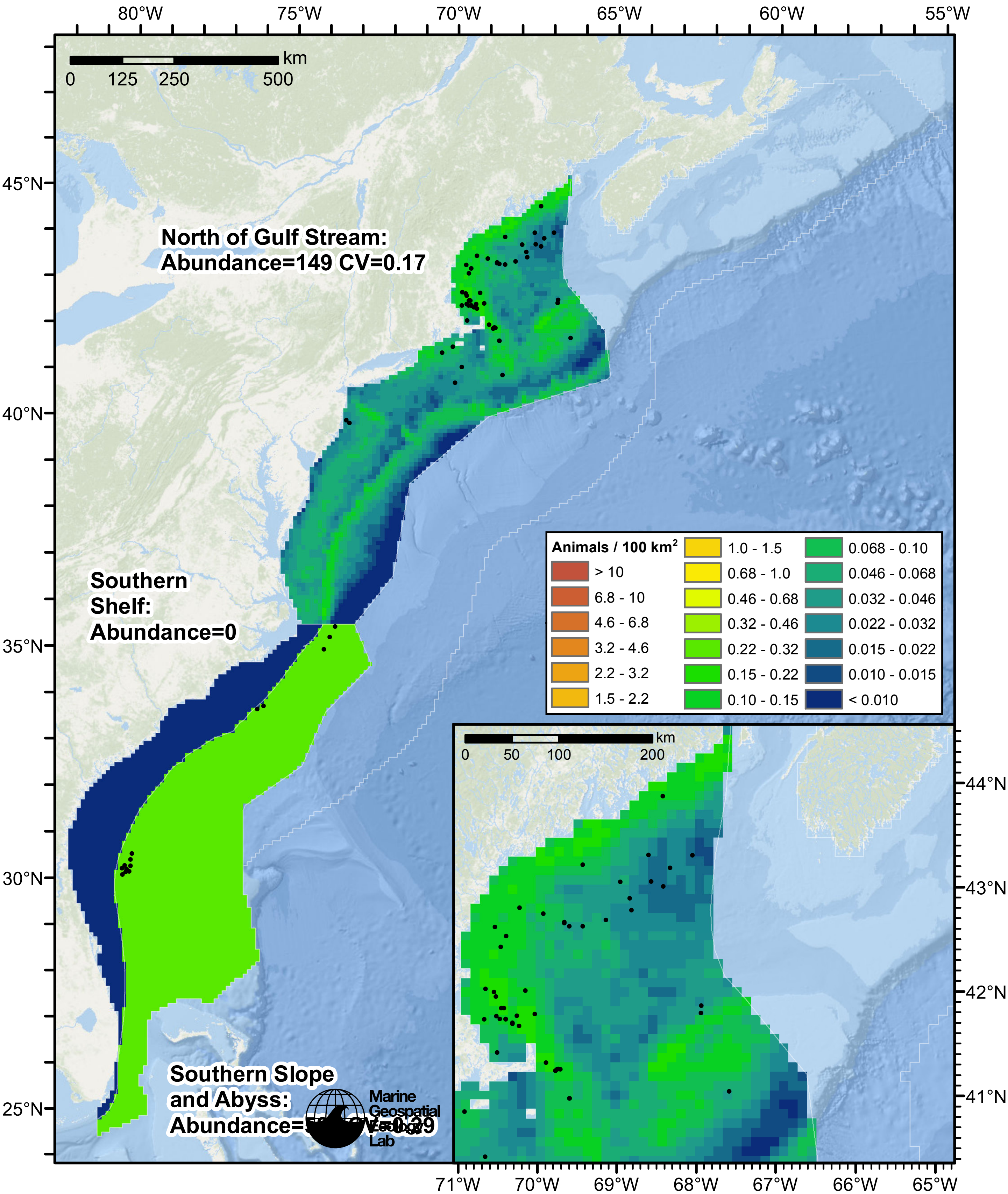

Figure 56: Minke whale density predicted by the Winter season climatological model that explained the most deviance. Pixels are 10x10 km. The legend gives the estimated individuals per pixel; breaks are logarithmic. The same scale is used for all seasons. Abundance for each region was computed by summing the density cells occuring in that region.

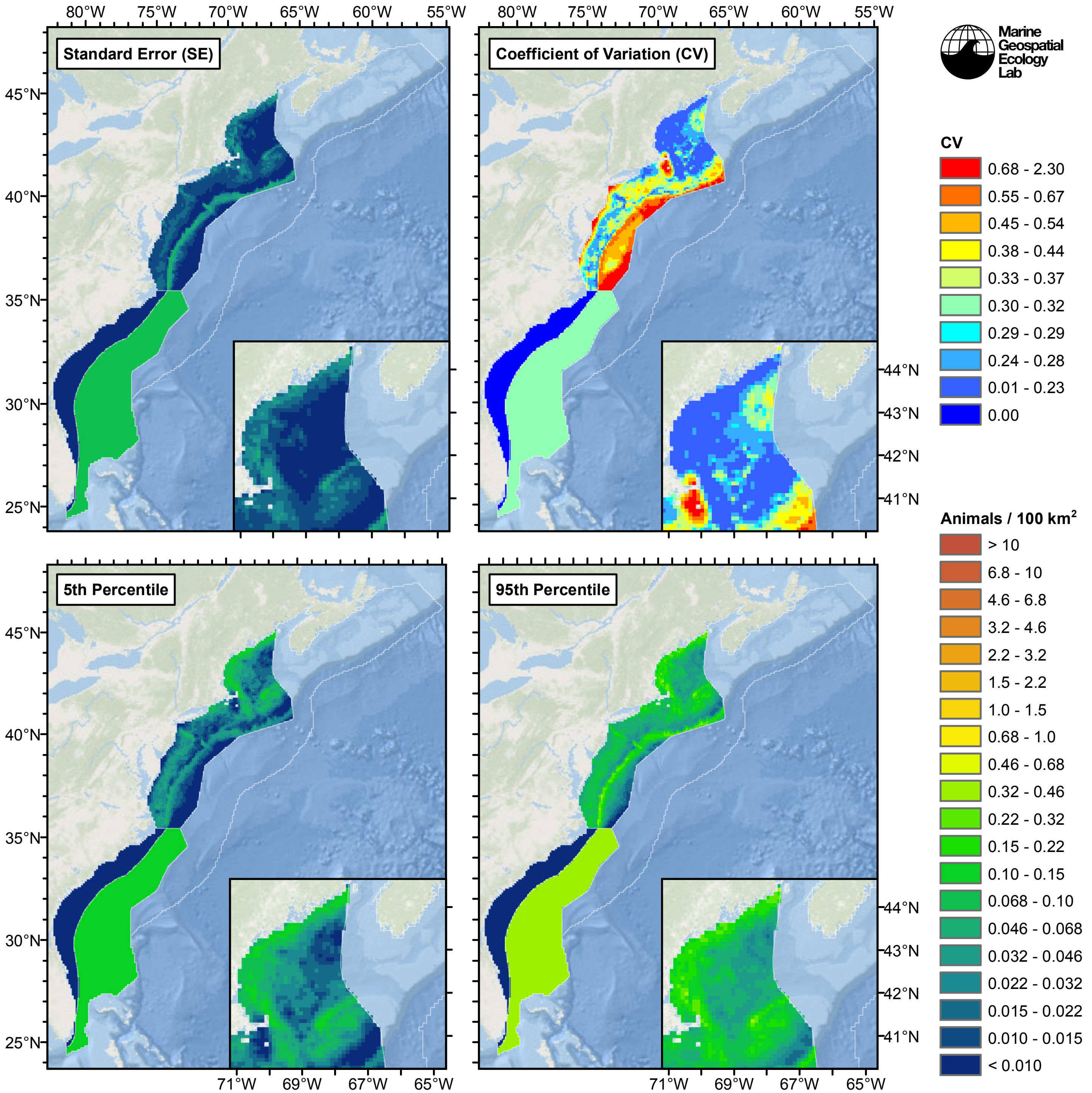

Figure 57: Estimated uncertainty for the Winter season climatological model that explained the most deviance. These estimates only incorporate the statistical uncertainty estimated for the spatial model (by the R mgcv package). They do not incorporate uncertainty in the detection functions, g(0) estimates, predictor variables, and so on.

North of Gulf Stream

Statistical output

```
Rscript.exe: This is mgcv 1.8-3. For overview type 'help("mgcv-package")'.


Family: Tweedie(p=1.106)
```

```
Link function: log

Formula:
abundance ~ offset(log(area_km2)) + s(log10(Slope), bs = "ts",
    k = 5) + s(ClimChl1, bs = "ts", k = 5)

Parametric coefficients:
            Estimate Std. Error t value Pr(>|t|)
(Intercept)  -7.6538     0.1859  -41.18   <2e-16 ***
---
Signif. codes:  0 '***' 0.001 '**' 0.01 '*' 0.05 '.' 0.1 ' ' 1

Approximate significance of smooth terms:
                  edf Ref.df     F  p-value
s(log10(Slope)) 1.012      4 3.316 0.000173 ***
s(ClimChl1)     2.453      4 4.225 0.000136 ***
---
Signif. codes:  0 '***' 0.001 '**' 0.01 '*' 0.05 '.' 0.1 ' ' 1

R-sq.(adj) =  0.00104   Deviance explained = 9.16%
-REML = 472.77  Scale est. = 18.704    n = 18415

All predictors were significant. This is the final model.
Creating term plots.
Diagnostic output from gam.check():

Method: REML   Optimizer: outer newton
full convergence after 12 iterations.
Gradient range [-9.482685e-07,1.048288e-06]
(score 472.7729 & scale 18.70364).
Hessian positive definite, eigenvalue range [0.3332399,513.7657].
Model rank =  9 / 9

Basis dimension (k) checking results. Low p-value (k-index<1) may
indicate that k is too low, especially if edf is close to k'.

                   k'   edf k-index p-value
s(log10(Slope)) 4.000 1.012   0.843    0.06
s(ClimChl1)     4.000 2.453   0.837    0.01

Predictors retained during the model selection procedure: Slope, ClimChl1

Predictors dropped during the model selection procedure: Depth, DistToShore, DistTo125m, DistTo300m,
ClimSST, ClimDistToFront1, ClimTKE
```

Model term plots

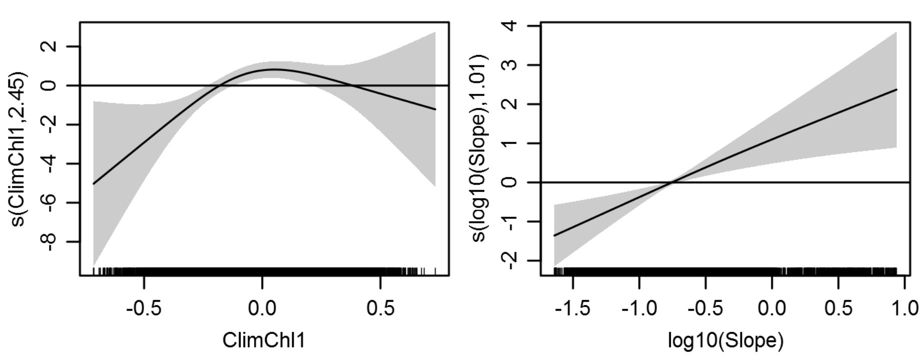

Diagnostic plots

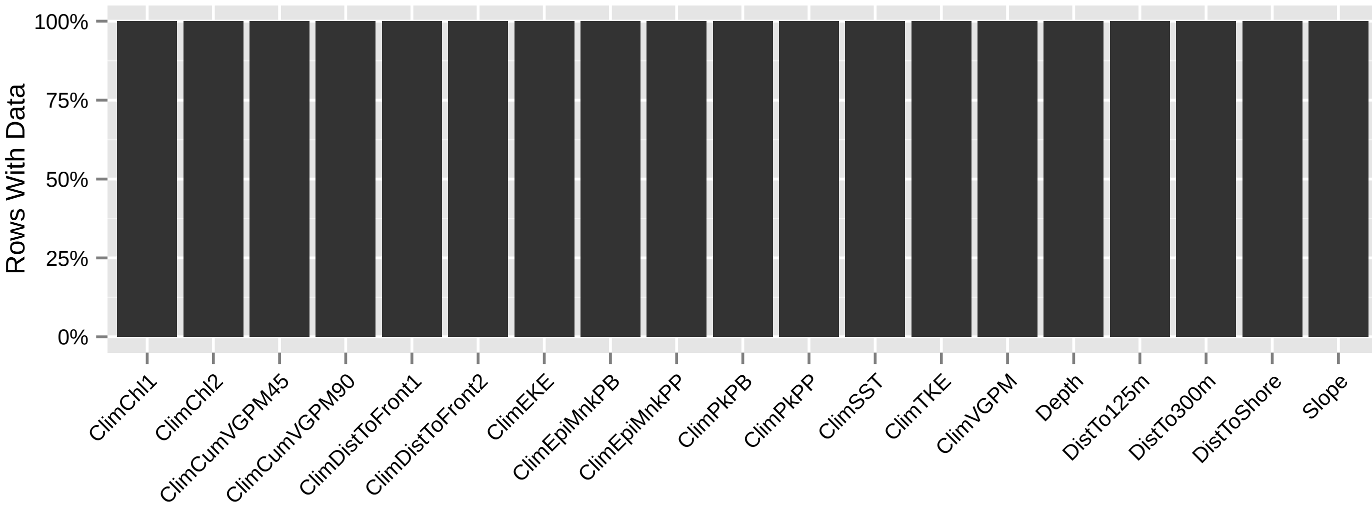

Figure 58: Segments with predictor values for the Minke whale Climatological model, Winter season, North of Gulf Stream. This plot is used to assess how many segments would be lost by including a given predictor in a model.

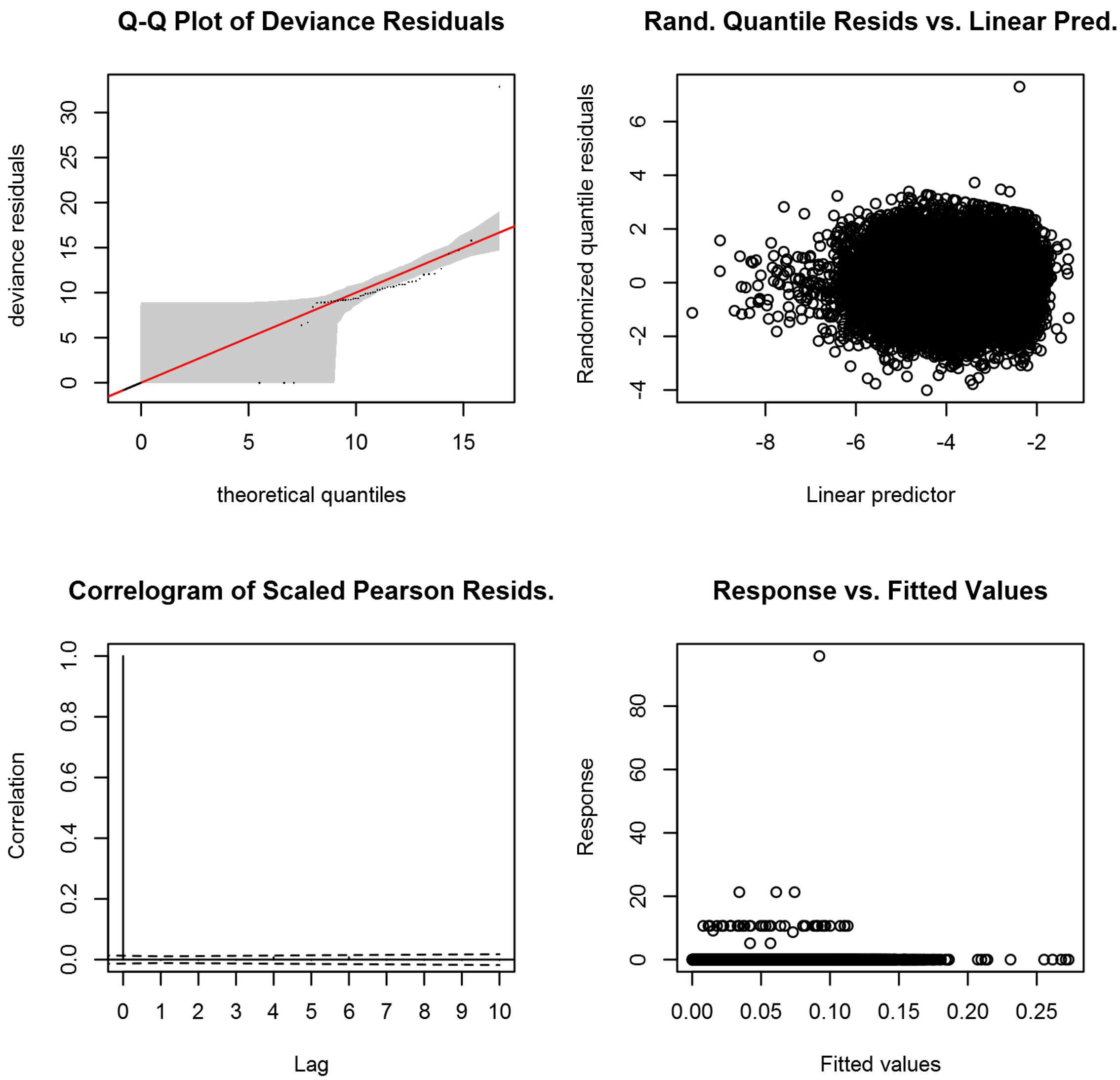

Figure 59: Statistical diagnostic plots for the Minke whale Climatological model, Winter season, North of Gulf Stream.

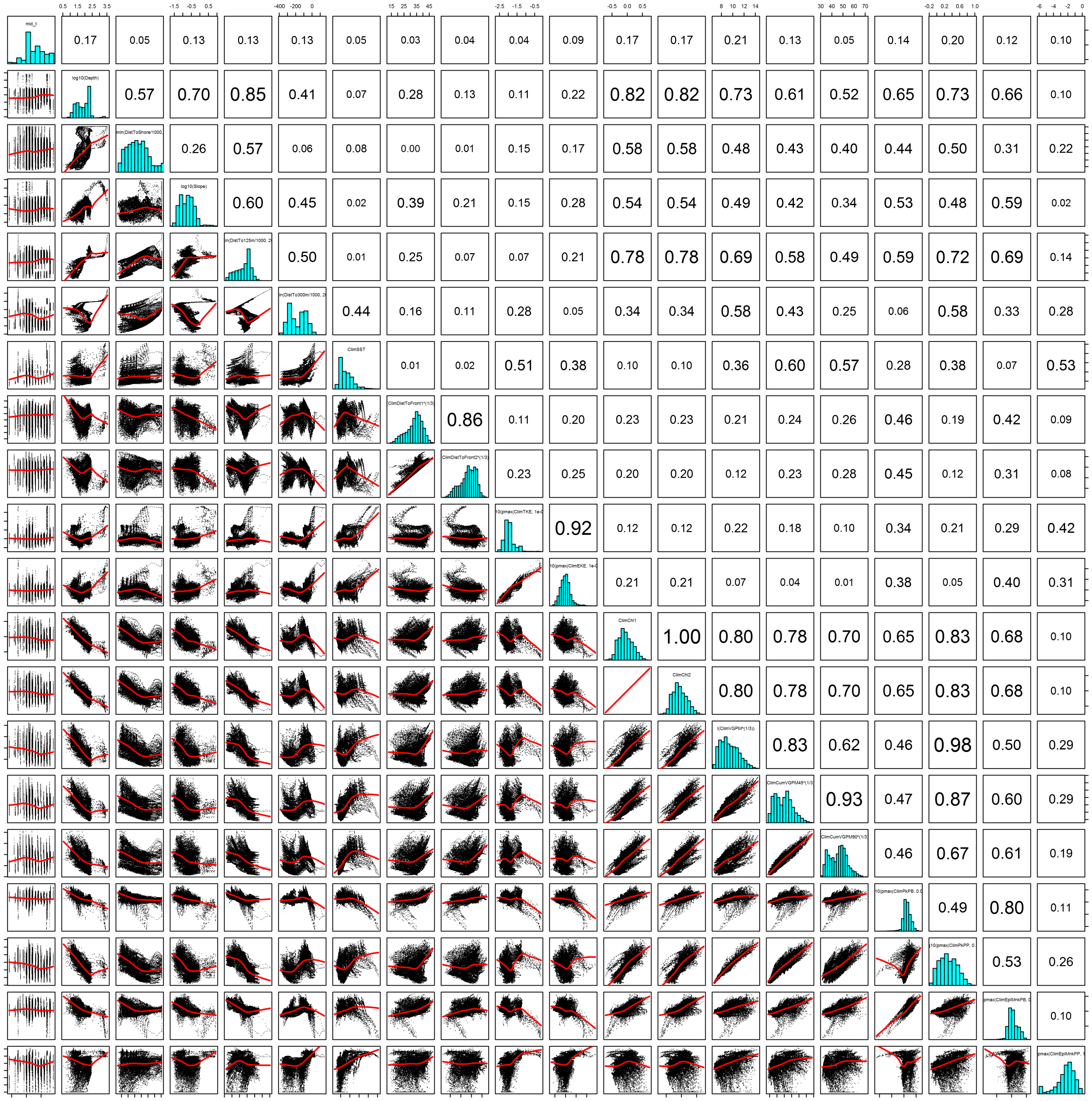

Figure 60: Scatterplot matrix for the Minke whale Climatological model, Winter season, North of Gulf Stream. This plot is used to inspect the distribution of predictors (via histograms along the diagonal), simple correlation between predictors (via pairwise Pearson coefficients above the diagonal), and linearity of predictor correlations (via scatterplots below the diagonal). This plot is best viewed at high magnification.

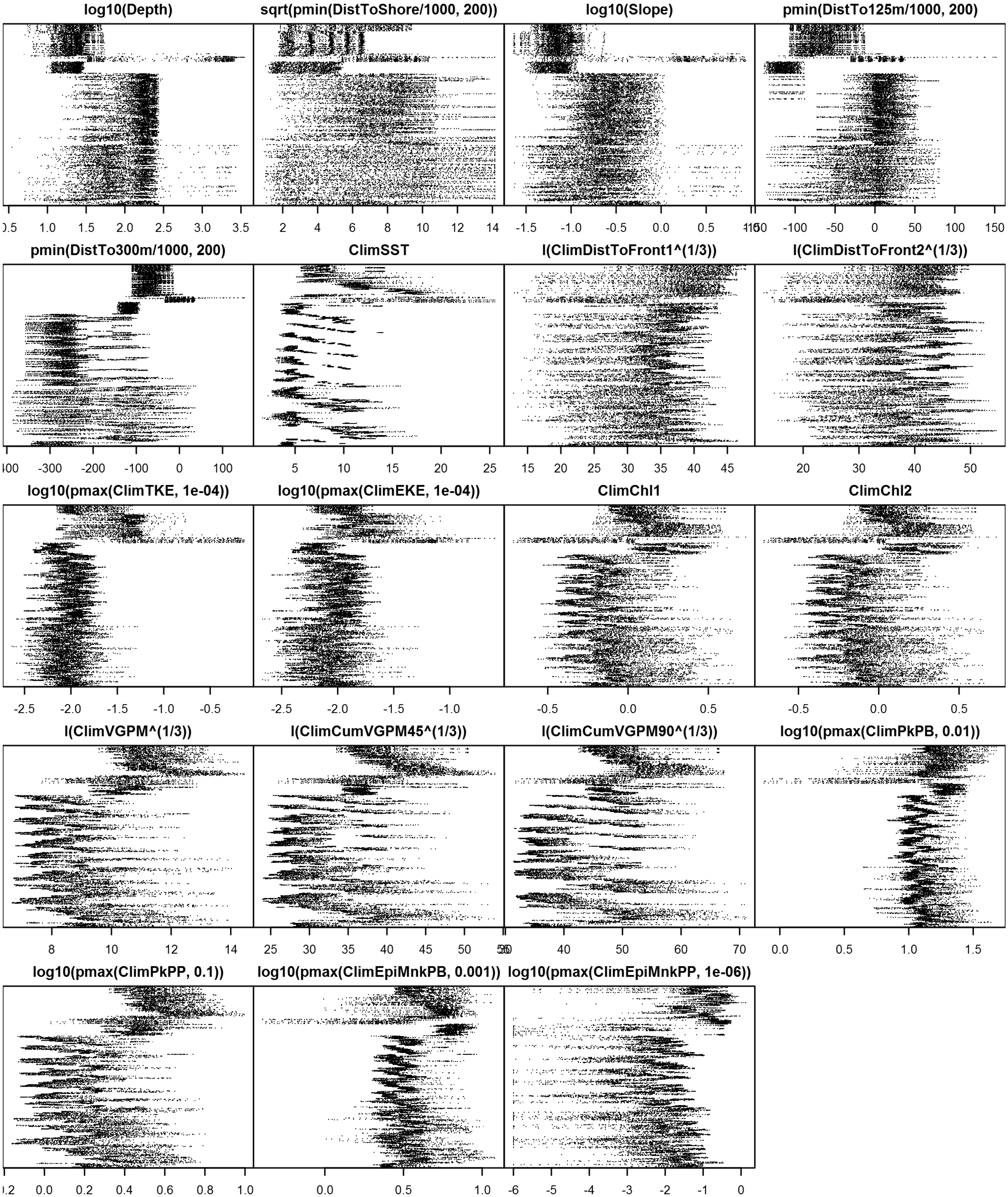

Figure 61: Dotplot for the Minke whale Climatological model, Winter season, North of Gulf Stream. This plot is used to check for suspicious patterns and outliers in the data. Points are ordered vertically by transect ID, sequentially in time.

Southern Slope and Abyss

A mean density estimate was made for this region. First, density (individuals per square kilometer) was calculated as the number of animals encountered divided by the area effectively surveyed, corrected by the detection functions and g(0) estimates. Then, density was multiplied by the size of each grid cell, in square kilometers, to obtain abundance (number of individuals) per grid cell. Finally, all grid cells in the region were assigned this abundance value.

Southern Shelf

Density assumed to be 0 in this region.

Low Effort Area

Density was not modeled for this region.

Contemporaneous Model

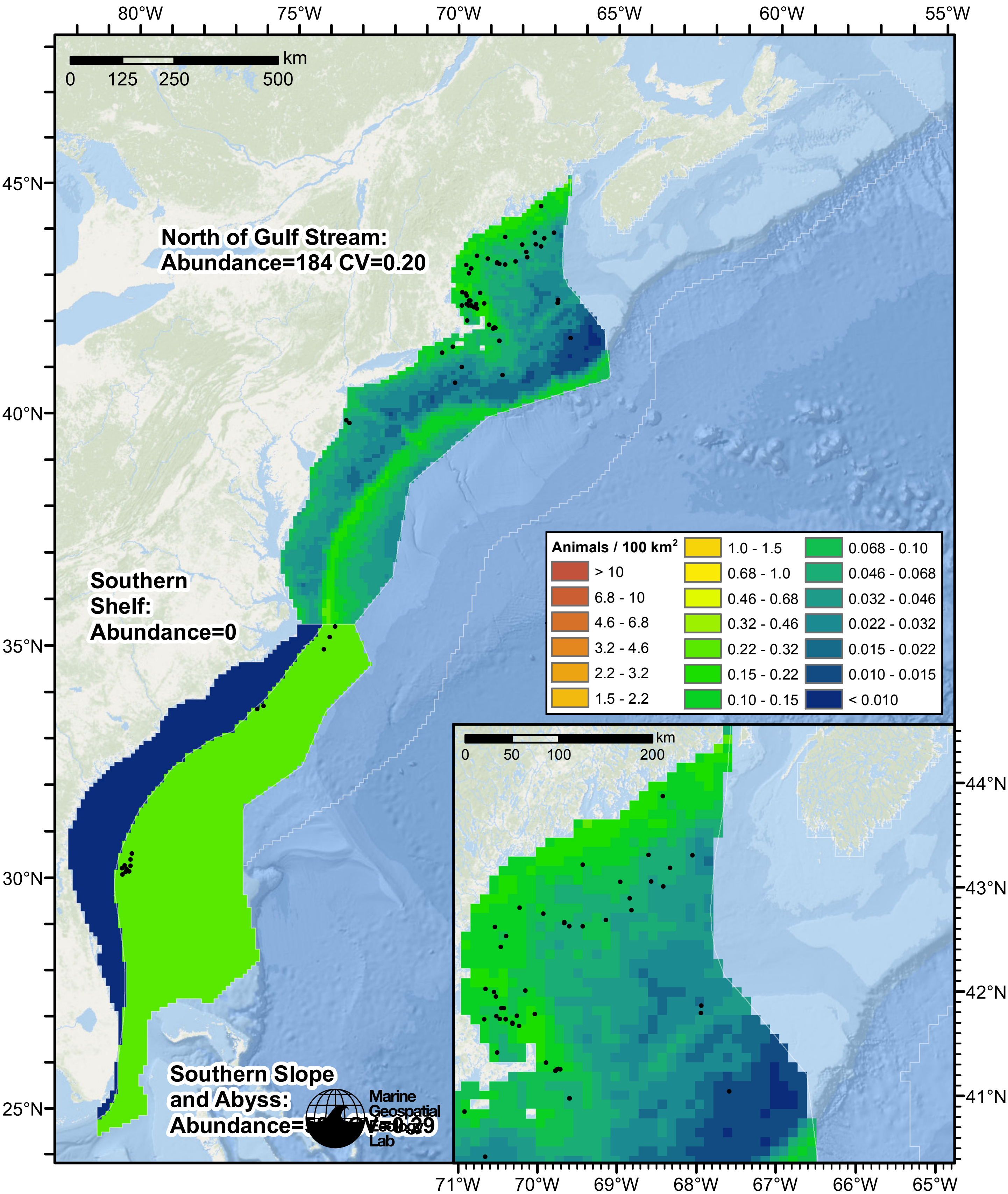

Figure 62: Minke whale density predicted by the Winter season contemporaneous model that explained the most deviance. Pixels are 10x10 km. The legend gives the estimated individuals per pixel; breaks are logarithmic. The same scale is used for all seasons. Abundance for each region was computed by summing the density cells occuring in that region.

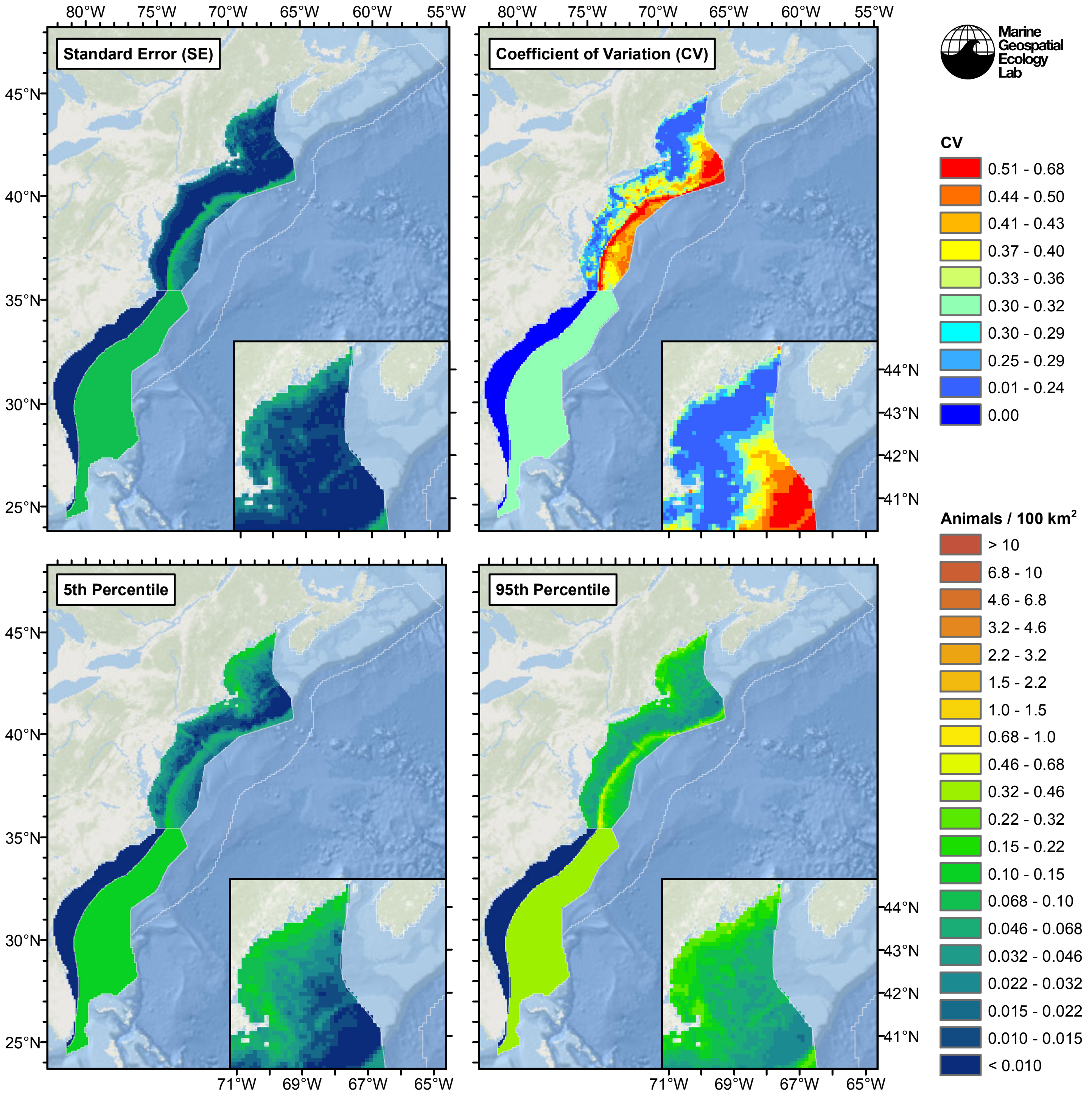

Figure 63: Estimated uncertainty for the Winter season contemporaneous model that explained the most deviance. These estimates only incorporate the statistical uncertainty estimated for the spatial model (by the R mgcv package). They do not incorporate uncertainty in the detection functions, g(0) estimates, predictor variables, and so on.

North of Gulf Stream

Statistical output

```
Rscript.exe: This is mgcv 1.8-3. For overview type 'help("mgcv-package")'.


Family: Tweedie(p=1.113)
```

```
Link function: log

Formula:
abundance ~ offset(log(area_km2)) + s(sqrt(pmin(DistToShore/1000,
    200)), bs = "ts", k = 5) + s(log10(Slope), bs = "ts", k = 5)

Parametric coefficients:
            Estimate Std. Error t value Pr(>|t|)
(Intercept)   -7.486      0.167  -44.82   <2e-16 ***
---
Signif. codes:  0 '***' 0.001 '**' 0.01 '*' 0.05 '.' 0.1 ' ' 1

Approximate significance of smooth terms:
                                       edf Ref.df     F  p-value
s(sqrt(pmin(DistToShore/1000, 200))) 0.9783      4 2.237 0.001677 **
s(log10(Slope))                      0.9787      4 2.596 0.000773 ***
---
Signif. codes:  0 '***' 0.001 '**' 0.01 '*' 0.05 '.' 0.1 ' ' 1

R-sq.(adj) =  0.000787   Deviance explained = 6.26%
-REML = 475.47  Scale est. = 19.624    n = 18415

All predictors were significant. This is the final model.
Creating term plots.
Diagnostic output from gam.check():

Method: REML   Optimizer: outer newton
full convergence after 10 iterations.
Gradient range [-0.0008479753,0.0003972762]
(score 475.47 & scale 19.62408).
Hessian positive definite, eigenvalue range [0.3152799,496.7147].
Model rank =  9 / 9

Basis dimension (k) checking results. Low p-value (k-index<1) may
indicate that k is too low, especially if edf is close to k'.

                                       k'   edf k-index p-value
s(sqrt(pmin(DistToShore/1000, 200))) 4.000 0.978   0.821    0.12
s(log10(Slope))                      4.000 0.979   0.781    0.02

Predictors retained during the model selection procedure: DistToShore, Slope

Predictors dropped during the model selection procedure: Depth, DistTo125m, DistTo300m, SST,
DistToFront1
```

Model term plots

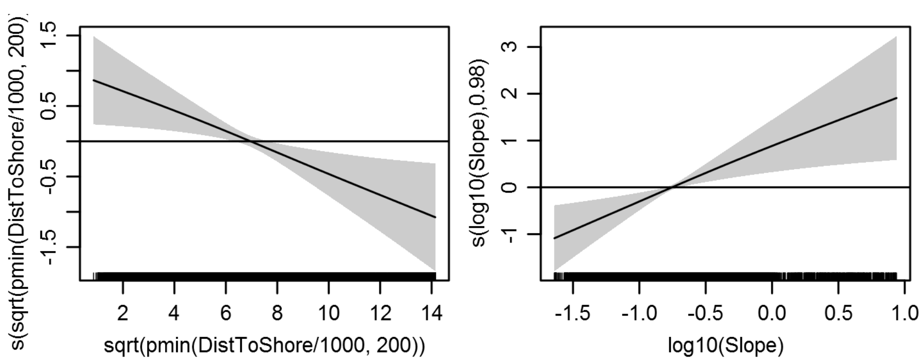

Diagnostic plots

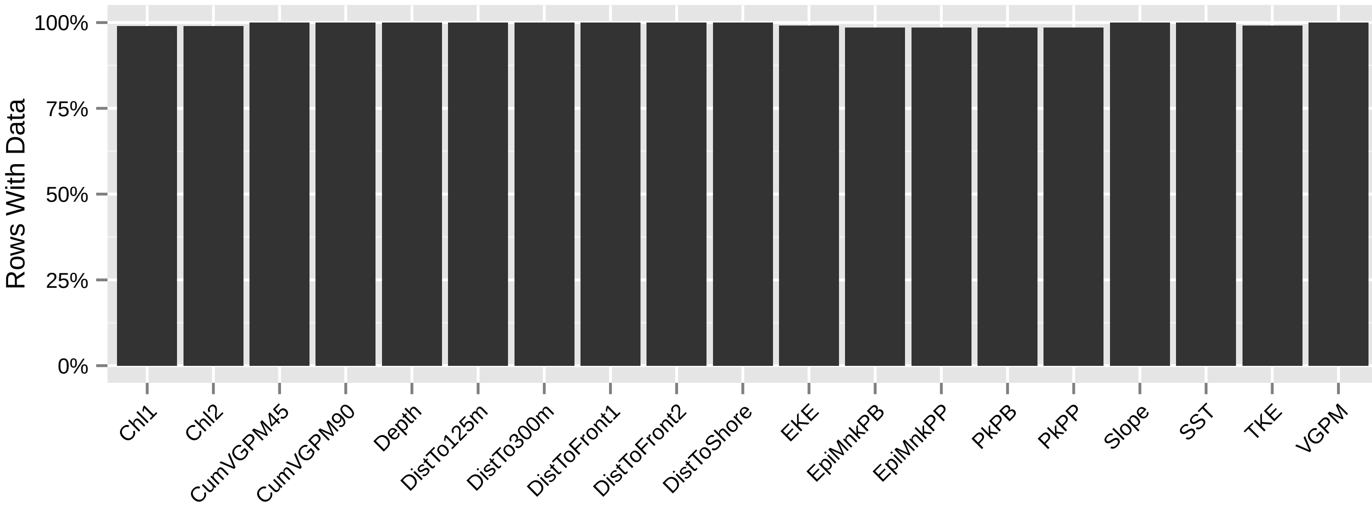

Figure 64: Segments with predictor values for the Minke whale Contemporaneous model, Winter season, North of Gulf Stream. This plot is used to assess how many segments would be lost by including a given predictor in a model.

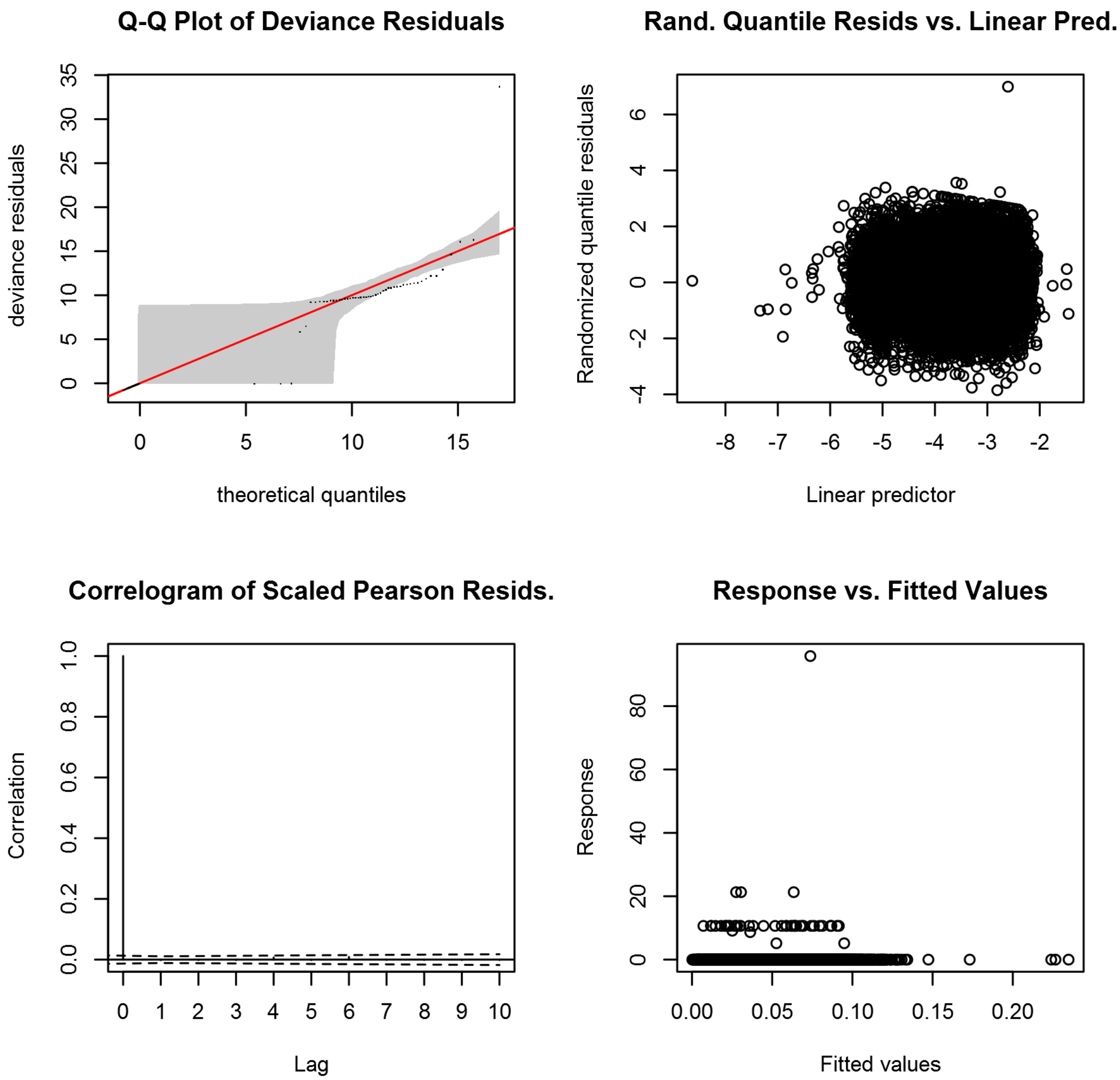

Figure 65: Statistical diagnostic plots for the Minke whale Contemporaneous model, Winter season, North of Gulf Stream.

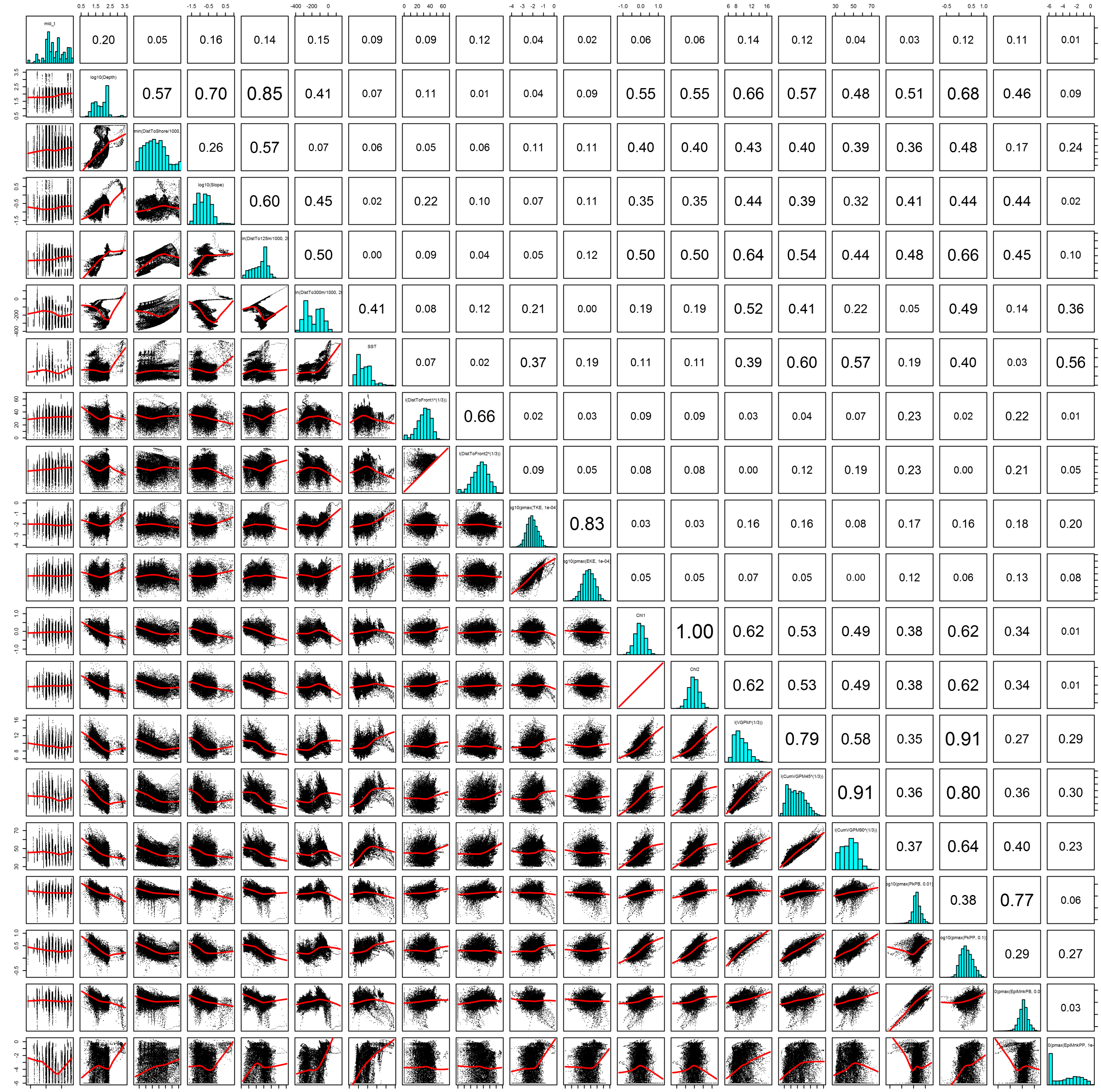

Figure 66: Scatterplot matrix for the Minke whale Contemporaneous model, Winter season, North of Gulf Stream. This plot is used to inspect the distribution of predictors (via histograms along the diagonal), simple correlation between predictors (via pairwise Pearson coefficients above the diagonal), and linearity of predictor correlations (via scatterplots below the diagonal). This plot is best viewed at high magnification.

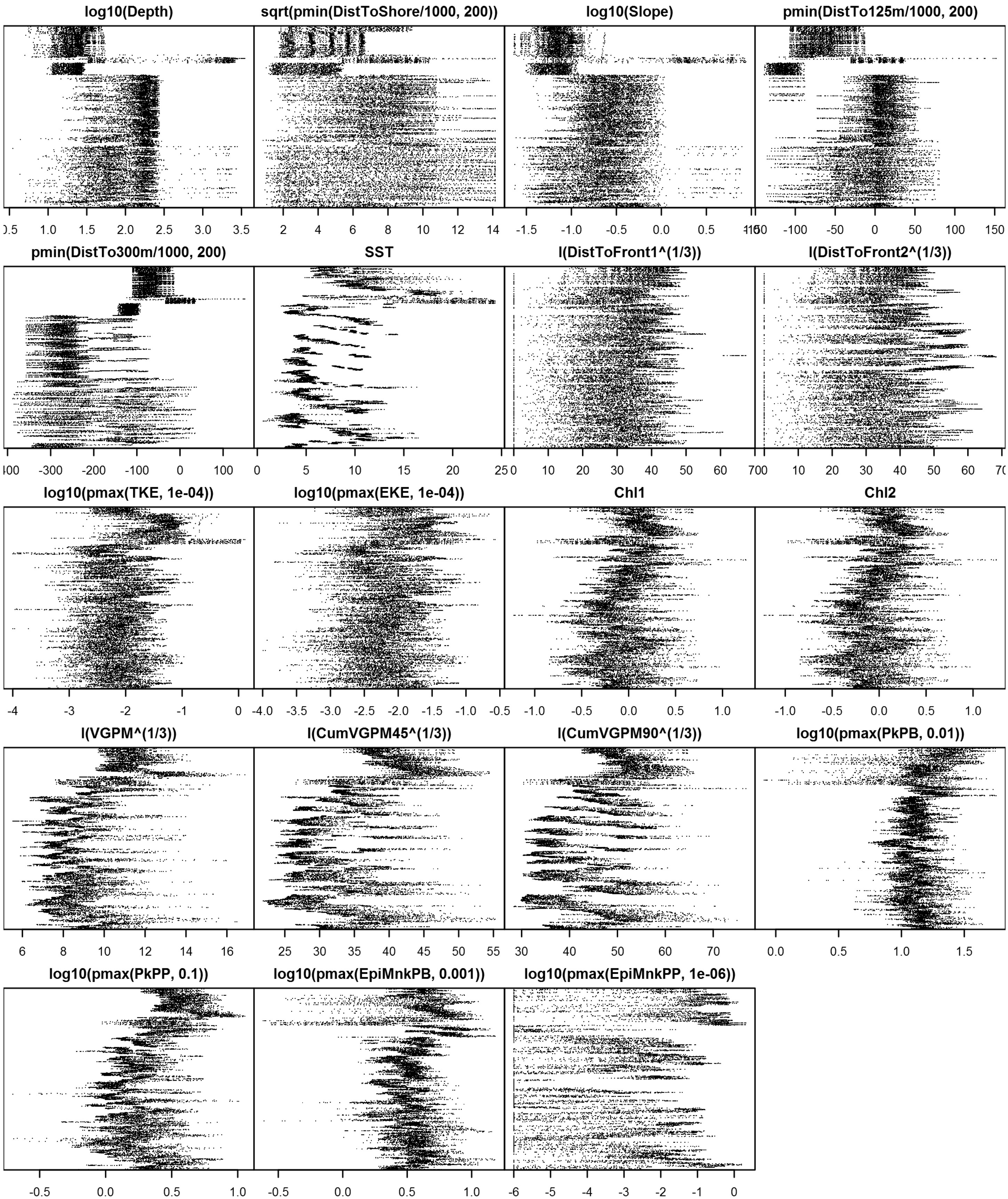

Figure 67: Dotplot for the Minke whale Contemporaneous model, Winter season, North of Gulf Stream. This plot is used to check for suspicious patterns and outliers in the data. Points are ordered vertically by transect ID, sequentially in time.

Southern Slope and Abyss

A mean density estimate was made for this region. First, density (individuals per square kilometer) was calculated as the number of animals encountered divided by the area effectively surveyed, corrected by the detection functions and g(0) estimates. Then, density was multiplied by the size of each grid cell, in square kilometers, to obtain abundance (number of individuals) per grid cell. Finally, all grid cells in the region were assigned this abundance value.

Southern Shelf

Density assumed to be 0 in this region.

Low Effort Area

Density was not modeled for this region.

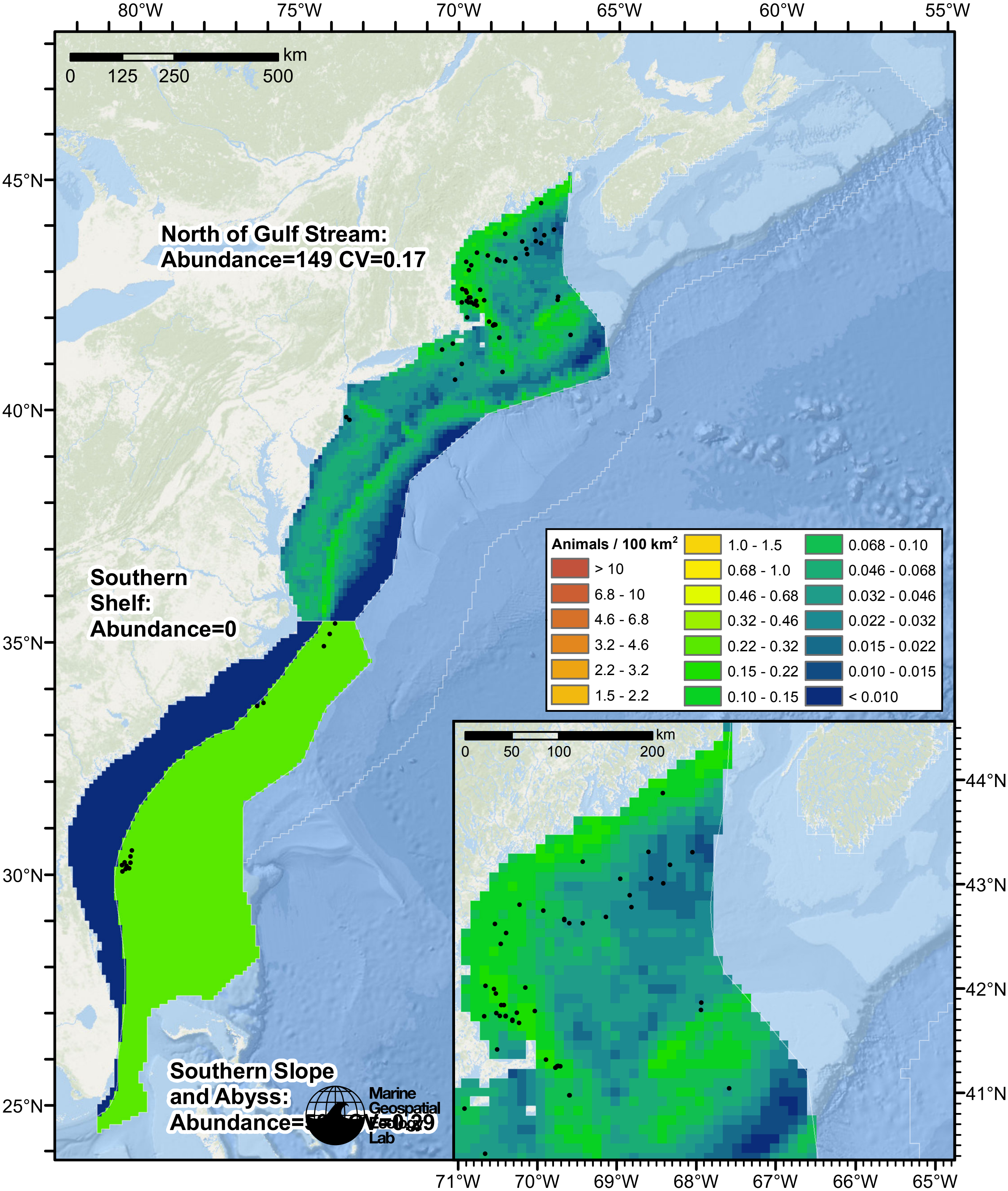

Figure 68: Minke whale density predicted by the Winter season climatological same segments model that explained the most deviance. Pixels are 10x10 km. The legend gives the estimated individuals per pixel; breaks are logarithmic. The same scale is used for all seasons. Abundance for each region was computed by summing the density cells occuring in that region.

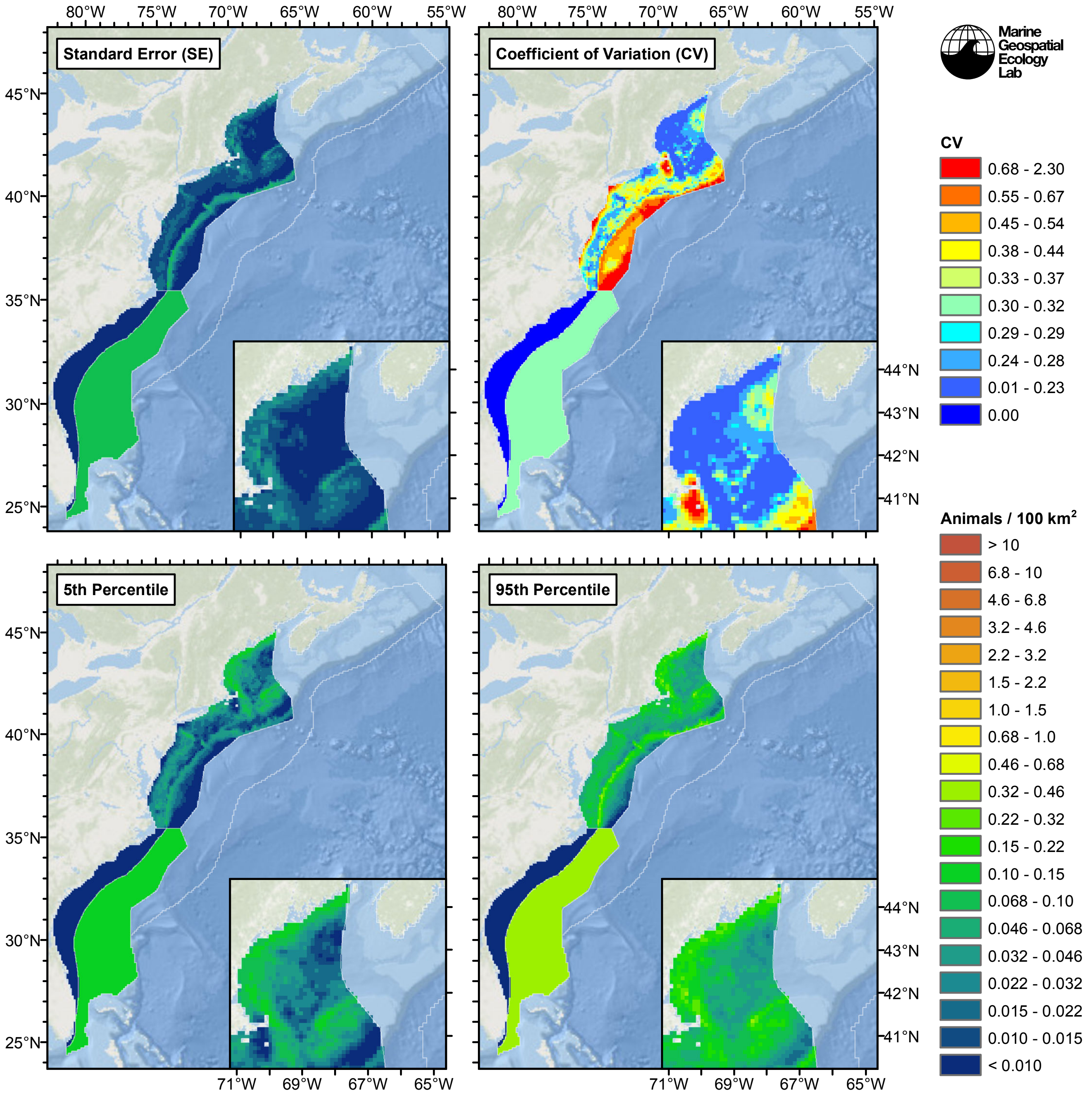

Figure 69: Estimated uncertainty for the Winter season climatological same segments model that explained the most deviance. These estimates only incorporate the statistical uncertainty estimated for the spatial model (by the R mgcv package). They do not incorporate uncertainty in the detection functions, g(0) estimates, predictor variables, and so on.

North of Gulf Stream

Statistical output

```
Rscript.exe: This is mgcv 1.8-3. For overview type 'help("mgcv-package")'.


Family: Tweedie(p=1.106)
```

```
Link function: log

Formula:
abundance ~ offset(log(area_km2)) + s(log10(Slope), bs = "ts",
    k = 5) + s(ClimChl1, bs = "ts", k = 5)

Parametric coefficients:
            Estimate Std. Error t value Pr(>|t|)
(Intercept)  -7.6538     0.1859  -41.18   <2e-16 ***
---
Signif. codes:  0 '***' 0.001 '**' 0.01 '*' 0.05 '.' 0.1 ' ' 1

Approximate significance of smooth terms:
                  edf Ref.df     F  p-value
s(log10(Slope)) 1.012      4 3.316 0.000173 ***
s(ClimChl1)     2.453      4 4.225 0.000136 ***
---
Signif. codes:  0 '***' 0.001 '**' 0.01 '*' 0.05 '.' 0.1 ' ' 1

R-sq.(adj) =  0.00104   Deviance explained = 9.16%
-REML = 472.77  Scale est. = 18.704    n = 18415

All predictors were significant. This is the final model.
Creating term plots.
Diagnostic output from gam.check():

Method: REML   Optimizer: outer newton
full convergence after 12 iterations.
Gradient range [-9.482685e-07,1.048288e-06]
(score 472.7729 & scale 18.70364).
Hessian positive definite, eigenvalue range [0.3332399,513.7657].
Model rank =  9 / 9

Basis dimension (k) checking results. Low p-value (k-index<1) may
indicate that k is too low, especially if edf is close to k'.

                   k'   edf k-index p-value
s(log10(Slope)) 4.000 1.012   0.866    0.06
s(ClimChl1)     4.000 2.453   0.869    0.06

Predictors retained during the model selection procedure: Slope, ClimChl1

Predictors dropped during the model selection procedure: Depth, DistToShore, DistTo125m, DistTo300m,
ClimSST, ClimDistToFront1, ClimTKE
```

Model term plots

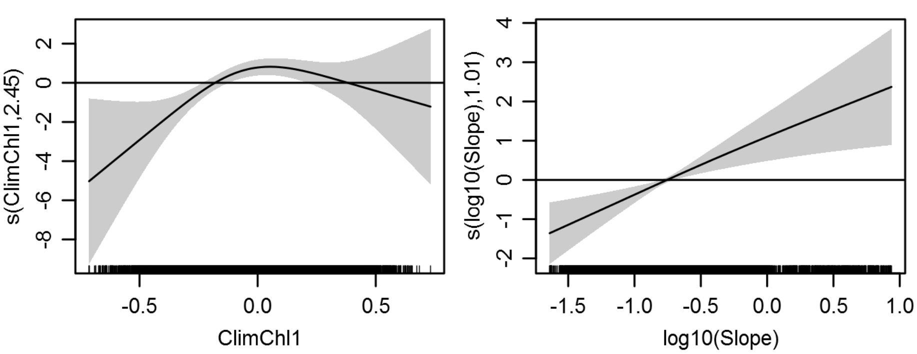

Diagnostic plots

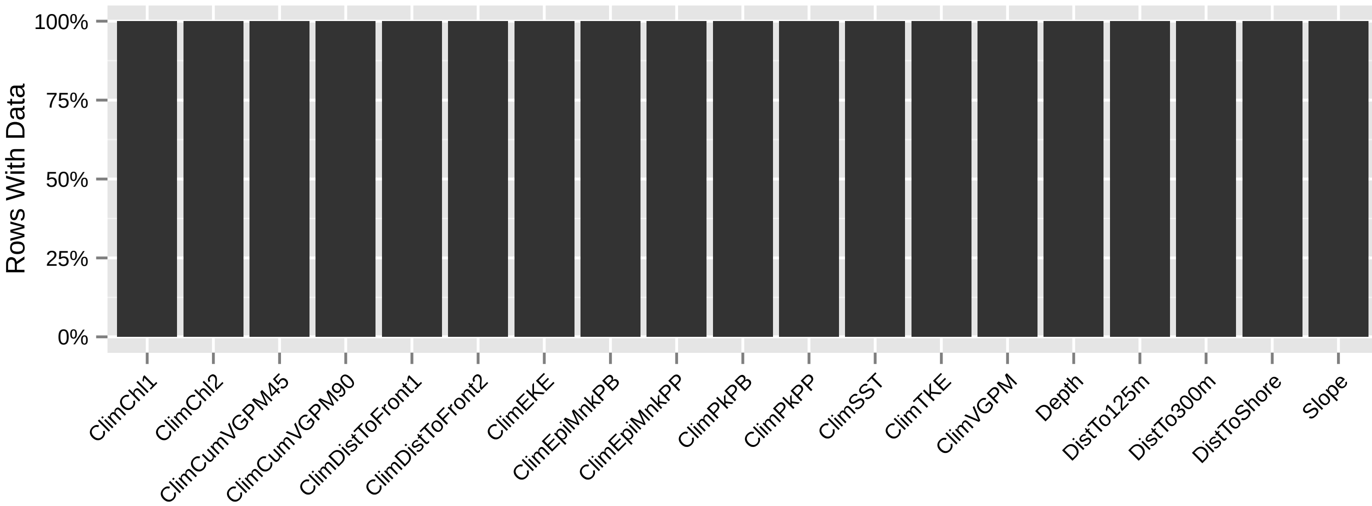

Figure 70: Segments with predictor values for the Minke whale Climatological model, Winter season, North of Gulf Stream. This plot is used to assess how many segments would be lost by including a given predictor in a model.

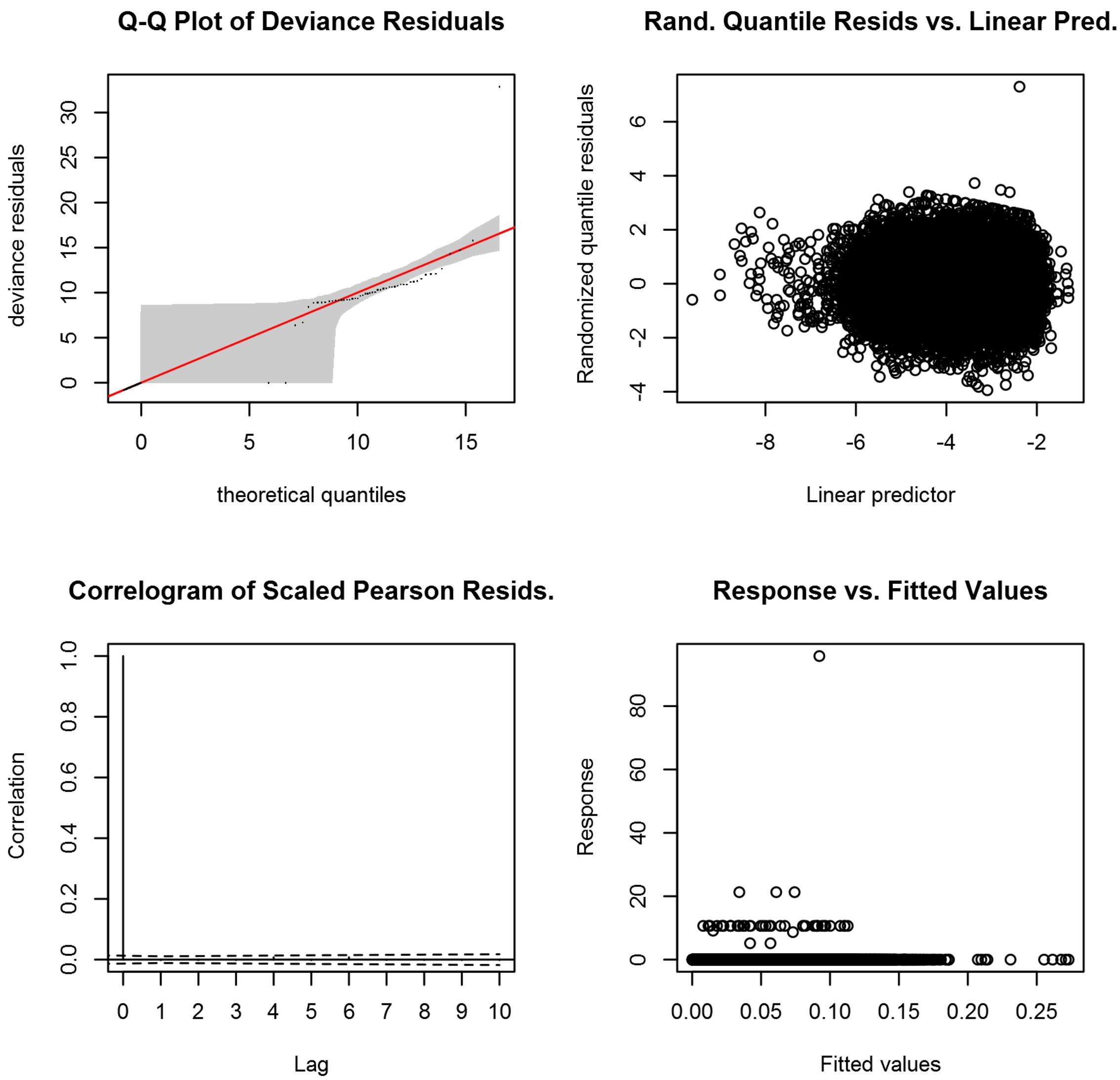

Figure 71: Statistical diagnostic plots for the Minke whale Climatological model, Winter season, North of Gulf Stream.

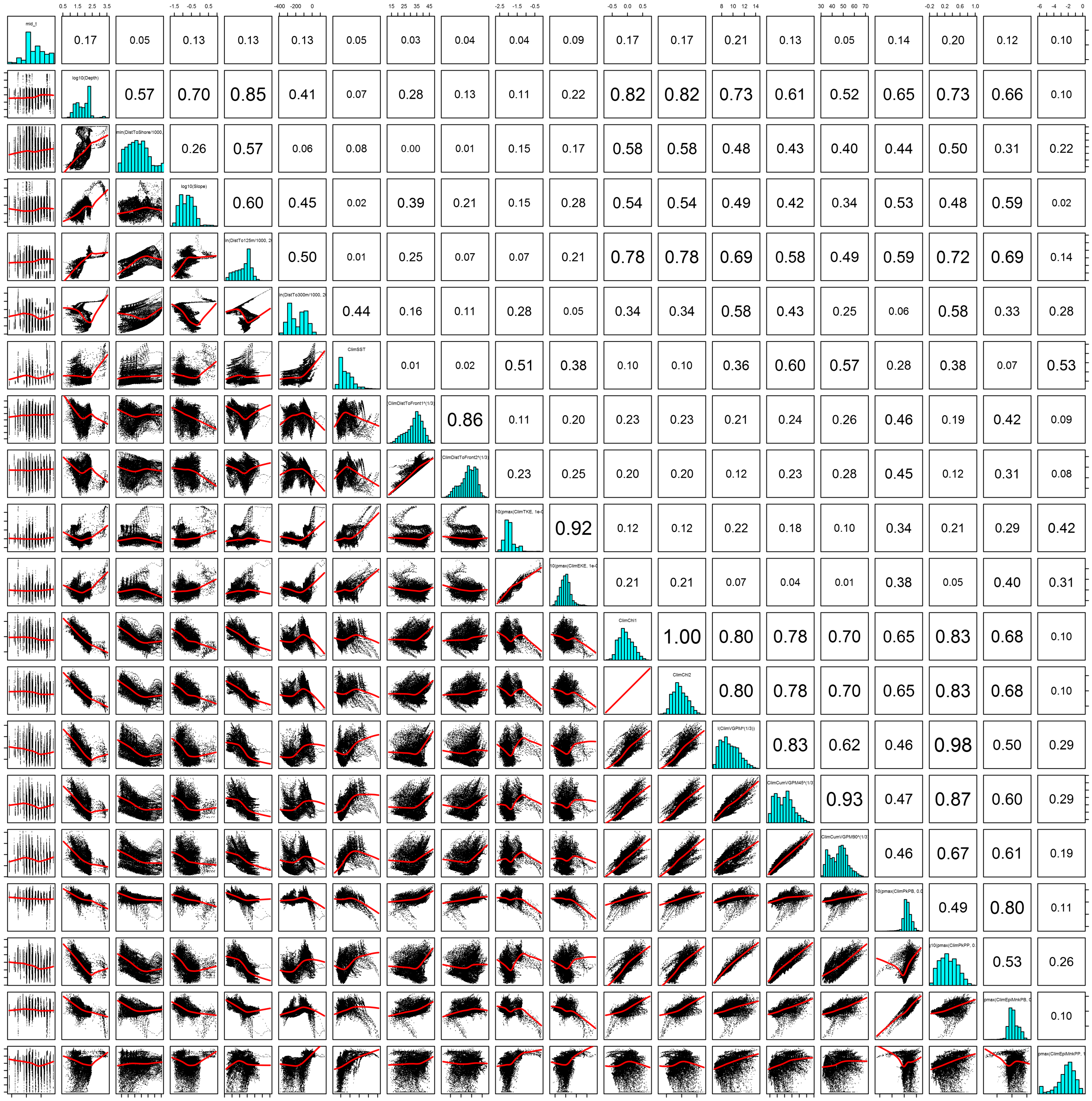

Figure 72: Scatterplot matrix for the Minke whale Climatological model, Winter season, North of Gulf Stream. This plot is used to inspect the distribution of predictors (via histograms along the diagonal), simple correlation between predictors (via pairwise Pearson coefficients above the diagonal), and linearity of predictor correlations (via scatterplots below the diagonal). This plot is best viewed at high magnification.

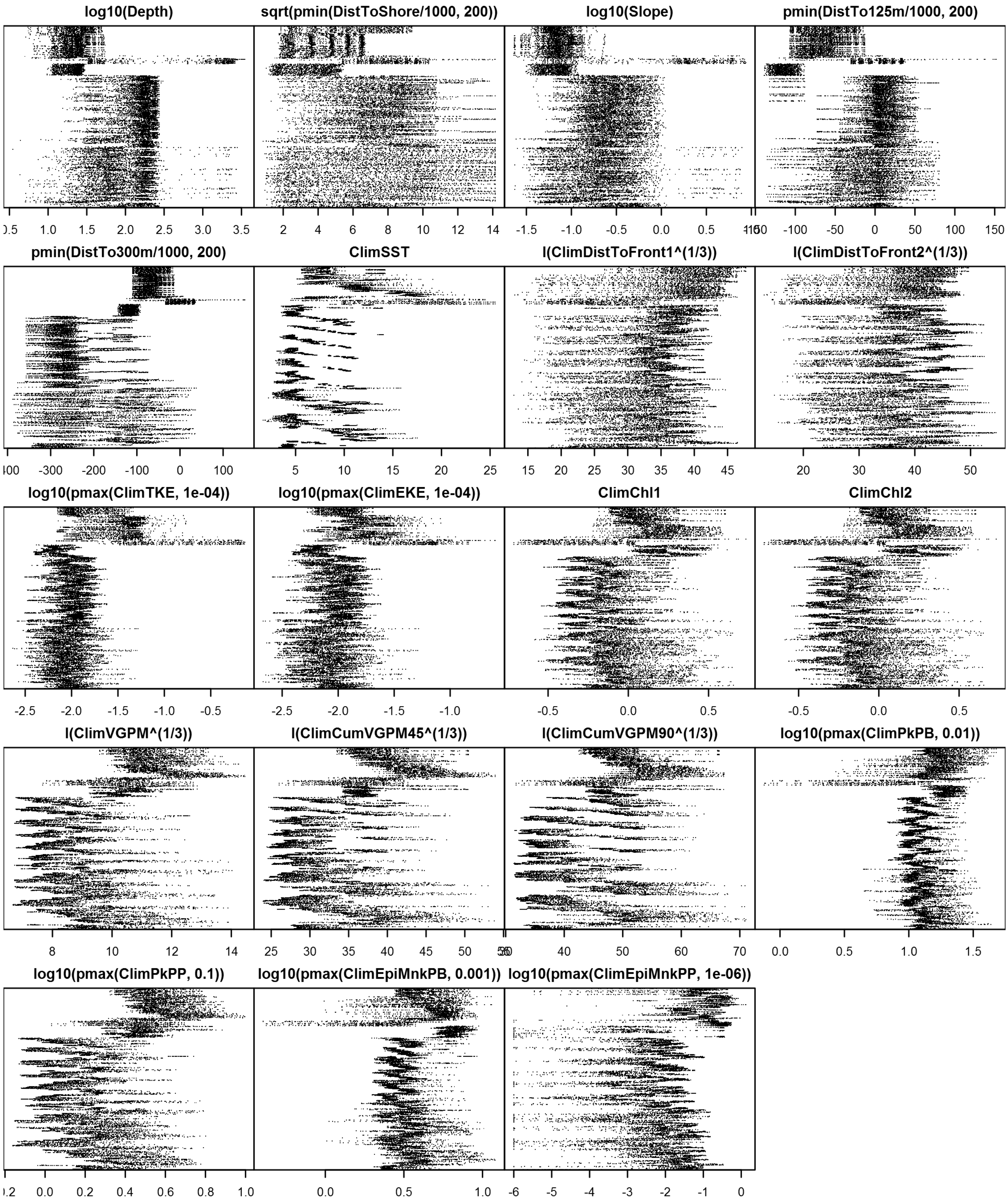

Figure 73: Dotplot for the Minke whale Climatological model, Winter season, North of Gulf Stream. This plot is used to check for suspicious patterns and outliers in the data. Points are ordered vertically by transect ID, sequentially in time.

Southern Slope and Abyss

A mean density estimate was made for this region. First, density (individuals per square kilometer) was calculated as the number of animals encountered divided by the area effectively surveyed, corrected by the detection functions and g(0) estimates. Then, density was multiplied by the size of each grid cell, in square kilometers, to obtain abundance (number of individuals) per grid cell. Finally, all grid cells in the region were assigned this abundance value.

Southern Shelf

Density assumed to be 0 in this region.

Low Effort Area

Density was not modeled for this region.

Summer

In this season, the entire study area was surveyed extensively (although the majority of effort occurred during the July-August period). All of the sightings reported by our surveys were over the continental shelf or slope, with the exception of one sighting far offshore at about 37 N on 10 July, 1998. We believed this sighting was anomalous; the area it occurred in does not represent good feeding habitat for minke whales. We split the study area 150 km from the self break and modeled the shelf-wards data with a full statistical model. In the far offshore area, we estimated mean density from the survey effort that occurred there.

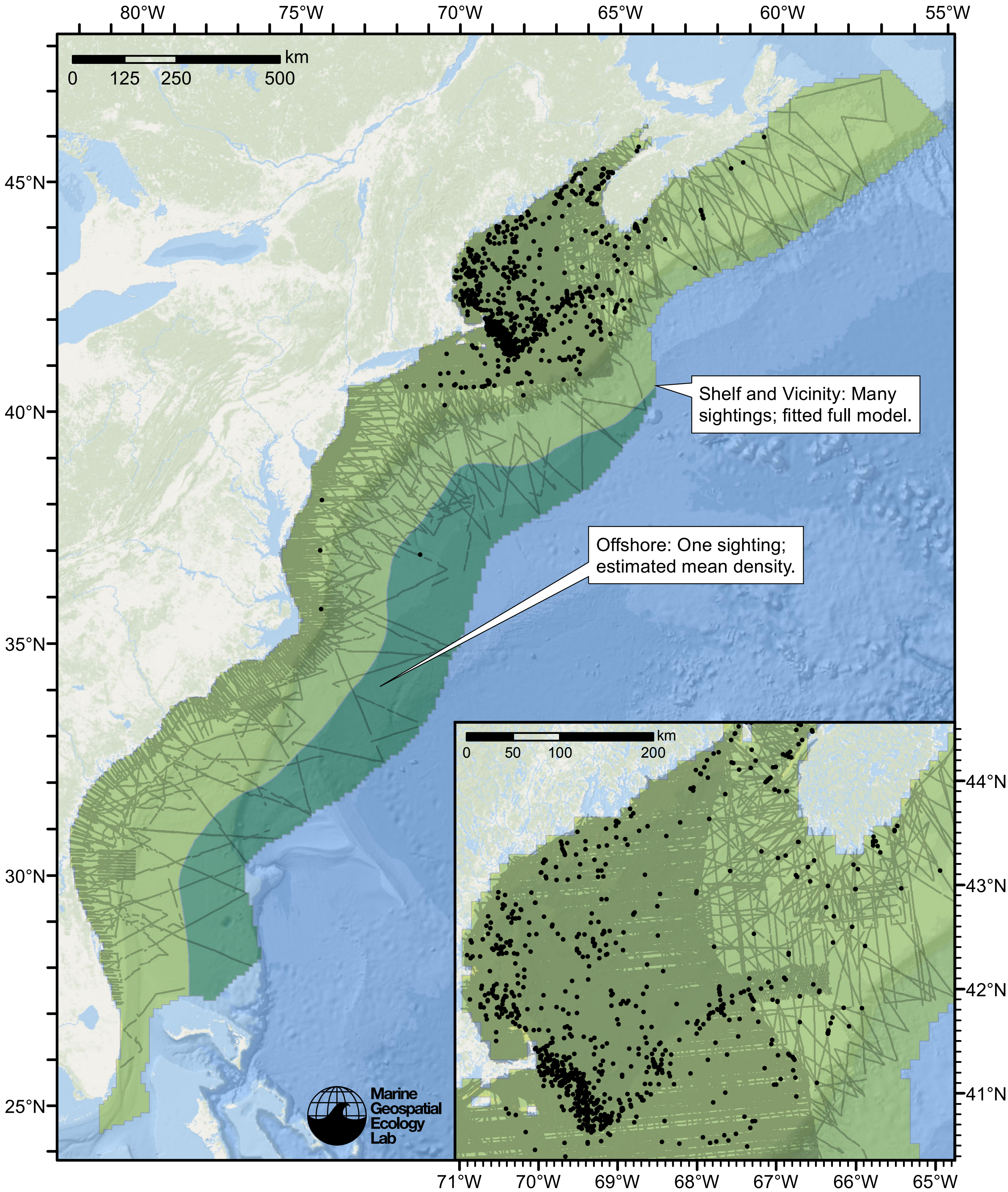

Figure 74: Minke whale density model schematic for Summer season. All on-effort sightings are shown, including those that were truncated when detection functions were fitted.

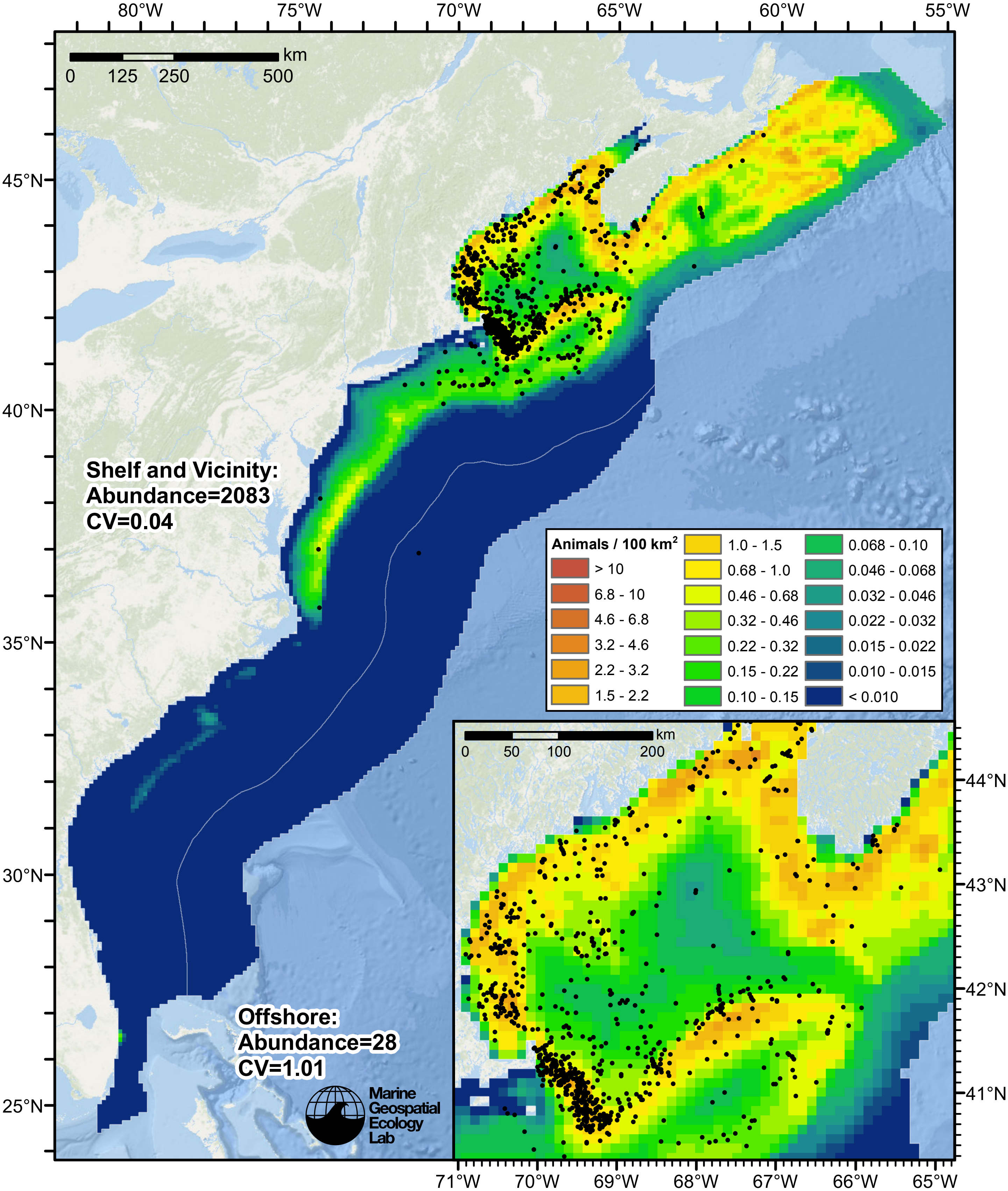

Figure 75: Minke whale density predicted by the Summer season climatological model that explained the most deviance. Pixels are 10x10 km. The legend gives the estimated individuals per pixel; breaks are logarithmic. The same scale is used for all seasons. Abundance for each region was computed by summing the density cells occuring in that region.

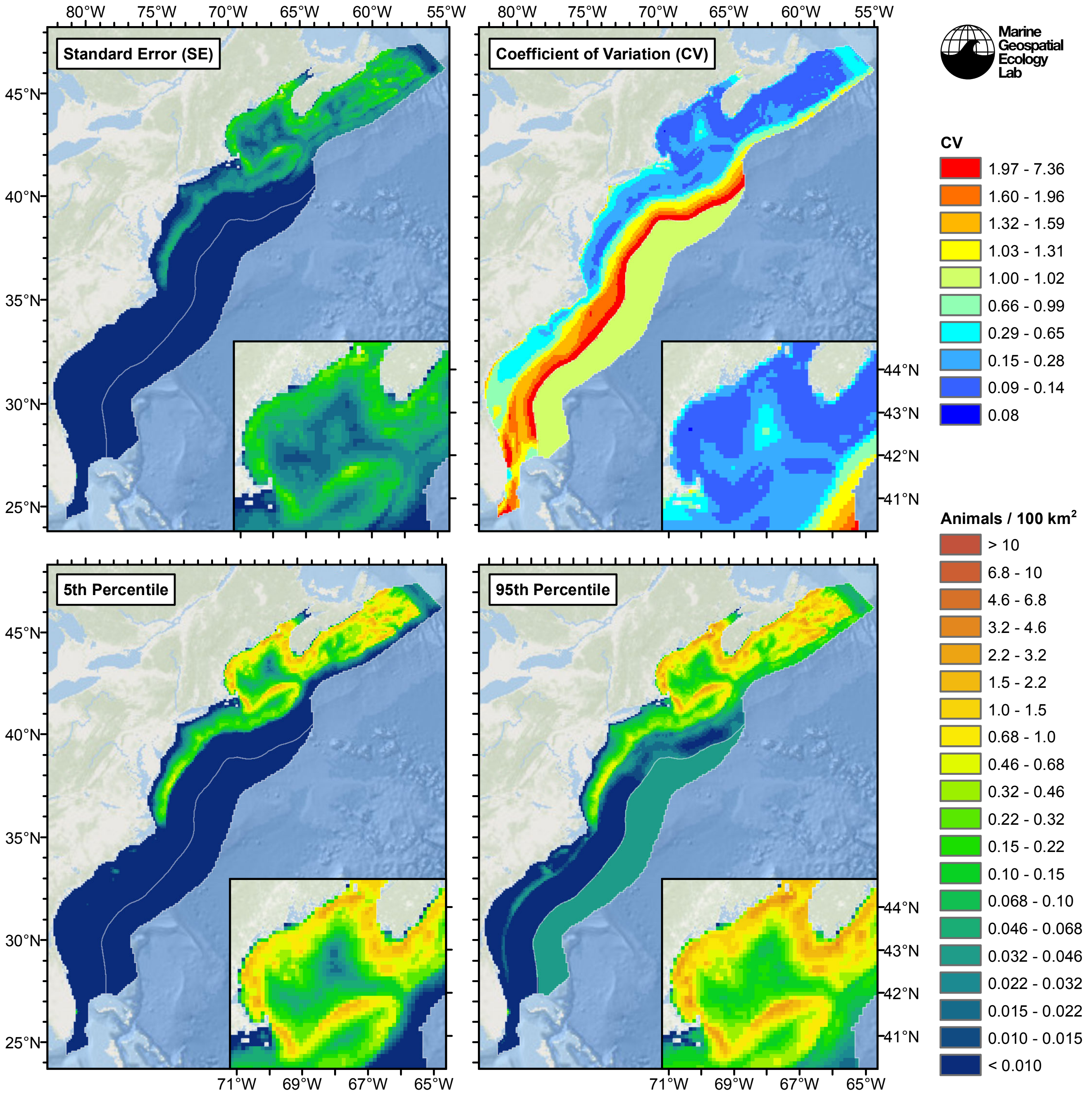

Figure 76: Estimated uncertainty for the Summer season climatological model that explained the most deviance. These estimates only incorporate the statistical uncertainty estimated for the spatial model (by the R mgcv package). They do not incorporate uncertainty in the detection functions, g(0) estimates, predictor variables, and so on.

Shelf and Vicinity

Statistical output

```
Rscript.exe: This is mgcv 1.8-3. For overview type 'help("mgcv-package")'.


Family: Tweedie(p=1.162)
```

```
Link function: log

Formula:
abundance ~ offset(log(area_km2)) + s(log10(Depth), bs = "ts",
    k = 5) + s(sqrt(pmin(DistToShore/1000, 200)), bs = "ts",
    k = 5) + s(pmin(DistTo125m/1000, 200), bs = "ts", k = 5) +
    s(I(ClimDistToFront1^(1/3)), bs = "ts", k = 5) + s(log10(pmax(ClimPkPB,
    0.01)), bs = "ts", k = 5)

Parametric coefficients:
            Estimate Std. Error t value Pr(>|t|)
(Intercept)  -8.3211     0.3826  -21.75   <2e-16 ***
---
Signif. codes:  0 '***' 0.001 '**' 0.01 '*' 0.05 '.' 0.1 ' ' 1

Approximate significance of smooth terms:
                                       edf Ref.df      F  p-value
s(log10(Depth))                      3.715      4 31.581  < 2e-16 ***
s(sqrt(pmin(DistToShore/1000, 200))) 3.556      4 11.386 2.92e-10 ***
s(pmin(DistTo125m/1000, 200))        3.595      4 56.725  < 2e-16 ***
s(I(ClimDistToFront1^(1/3)))         1.866      4  1.751   0.0171 *
s(log10(pmax(ClimPkPB, 0.01)))       2.984      4 39.480  < 2e-16 ***
---
Signif. codes:  0 '***' 0.001 '**' 0.01 '*' 0.05 '.' 0.1 ' ' 1

R-sq.(adj) =  0.0288   Deviance explained =   28%
-REML = 5649.3  Scale est. = 18.132    n = 65833

All predictors were significant. This is the final model.
Creating term plots.
Diagnostic output from gam.check():

Method: REML   Optimizer: outer newton
full convergence after 15 iterations.
Gradient range [-0.0003550892,4.90408e-05]
(score 5649.255 & scale 18.13151).
Hessian positive definite, eigenvalue range [0.1956175,4544.991].
Model rank =  21 / 21

Basis dimension (k) checking results. Low p-value (k-index<1) may
indicate that k is too low, especially if edf is close to k'.

                                        k'   edf k-index p-value
s(log10(Depth))                      4.000 3.715   0.818    0.00
s(sqrt(pmin(DistToShore/1000, 200))) 4.000 3.556   0.857    0.46
s(pmin(DistTo125m/1000, 200))        4.000 3.595   0.849    0.25
s(I(ClimDistToFront1^(1/3)))         4.000 1.866   0.855    0.40
s(log10(pmax(ClimPkPB, 0.01)))       4.000 2.984   0.788    0.00

Predictors retained during the model selection procedure: Depth, DistToShore, DistTo125m,
ClimDistToFront1, ClimPkPB

Predictors dropped during the model selection procedure: Slope, ClimSST, ClimTKE
```

Model term plots

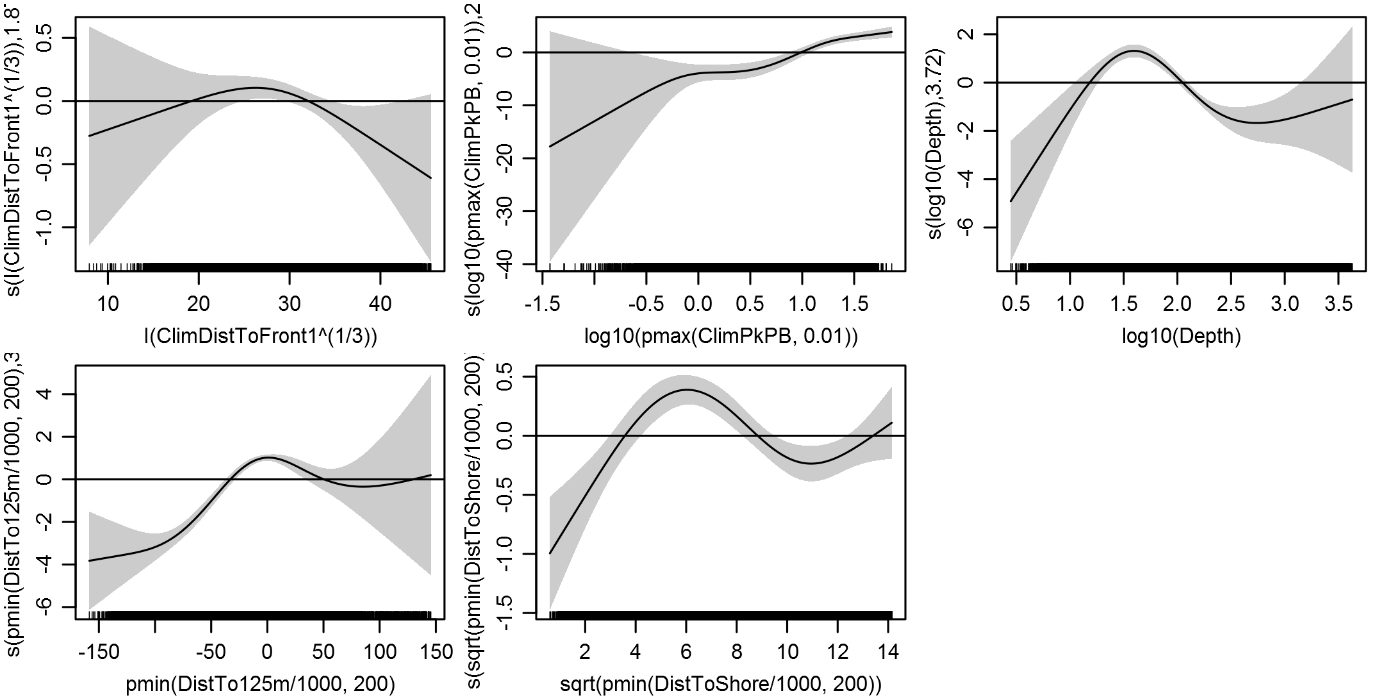

Diagnostic plots

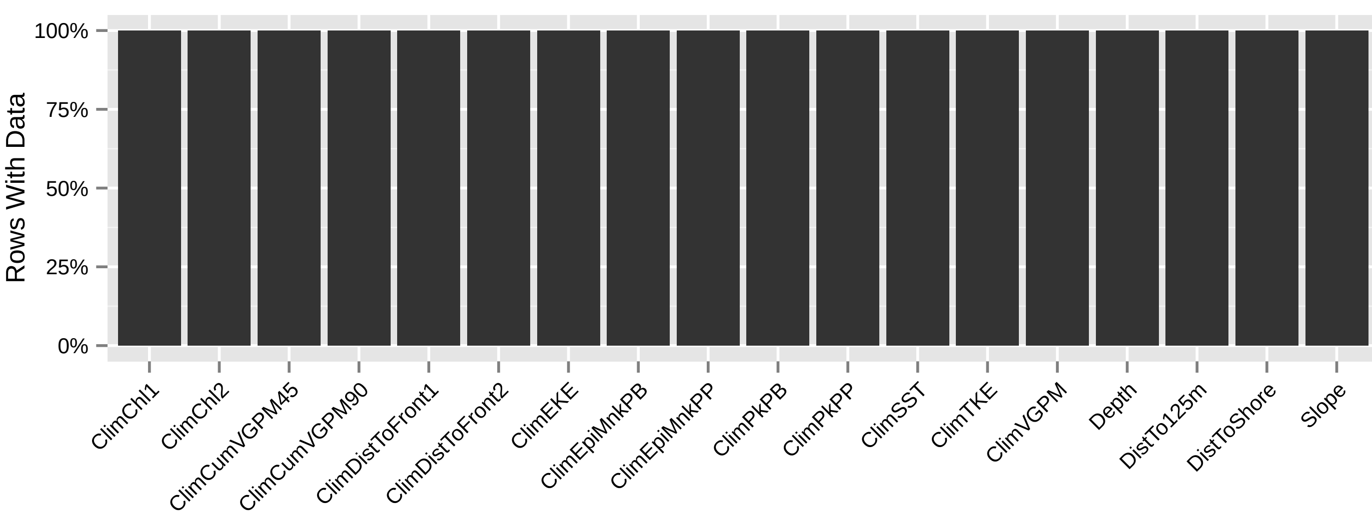

Figure 77: Segments with predictor values for the Minke whale Climatological model, Summer season, Shelf and Vicinity. This plot is used to assess how many segments would be lost by including a given predictor in a model.

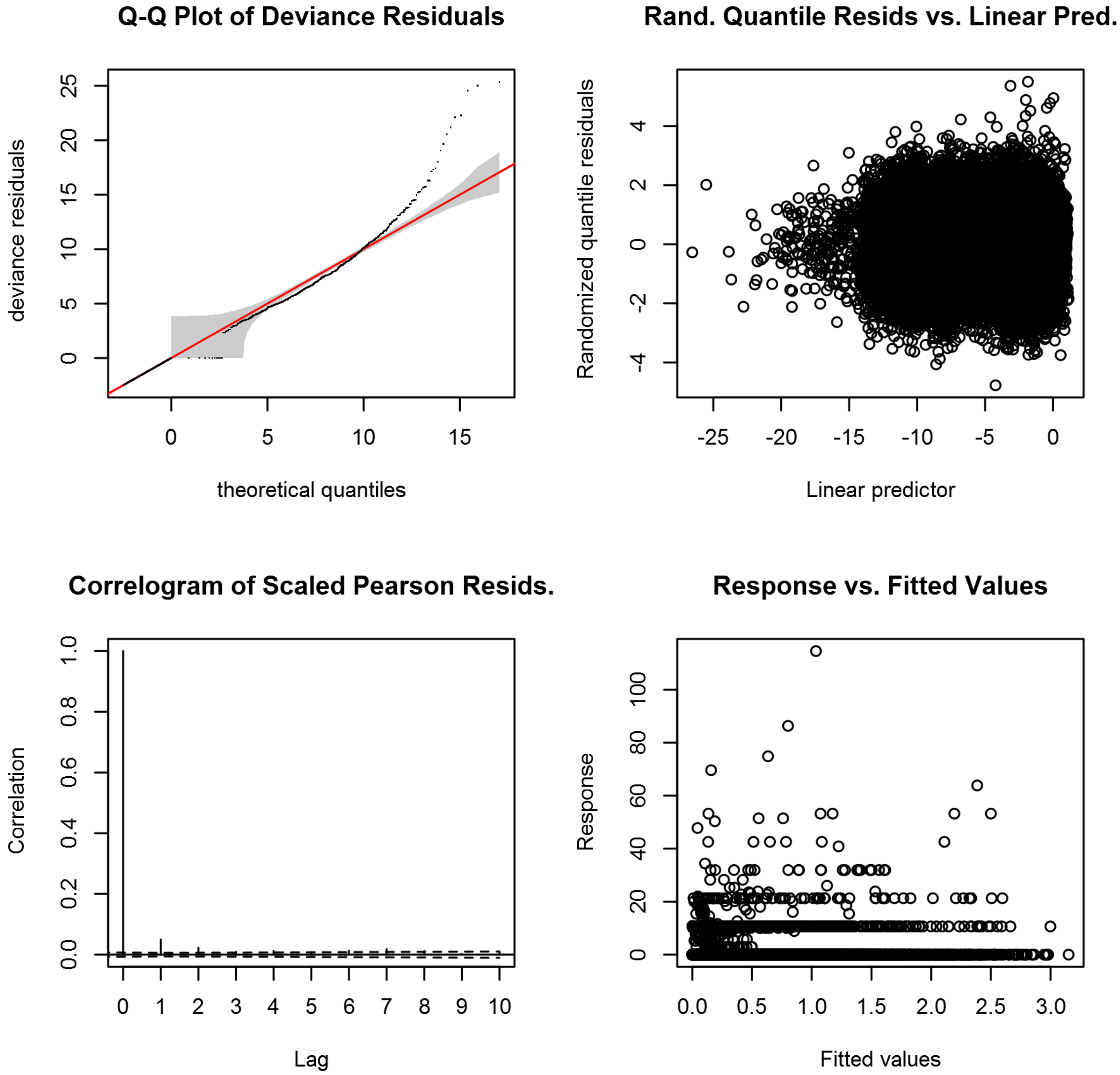

Figure 78: Statistical diagnostic plots for the Minke whale Climatological model, Summer season, Shelf and Vicinity.

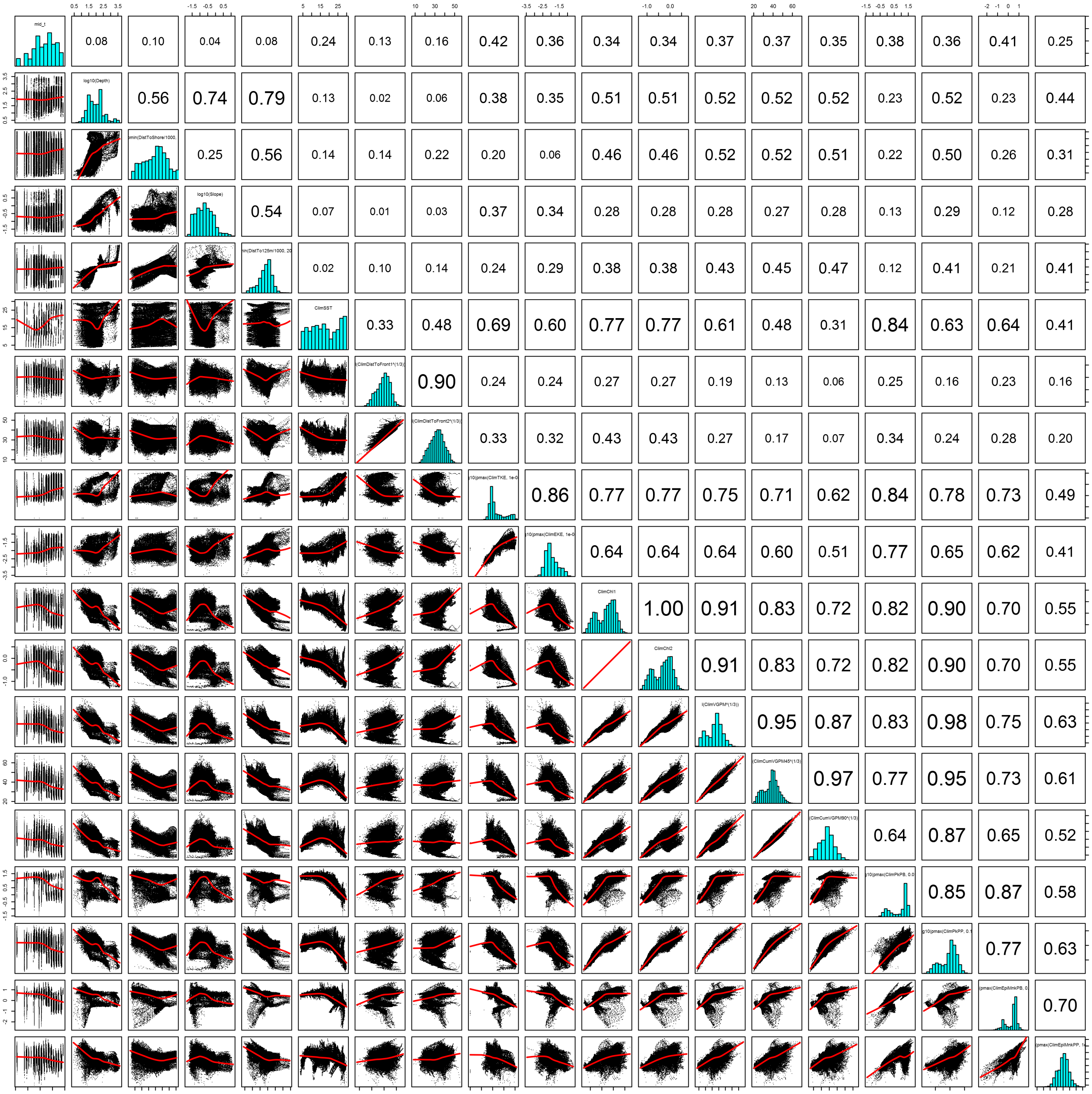

Figure 79: Scatterplot matrix for the Minke whale Climatological model, Summer season, Shelf and Vicinity. This plot is used to inspect the distribution of predictors (via histograms along the diagonal), simple correlation between predictors (via pairwise Pearson coefficients above the diagonal), and linearity of predictor correlations (via scatterplots below the diagonal). This plot is best viewed at high magnification.

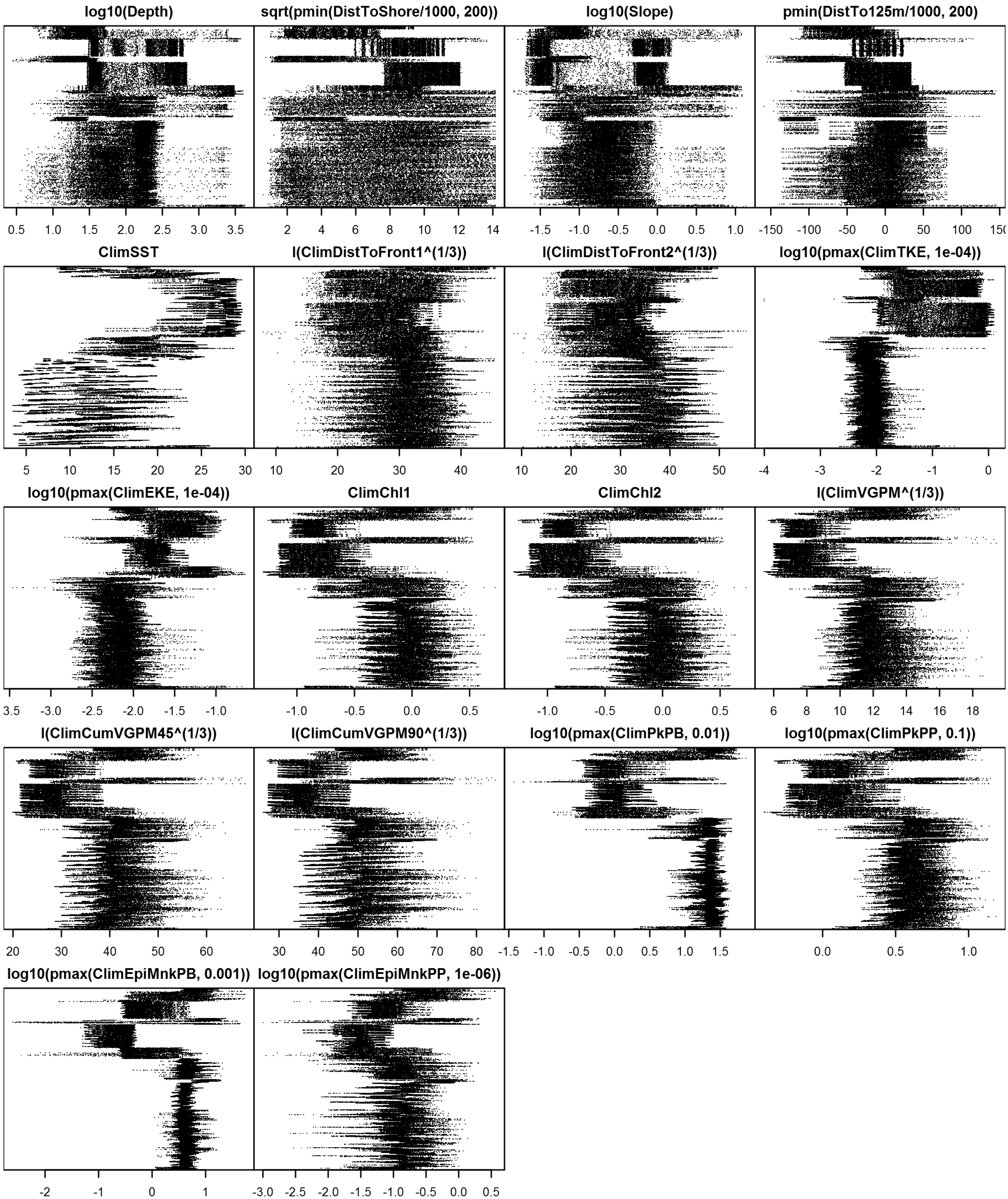

Figure 80: Dotplot for the Minke whale Climatological model, Summer season, Shelf and Vicinity. This plot is used to check for suspicious patterns and outliers in the data. Points are ordered vertically by transect ID, sequentially in time.

Offshore

A mean density estimate was made for this region. First, density (individuals per square kilometer) was calculated as the number of animals encountered divided by the area effectively surveyed, corrected by the detection functions and g(0) estimates. Then, density was multiplied by the size of each grid cell, in square kilometers, to obtain abundance (number of individuals) per grid cell. Finally, all grid cells in the region were assigned this abundance value.

Contemporaneous Model

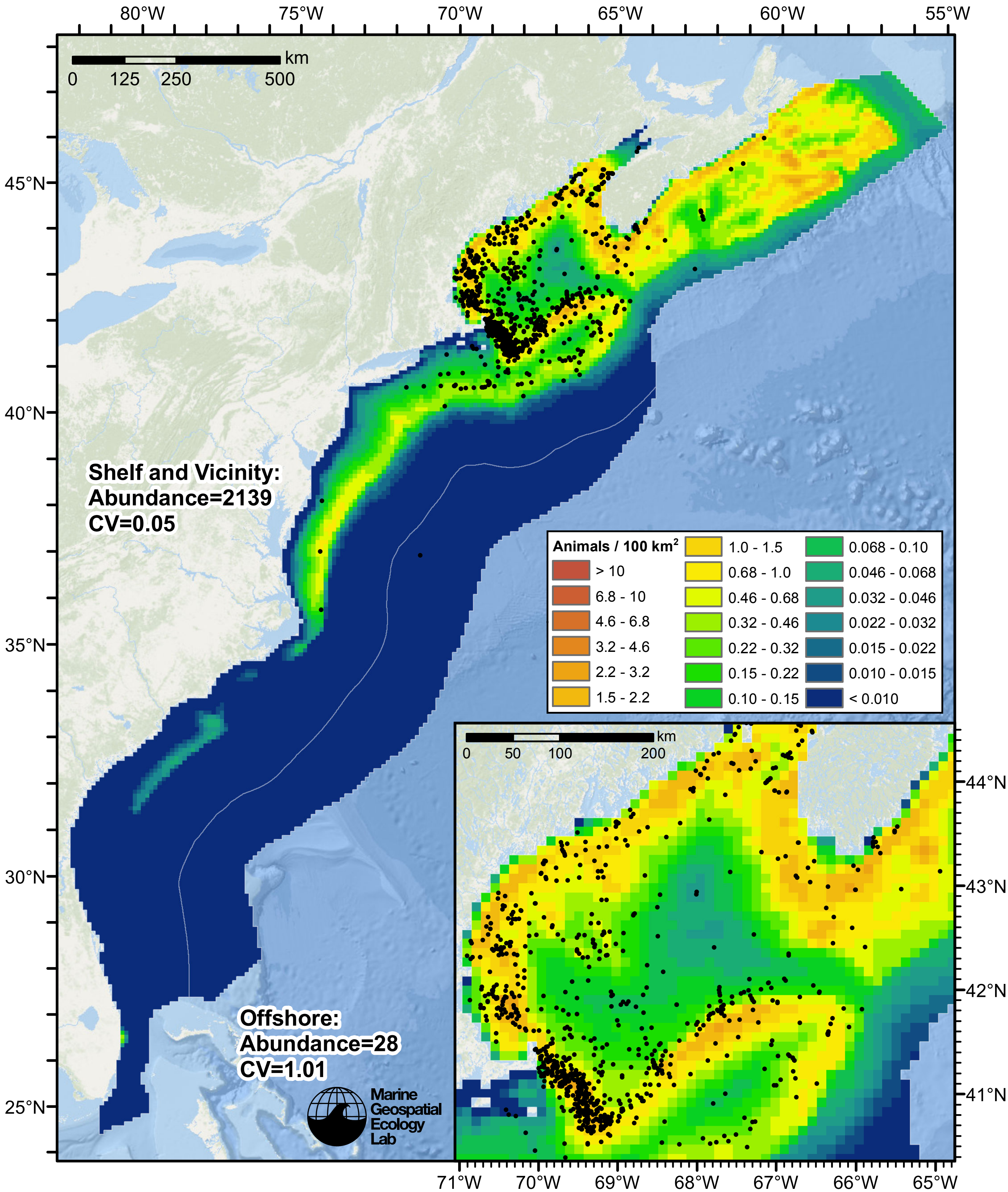

Figure 81: Minke whale density predicted by the Summer season contemporaneous model that explained the most deviance. Pixels are 10x10 km. The legend gives the estimated individuals per pixel; breaks are logarithmic. The same scale is used for all seasons. Abundance for each region was computed by summing the density cells occuring in that region.

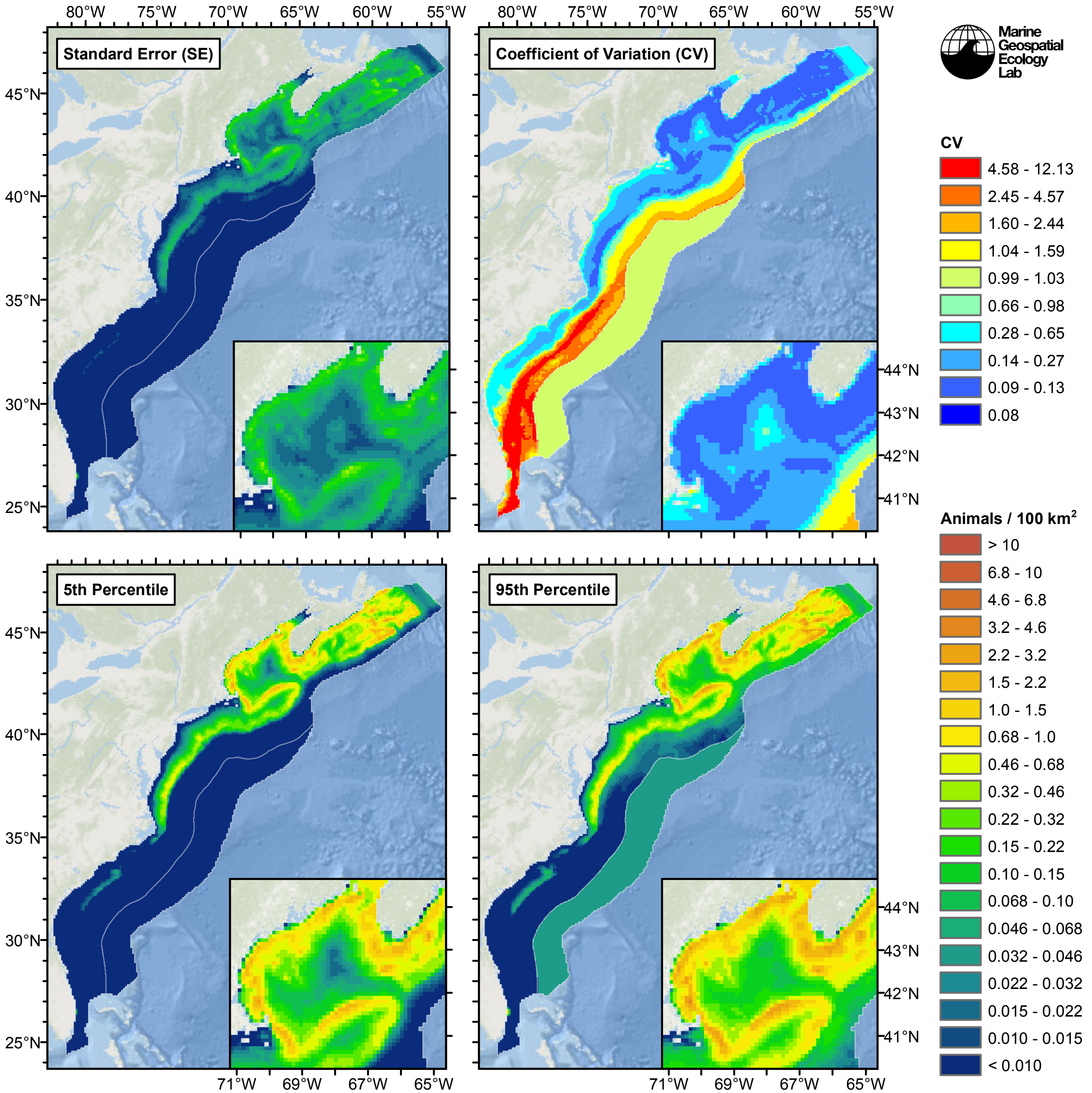

Figure 82: Estimated uncertainty for the Summer season contemporaneous model that explained the most deviance. These estimates only incorporate the statistical uncertainty estimated for the spatial model (by the R mgcv package). They do not incorporate uncertainty in the detection functions, g(0) estimates, predictor variables, and so on.

Shelf and Vicinity

Statistical output

```
Rscript.exe: This is mgcv 1.8-3. For overview type 'help("mgcv-package")'.


Family: Tweedie(p=1.163)
```

```
Link function: log

Formula:
abundance ~ offset(log(area_km2)) + s(log10(Depth), bs = "ts",
    k = 5) + s(sqrt(pmin(DistToShore/1000, 200)), bs = "ts",
    k = 5) + s(pmin(DistTo125m/1000, 200), bs = "ts", k = 5) +
    s(SST, bs = "ts", k = 5) + s(log10(pmax(PkPB, 0.01)), bs = "ts",
    k = 5)

Parametric coefficients:
            Estimate Std. Error t value Pr(>|t|)
(Intercept)  -10.657      2.499  -4.264 2.01e-05 ***
---
Signif. codes:  0 '***' 0.001 '**' 0.01 '*' 0.05 '.' 0.1 ' ' 1

Approximate significance of smooth terms:
                                       edf Ref.df     F  p-value
s(log10(Depth))                      3.701      4 32.81  < 2e-16 ***
s(sqrt(pmin(DistToShore/1000, 200))) 3.550      4 11.46 2.59e-10 ***
s(pmin(DistTo125m/1000, 200))        3.626      4 65.56  < 2e-16 ***
s(SST)                               3.337      4 13.06 9.94e-12 ***
s(log10(pmax(PkPB, 0.01)))           2.202      4 15.11 1.75e-14 ***
---
Signif. codes:  0 '***' 0.001 '**' 0.01 '*' 0.05 '.' 0.1 ' ' 1

R-sq.(adj) =  0.0299   Deviance explained = 28.1%
-REML = 5616.4  Scale est. = 18.082    n = 62935

All predictors were significant. This is the final model.
Creating term plots.
Diagnostic output from gam.check():

Method: REML   Optimizer: outer newton
full convergence after 11 iterations.
Gradient range [-5.199276e-05,1.957538e-05]
(score 5616.394 & scale 18.08179).
Hessian positive definite, eigenvalue range [0.8195703,4480.738].
Model rank =  21 / 21

Basis dimension (k) checking results. Low p-value (k-index<1) may
indicate that k is too low, especially if edf is close to k'.

                                        k'   edf k-index p-value
s(log10(Depth))                      4.000 3.701   0.886    0.04
s(sqrt(pmin(DistToShore/1000, 200))) 4.000 3.550   0.832    0.00
s(pmin(DistTo125m/1000, 200))        4.000 3.626   0.908    0.38
s(SST)                               4.000 3.337   0.828    0.00
s(log10(pmax(PkPB, 0.01)))           4.000 2.202   0.852    0.00

Predictors retained during the model selection procedure: Depth, DistToShore, DistTo125m, SST, PkPB

Predictors dropped during the model selection procedure: Slope, DistToFront1, TKE
```

Model term plots

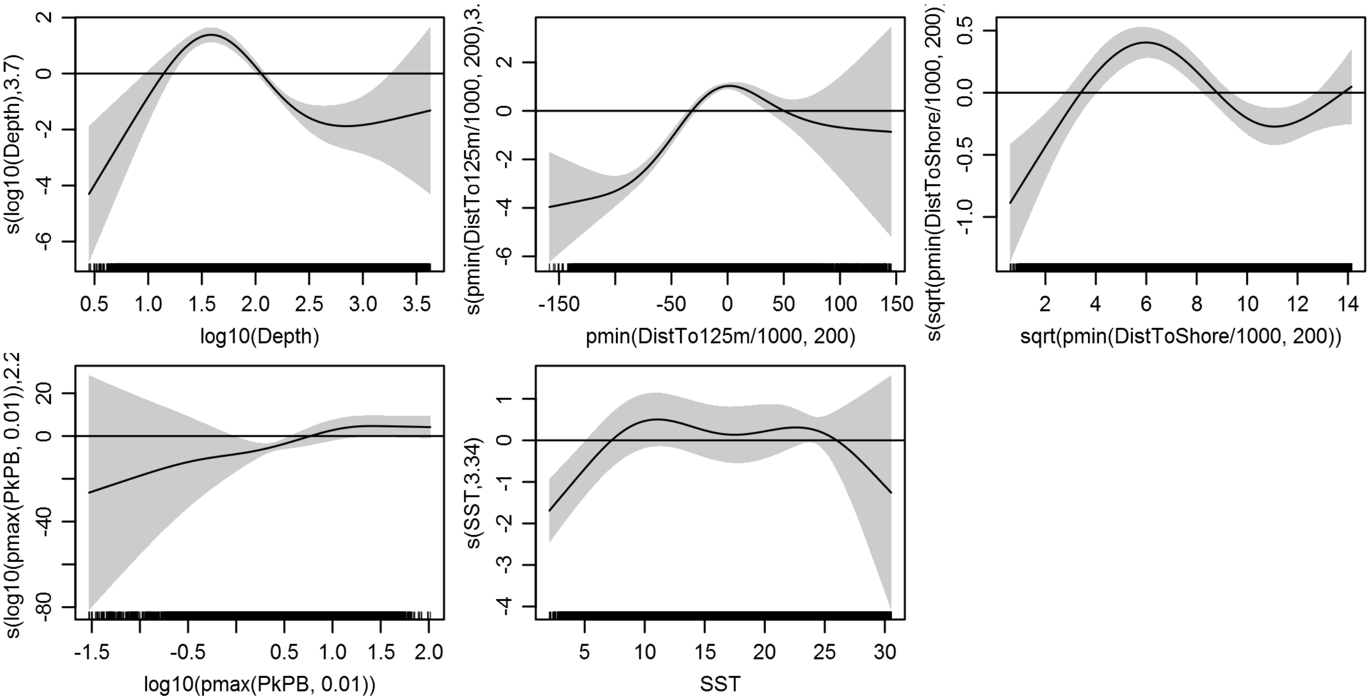

Diagnostic plots

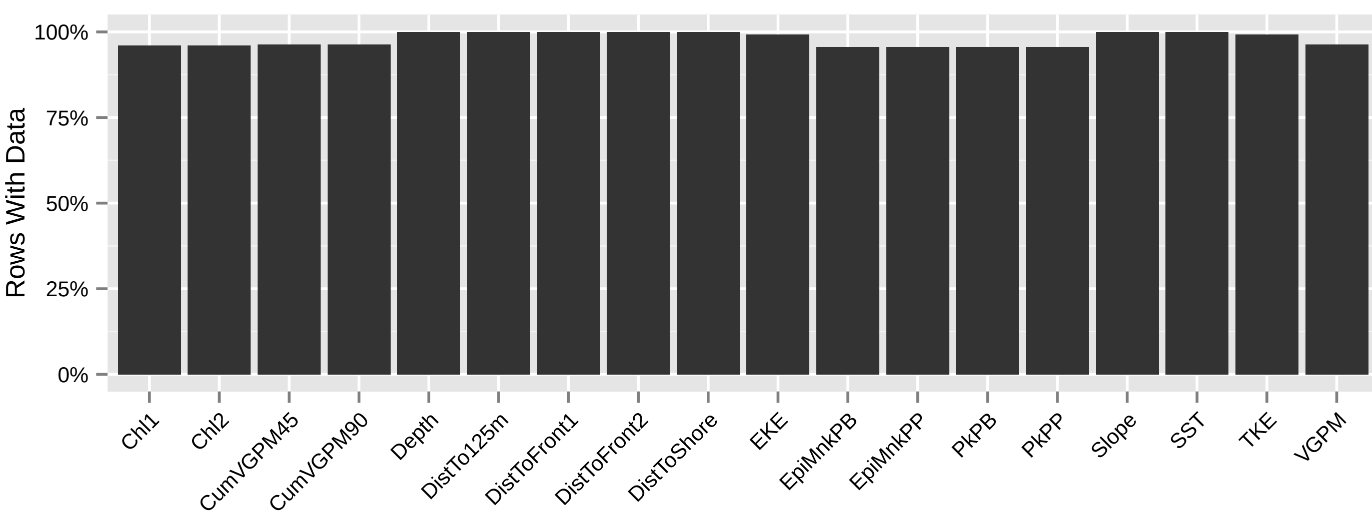

Figure 83: Segments with predictor values for the Minke whale Contemporaneous model, Summer season, Shelf and Vicinity. This plot is used to assess how many segments would be lost by including a given predictor in a model.

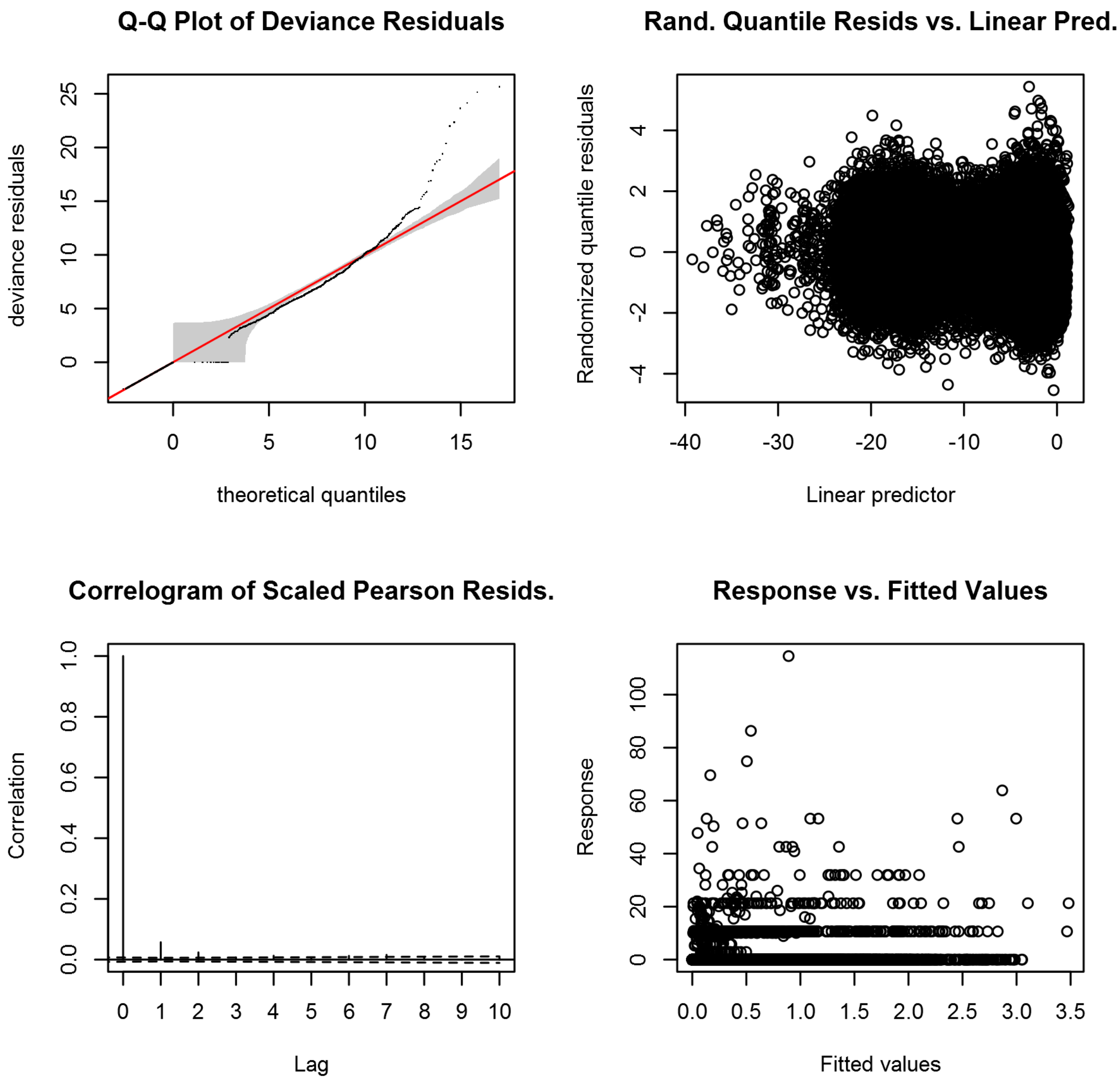

Figure 84: Statistical diagnostic plots for the Minke whale Contemporaneous model, Summer season, Shelf and Vicinity.

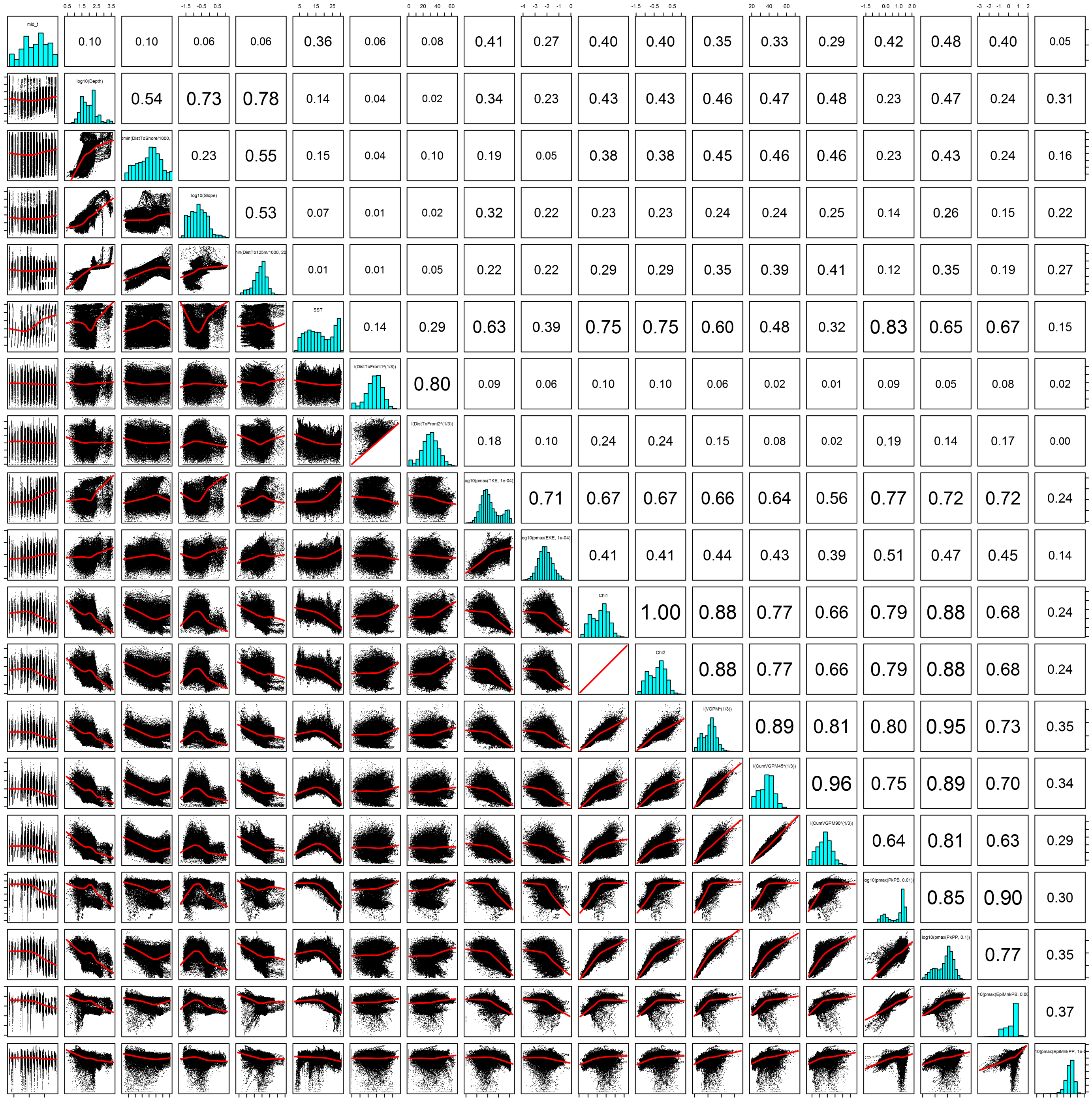

Figure 85: Scatterplot matrix for the Minke whale Contemporaneous model, Summer season, Shelf and Vicinity. This plot is used to inspect the distribution of predictors (via histograms along the diagonal), simple correlation between predictors (via pairwise Pearson coefficients above the diagonal), and linearity of predictor correlations (via scatterplots below the diagonal). This plot is best viewed at high magnification.

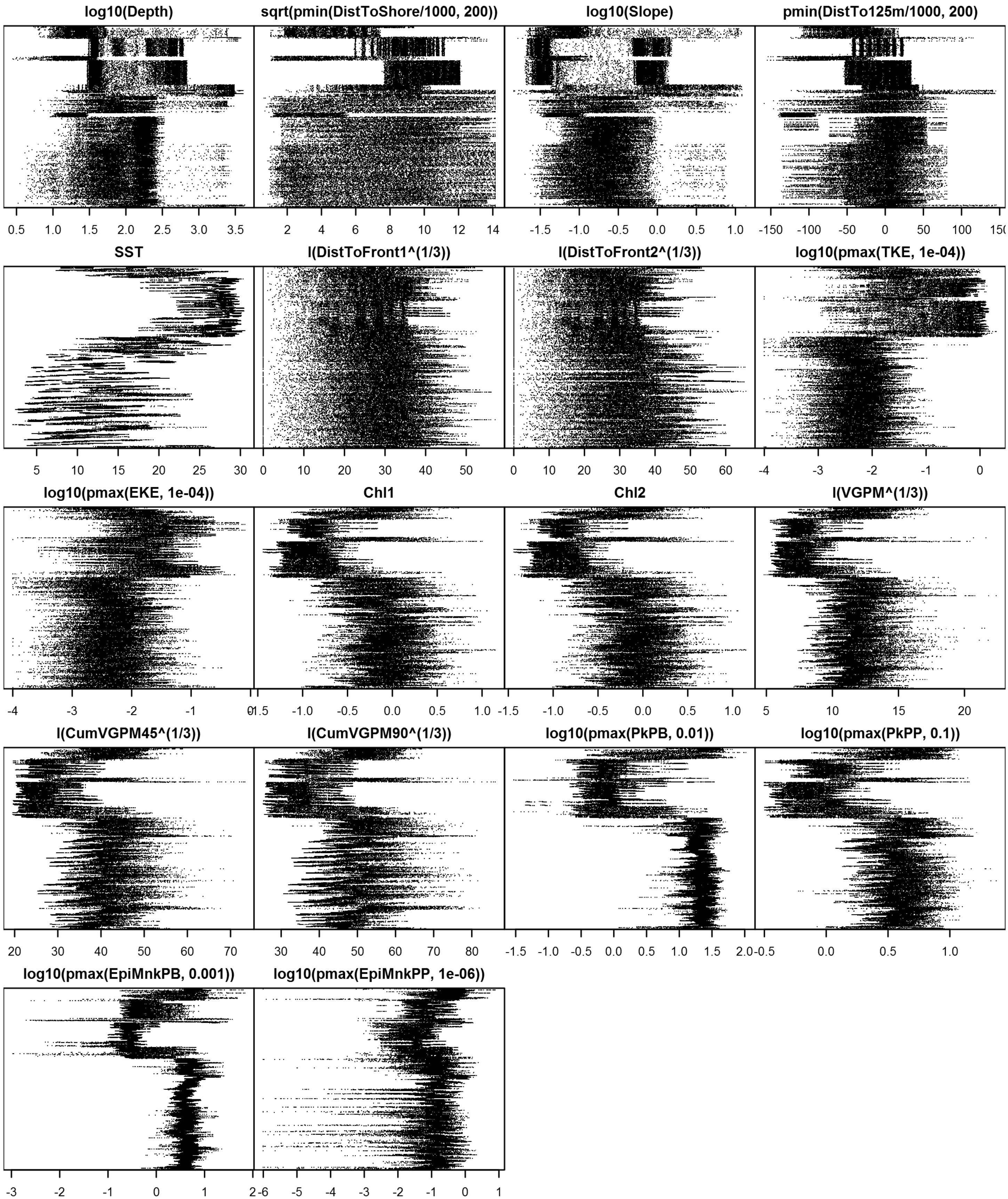

Figure 86: Dotplot for the Minke whale Contemporaneous model, Summer season, Shelf and Vicinity. This plot is used to check for suspicious patterns and outliers in the data. Points are ordered vertically by transect ID, sequentially in time.

Offshore

A mean density estimate was made for this region. First, density (individuals per square kilometer) was calculated as the number of animals encountered divided by the area effectively surveyed, corrected by the detection functions and g(0) estimates. Then, density was multiplied by the size of each grid cell, in square kilometers, to obtain abundance (number of individuals) per grid cell. Finally, all grid cells in the region were assigned this abundance value.

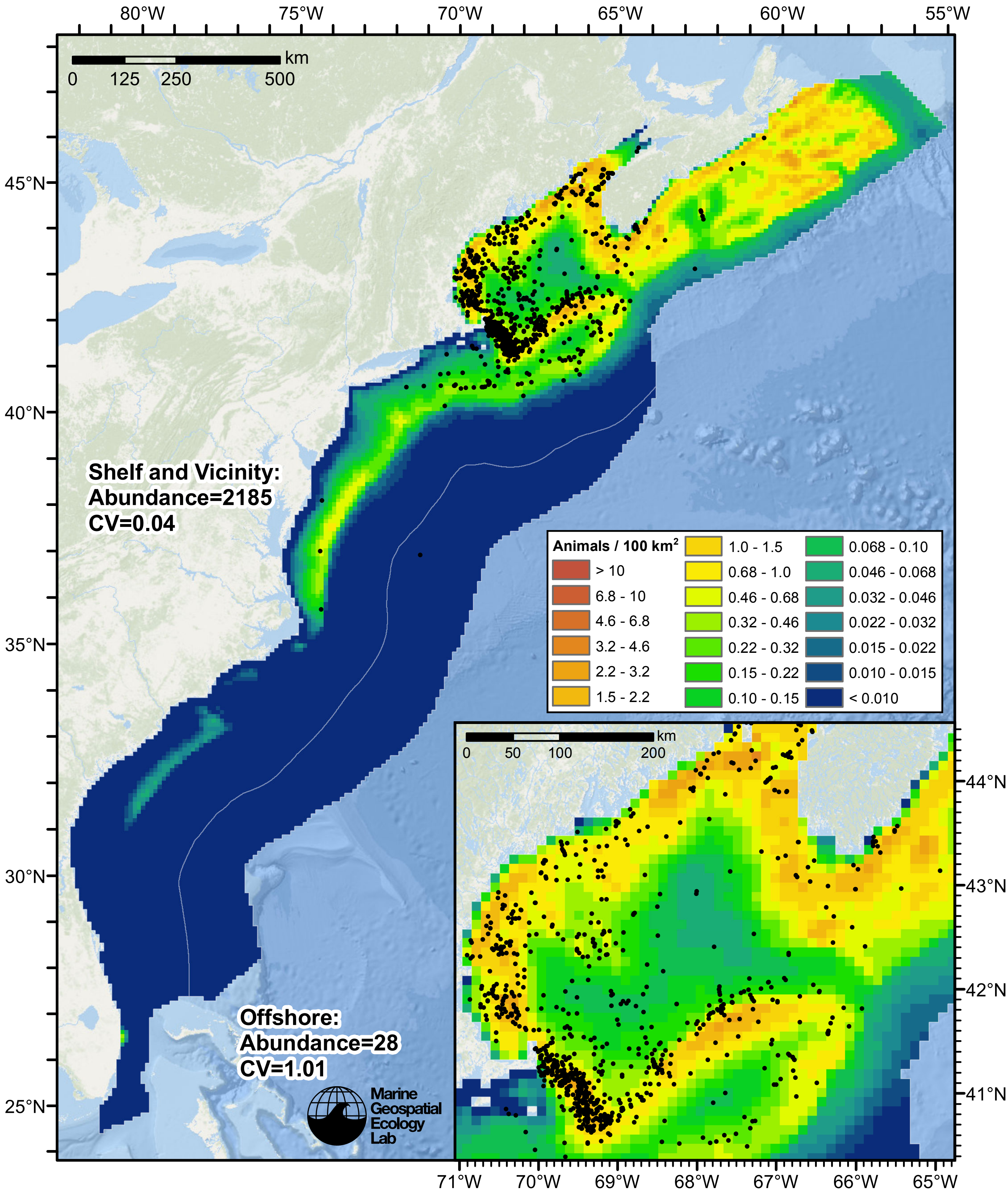

Figure 87: Minke whale density predicted by the Summer season climatological same segments model that explained the most deviance. Pixels are 10x10 km. The legend gives the estimated individuals per pixel; breaks are logarithmic. The same scale is used for all seasons. Abundance for each region was computed by summing the density cells occuring in that region.

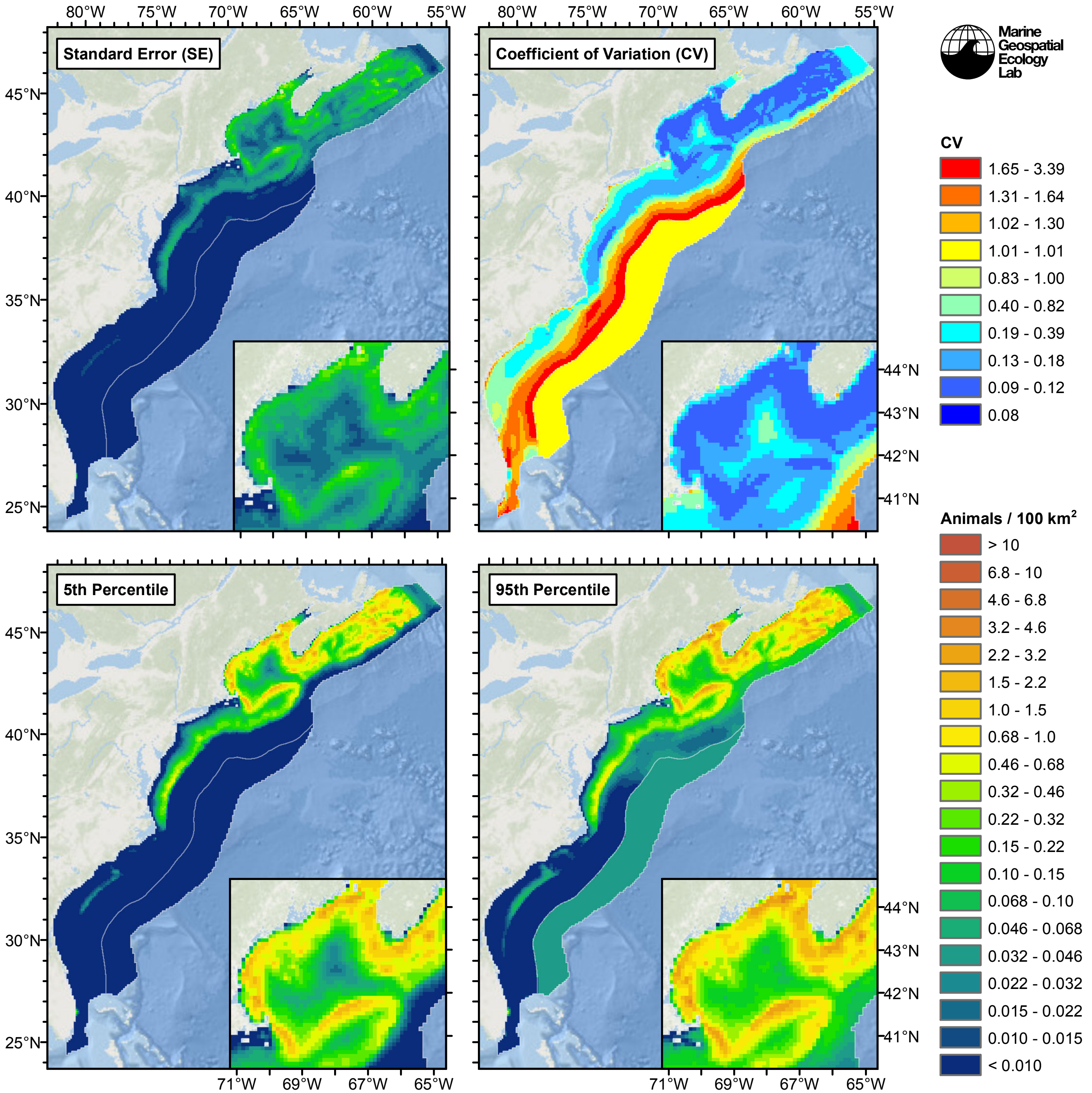

Figure 88: Estimated uncertainty for the Summer season climatological same segments model that explained the most deviance. These estimates only incorporate the statistical uncertainty estimated for the spatial model (by the R mgcv package). They do not incorporate uncertainty in the detection functions, g(0) estimates, predictor variables, and so on.

Shelf and Vicinity

Statistical output

```
Rscript.exe: This is mgcv 1.8-3. For overview type 'help("mgcv-package")'.


Family: Tweedie(p=1.163)
```

```
Link function: log

Formula:
abundance ~ offset(log(area_km2)) + s(log10(Depth), bs = "ts",
    k = 5) + s(sqrt(pmin(DistToShore/1000, 200)), bs = "ts",
    k = 5) + s(pmin(DistTo125m/1000, 200), bs = "ts", k = 5) +
    s(log10(pmax(ClimPkPB, 0.01)), bs = "ts", k = 5)

Parametric coefficients:
            Estimate Std. Error t value Pr(>|t|)
(Intercept)  -8.4403     0.3675  -22.97   <2e-16 ***
---
Signif. codes:  0 '***' 0.001 '**' 0.01 '*' 0.05 '.' 0.1 ' ' 1

Approximate significance of smooth terms:
                                      edf Ref.df     F  p-value
s(log10(Depth))                     3.705      4 30.18  < 2e-16 ***
s(sqrt(pmin(DistToShore/1000, 200))) 3.576      4 12.39 3.87e-11 ***
s(pmin(DistTo125m/1000, 200))       3.686      4 66.10  < 2e-16 ***
s(log10(pmax(ClimPkPB, 0.01)))      1.786      4 40.21  < 2e-16 ***
---
Signif. codes:  0 '***' 0.001 '**' 0.01 '*' 0.05 '.' 0.1 ' ' 1

R-sq.(adj) =  0.0269   Deviance explained = 27.5%
-REML = 5619.3  Scale est. = 18.146    n = 62935

All predictors were significant. This is the final model.
Creating term plots.
Diagnostic output from gam.check():

Method: REML   Optimizer: outer newton
full convergence after 11 iterations.
Gradient range [-2.644177e-05,0.002818238]
(score 5619.315 & scale 18.14555).
Hessian positive definite, eigenvalue range [0.1303163,4492.229].
Model rank =  17 / 17

Basis dimension (k) checking results. Low p-value (k-index<1) may
indicate that k is too low, especially if edf is close to k'.

                                       k'   edf k-index p-value
s(log10(Depth))                     4.000 3.705   0.856    0.00
s(sqrt(pmin(DistToShore/1000, 200))) 4.000 3.576   0.896    0.60
s(pmin(DistTo125m/1000, 200))       4.000 3.686   0.886    0.18
s(log10(pmax(ClimPkPB, 0.01)))      4.000 1.786   0.849    0.00
```

Predictors retained during the model selection procedure: Depth, DistToShore, DistTo125m, ClimPkPB

Predictors dropped during the model selection procedure: Slope, ClimSST, ClimDistToFront1, ClimTKE

Model term plots

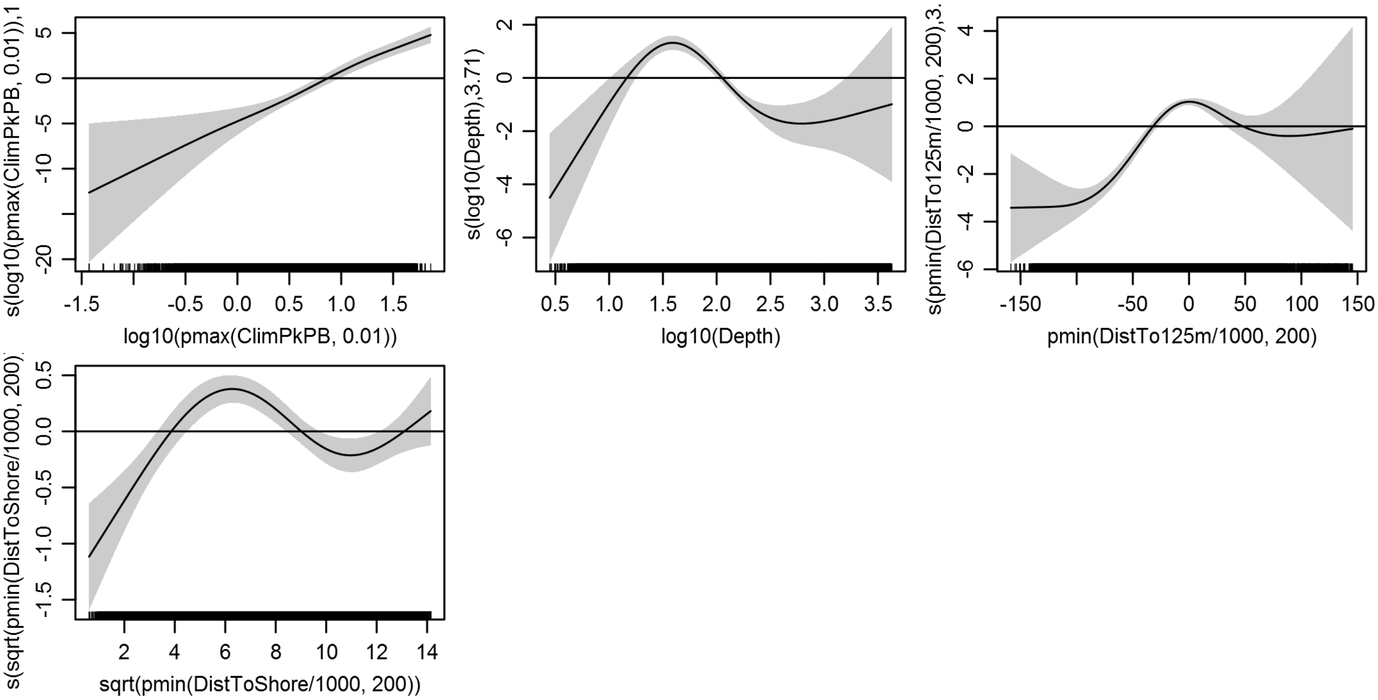

Diagnostic plots

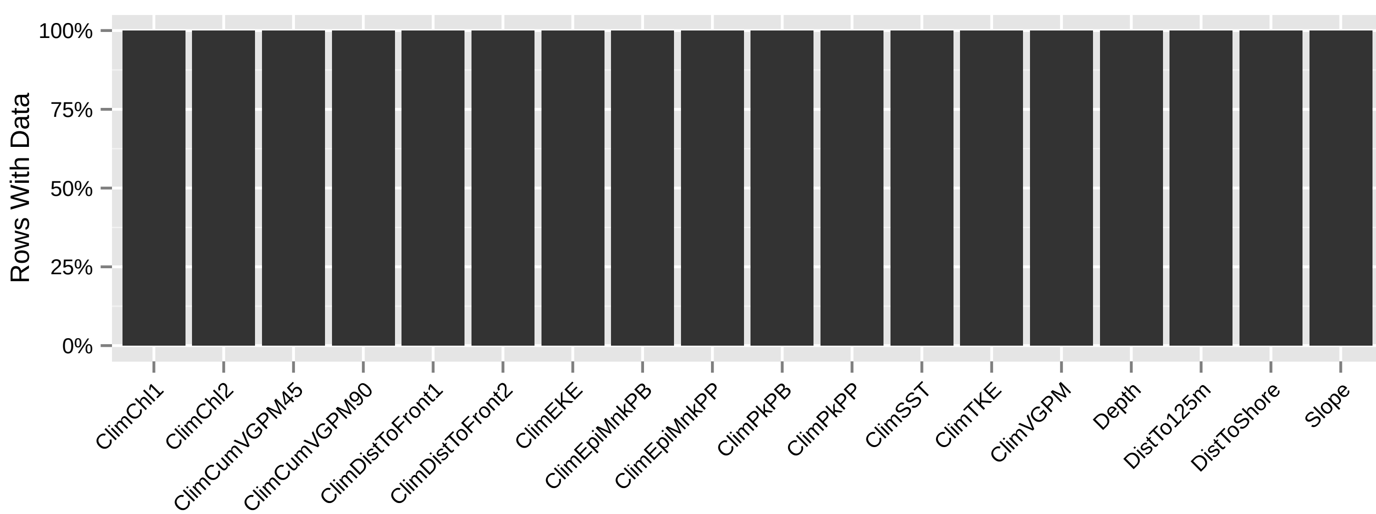

Figure 89: Segments with predictor values for the Minke whale Climatological model, Summer season, Shelf and Vicinity. This plot is used to assess how many segments would be lost by including a given predictor in a model.

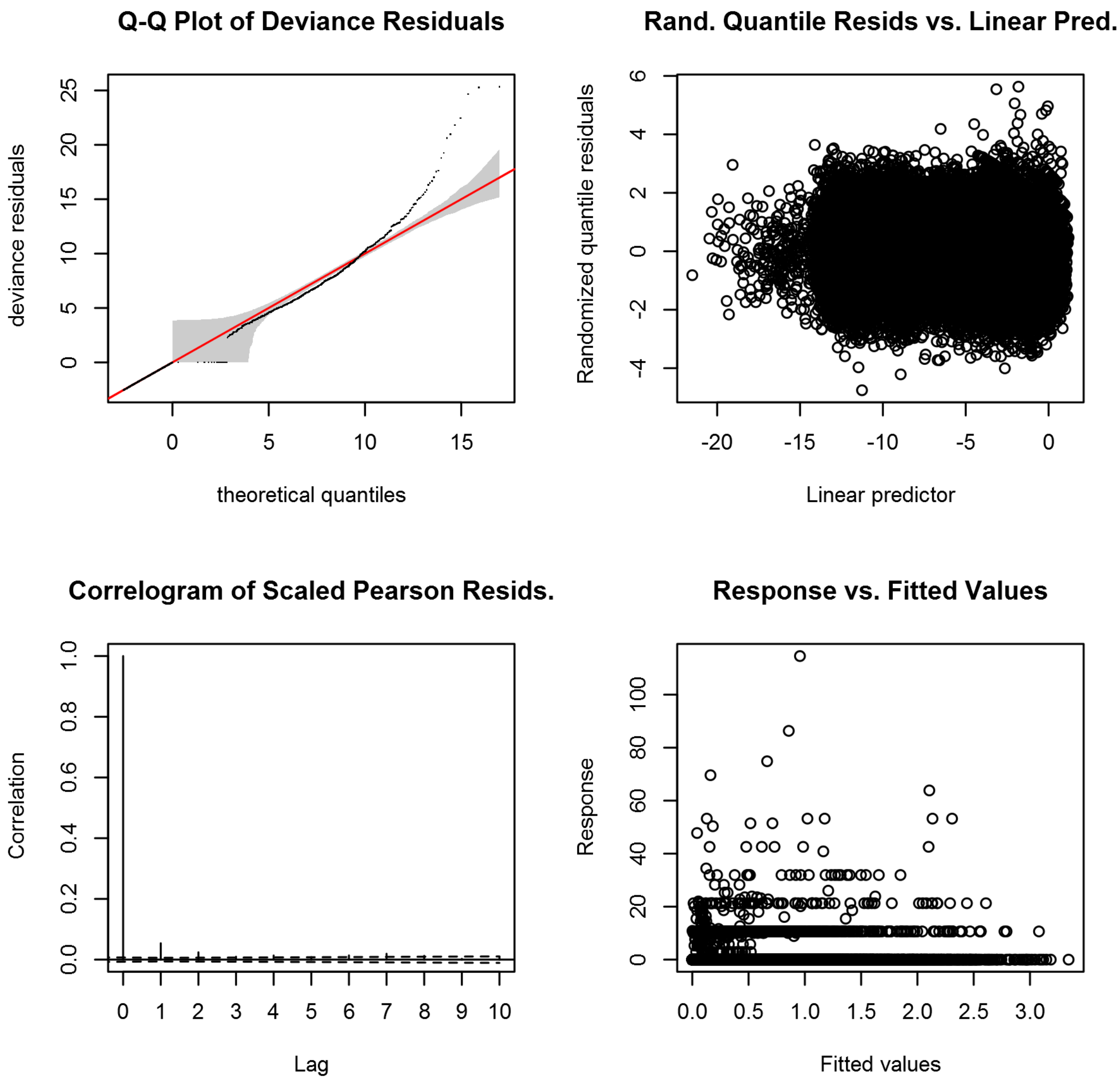

Figure 90: Statistical diagnostic plots for the Minke whale Climatological model, Summer season, Shelf and Vicinity.

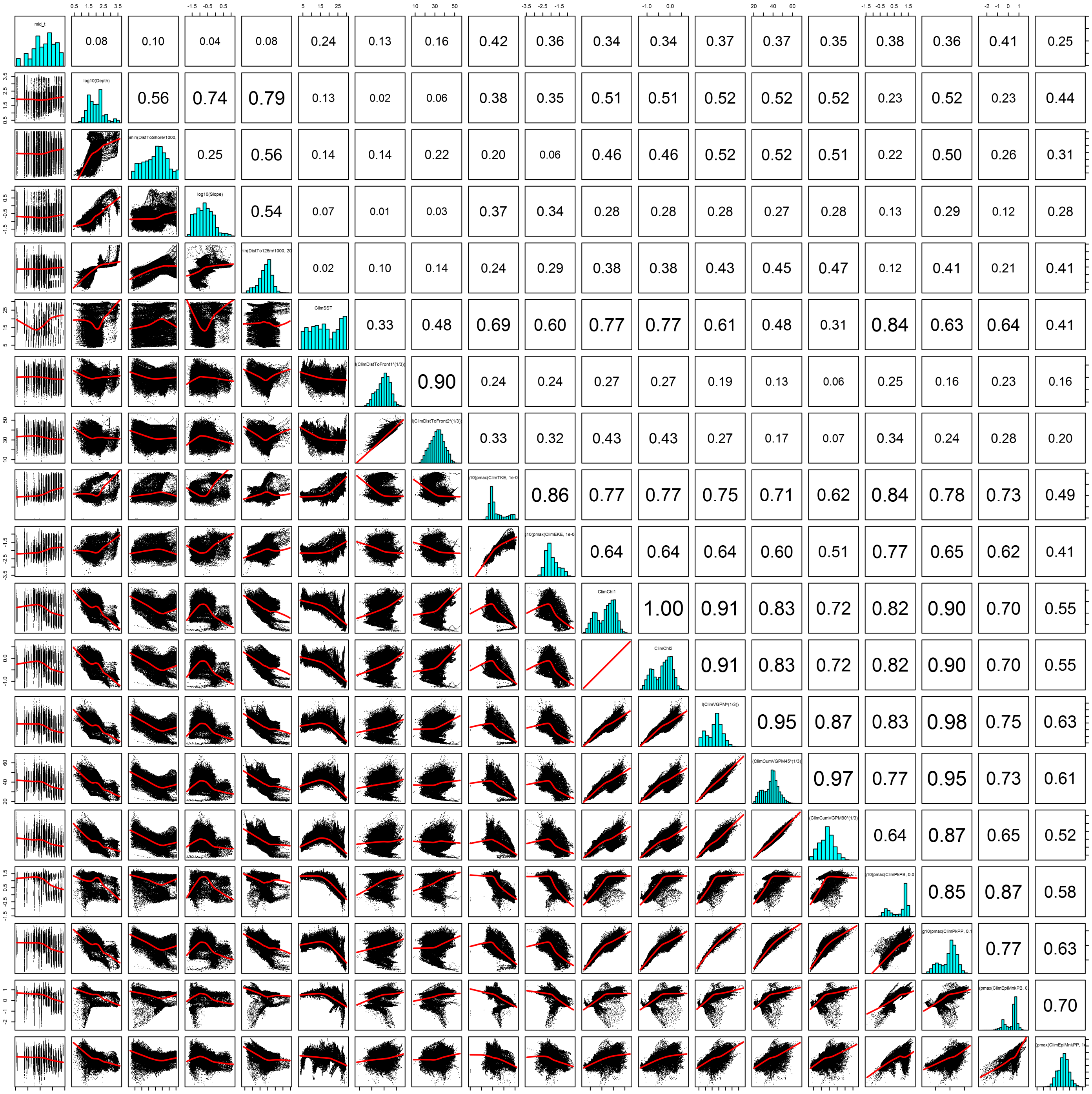

Figure 91: Scatterplot matrix for the Minke whale Climatological model, Summer season, Shelf and Vicinity. This plot is used to inspect the distribution of predictors (via histograms along the diagonal), simple correlation between predictors (via pairwise Pearson coefficients above the diagonal), and linearity of predictor correlations (via scatterplots below the diagonal). This plot is best viewed at high magnification.

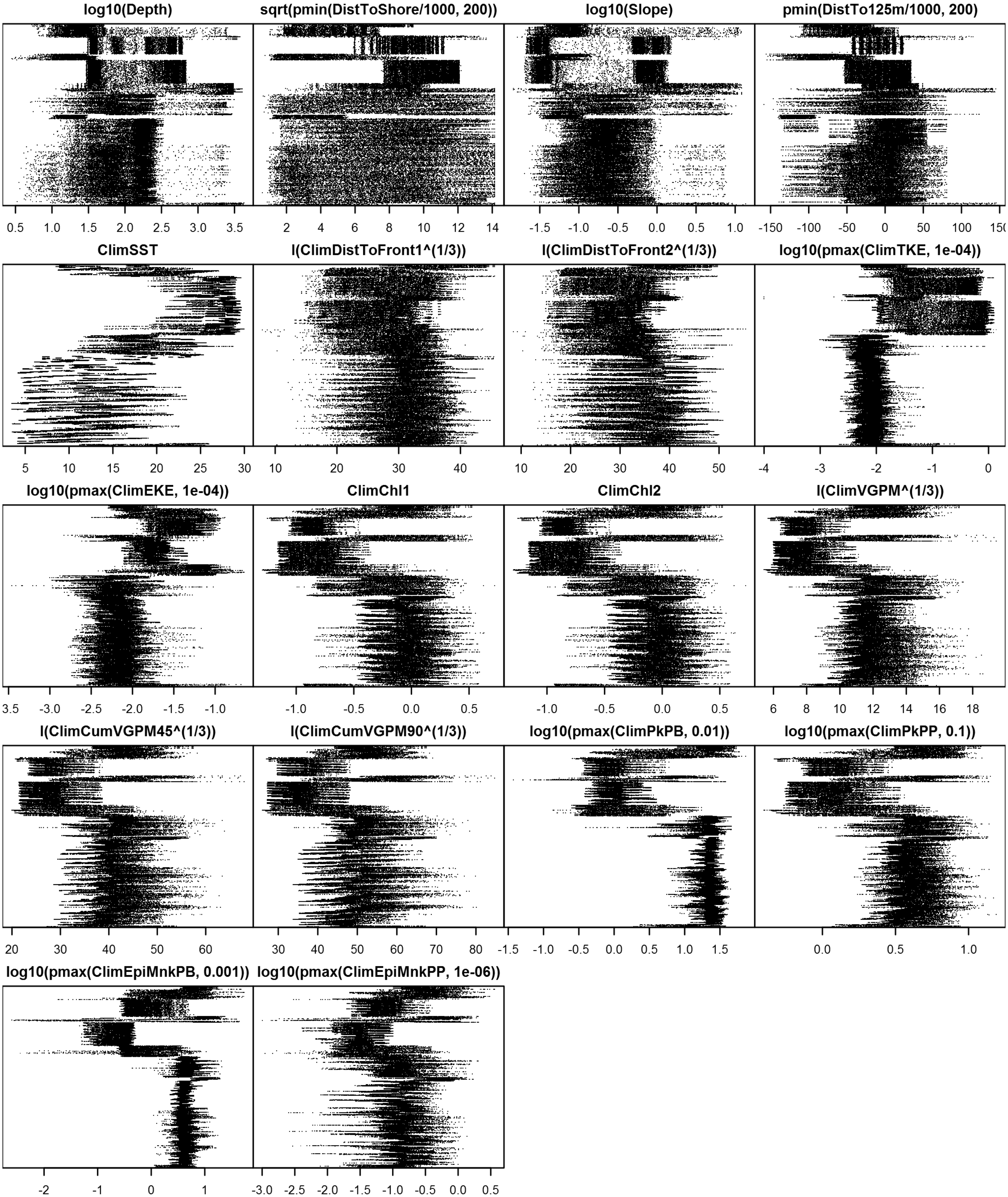

Figure 92: Dotplot for the Minke whale Climatological model, Summer season, Shelf and Vicinity. This plot is used to check for suspicious patterns and outliers in the data. Points are ordered vertically by transect ID, sequentially in time.

Offshore

A mean density estimate was made for this region. First, density (individuals per square kilometer) was calculated as the number of animals encountered divided by the area effectively surveyed, corrected by the detection functions and g(0) estimates. Then, density was multiplied by the size of each grid cell, in square kilometers, to obtain abundance (number of individuals) per grid cell. Finally, all grid cells in the region were assigned this abundance value.

Model Comparison

Spatial Model Performance

The table below summarizes the performance of the candidate spatial models that were tested. For each season, the first model contained only physiographic predictors. Subsequent models added additional suites of predictors of based on when they became available via remote sensing.

For each model, three versions were fitted; the % Dev Expl columns give the % deviance explained by each one. The "climatological" models were fitted to 8-day climatologies of the environmental predictors. Because the environmental predictors were always available, no segments were lost, allowing these models to consider the maximal amount of survey data. The "contemporaneous" models were fitted to day-of-sighting images of the environmental predictors; these were smoothed to reduce data loss due to clouds, but some segments still failed to retrieve environmental values and were lost. Finally, the "climatological same segments" models fitted climatological predictors to the segments retained by the contemporaneous model, so that the explantory power of the two types of predictors could be directly compared. For each of the three models, predictors were selected independently via shrinkage smoothers; thus the three models did not necessarily utilize the same predictors.

Predictors derived from ocean currents first became available in January 1993 after the launch of the TOPEX/Poseidon satellite; productivity predictors first became available in September 1997 after the launch of the SeaWiFS sensor. Contemporaneous and climatological same segments models considering these predictors usually suffered data loss. Date Range shows the years spanned by the retained segments. The Segments column gives the number of segments retained; % Lost gives the percentage lost.

Season	Predictors	Climatol % Dev Expl	Contemp % Dev Expl	Climatol Same Segs % Dev Expl	Segments	% Lost	Date Range
Winter							
	Phys	6.3			18415		1999-2014
	Phys+SST	6.3	6.3	6.3	18415	0.0	1999-2014
	Phys+SST+Curr	6.3	6.3	6.3	18415	0.0	1999-2014
	Phys+SST+Curr+Prod	9.2	6.3	9.2	18415	0.0	1999-2014
Summer							
	Phys	20.8			65833		1995-2014
	Phys+SST	26.0	26.2	26.0	65833	0.0	1995-2014
	Phys+SST+Curr	26.9	26.7	26.9	65344	0.7	1995-2013
	Phys+SST+Curr+Prod	28.0	28.1	27.5	62935	4.4	1998-2013

Table 34: Deviance explained by the candidate density models.

Abundance Estimates

The table below shows the estimated mean abundance (number of animals) within the study area, for the models that explained the most deviance for each model type. Mean abundance was calculated by first predicting density maps for a series of time steps, then computing the abundance for each map, and then averaging the abundances. For the climatological models, we used 8-day climatologies, resulting in 46 abundance maps. For the contemporaneous models, we used daily images, resulting in 365 predicted abundance maps per year that the prediction spanned. The Dates column gives the dates to which the estimates apply. For our models, these are the years for which both survey data and remote sensing data were available.

The Assumed g(0)=1 column specifies whether the abundance estimate assumed that detection was certain along the survey trackline. Studies that assumed this did not correct for availability or perception bias, and therefore underestimated abundance. The In our models column specifies whether the survey data from the study was also used in our models. If not, the study provides a completely independent estimate of abundance.

Season	Dates	Model or study	Estimated abundance	CV	Assumed g(0)=1	In our models
Winter						
	1999-2014	Climatological model*	740	0.23	No	
	1999-2013	Contemporaneous model	775	0.23	No	
	1999-2014	Climatological same segments model	740	0.23	No	
Summer						
	1995-2014	Climatological model*	2112	0.05	No	
	1998-2004	Contemporaneous model	2167	0.05	No	
	1995-2014	Climatological same segments model	2214	0.05	No	
	Jun-Aug 2011	Central Virginia to lower Bay of Fundy (Waring et al. 2014)	2591	0.81	No	No
	Jul-Aug 2007	Scotian Shelf to Northern Labrador (Lawson and Gosselin 2011)	20741	0.30	No	No
	August 2006	Southern Gulf of Maine to Bay of Fundy and Gulf of St. Lawrence (Waring et al. 2014)	3312	0.74	No	Yes
	Jun-Jul 2004	Gulf of Maine to lower Bay of Fundy (Waring et al. 2013; Palka 2006)	600	0.61	No	Yes

Table 35: Estimated mean abundance within the study area. We selected the model marked with * as our best estimate of the abundance and distribution of this taxon. For comparison, independent abundance estimates from NOAA technical reports and/or the scientific literature are shown. Please see the Discussion section below for our evaluation of our models compared to the other estimates. Our coefficients of variation (CVs) underestimate the true uncertainty in our estimates, as they only incorporated the uncertainty of the GAM stage of our models. Other sources of uncertainty include the detection functions and g(0) estimates. It was not possible to incorporate these into our CVs without undertaking a computationally-prohibitive bootstrap; we hope to attempt that in a future version of our models.

Density Maps

Climatological Model

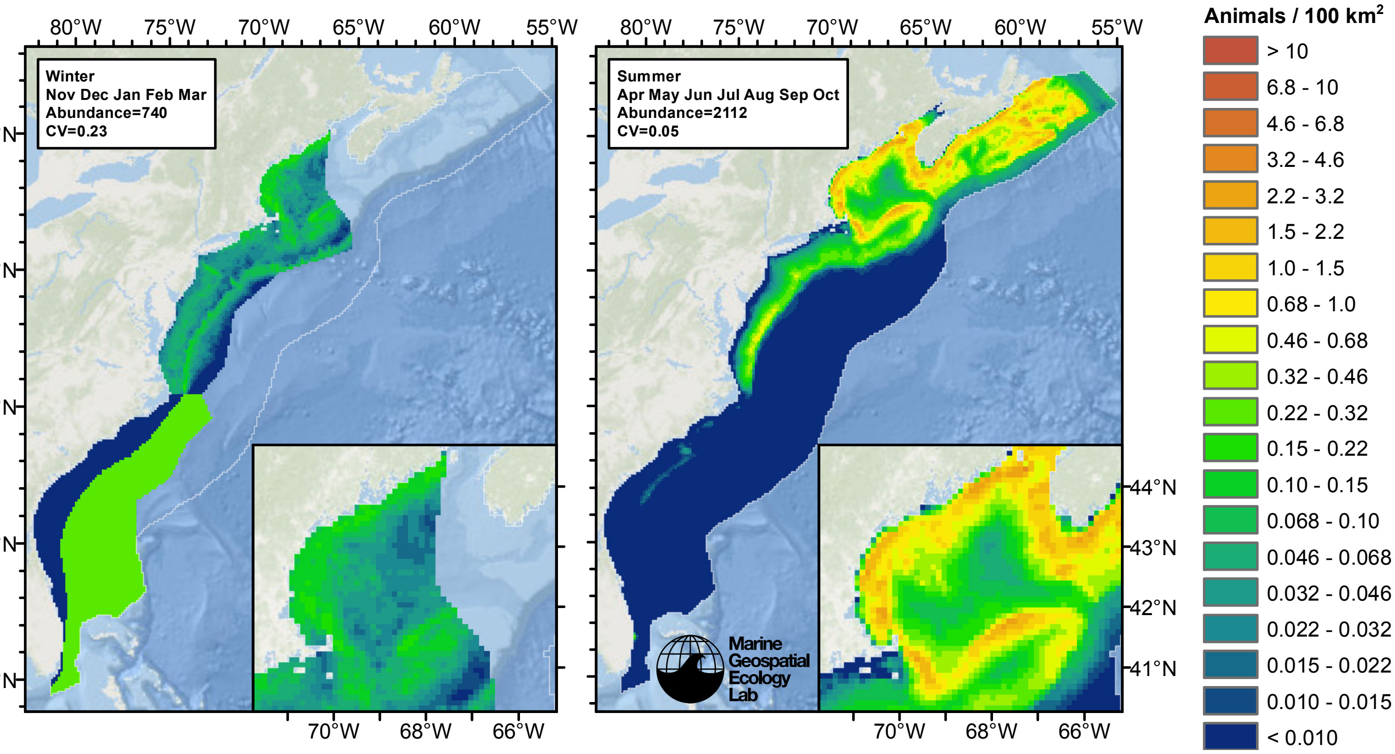

Figure 93: Minke whale density and abundance predicted by the climatological model that explained the most deviance. Regions inside the study area (white line) where the background map is visible are areas we did not model (see text).

Contemporaneous Model

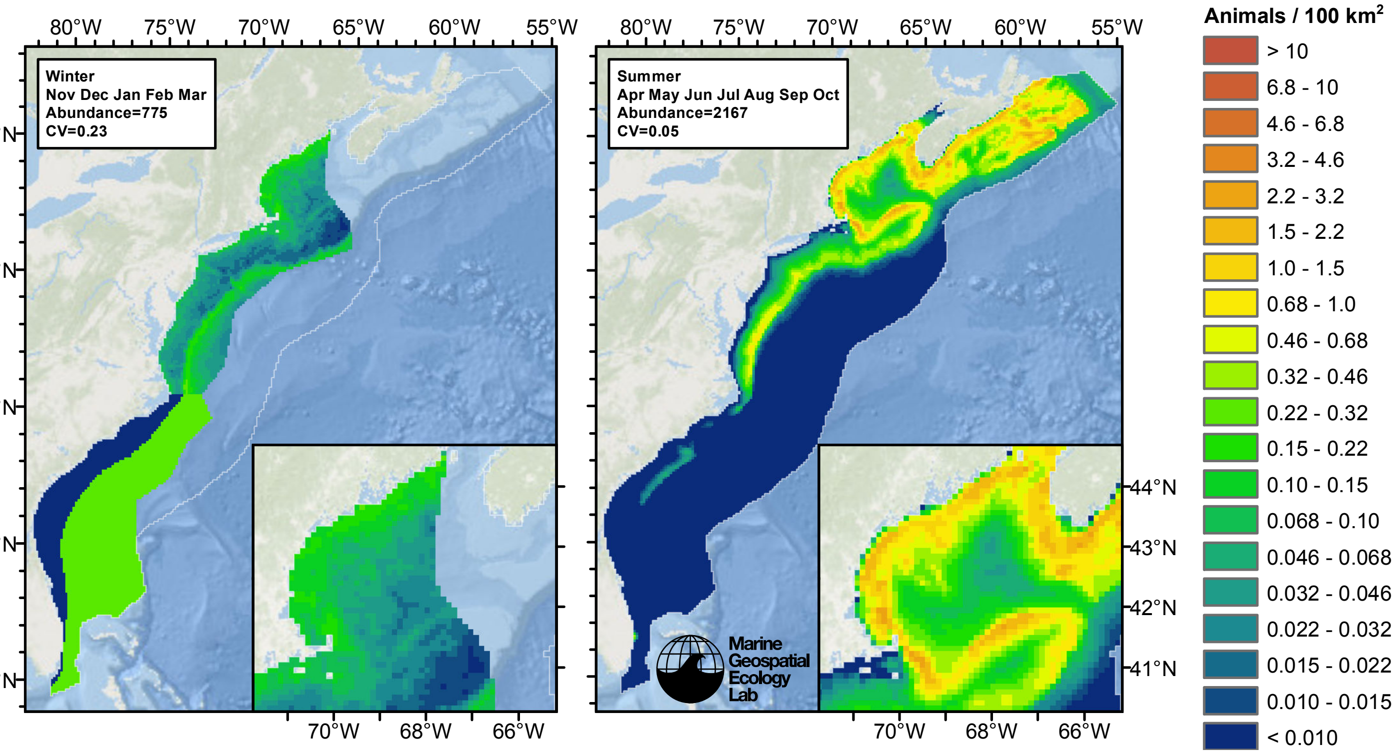

Figure 94: Minke whale density and abundance predicted by the contemporaneous model that explained the most deviance. Regions inside the study area (white line) where the background map is visible are areas we did not model (see text).

Climatological Same Segments Model

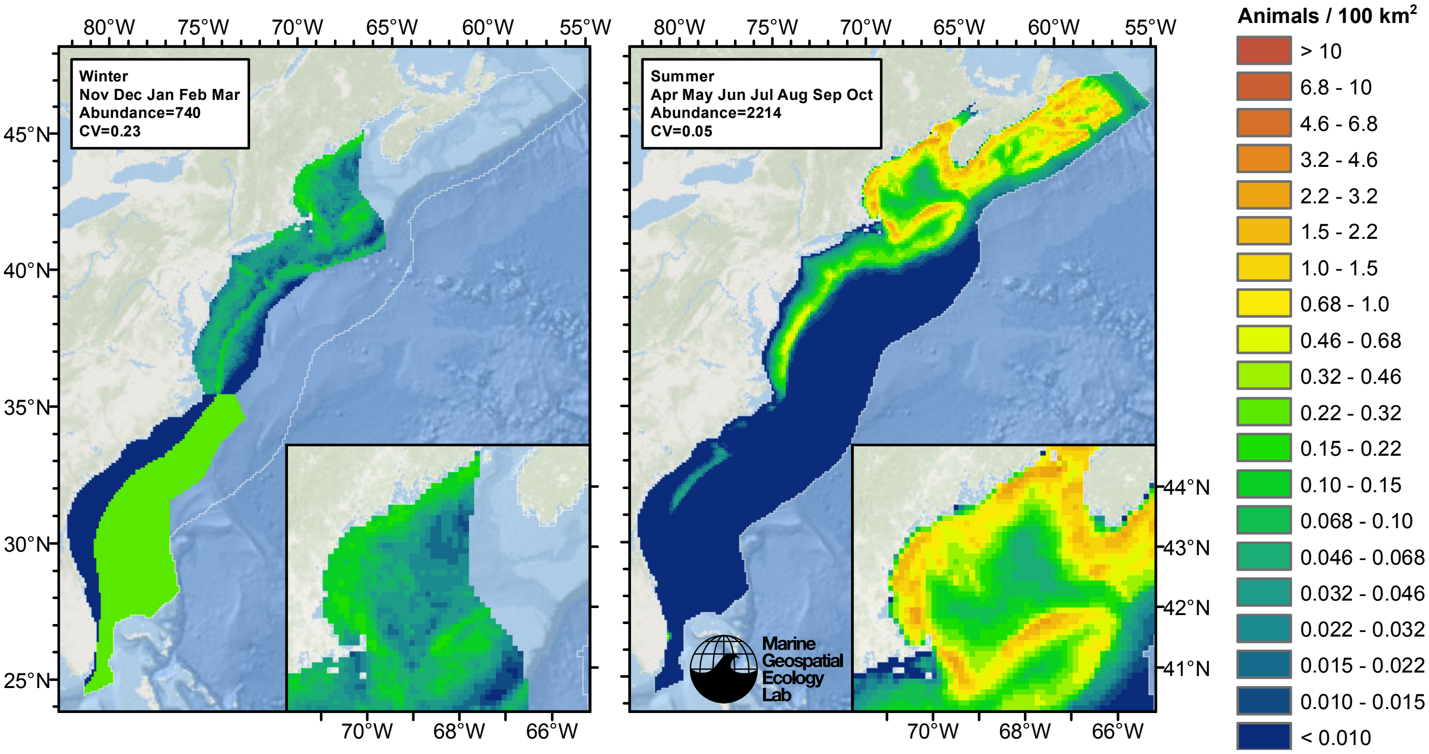

Figure 95: Minke whale density and abundance predicted by the climatological same segments model that explained the most deviance. Regions inside the study area (white line) where the background map is visible are areas we did not model (see text).

Temporal Variability

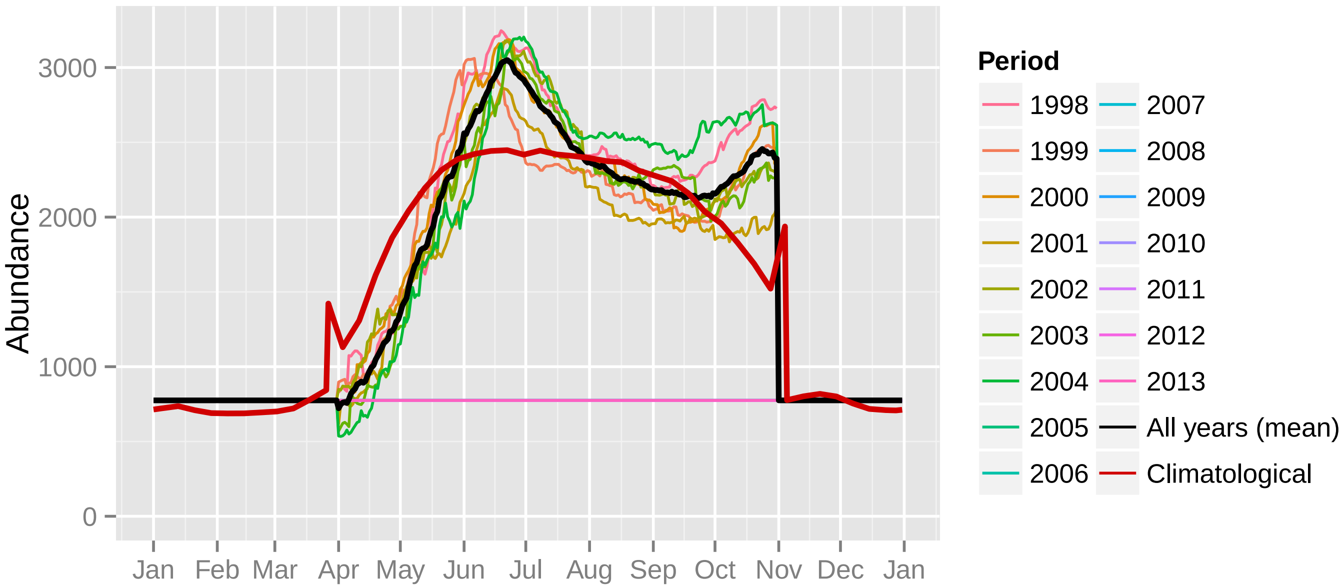

Figure 96: Comparison of Minke whale abundance predicted at a daily time step for different time periods. Individual years were predicted using contemporaneous models. "All years (mean)" averages the individual years, giving the mean annual abundance of the contemporaneous model. "Climatological" was predicted using the climatological model. The results for the climatological same segments model are not shown.

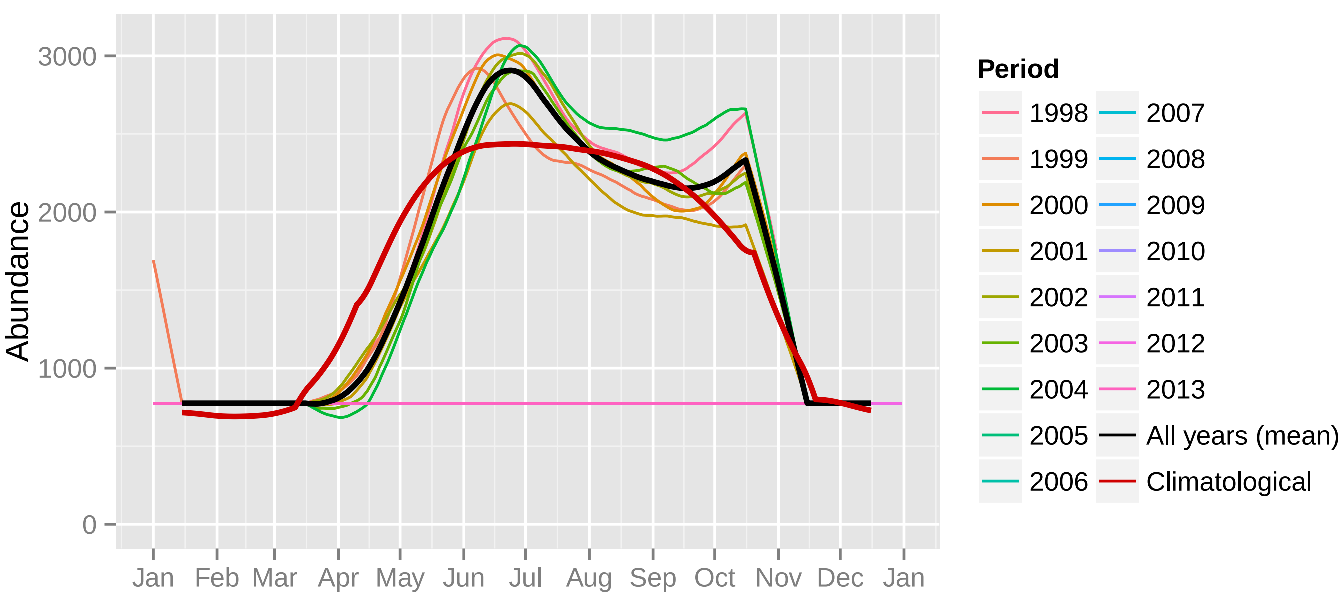

Figure 97: The same data as the preceding figure, but with a 30-day moving average applied.

Climatological Model

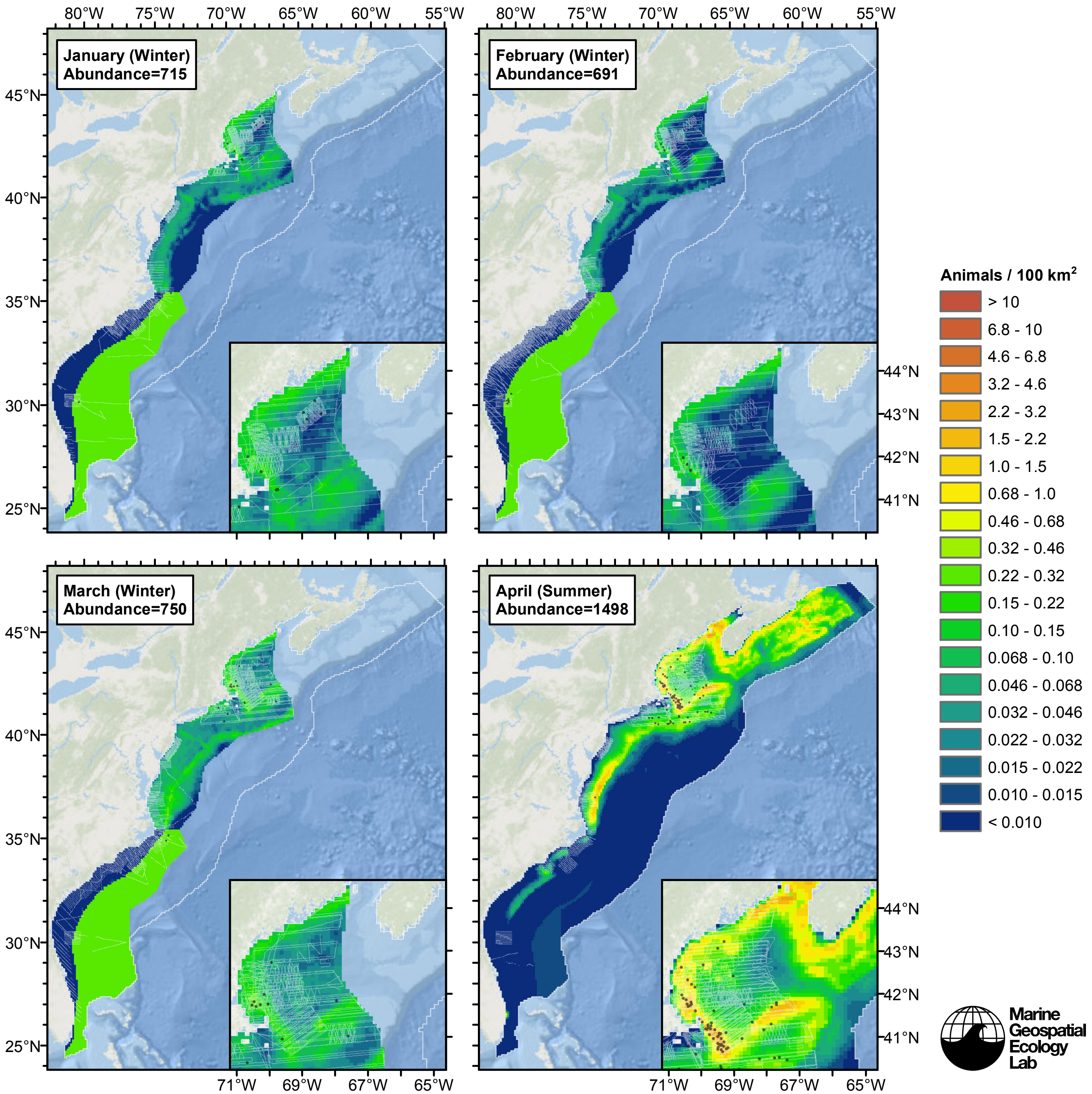

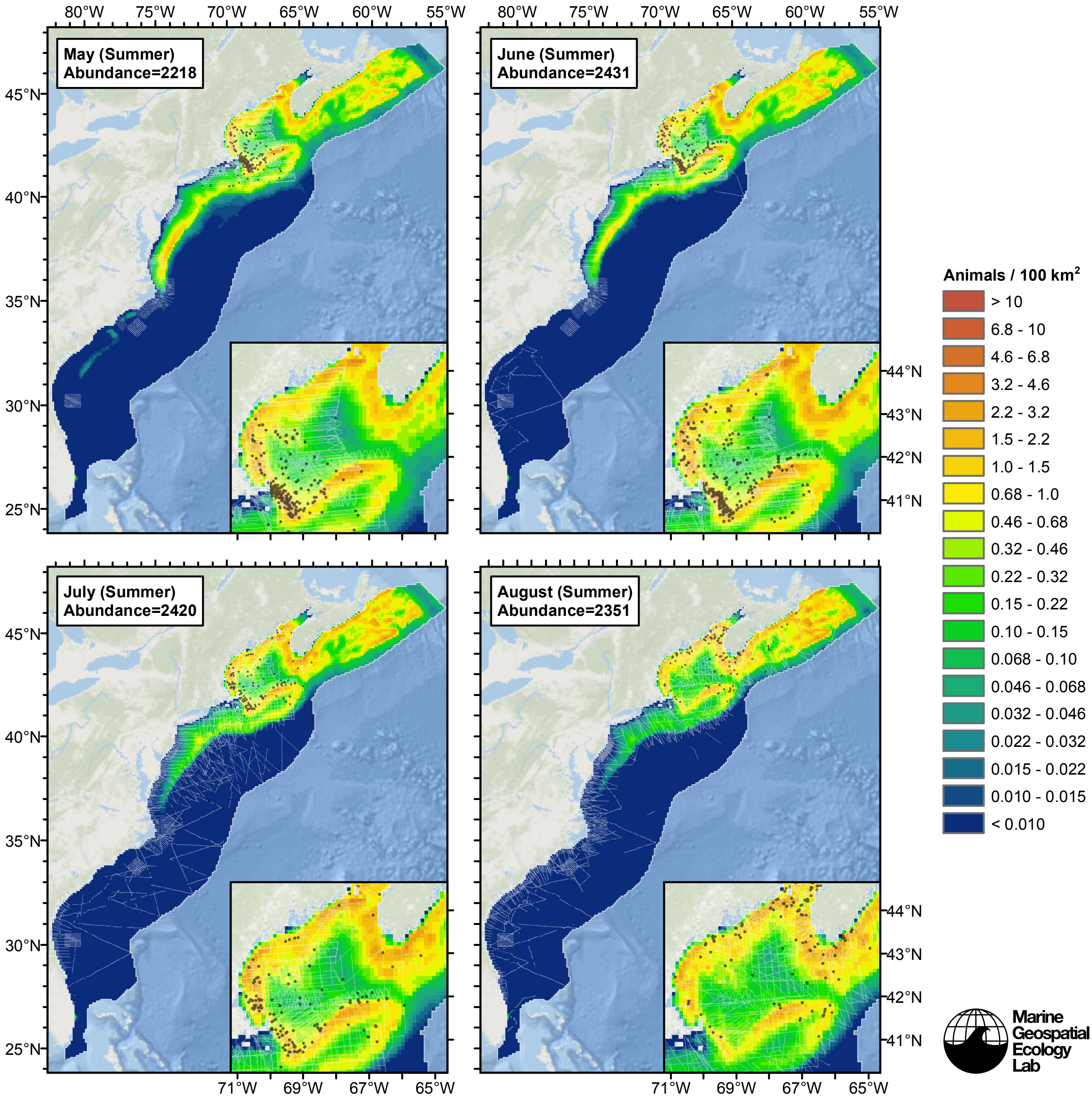

May (Summer)
Abundance=2218
June (Summer)
Abundance=2431
July (Summer)
Abundance=2420
August (Summer)
Abundance=2351
80°W
75°W
70°W
65°W
60°W
55°W
45°N
40°N
35°N
30°N
25°N
44°N
43°N
42°N
41°N
71°W
69°W
67°W
65°W
Animals / 100 km^2
> 10
6.8 - 10
4.6 - 6.8
3.2 - 4.6
2.2 - 3.2
1.5 - 2.2
1.0 - 1.5
0.68 - 1.0
0.46 - 0.68
0.32 - 0.46
0.22 - 0.32
0.15 - 0.22
0.10 - 0.15
0.068 - 0.10
0.046 - 0.068
0.032 - 0.046
0.022 - 0.032
0.015 - 0.022
0.010 - 0.015
< 0.010
Marine Geospatial Ecology Lab

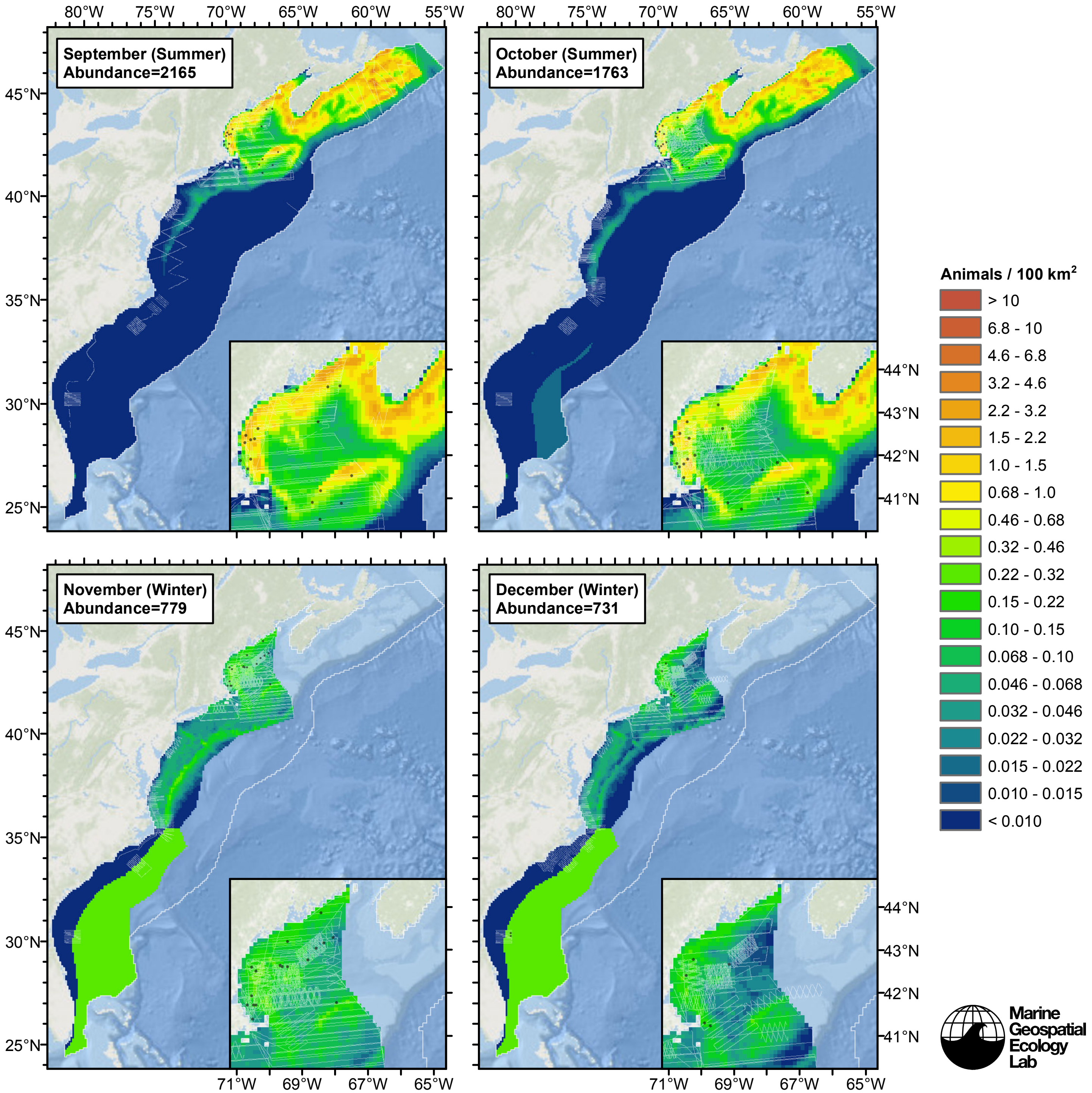
September (Summer)
Abundance=2165
October (Summer)
Abundance=1763
November (Winter)
Abundance=779
December (Winter)
Abundance=731
80°W
75°W
70°W
65°W
60°W
55°W
45°N
40°N
35°N
30°N
25°N
44°N
43°N
42°N
41°N
71°W
69°W
67°W
65°W
Animals / 100 km²
> 10
6.8 - 10
4.6 - 6.8
3.2 - 4.6
2.2 - 3.2
1.5 - 2.2
1.0 - 1.5
0.68 - 1.0
0.46 - 0.68
0.32 - 0.46
0.22 - 0.32
0.15 - 0.22
0.10 - 0.15
0.068 - 0.10
0.046 - 0.068
0.032 - 0.046
0.022 - 0.032
0.015 - 0.022
0.010 - 0.015
< 0.010
Marine
Geospatial
Ecology
Lab

Contemporaneous Model

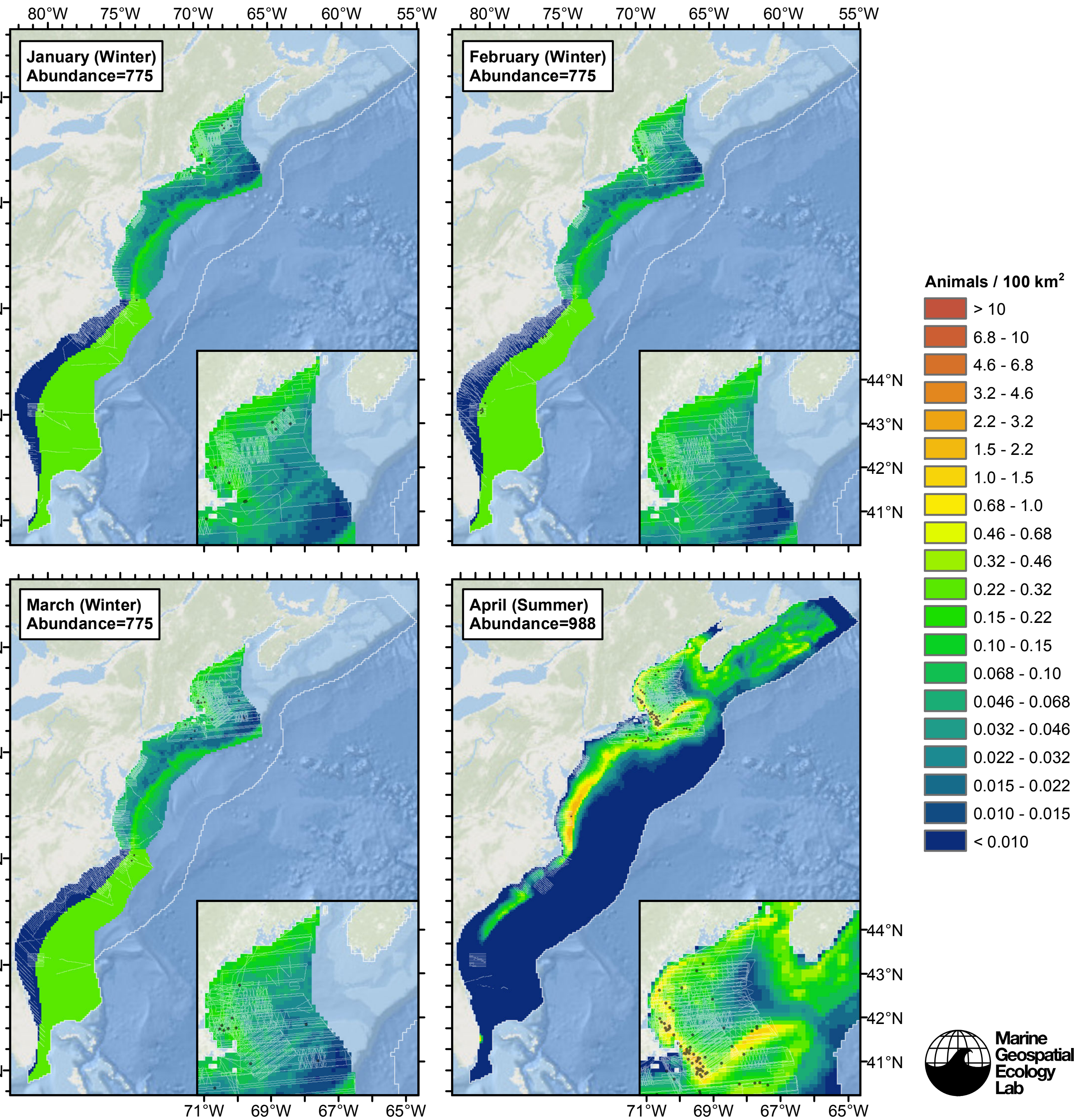

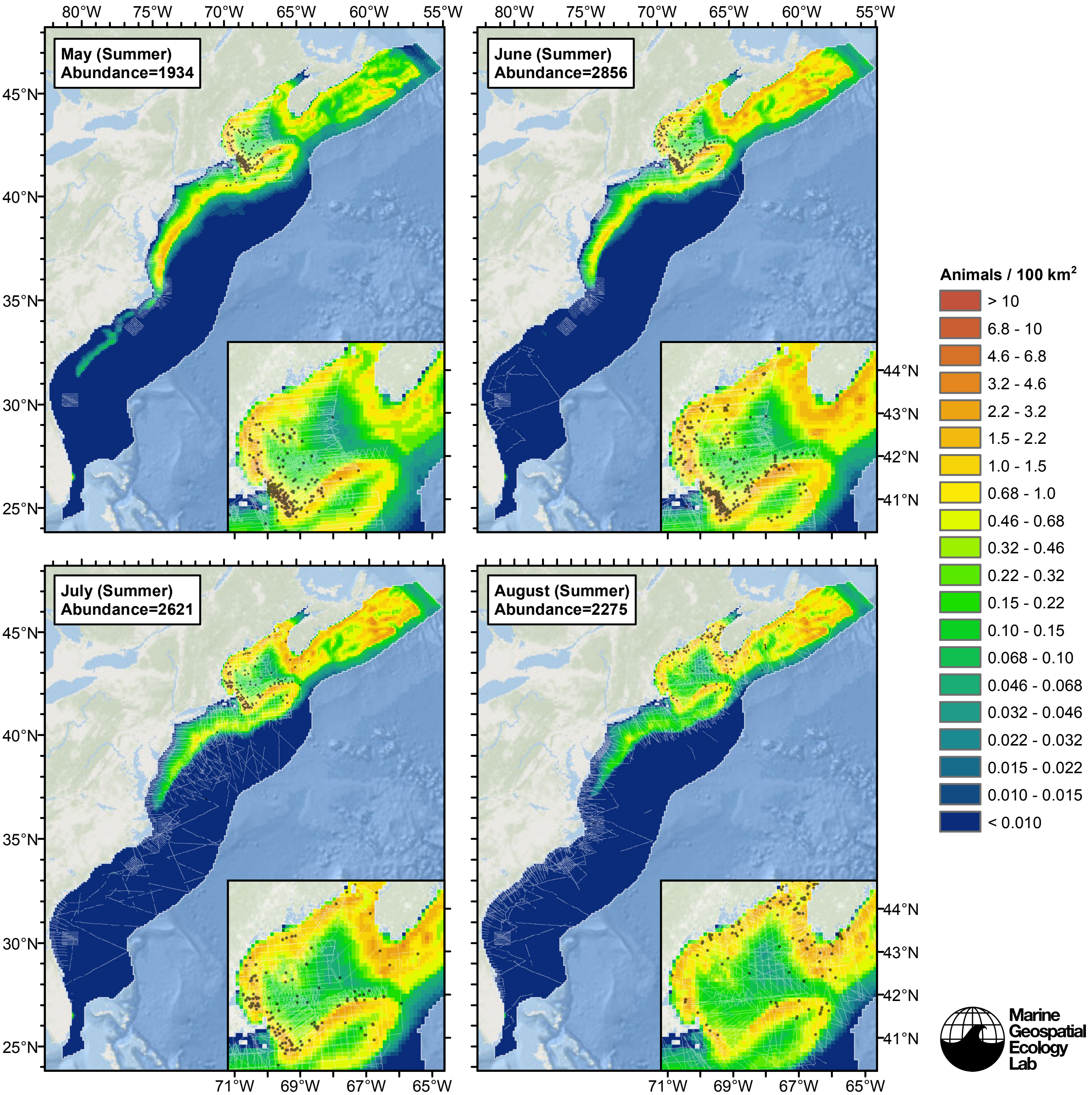
May (Summer)
Abundance=1934
June (Summer)
Abundance=2856
July (Summer)
Abundance=2621
August (Summer)
Abundance=2275
80°W
75°W
70°W
65°W
60°W
55°W
45°N
40°N
35°N
30°N
25°N
44°N
43°N
42°N
41°N
71°W
69°W
67°W
65°W
Animals / 100 km²
> 10
6.8 - 10
4.6 - 6.8
3.2 - 4.6
2.2 - 3.2
1.5 - 2.2
1.0 - 1.5
0.68 - 1.0
0.46 - 0.68
0.32 - 0.46
0.22 - 0.32
0.15 - 0.22
0.10 - 0.15
0.068 - 0.10
0.046 - 0.068
0.032 - 0.046
0.022 - 0.032
0.015 - 0.022
0.010 - 0.015
< 0.010
Marine Geospatial Ecology Lab

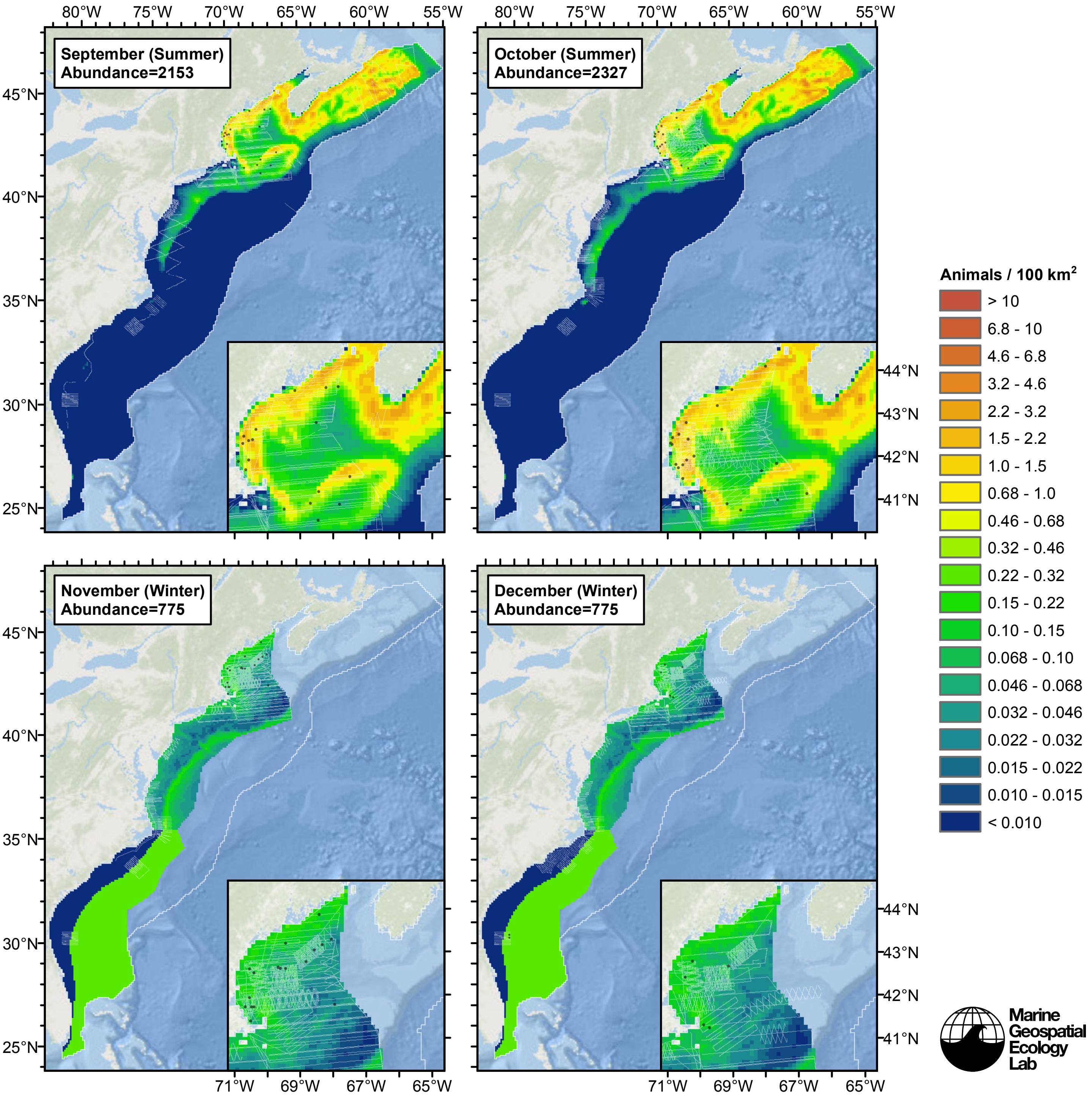

September (Summer)
Abundance=2153
October (Summer)
Abundance=2327
November (Winter)
Abundance=775
December (Winter)
Abundance=775
80°W
75°W
70°W
65°W
60°W
55°W
45°N
40°N
35°N
30°N
25°N
44°N
43°N
42°N
41°N
71°W
69°W
67°W
65°W
Animals / 100 km²
> 10
6.8 - 10
4.6 - 6.8
3.2 - 4.6
2.2 - 3.2
1.5 - 2.2
1.0 - 1.5
0.68 - 1.0
0.46 - 0.68
0.32 - 0.46
0.22 - 0.32
0.15 - 0.22
0.10 - 0.15
0.068 - 0.10
0.046 - 0.068
0.032 - 0.046
0.022 - 0.032
0.015 - 0.022
0.010 - 0.015
< 0.010
Marine
Geospatial
Ecology
Lab

Climatological Same Segments Model

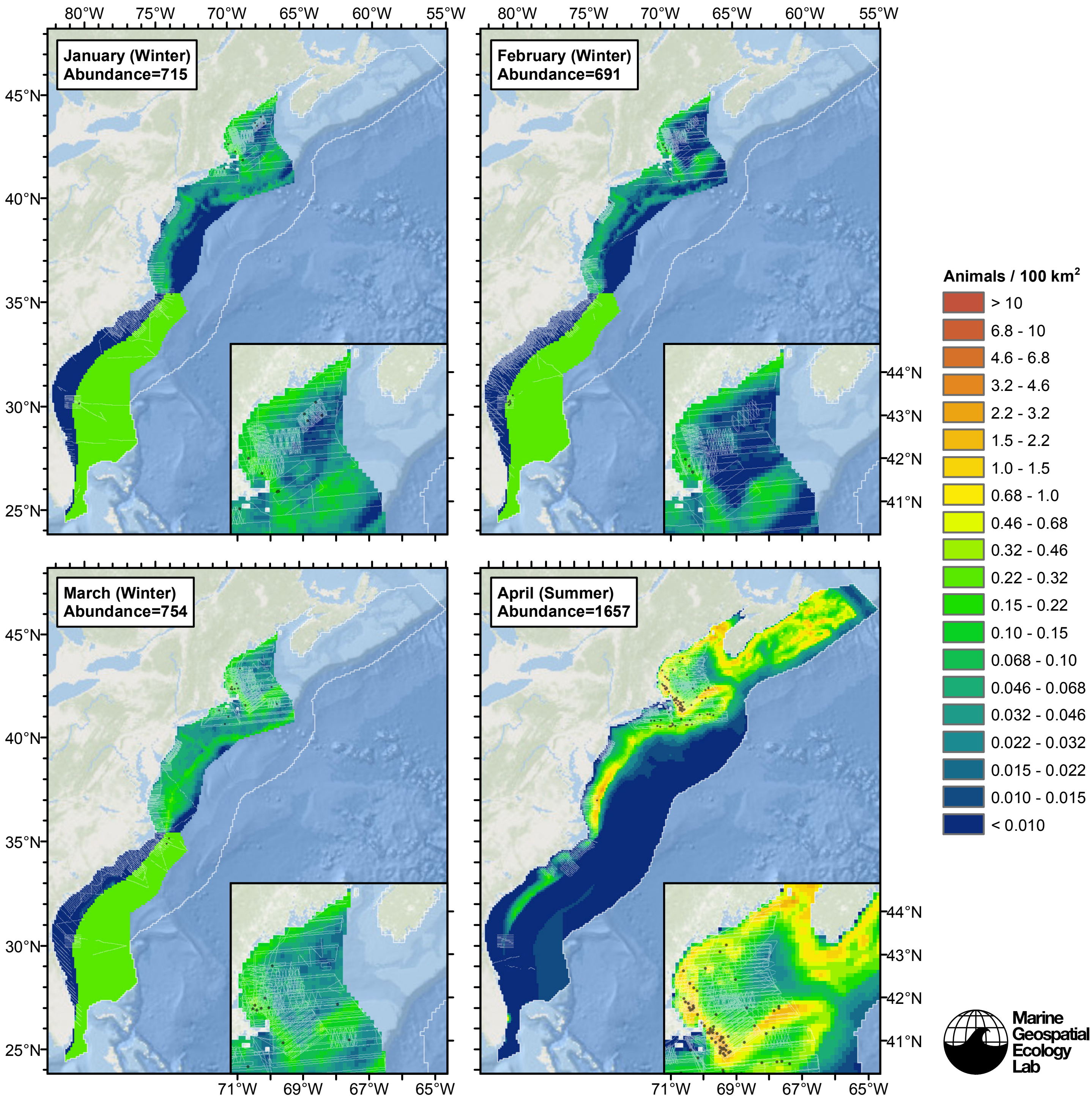

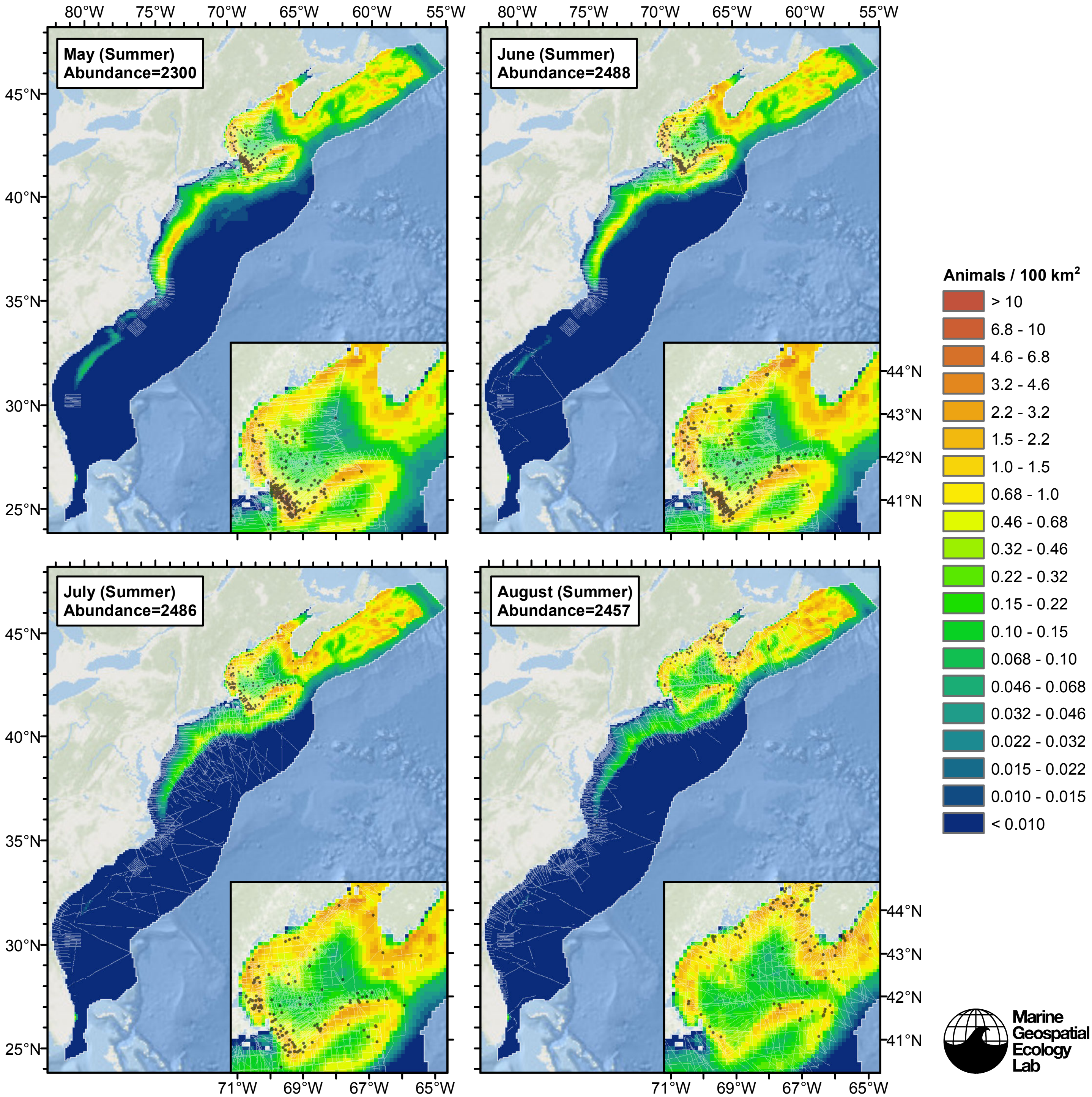

Marine Geospatial Ecology Lab

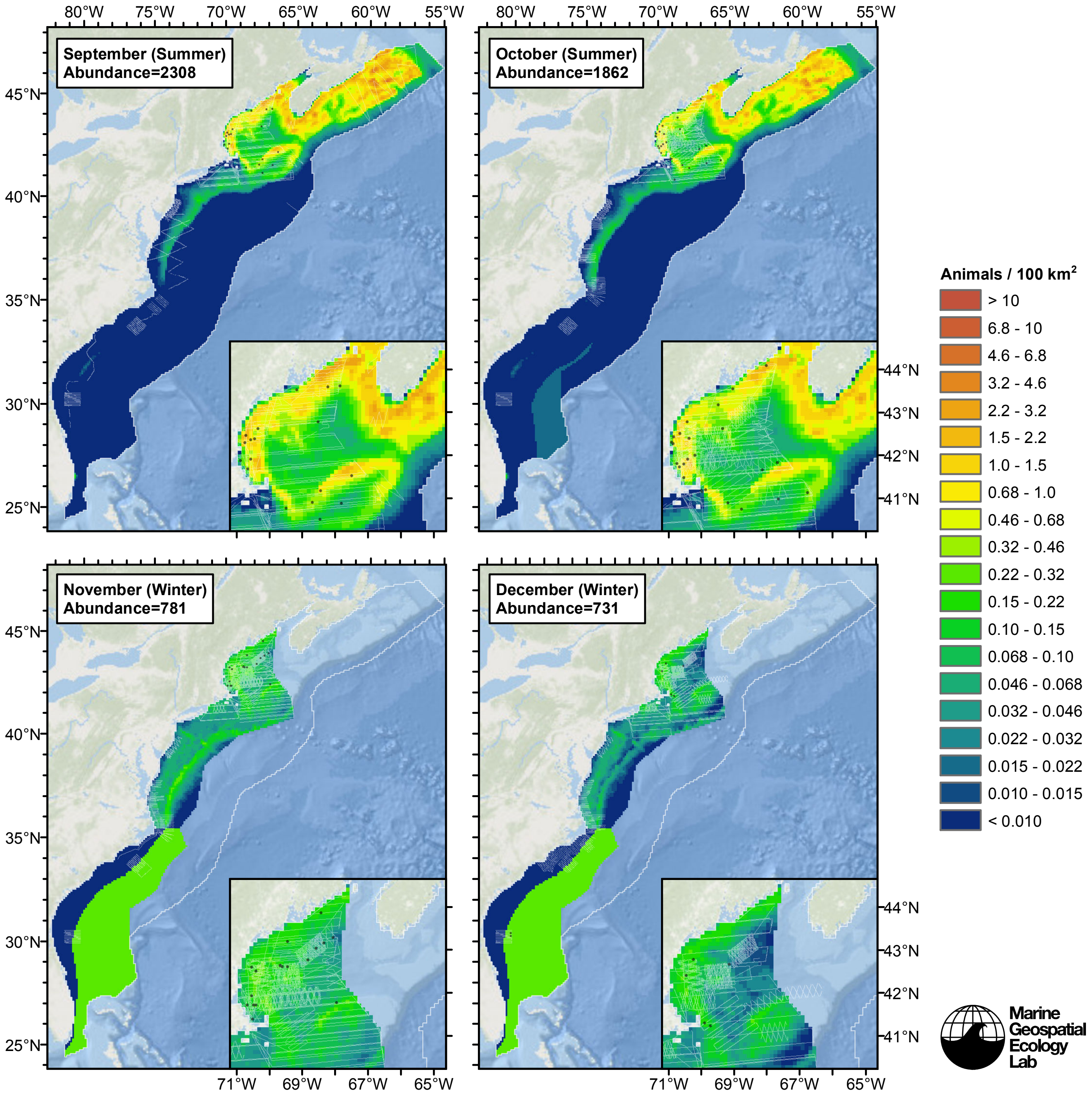

Discussion

Winter

In the northern sub-region, the models that used climatological predictor variables explained substantially more deviance than the models that used contemporaneous predictors, selecting slope and chlorophyll as predictors instead of slope and distance to shore. On the basis of higher explained deviance, we selected the climatological model that considered all segments as our best estimate of minke whale winter distribution and abundance in this sub-region.

In the southern slope and abyss sub-region, abundance was markedly higher than in the northern region. This is consistent with the view that most minkes depart the northern feeding grounds in the summer and migrate south.

No other estimates of winter abundance were available in the literature so we have no basis with which to compare our total abundance estimate.

Summer

In this season, the climatological model that considered all segments and the contemporaneous model essentially performed equally well; the latter model explained 0.1% more deviance but also predicted slightly higher abundance along the shelf break off South Carolina, which we consider to be in error (no sightings occurred there, and it does not represent good feeding habitat for minke whales). On the basis of avoiding that error, and because it considered more survey segments, we selected the climatological model that considered all segments as our best estimate of summertime minke whale distribution and abundance. The climatological model that considered the contemporaneous model's segments scored 0.5% lower than the other two, so we did not consider it.

At the broad scale, the model displayed plausible temporal dynamics, with abundance starting low in April, increasing and shifting north in the mid-summer months, then falling in October. Although minke whale migration patterns for this area have not been fully described in the literature, we are confident enough in the temporal dynamics of our model to recommend that our monthly predictions be used for federal regulatory purposes and marine spatial planning applications.

The total abundance predicted by our model is lower than the other estimates reported in recent NOAA stock assessment reports (Table 35) but within their confidence limits. A direct comparison is difficult due to the differing spatial and temporal extents of those studies and ours. Interestingly, our estimate is roughly 30% lower than Palka's 2006 estimate, yet our aerial g(0) of 0.385 was lower than Palka's g(0) of 0.53. Abundance changes inversely with g(0), so it is noteworthy that our abundance estimate was lower than Palka's even though our g(0) was lower. With other species, such as fin whales, the difference between our estimate and Palka's could plausibly be attributed to a difference in g(0). Not so, here.

Lawson and Gosselin (2011) estimated an order of magnitude more minke whales present from the Scotian Shelf to northern Labrador. Their estimate reflects the higher abundance of minke whales in Canada, especially in the far north. We believe our models could be improved by incorporating the data they used, the Canadian TNASS survey from July 2007 (Lawson and Gosselin, 2009). We made several attempts to contact J. Lawson regarding this survey, but received no response. We remain hopeful that a collaboration can be established in the future, and the Canadian TNASS data may be incorporated into a new version of our models.

References

Barlow J, Forney KA (2007) Abundance and density of cetaceans in the California Current ecosystem. Fish. Bull. 105: 509-526.

CETAP (1982) A characterization of marine mammals and turtles in the mid-and north Atlantic areas of the US outer continental shelf. Final Report. Bureau of Land Management, Washington, DC. Ref. AA551-CT8-48.

Carretta JV, Lowry MS, Stinchcomb CE, Lynn MS, Cosgrove RE (2000) Distribution and abundance of marine mammals at San Clemente Island and surrounding offshore waters: results from aerial and ground surveys in 1998 and 1999. Administrative Report LJ-00-02, available from Southwest Fisheries Science Center, P.O. Box 271, La Jolla, CA USA 92038. 44 p.

Chelton DB, Schlax MG, Samelson RM (2011) Global observations of nonlinear mesoscale eddies. Prog. Oceanogr. 91: 167-216.

Debich AJ, Baumann-Pickering A, Sirovic A, Buccowich JS, Gentes ZE, et al. (2014) Passive Acoustic Monitoring for Marine Mammals in the Cherry Point OPAREA 2011-2012. MPL Technical Memorandum #545. Marine Physical Laboratory, Scripps Institution of Oceanography, University of California San Diego, La Jolla, California. 83 p. Available online: http://www.navymarinespeciesmonitoring.us/index.php/download_file/view/660/

Debich AJ, Baumann-Pickering A, Sirovic A, Kerosky SA, Roche LK, et al. (2013) Passive Acoustic Monitoring for Marine Mammals in the Jacksonville Range Complex 2010-2011. MPL Technical Memorandum #541. Marine Physical Laboratory, Scripps Institution of Oceanography, University of California San Diego, La Jolla, California. 57 p. Available online: http://www.navymarinespeciesmonitoring.us/index.php/download_file/view/465/

Hodge L, Reed A (2014) Passive Acoustic Monitoring for Marine Mammals in Onslow Bay (multiple documents). Reports by the Duke University Marine Laboratory, Beaufort, North Carolina. Available online: http://www.navymarinespeciesmonitoring.us/reading-room/atlantic/ under Technical Reports.

Lawson JW, Gosselin J-F (2011) Fully-corrected cetacean abundance estimates from the Canadian TNASS survey. Working Paper 10. National Marine Mammal Peer Review Meeting. Ottawa, Can. 28 p.

Mitchell ED (1991) Winter records of the minke whale (Balaenoptera acutorostrata Lacepede 1804) in the southern North Atlantic. Rep. Int. Whal. Comm. 41: 455-457.

Norris TF, Oswald JO, Yack TM, Ferguson EL (2014) An Analysis of Marine Acoustic Recording Unit (MARU) Data Collected off Jacksonville, Florida in Fall 2009 and Winter 2009-2010. Final Report. Submitted to Naval Facilities Engineering Command (NAVFAC) Atlantic, Norfolk, Virginia, under Contract No. N62470-10-D-3011, Task Order 021, issued to HDR Inc., Norfolk, Virginia. Prepared by Bio-Waves Inc., Encinitas, CA. 21 November 2012. Revised January 2014.

Palka DL (2006) Summer Abundance Estimates of Cetaceans in US North Atlantic Navy Operating Areas. US Dept Commer, Northeast Fish Sci Cent Ref Doc. 06-03: 41 p.

Risch D, Castellote M, Clark CW, Davis GE, Dugan PJ, et al. (2014) Seasonal migrations of North Atlantic minke whales: Novel insights from large-scale passive acoustic monitoring networks. Movement Ecology 2: 24.

Stanistreet J, Hodge L, Reed A (2013) Passive Acoustic Monitoring for Marine Mammals at Site A in the Cape Hatteras Survey Area, March - April 2012. A report by the Duke University Marine Laboratory, Beaufort, North Carolina. 13 p. Available online: http://www.navymarinespeciesmonitoring.us/index.php/download_file/view/471/

Stern JS (1992) Surfacing rates and surfacing patterns of minke whales (Balaenoptera acutorostrata) off central California, and the probability of a whale surfacing within visual range. Paper SC/43/Mi2. Rep. Int. Whal. Commn. 42:379-385.

Waring GT, Josephson E, Maze-Foley K, Rosel PE, eds. (2013) U.S. Atlantic and Gulf of Mexico Marine Mammal Stock Assessments – 2012. NOAA Tech Memo NMFS NE 223; 419 p.

Waring GT, Josephson E, Maze-Foley K, Rosel PE, eds. (2014) U.S. Atlantic and Gulf of Mexico Marine Mammal Stock Assessments – 2013. NOAA Tech Memo NMFS NE 228; 464 p.